

Titre: Conceptual metallogenic modelling of archean volcanogenic massive sulphide and lode-gold deposits in Bourlamaque and Louvicourt townships, Val d'Or district, Québec
Title:

Auteur: Cecilia Louise Jenkins
Author:

Date: 1994

Type: Mémoire ou thèse / Dissertation or Thesis

Référence: Jenkins, C. L. (1994). Conceptual metallogenic modelling of archean volcanogenic massive sulphide and lode-gold deposits in Bourlamaque and Louvicourt townships, Val d'Or district, Québec [Ph.D. thesis, École Polytechnique de Montréal]. PolyPublie. <https://publications.polymtl.ca/33190/>
Citation:

 **Document en libre accès dans PolyPublie**
Open Access document in PolyPublie

URL de PolyPublie: <https://publications.polymtl.ca/33190/>
PolyPublie URL:

Directeurs de recherche: Alexander C. Brown
Advisors:

Programme: Unspecified
Program:

UNIVERSITÉ DE MONTRÉAL

CONCEPTUAL METALLOGENIC MODELLING
OF ARCHEAN VOLCANOGENIC MASSIVE SULPHIDE
AND LODE-GOLD DEPOSITS IN BOURLAMAQUE AND
LOUVICOURT TOWNSHIPS, VAL D'OR DISTRICT, QUEBEC.

par

Cecilia Louise JENKINS

DÉPARTEMENT DE GÉNIE MINÉRAL

ÉCOLE POLYTECHNIQUE

THÈSE PRÉSENTÉE EN VUE DE L'OBTENTION
DU GRADE DE PHILOSOPHIAE DOCTOR (Ph.D.)

(GÉNIE MINÉRAL)

mai 1994



National Library
of Canada

Acquisitions and
Bibliographic Services Branch

395 Wellington Street
Ottawa, Ontario
K1A 0N4

Bibliothèque nationale
du Canada

Direction des acquisitions et
des services bibliographiques

395, rue Wellington
Ottawa (Ontario)
K1A 0N4

Your file *Votre référence*

Our file *Notre référence*

THE AUTHOR HAS GRANTED AN IRREVOCABLE NON-EXCLUSIVE LICENCE ALLOWING THE NATIONAL LIBRARY OF CANADA TO REPRODUCE, LOAN, DISTRIBUTE OR SELL COPIES OF HIS/HER THESIS BY ANY MEANS AND IN ANY FORM OR FORMAT, MAKING THIS THESIS AVAILABLE TO INTERESTED PERSONS.

L'AUTEUR A ACCORDE UNE LICENCE IRREVOCABLE ET NON EXCLUSIVE PERMETTANT A LA BIBLIOTHEQUE NATIONALE DU CANADA DE REPRODUIRE, PRETER, DISTRIBUER OU VENDRE DES COPIES DE SA THESE DE QUELQUE MANIERE ET SOUS QUELQUE FORME QUE CE SOIT POUR METTRE DES EXEMPLAIRES DE CETTE THESE A LA DISPOSITION DES PERSONNE INTERESSEES.

THE AUTHOR RETAINS OWNERSHIP OF THE COPYRIGHT IN HIS/HER THESIS. NEITHER THE THESIS NOR SUBSTANTIAL EXTRACTS FROM IT MAY BE PRINTED OR OTHERWISE REPRODUCED WITHOUT HIS/HER PERMISSION.

L'AUTEUR CONSERVE LA PROPRIETE DU DROIT D'AUTEUR QUI PROTEGE SA THESE. NI LA THESE NI DES EXTRAITS SUBSTANTIELS DE CELLE-CI NE DOIVENT ETRE IMPRIMES OU AUTREMENT REPRODUITS SANS SON AUTORISATION.

ISBN 0-315-97146-0

UNIVERSITÉ DE MONTRÉAL

ÉCOLE POLYTECHNIQUE

Cette thèse intitulée:

CONCEPTUAL METALLOGENIC MODELLING
OF ARCHEAN VOLCANOGENIC MASSIVE SULPHIDE
AND LODE-GOLD DEPOSITS IN BOURLAMAQUE AND
LOUVICOURT TOWNSHIPS, VAL D'OR DISTRICT, QUEBEC.

présentée par: Cecilia Louise JENKINS

en vue de l'obtention du grade de: Philosophiae Doctor (Ph.D.)

a été dûment acceptée par le jury d'examen constitué de:

M. TANGUAY Marc, Ph.D., président

M. BROWN Alex, C., Ph.D., membre et directeur de recherche

M. DARLING Richard, Ph.D., membre

M. SAUVÉ Pierre, Ph.D., membre

SOMMAIRE

Cette étude se rapporte à la modélisation conceptuelle métallogénique de la ceinture de roches vertes de l'Abitibi au niveau du camp minier de Val d'Or, dans les cantons de Bourlamaque et de Louvicourt. Les objectifs visés sont 1) de fournir une vision globale sur le développement et l'évolution tectonostratigraphique de cette région et 2) d'expliquer l'origine des gisements de sulfures massifs volcanogènes (SMV) et des gisements d'or filonien mésothermaux (OFM) en faisant appel d'une part, aux interprétations géologiques connues pour ce secteur et d'autre part, aux modèles génétiques les plus plausibles pour la formation de tels gisements à l'Archéen.

Le modèle lithotectonique proposé par Desrochers et al. (1993) pour le développement géologique de la région de Val d'Or-Malartic suggère que le groupe de Malartic résulte d'une accrétion de fragments de plateau océanique (les domaines Nord, Vassan, Centre et Sud) sur lesquels est venu se superposer un volcanisme calco-alcalin relié à une distension intraplaque (domaine de Val d'Or). Les roches du domaine de Val d'Or ont subi une altération hydrothermale intense (associée aux SMV), visible par la présence d'une signature peralumineuse dans les roches calco-alcalines affectées. Les domaines représentant les fragments océaniques ont une affinité tholéiitique à komatiitique. Les roches volcaniques mafiques des domaines Central et Sud exhibent deux types de patrons des éléments des terres rares (ETR), ce qui suggère l'existence d'au moins deux sources mantelliques distinctes pour ces roches.

Le modèle de cellule de convection hydrothermale (CCH) est préconisé pour expliquer la formation des gisements SMV anciens et actuels. Ce modèle suppose l'existence d'une intrusion sub-volcanique à une profondeur relativement faible (2-3 km de profondeur) pour chauffer l'eau de mer et ainsi engendrer un mouvement de convection au sein d'une dorsale océanique. L'étude des gisements SMV de la région démontre qu'ils appartiennent au groupe Cu-Zn et au sous-type Mattabi. Ces gisements sont caractérisés par 1) des quantités relativement abondantes de fragments de roches volcaniques, 2) des cheminées d'altération relativement larges aux contacts mal définis, 3) des grandes zones d'altération bien développées et en semi-conformité, et 4) la présence de carbonates de fer et/ou de chloritoïdes dans les cheminées et/ou les zones d'altération.

Parmi les principaux modèles génétiques pour les gisements OFM (modèle eau météorique, modèle orthomagmatique, modèle métamorphogénique et le modèle de dégazage mantellique-granulitisation), le modèle de dégazage mantellique-granulitisation (DMG) offre l'explication la plus complète pour la formation de la majorité de la minéralisation OFM de la région d'intérêt. Suivant ce modèle, les gisements OFM archéens sont intimement liés à la cratonisation de la province du Supérieur. En fournissant magma, chaleur et éléments volatiles à la croûte inférieure, le diapirisme mantellique aurait contribué à la formation d'un résidu granulitique déshydraté et d'un fluide hydrothermal riche en éléments incompatibles (Li, Rb, B, Cs, U, Th, K), H₂O, CO₂ et or. Ce fluide, dérivant soit de l'exsolution des magmas silicatés ascendants, soit

directement de la source déshydratée, aurait ensuite été canalisé dans les structures profondes de la déformation régionale. Les fluides métamorphiques, générés lors du métamorphisme de faciès schistes verts-amphibolite inférieur, ou les fluides d'eau météoriques provenant de la surface peuvent avoir joué un rôle, au même titre que les fluides riches en CO₂ émanant des SMV, dans le lessivage, le transport et la déposition de l'or et des éléments associés, dans l'est du secteur de Val d'Or.

L'examen du secteur des cantons Bourlamaque-Louvicourt montre que plusieurs caractéristiques géologiques de cette région et de sa minéralisation OFM sont en accord avec les principaux éléments du modèle DMG: 1) la minéralisation aurifère est généralement associée à la zone tectonique de Larder Lake-Cadillac (ZTLLC) et se rencontre essentiellement dans les zones de cisaillement subsidiaires aux failles régionales; 2) des quantités importantes de carbonates sont associées aux zones de cisaillement et aux veines de quartz, ce qui témoigne d'une teneur élevée en CO₂ dans le fluide hydrothermal; 3) des enrichissements en K, Rb, U, B, CO₂ sont observés dans les zones d'altération adjacentes aux veines; et 4) la minéralisation aurifère dans la région étudiée semble plus jeune de 80-100 Ma par rapport au magmatisme syn- à post-tectonique et au métamorphisme régional, celle-ci pouvant être reliée aux processus magmatiques et métamorphiques en opération dans la croûte inférieure.

La modélisation lithotectonique suggère premièrement, que la croûte abitibienne a évolué par accréation du nord vers le sud sur une période s'étendant de 2,750-2,700 Ma

et deuxièmement, que le secteur de Val d'Or-Malartic est constitué de quatre domaines distincts qui se sont amalgamés du côté sud du protocontinent abitibien avant 2,705 Ma, âge qui correspond au volcanisme calco-alcalin dans le domaine de Val d'Or. Ce domaine et le pluton comagmatique de Bourlamaque se sont formés dans un régime d'extension au sein des 4 domaines amalgamés. Étant à l'intérieur d'une marge continentale, deux situations tectoniques sont possibles: 1) un bassin marginal intracontinental et 2) une dorsale océanique subductée. Le pluton de Bourlamaque aurait agi comme source de chaleur pour faire circuler l'eau de mer minéralisée à l'origine des gisements SMV dans la région étudiée. Suite à l'événement de formation des gisements SMV, l'Abitibi-Sud aurait subi un événement de déformation N-S entre 2,700-2,688 Ma, probablement relié à la fermeture de l'océan entre les sous-provinces de l'Abitibi et du Pontiac. La zone de suture de cette collision serait représentée par la ZTLLC et ses failles subsidiaires de deuxième et troisième ordre. Les fluides aurifères produits en profondeur par DMG (et possiblement par le métamorphisme de faciès schistes verts-amphibolite) pourraient avoir été canalisés pour ensuite remonter vers la surface à travers un système hydrothermal constitué de failles. En se basant sur cette modélisation, il nous est possible de bien cerner le développement (temporel, tectonique, lithologique et géochimique) et l'évolution crustale de la ceinture verte de l'Abitibi-Sud à laquelle sont associés les deux principaux types de minéralisation archéenne.

ABSTRACT

This study concerns conceptual metallogenic modelling for the Abitibi terrane of the Val d'Or-east mining camp located in the Bourlamaque and Louvicourt townships. Its intent is 1) to provide a global review of the development and evolution of the strata and structures of this district and 2) to explain the base-metal and gold mineralization in this district, based on the best-known geological interpretations for the district and on the most plausible crustal-to-local-scale models for Archean base-metal volcanogenic massive sulphide (VMS) deposits and mesothermal lode-gold (MLG) deposits.

The lithotectonic model of Desrochers et al. (1993) for the geological development of the Val d'Or-Malartic district suggests that the Malartic Group consists of an amalgamation of fragments of oceanic plateau (the Northern, Vassan, Central and Southern domains) upon which was superimposed extension-related calc-alkalic volcanism (the Val d'Or domain). The rocks of the Val d'Or domain have experienced intense VMS-related hydrothermal alteration, resulting in a peraluminous overprint on calc-alkalic rocks. The oceanic plateau domains have tholeiitic to komatiitic affinities. Contrasting rare-earth element (REE) profiles (flat REE profiles versus LREE-depleted/HREE-enriched profiles) suggest that the mafic flow rocks of both the Central and Southern domains come from two distinct mantle sources.

The most favourable explanation for modern and ancient VMS mineralization is

given by the hydrothermal convection-cell (HCC) model. This model requires a relatively shallow (2-3 km below seafloor) subvolcanic intrusion to heat and convect seawater in an oceanic rift environment. Evaluation of the known VMS deposits in the study area suggests that they belong to the Cu-Zn group and to the Mattabi-subtype. These deposits are characterized by 1) relatively abundant felsic fragmental volcanic rocks, 2) relatively broad, poorly-defined alteration pipes, 3) large, well-developed, semi-conformable alteration zones, and 4) iron carbonate and/or chloritoid in the alteration pipes and/or zones.

Of the current four MLG models (meteoric water, orthomagmatic, metamorphic dehydration, and mantle degassing-granulitization), the mantle degassing-granulitization (MDG) concept appears to be the most comprehensive explanation of most Archean MLG mineralization in the study area. In this model, Archean MLG mineralization is proposed to be an integral part of the cratonization of the Superior Province. Briefly, mantle diapirism supplies magma, heat and volatiles to the lower crust, resulting in the formation of a dehydrated granulitic residue and a hydrothermal fluid containing CO₂, H₂O, incompatible elements (Li, Rb, B, Cs, U, Th, K) and gold. This fluid, which comes either from exsolution of ascending silicate magmas or directly from the dehydrating source, is channelled into deep regional deformation structures. Metamorphic fluids generated at the upper greenschist-lower amphibolite transition or meteoric water descending from surface recharge areas may also have played a role, along with abundant CO₂-rich fluids from MDG, in the leaching, transport and deposition

of gold and associated elements in the Val d'Or-east district.

Several characteristics of the study area and its MLG deposits agree with the central elements of the MDG model: 1) gold mineralization is associated regionally with the crustal-scale Larder Lake-Cadillac Tectonic Zone (LLCTZ), and is hosted essentially by shear zones subsidiary to the regional fault; 2) abundant carbonate is associated with all scales of shearing and quartz veining, and CO₂ is in fact recognized as an important hydrothermal fluid component; 3) enrichments in K, Rb, U, B, CO₂ and Au are noted in alteration zones adjacent to quartz veins; and 4) gold mineralization in the study area is apparently ca 80-100 Ma younger than syn- to post-tectonic magmatism and regional metamorphism, and may be correlated with lower crustal magmatism and metamorphism.

Lithotectonic modelling suggests that the Abitibi crust evolved by accretion from north to south over a period extending from ca 2,750-2,700 Ma, and that the Val d'Or-Malartic district consists of four discrete terranes that were accreted to the southern side of the Abitibi protocontinent before ca 2,705 Ma, the age of volcanism for the superimposed Val d'Or domain. The Val d'Or domain and its apparently comagmatic Bourlamaque pluton formed in an extensional regime within the four accreted terranes. Being within a continental margin, two tectonic situations are possible: 1) an intra-continental back-arc, and 2) a subducted oceanic ridge. The Bourlamaque pluton would have acted as the heat engine to circulate mineralized modified seawater that generated the VMS deposits of the study area. Subsequent to the VMS environment, the Southern

Abitibi underwent a north-south deformational event lasting from ca 2,700 to at least 2,688 Ma, probably tied to the closure of the oceanic crust between the Abitibi and Pontiac subprovinces. The suture zone of this collision is characterized by the LLCTZ and its subsidiary second- and third-order faults. Auriferous fluids produced at depth by MDG (and possibly greenstone-amphibolite-type metamorphism) could be tapped and rise through a fault-valve-type hydrothermal system. Based on this modelling, we see a fairly well-constrained (temporal, tectonic, lithologic and geochemical) development and evolution of the southern Abitibi greenstone belt geology, within which two very major types of Archean mineralization formed as normal products of this crustal evolution.

RÉSUMÉ

Cette étude se rapporte à la modélisation conceptuelle métallogénique de la ceinture de roches vertes de l'Abitibi au niveau du camp minier de Val d'Or, dans les cantons de Bourlamaque et de Louvicourt. Ce camp minier est connu pour ses gisements d'or filonien mésothermaux (OFM) archéens depuis leur découverte au début des années 1900. Cette région recèle également de nombreux gisements de sulfures massifs volcanogènes (SMV) de dimensions moyennes qui furent exploités de 1942 à 1981, avant la découverte en 1989 de l'important gisement de Louvicourt. Plusieurs études régionales ont été réalisées pour comprendre la stratigraphie, la structure et l'évolution tectonique de la ceinture de roches vertes de l'Abitibi-Sud où se situent ces deux types de gisements. Les objectifs visés dans la présente étude sont 1) de fournir une vision globale sur le développement et l'évolution tectonostratigraphique de cette région et 2) d'expliquer l'origine des gisements de SMV et des gisements d'OFM, dans les cantons de Bourlamaque et de Louvicourt, en faisant appel d'une part aux interprétations géologiques connues pour ce secteur, et d'autre part, aux modèles génétiques les plus plausibles pour la formation de tels gisements à l'Archéen.

Une recherche bibliographique a révélé la rareté des données géochimiques se rapportant aux lithologies du secteur de Val d'Or. Les nouvelles analyses présentées ici des éléments majeurs indiquent que les roches volcaniques des domaines Vassan, Centre et Sud ont une affinité tholéïitique à komatiitique. La majorité de ces échantillons ont

des rapports Y/Zr chondritiques à l'exception d'un petit groupe de basaltes, provenant des domaines Centre et Sud qui ont des teneurs élevées en Y. Ces teneurs peuvent être attribuées à une certaine mobilité de l'Y ou plutôt à une accumulation de clinopyroxène, minéral au sein duquel l'Y est compatible. Toutes les roches tholéitiques exhibent des anomalies positives en Nb et Zr et semblent comagmatiques d'après les diagrammes Ni-Y, Co-Y, V-Y et Sc-Y. Cependant, les patrons des terres rares [patrons plats versus patrons inclinés où les terres rares légères (TRLé) sont appauvries par rapport aux terres rares lourdes (TRL_o)] suggèrent que les roches volcaniques des domaines Centre et Sud proviennent de deux sources mantelliques distinctes: une source mantellique tholéitique appauvrie et une source mantellique tholéitique également appauvrie en TRLé.

La majorité des roches extrusives et intrusives du domaine de Val d'Or sont altérées, comme en témoigne la présence de corindon normatif dans leur norme CIPW. Cependant, les roches avec ou sans corindon dans leur norme se comportent de façon similaire sur les diagrammes Y versus Zr, indiquant que malgré une altération intense les éléments incompatibles tels que Y et Zr retiennent leur caractère immobile pour la plupart des échantillons.

Malgré l'importance de l'altération, les tendances magmatiques, basées sur le comportement des éléments majeurs, demeurent évidentes. Pour leur part, les éléments traces et les terres rares (anomalies négatives en Nb et Ti et positive en Zr, enrichissement en TRLé) sont en accord avec une affinité calco-alkaline pour les roches

du domaine de Val d'Or. Aussi, les roches intrusives et extrusives de ce domaine ont des caractéristiques géochimiques similaires impliquant un lien cogénétique.

Les gisements de SMV du camp minier de Val d'Or-Est appartiennent au groupe Cu-Zn et s'apparentent aux gisements du sous-type Mattabi. Ils sont caractérisés par une minéralisation Cu-Zn qui apparaît sous forme de lentilles stratiformes ou de stockworks. Les roches encaissantes sont felsiques et volcanoclastiques et ont des compositions peralumineuses suite à un lessivage intense du Ca et du Na. Plusieurs types d'altération sont visibles au sein de ces roches: 1) une chloritisation à proximité des systèmes de stockwork; 2) une séricitisation semi-concordante à l'extérieur de la zone de chloritisation; et 3) une altération en carbonates +/- chloritoïdes +/- grenat.

Le modèle de la cellule de convection hydrothermale (CCH) est préconisé pour expliquer la formation des gisements de SMV anciens et actuels. Ce modèle requiert la présence d'une intrusion sub-volcanique à une profondeur de 2 à 3 km pour chauffer l'eau de mer et ainsi engendrer un mouvement de convection au niveau d'une zone d'expansion océanique. Suivant ce modèle, l'eau de mer percole à travers la croûte océanique et réagit avec les roches basaltiques chaudes pour former des précipités minéraux et une solution hydrothermale chaude et minéralisée. Cette solution hydrothermale remonte ensuite vers le plancher océanique et précipite des sulfures métalliques lorsqu'elle entre en contact avec l'eau de mer froide. Il est à noter qu'une faible proportion du fluide minéralisé pourrait provenir de l'intrusion sub-volcanique.

La grande majorité des systèmes de SMV sont recouverts d'une couverture de sédiments ou d'une couche de silice et/ou carbonates entre le plancher océanique et le gisement. Il est également possible que ces systèmes soient formés d'une certaine épaisseur de roches volcaniques non fracturées lorsque les sédiments sont absents. Dans tous ces cas, la source de chaleur et les fluides hydrothermaux se trouvent isolés, ce qui empêche une incursion trop rapide de l'eau de mer froide. La fracturation locale de la couverture sédimentaire ou volcanique prévient également une percolation des fluides à travers la croûte. En effet, les fluides hydrothermaux auraient plutôt tendance à remonter vers le plancher océanique, le long des failles et des fractures synvolcaniques, ces dernières étant le résultat d'une distension crustale ou d'explosions bréchiques.

Les analogues modernes les plus représentatifs de la minéralisation de SMV archéenne ont été décrits pour 1) la fosse d'Okinawa qui correspond à un bassin marginal intracontinental au sein duquel on rencontre des gisements de SMV de type Kuroko; 2) le bassin marginal de Lau dont les gisements de métaux de base sont intermédiaires entre la minéralisation typique associée aux dorsales océaniques et à celle de type Kuroko; 3) l'est du bassin de Manus qui représente un bassin marginal en extension auquel sont associés des gisements de sulfures polymétalliques; et 4) le guyot de Franklin, localisé près de la terminaison ouest de la dorsale, dans le bassin de Woodlark, où l'activité hydrothermale est associée à une marge continentale.

Les principaux modèles génétiques pour les gisements d'OFM (modèles eau

météorique, orthomagmatique, métamorphogénique et le modèle de dégazage mantellique-granulitisation (DMG)), proposent plusieurs sources variées de fluides et de solutés, et différentes hypothèses pour expliquer cette minéralisation. Le modèle eau météorique, basé principalement sur les gisements d'or filonien épithermaux et mésothermaux rencontrés dans la Cordillère canadienne, propose que les gisements d'OFM archéens se sont formés par la convection profonde des eaux météoriques descendantes. De son côté le modèle orthomagmatique suggère que, lors de la cristallisation d'une intrusion, il y a exsolution de fluides hydrothermaux chargés de métaux, soufre et minéraux de gangue pour éventuellement former des gisements d'OFM. Pour sa part le modèle métamorphogénique envisage l'écoulement de fluides de faibles densité et salinité, mais riches en CO₂ et H₂O à travers les failles crustales. Ces fluides proviendraient de la dévolatilisation des roches volcaniques mafiques lors du métamorphisme au faciès amphibolite-schistes verts, phénomène à peu près synchrone à la déformation et au plutonisme tardifs. Suivant le modèle DMG, le diapirisme mantellique, en fournissant magma, chaleur et éléments volatiles à la croûte inférieure, aurait contribué à la formation d'un résidu granulitique déshydraté et d'un fluide hydrothermal riche en éléments incompatibles (Li, Rb, B, Cs, U, Th, K), H₂O, CO₂ et or. Ce fluide dont l'origine est reliée soit à l'exsolution des magmas silicatés ascendants, soit directement à la source déshydratée, aurait ensuite été canalisé dans les structures profondes de la déformation régionale. De petits corps intrusifs seraient aussi piégés dans ces zones de déformation. Notre évaluation de ces principaux modèles favorise le modèle DMG qui offre l'explication la plus complète pour la minéralisation d'OFM

archéenne, dans le contexte de l'évolution des ceintures de roches vertes. Selon Colvine et al. (1988), les gisements d'OFM archéens sont intimement liés à la cratonisation de la province du Supérieur. D'ailleurs, la présente étude suggère que les fluides métamorphiques, générés lors du métamorphisme de faciès schistes verts-amphibolite inférieur, ou possiblement les fluides d'eau météoriques provenant de la surface peuvent avoir joué un rôle, au même titre que les fluides riches en CO₂ provenant du DMG, dans le lessivage, le transport et la déposition de l'or et des éléments associés, dans le secteur aurifère à l'est de Val d'Or.

Probablement, les analogues les plus représentatifs de la minéralisation d'OFM archéenne sont les gisements d'OFM retrouvés sur la côte ouest du continent nord-américain. Cette région est formée d'une série de terrains allochtones qui se sont agglomérés à la marge continentale pour ensuite être subductés sous celle-ci. Les gisements d'OFM des Cordillères sont 1) retrouvés seulement dans des terrains allochtones, 2) associés à des failles régionales crustales et post-métamorphiques qui pourraient représenter des zones de suture entre les différents terrains et 3) souvent associés à des failles inverses subverticales, subsidiaires aux zones de failles majeures. Certains domaines phanérozoïques (ex.: les Monte Rosa Lodes dans les Alpes italiennes ou la ceinture de schistes de Ballarat en Australie) renferment des gisements d'OFM qui partagent des emplacements géodynamiques similaires.

L'examen du secteur des cantons Bourlamaque-Louvicourt montre que plusieurs

caractéristiques géologiques de cette région et de sa minéralisation d'OFM sont en accord avec les principaux éléments du modèle de DMG: 1) la minéralisation aurifère est généralement associée à la zone tectonique de Larder Lake-Cadillac (ZTLLC) et se rencontre essentiellement dans les zones de cisaillement subsidiaires aux failles régionales, à l'intérieur de veines non déformées de quartz-tourmaline-carbonates-pyrite; 2) des quantités importantes de carbonates sont associées aux zones de cisaillement et aux veines de quartz, ce qui témoigne d'une teneur élevée en CO₂ dans le fluide hydrothermal; 3) des enrichissements en K, Rb, U, B, CO₂ et Au ont été observés dans les zones d'altération adjacentes aux veines de quartz; et 4) les gisements d'OFM de la région étudiée sont spatialement reliés à, ou sont à l'intérieur des intrusions de compositions intermédiaires à felsiques; et 5) la minéralisation aurifère dans la région étudiée semble plus jeune de 80-100 Ma par rapport au magmatisme syn- à post-tectonique et au métamorphisme régional et peut être reliée aux processus magmatiques et métamorphiques en opération dans la croûte inférieure, comme en témoigne l'histoire tectonique de la zone structurale de Kapuskasing.

Finalement, la présente étude s'intéresse à la métallogénie du secteur est de Val d'Or. Dimroth et al. (1983a,b), Ludden et Hubert (1986) et Jackson et Fyon (1991) proposent que la croûte abitibienne a évolué par un processus d'accrétion du nord vers le sud sur une période s'étendant de 2,750-2,700 Ma. En considérant le secteur de Val d'Or-Malartic, il semble que même à l'intérieur d'une petite portion de la ceinture verte de l'Abitibi-Sud, ici représentée par le bloc composite de Malartic (BCM), il y a eu des

phénomènes d'accrétion. Effectivement, Desrochers et al. (1993) stipulent que le BCM est formé de quatre domaines distincts qui se seraient agglomérés du côté sud du protocontinent abitibien, un par un ou par une combinaison de regroupements. Chaque domaine a enregistré une déformation D_1 bien marquée, ce qui indique probablement différents événements obliques. Cette accrétion devait être nécessairement complétée à 2,705 Ma, l'âge qui correspond au volcanisme calco-alcalin du domaine de Val d'Or. Présentement, nous ignorons si certains, ou tous les domaines du BCM, se retrouvent à l'est de Val d'Or. Si tel n'est pas le cas, nous pouvons supposer que des domaines similaires se sont agglomérés plus à l'est. Le domaine Sud semble se prolonger au sud du domaine de Val d'Or, quoique cet empilement volcanique de roches tholéitiques pourrait représenter un tout autre domaine.

Dans tous ces cas, la possibilité que le domaine calco-alcalin de Val d'Or repose en discordance sur les domaines accrétés D_1 du BCM représente une situation anormale en soi. Nous devons faire appel à un régime en extension à l'intérieur d'une marge continentale formée des quatre domaines D_1 déformés et nouvellement agglomérés. L'extension crustale, dans un tel environnement, est consistante avec la composition calco-alcaline du domaine de Val d'Or et aussi avec la formation de la minéralisation de SMV associée. Étant à l'intérieur d'une marge continentale, nous pouvons envisager deux scénarios tectoniques possibles: 1) extension au sein d'un bassin marginal intra-continental; et 2) subduction d'une dorsale océanique. Afin d'expliquer le phénomène d'extension et les affinités calco-alcalines, Desrochers et al. (1993) ont fait appel au

deuxième scénario, où la subduction de la ride océanique sous le BCM s'accompagne d'une montée de magma (plume) qui serait à l'origine du volcanisme calco-alcalin et du plutonisme sub-volcanique recoupant le BCM. Cependant, dans le cadre de cette étude, nous favorisons le premier scénario où l'extension crustale survient dans un bassin marginal surmontant une plaque océanique subductée (ex.: la mer du Japon).

Le pluton de Bourlamaque, qui est probablement comagmatique avec le domaine de Val d'Or, s'est mis en place dans le BCM, autour de 2,705 Ma et a agité comme source de chaleur pour modifier et faire circuler l'eau de mer. Étant donné les dimensions importantes de ce pluton, on peut supposer, si son volume entier était contemporain au volcanisme, qu'il aurait été suffisamment grand pour générer les gisements de SMV équivalents à plusieurs camps de SMV de Rouyn-Noranda.

Suite à l'événement de formation des gisements de SMV, l'Abitibi-Sud aurait subi une déformation N-S entre 2,700 et 2,688 Ma. Cette déformation est visible par un métamorphisme régional kénoréen de faciès schistes verts et par une déformation D_2 est-ouest. Cet événement pourrait être relié à la fermeture de l'océan entre les sous-provinces de l'Abitibi et du Pontiac par la subduction d'une plaque océanique vers le nord, pour former la grande suite plutonique syn-tectonique. La collision de la croûte océanique avec la croûte continentale serait aujourd'hui visible par la présence d'une zone de suture, représentée par la ZTLLC et par un réseau de failles subsidiaires de deuxième et troisième ordre.

Durant les derniers stades de la déformation D_2 , les gisements d'OFM de type Sigma se sont formés au-dessus de la ZTLLC. Les fluides aurifères générés en profondeur par DMG (et possiblement par le métamorphisme de faciès schistes verts-amphibolite) pourraient avoir été canalisés pour ensuite remonter vers la surface à partir d'un système de pompage sismique. Selon Robert (1990), le système de veines se serait étendu à l'échelle de la zone de déformation (jusqu'à 15 km au nord de la principale zone de suture) et peut-être à plus de 40 km le long de la faille. La nature des veines et de l'altération de la roche encaissante sont remarquablement similaires pour les gisements d'OFM du secteur est de Val d'Or. Toutefois, il y a des indices sur les roches-source en profondeur, comme par exemple, la présence de tourmaline dans les veines, dont le bore pourrait provenir des sédiments du Pontiac chevauchés par le BCM. La minéralisation d'OFM semble être le dernier événement géologique archéen d'importance.

En étudiant les différentes facettes de la géologie de l'Abitibi, il nous a été possible de bien cerner le développement (temporel, tectonique, lithologique et géochimique) et l'évolution de la ceinture de roches vertes de l'Abitibi-Sud, au sein de laquelle on retrouve les deux principaux types de minéralisation associés à son histoire crustale. Si, dans le futur, il y a des changements significatifs dans les modèles génétiques des gisements et dans nos conceptions du développement crustal, ces nouveaux modèles ou interprétations fourniront sans nul doute une meilleure compréhension de l'Abitibi et de sa métallogénie.

ACKNOWLEDGEMENTS

This thesis has been financed by the Ministère de l'Énergie et des Ressources du Québec (MERQ) and I wish to thank Dr. Alain Simard and Dr. Francis Chartrand of the MERQ for sponsoring my project.

I wish to express my sincerest thanks to Alex Brown, my thesis advisor, for accepting to guide me through the challenge of this doctorate study. His constant understanding of the project and his confidence in me are greatly appreciated.

The following companies, Aur Resources Inc., les Mines Aurizon Ltée, Cambior Inc., Lac Minerals Ltd., and Placer Dome Inc., are acknowledged for access to their Val d'Or properties and documents.

Special thanks go to:

Mr. Jean-Philippe Desrochers who gave me permission to use some of his geochemical analyses;

Dr. John Ludden and Ms. Shirley Peloquin who helped me better understand the geochemical data;

Mr. Christian Dallaire of the Mineral Engineering Department and all my friends from the 6th floor computer lab who helped me immensely along my way with all my !*#! computer problems!;

Dr. Guy Valiquette for his assistance with thin section observations;

Ms. Brigitte Dionne for French translations;

Mr. Pierre Bédard for drafting several figures in this thesis; and

Mr. Gaston Gélinas and Mr. Louis Évrard for the preparation of thin sections.

This thesis was funded by the MERQ, the NSERC Strategic Grant #STR0045303, the NSERC Operating Grant OGP0007814 to A.C. Brown, an NSERC scholarship, financial aid from the Department of Mineral Engineering of l'École Polytechnique, and the bursary "Commémoration du 6 décembre, 1989" offered by the Comité Femmes du Syndicat général des professeurs de l'Université de Montréal, École Polytechnique.

TABLE OF CONTENTS

	<u>PAGE</u>
SOMMAIRE	iv
ABSTRACT	viii
RÉSUMÉxii
ACKNOWLEDGEMENTS	xxii
TABLE OF CONTENTS	xxiv
LIST OF FIGURES	xxix
LIST OF TABLES	xxxvi
LIST OF APPENDICES	xxxvii
INTRODUCTION	1
CHAPTER 1 - REGIONAL AND LOCAL GEOLOGY	4
1.1 Regional Geology	4
1.2 Local Geology	11
1.2.1 Historical Development	11
1.2.2 Group Descriptions (Figs. 3 and 4)	18
1.2.3 Structure	26
1.2.4 Metamorphism	26
1.2.5 Major Intrusions	27
1.2.6 Interpretations of Local Geology	28

1.3 Peculiarities of the Bourlamaque and Louvicourt Townships Geology	42
CHAPTER 2 - GEOCHEMICAL DATA FOR ROCKS OF THE VAL D'OR DISTRICT	47
2.1 Introduction	47
2.2 Literature Review of the Geochemistry of Rocks in the Val d'Or Region	48
2.3 New Geochemical Data for Val d'Or District Rocks	55
2.3.1 Introduction	55
2.3.2 Characterization of Least-Altered Samples	56
2.3.3 Evaluation of Geochemical Data	61
2.3.3.1 Geochemical Data of Flow Rocks	61
2.3.3.2 Geochemical Data of Intrusive Rocks	84
2.4 Summary and Conclusion	92
CHAPTER 3 - VOLCANOGENIC MASSIVE SULPHIDE MODELLING FOR THE BOURLAMAQUE AND LOUVICOURT TOWNSHIPS	95
3.1 Volcanogenic Massive Sulphide Mineralization in the Study Area	95
3.2 Volcanogenic Massive Sulphide Classification	101
3.2.1 Significance of Water Depth	103
3.3 Hydrothermal Convection-Cell Model	109
3.3.1 Introduction	109

3.3.2 Oceanic Environment	111
3.3.3 Heat Source	111
3.3.4 Extensional Fracture System	114
3.3.5 "Cap" on the Hydrothermal Reaction Zone	114
3.3.6 Source of Fluids and Metals	115
3.3.7 Ore-Metal Transport	119
3.3.8 Chemical Reactions Causing Alteration	120
3.3.9 Alteration Pipes	121
3.3.10 Mechanisms for Precipitating and Accumulating Sulphides	123
3.4 Modern Analogues	125
3.5 Case Study: Bourlamaque and Louvicourt Townships	133
3.6 Conclusion	138
CHAPTER 4 - ARCHEAN MESOTHERMAL LODGE-GOLD DEPOSITS	140
4.1 Introduction	140
4.2 Synvolcanic Gold Mineralization Environments	150
4.2.1 Porphyry Copper Deposits	150
4.2.2 Gold Skarn Deposits	153
4.2.3 Epithermal Precious Metal Deposits	155
4.2.4 Volcanogenic Massive Sulphide Deposits	158
4.2.5 Banded Iron-Formation-Hosted Gold Deposits	163
4.3 Late- to Post-Tectonic Gold Mineralization Environments	165
4.3.1 Quartz-Vein Gold Deposits	165

4.3.2 Pyritic Gold Deposits	170
4.4 Models for Archean Mesothermal Lode-Gold Mineralization	172
4.4.1 Introduction	172
4.4.2 Meteoric Water Model	173
4.4.3 Orthomagmatic Model	177
4.4.4 Metamorphic Dehydration Model	182
4.4.5 Mantle Degassing-Granulitization Model	187
4.4.6 Conclusion	196
4.5 Phanerozoic Analogues	199
4.6 Geochronological and Geotectonic Developments Pertinent to the Bourlamaque-Louvicourt Townships Study Area	202
4.7 Application of the Mantle Degassing—Granulitization Model to the Bourlamaque-Louvicourt Townships Study Area	216
4.8 Summary	227
CHAPTER 5 - DISCUSSION AND SUMMARY	229
5.1 Introduction	229
5.2 Summary of Geochemical Data and VMS and Lode-Gold Models Applied to the Val d'Or-East District	230
5.2.1 Geochemical Data for the Val d'Or District	230
5.2.2 The Hydrothermal Convection-Cell Model for VMS Mineralization	231

5.2.3 The Mantle Degassing-Granulitization Model for Archean Lode-Gold Mineralization	233
5.3 Crustal-Scale Metallogenic Interpretation of the Val d'Or-East Geology	234
CHAPTER 6 - CONCLUSION AND RECOMMENDATIONS	239
REFERENCES	244
APPENDICES	287

LIST OF FIGURES

	<u>PAGE</u>
Figure 1: Superior Province location map (modified after Card, 1990)	5
Figure 2: General map of the Abitibi Subprovince divided into lozenge-shaped blocks. CBZ = Casa Berardi Tectonic Zone, LWZ = Lac Waswanipi Tectonic Zone, CLZ = Chicobi Lake Tectonic Zone, DZ = Dumagami Tectonic Zone, LCZ = Larder Lake-Cadillac Tectonic Zone (taken from Hubert, 1990 as modified from Ludden and Hubert, 1986)	7
Figure 3: General geologic map of the Val d'Or region illustrating the regional syncline interpreted by Gunning and Ambrose (1940) and the division (broken line) of the Malartic Group into upper and lower subgroups (Latulippe, 1976). The dotted lines represent township boundaries. The Bourlamaque and Louvicourt townships comprise the study area	12
Figure 4: Geologic map of the Val d'Or region interpreted by Imreh (1984). The La Motte-Vassan overturned anticline is the dominant, regional structure and the Malartic Group is divided into the La Motte-Vassan, Dubuisson, Jacola, Val d'Or and Héva formations. The dotted line outlines the study area	14
Figure 5: Tectonostratigraphic map of the Val d'Or region highlighting the five lithotectonic domains of the Malartic Composite Block (modified after Desrochers et al. (1993). The dotted line outlines the study area	16

- Figure 6a: Model for the formation of a Malartic Composite Block (shaded = MCB). Top: Progressive collage of oceanic plateaux (N = Northern, V = Vassan, C = Central, S = Southern domain) prior to 2,705 Ma on the Superior protocontinent. Bottom: Back-stepping of the subduction zone and ridge subduction resulting in calc-alkalic volcanism (Black = Val d'Or domain) on top of accreted plateaux at 2,705 Ma (modified after Desrochers et al., 1993) 17
- Figure 6b: Block diagram of assembled Malartic Composite Block. Thick lines represent fault zones bounding domains, dotted lines represent unconformities, and thin lines indicate bedding attitudes (modified after Desrochers et al., 1993) 17
- Figure 7: Schematic diagram of the tectonic interplay in the Indonesian region (taken from Jackson and Fyon, 1991 as modified from Hamilton, 1988) 40
- Figure 8: General geologic map of the Val d'Or-east district (modified after Sauvé et al., 1986 and Desrochers et al., 1993) with the location of the Central Pyroclastic Belt as defined by Sharpe (1968) and Chartrand (1991) 43
- Figure 9: Binary diagram of normative corundum versus Al_2O_3 for flow and intrusive rocks of the Val d'Or domain. Solid boxes = flow rocks (author's data); triangles = intrusive rocks (author's data); open boxes = flow rocks (data from Girault, 1986 and Gaudreau et al., 1986) 59
- Figure 10: Alkalis-silica plot (Irvine and Baragar, 1971) for flow rocks of the Val d'Or district. Triangles = Val d'Or domain (author's data); circles = Southern and Vassan domains (author's data); and boxes = Southern, Central and Vassan domains (data from Desrochers, 1994) 63
- Figure 11: (a) AFTiM (Jensen, 1976) and (b) AFM (Irvine and Baragar, 1971) plots for flow rocks of the Val d'Or district. Triangles = Val d'Or domain (author's data); circles = Southern and Vassan domains (author's data); and boxes = Southern, Central and Vassan domains (data from Desrochers, 1994) 64

- Figure 12: Binary major element oxide diagrams for flow rocks of the Val d'Or district. Triangles = Val d'Or domain (author's data); circles = Southern and Vassan domains (author's data); and boxes = Southern, Central and Vassan domains (data from Desrochers, 1994) 65
- Figure 13: Rare-earth element profiles for Val d'Or domain flow rocks. (a) = low-SiO₂, (b) = medium-SiO₂, (c) = high-SiO₂ samples grouped according to their position in Figure 12e (P₂O₅ vs SiO₂). Elements normalized to the C1 chondrite (Sun and McDonough, 1989) 68
- Figure 14: Extended trace-element abundance profiles for Val d'Or domain flow rocks. (a) = low-SiO₂, (b) = medium-SiO₂, (c) = high-SiO₂ samples grouped according to their position in Figure 12e (P₂O₅ vs SiO₂). Elements, normalized to the C1 chondrite (Sun and McDonough, 1989), exhibit decreasing incompatibilities from left to right 70
- Figure 15: Field for composite extended trace element abundance profiles for Val d'Or domain flow rocks. See Figure 14 for individual profiles 71
- Figure 16: Binary trace element diagrams for flow rocks of the Val d'Or district. (a) = Y vs Zr, (b) = Zr/Y vs Zr, (c) = Zr/Nb vs Zr. Triangles = Val d'Or domain (author's data); circles = Southern and Vassan domains (author's data); boxes = Southern, Central and Vassan domains (data from Desrochers, 1994) 72
- Figure 17: Binary trace-element diagrams for flow rocks of the Val d'Or district. (a) = Ni vs Y, (b) = Co vs Y, (c) = V vs Y, (d) Sc vs Y. Triangles = Val d'Or domain (author's data); circles = Southern and Vassan domains (author's data); boxes = Southern, Central and Vassan domains (data from Desrochers, 1994) 74

- Figure 18: (a) Relatively flat rare-earth element profiles and (b) heavy rare-earth element enriched profiles for flow rocks from the Vassan (3864-91), Central (3833-91, 3834-91, 3837-91) and Southern (3838-91, 3865-91, 5667-92, 5668-92) domains. Elements are normalized to the C1 chondrite (Sun and McDonough, 1989) 76
- Figure 19: Extended trace element abundance profiles for flow rocks grouped according to (a) relatively flat REE and (b) HREE-enriched profiles in Figure 18. Samples are from the Vassan (3964-91), Central (3833-91, 3834-91, 3837-91) and Southern (3838-91, 3865-91, 5667-92, 5668-92) domains. Elements, normalized to the C1 chondrite (Sun and McDonough, 1989), exhibit decreasing incompatibilities from left to right 79
- Figure 20: (a) P_2O_5 vs SiO_2 and (b) TiO_2 vs SiO_2 plots for various rock samples by Girault (1986) in the Val d'Or domain. Trends taken from Figures 12d and 12e. Open circle = basalt, half-filled circle = andesite, filled circle = porphyritic lava, open box = rhyolite, half-filled box = rhyolitic pyroclastic block, filled box = dacite, filled upright triangle = diorite sill, open inverted triangle = albite microgranite, asterisk = tuff 80
- Figure 21: Y versus Zr plot for flow rocks of the Val d'Or domain (data from Girault, 1986 and Gaudreau et al., 1986). Empty diamonds = no normative corundum, full diamonds = with normative corundum (data from Gaudreau et al., 1986); empty circles = no normative corundum, full circles = with normative corundum (data from Girault, 1986) 83
- Figure 22: Y versus Zr plot for intrusive rocks of the Val d'Or and Southern domains. Triangles = Southern domain; empty boxes = feldspar ± quartz porphyries; full box = feldspar porphyry; empty circles = Val d'Or domain; full circles = Bourlamaque intrusion. Samples not plotted: 5669-92 (triangle: 73 ppm Y, 160 ppm Zr) and 3880-91 (full circle: 34 ppm Y, 1,000 ppm Zr) 86
- Figure 23: Y versus Zr plot of porphyries and plugs of the Lamaque mine, Val d'Or (modified after Daigneault et al., 1983) 87

- Figure 24: Rare-earth element profiles for intrusive rocks from the (a) Val d'Or and (b) Southern domains; and (c) for two feldspar±quartz porphyries (3846-91; 3857-91) and one gabbroic intrusion (3860-91) from the Val d'Or and Southern domains. Elements are normalized to the C1 chondrite (Sun and McDonough, 1989) 88
- Figure 25: Extended trace-element abundance profiles for intrusiverocks from the (a) Southern and (b) Val d'Or domains; and (c) for two feldspar±quartz porphyries (3846-91; 3857-91) and one gabbroic intrusion (3860-91) from the Val d'Or and Southern domains. Elements are normalized to the C1 chondrite (Sun and McDonough, 1989) 89
- Figure 26: Location map of major and minor base-metal sulphide deposits in the Val d'Or-east region, Quebec; modified after Sauvé et al. (1986), Chartrand (1991) and Desrochers et al. (1993). Numbers correspond to deposits described in Table 1 96
- Figure 27: General geologic map of the Yilgarn Craton, Australia with localization of the Scuddles VMS deposit in the Golden Grove greenstone belt (modified after Swager et al., 1992) 106
- Figure 28: Boiling point curves for H₂O liquid (0 wt. percent) and for brine of constant composition given in wt. percent NaCl. The insert expands the relations between 100°C and 150°C. The temperature at 0 metres for each curve is the boiling point for the liquid at 1.013 bars (1.0 atm) load pressure which is equivalent to atmospheric pressure at sea level. The uncertainty is contained within the width of the lines (original curves from Haas, 1971) 107
- Figure 29: Schematic representation of the hydrothermal convection-cell model. Caprock = sediments, ashflow material, silicification±epidotization or carbonatization 112
- Figure 30: Composite representation of the various alteration assemblages that have been reported for alteration pipes of VMS deposits (from Lydon, 1988) 122

Figure 31:	Location map of the Okinawa Trough and the Jade deposit (from Urabe and Marumo, 1991)	127
Figure 32:	General map (a) of the Lau back-arc basin and (b) location of hydrothermal fields along the Valu Fa Ridge (from Fouquet et al., 1991)	128
Figure 33:	General location map of the Manus and Woodlark basins east of Papua New Guinea (PNG) (modified after Binns and Scott, 1993)	131
Figure 34:	Location map of major gold deposits in Bourlamaque and Louvicourt townships; modified after Sauv�� et al. (1986) and Desrochers et al. (1993). Numbers correspond to deposits described in Table 2	149
Figure 35a:	Sequence of development of alteration zones and subzones around tension veins. Horizontal axis represents time as well as intensity of alteration. (CH: chlorite, CB: carbonate, MI: white mica, AB: albite, ep: epidote, ch: chlorite, mi: white mica, pg: plagioclase, qz: quartz, ca: calcite, ap: apatite, tm: tourmaline, py: pyrite, po: pyrrhotite, il: ilmentie, Au: gold, te: tellurobismuthite). (from Robert and Brown, 1986)	167
Figure 35b:	A schematic representation of the distribution of cryptic and visible alteration zones around flat veins and dike stringers. Visible alteration may be absent and grade laterally to asymmetrical or to symmetrical alteration envelopes (from Robert and Brown, 1984)	167
Figure 36:	Schematic representation of the meteoric water model for epithermal and mesothermal gold deposits (modified after Nesbitt et al., 1989)	174
Figure 37:	Schematic representation of the orthomagmatic model for Archean lode-gold deposits (modified after Rogers and Greenberg, 1990)	178
Figure 38:	Schematic representation of the metamorphic dehydration model for Archean lode-gold deposits (modified after Kerrich and Fryer, 1979)	183

- Figure 39: Schematic representation of the mantle degassing—granulitization model for Archean lode-gold deposits (modified after Colvine et al., 1988) 189
- Figure 40a: Part of the generalized geologic map, modified after Feng and Kerrich (1990), showing the distribution of emplacement pressure (number in kilobars) of granitic plutons and metallogenic provinces. Underlined numbers are pressures for gold mineralization. Numbers in squares represent structural blocks: 2-Blake River-Rouyn, 3-Val d'Or, 4-Lacorne, 5-Amos, 6-Lac Abitibi, 8-Pontiac. LCF: Larder Lake-Cadillac fault 210
- Figure 40b: Schematic composite crustal structure for the Southern Volcanic Zone before differential uplift caused by strike-slip faulting during oblique collisional tectonics in late Archean time. Types of mineralization also given (from Feng and Kerrich, 1990) 210
- Figure 41: Simplified tectonic model for the evolution of the Abitibi Southern Volcanic Zone (SVZ) and the Pontiac Subprovince 211
- Figure 42: Schematic cross-section through the Val d'Or district showing relationships between veins and different orders of shear zones (LLCF: Larder Lake-Cadillac Fault) (from Robert and Bouiller, in press) 217

LIST OF TABLES

	<u>PAGE</u>
Table 1: Summary of characteristics of major and minor base metal sulphide deposits in the Val d'Or district (modified after Chartrand, 1991 and the author's compilation)	97
Table 2: Summary of characteristics of gold deposits in Bourlamaque and Louvicourt townships, Val d'Or-East district	142
Table 3: Characteristics of Canadian Cordillera mesothermal lode-gold deposits (from Nesbitt and Muehlenbachs, 1988)	201

LIST OF APPENDICES

	<u>PAGE</u>
Appendix 1: Sampling and Laboratory Analytical Techniques	287
Appendix 2: Sampling Location Map, Major, Trace and Rare-Earth Element Analyses, and the CIPW Norm for Flow and Intrusive Rock Samples from the Vassan, Central, Southern and Val d'Or Domains	297
Appendix 3: Macroscopic and Microscopic Descriptions of Flow and Intrusive Rock Samples from the Vassan, Central, Southern and Val d'Or Domains	317
Appendix 4: Selected Major and Trace Element Analyses from Desrochers (1994) and the CIPW Norm of Mafic to Ultramafic Extrusive Flow Rocks from the Vassan, Central and Southern Domains	327
Appendix 5: Sampling Location Maps, Selected Major and Trace Element Analyses from Girault (1986) and Gaudreau et al. (1986), and the CIPW Norm for these Flow Rocks from the Val d'Or Domain	334

INTRODUCTION

This study concerns conceptual metallogenic modelling for the Abitibi terrane of the Val d'Or-east mining camp located in Bourlamaque and Louvicourt townships. The study area lies along the southern margin of the Abitibi greenstone belt and the northern margin of the Pontiac metasedimentary Subprovince.

The Abitibi subprovince is known for its abundant Archean volcanogenic and lode-gold mineralization. As shown by Spooner and Barrie (1993) for the Abitibi, volcanogenic massive sulphide production and reserves to 1989-1990 total approximately 424 million tonnes (at 4.4% Zn, 2.1% Cu, 0.1% Pb, 46 g/t Ag, \approx 1.3 g/t Au) and gold production and reserves for Abitibi gold deposits (as of January, 1990) totalled to be approximately 600 million tonnes at an average gold grade of approximately 8 g/t. For the Val d'Or district, volcanogenic massive sulphide production and reserves total approximately 44 million tonnes (\approx 740 000 metric tons of Cu and \approx 780 000 tonnes of Zn) (author's compilation from Couture, 1991, M.E.R.Q. microfiche deposit # 32C/4-77 and The Northern Miner, 1994). Gold production from 1941 to 1991 for the Val d'Or district is estimated to be approximately 195 million tonnes resulting in approximately 630 tonnes of gold (Dussault, 1992).

Located in the Abitibi greenstone belt, the Val d'Or mining district of Quebec has been known for its Archean mesothermal lode-gold deposits since their discovery in the

early 1900s (Lulin, 1990), and for its volcanogenic massive sulphide (VMS) deposits exemplified by several modest deposits mined from 1942 to 1981 and most recently by the major Louvicourt deposit discovered in 1989 (Bubar et al., 1989). Regional-scale studies by Norman (1941, 1942, 1943a, 1943b) and Gunning and Ambrose (1940) and more recently by Imreh (1976, 1984), Dimroth et al. (1982, 1983a, 1983b), Babineau (1985) and Desrochers et al. (1993) have examined closely the stratigraphic and structural evolution of sectors of the southeastern Abitibi greenstone belt which we find favourable for these types of deposits. The present study comprises a synthesis of these studies, complemented by additional geochemical analyses, with the intent to provide a global review of the development and evolution of these strata and structures, and to relate VMS and lode-gold mineralization to this geologic history.

Stimulated by high gold prices in the 1970s and 1980s, gold mining experienced a rebirth that continues to this day, and subsequently, a wealth of mine-scale studies has been published. During this same period, two VMS deposits in this mining camp have been documented (Spitz and Darling, 1973, 1975, 1978; Robert, 1980). Concurrently, research on detailed- to large-scale modelling of both VMS and mesothermal lode-gold deposits has made substantial advances. Thus, the principal purpose of this thesis has been to explain the occurrence of base-metal and gold mineralization in Bourlamaque and Louvicourt townships east of Val d'Or, based on the best-known geologic interpretations for the district and on the widely-accepted, large-scale models for Archean, VMS and mesothermal lode-gold deposits. The potential for other less important deposit types is

also discussed. The following is a brief outline of the thesis.

The section entitled "Regional Geology" contains a summary of Abitibi greenstone belt characteristics intended to provide the reader with the overall geological context of the study area. The section entitled "Local Geology" covers in detail the various explanations of the geological development of this area so that the reader has a clear understanding of the evolving lithotectonic interpretations of the study area. New geochemical data are presented and discussed for rocks from the study area and from the Val d'Or-west sector. VMS deposit mineralization follows, in which the known VMS deposits of the study area are discussed and the required "elements" of VMS formation are examined. Subsequently, possible modern analogues are discussed, followed by modelling of VMS formation for this camp.

With regard to the formation of lode-gold deposits, epithermal deposit mineralization is briefly addressed whereas a more lengthy description of the various mesothermal deposit models is given because of the mesothermal lode-gold mineralization well-known in the study area. From these models, processes are identified that best explain fluid formation, migration and gold deposition. In conclusion, the metallogenic evolution of the Bourlamaque and Louvicourt townships area is discussed as well as additional, recommended studies that may clarify specific problems and therefore, better explain the occurrence of Archean VMS and mesothermal lode-gold deposit types.

CHAPTER 1

REGIONAL AND LOCAL GEOLOGY

1.1 REGIONAL GEOLOGY

The following section presents descriptions of the two subprovinces the Abitibi and Pontiac terranes that comprise the study area.

The Abitibi Subprovince, composed mainly of volcanic and plutonic rocks with minor sedimentary units, (Fig. 1) (Card and Ciesielski, 1986; Card, 1990) is the largest (≈ 700 km x ≈ 200 km) volcano-plutonic belt of the Archean Superior Province. It is bound to the north by the predominantly metasedimentary River Nemiscau and River Opinaca subprovinces, to the south by the predominantly metasedimentary Pontiac Subprovince, and to the southwest it is unconformably overlain by Early Proterozoic sediments of the Huronian Supergroup and by Middle Proterozoic (Keweenawan) volcanics and sediments. The Abitibi belt is truncated to the east by the Proterozoic Grenville Front, to the west by the Kapuskasing Structural Zone (Percival, 1989; Geis et al., 1990), and to the northwest by metasedimentary schists and gneisses of the Opatoca Subprovince.

The Larder Lake Cadillac Tectonic Zone (LLCTZ; Robert, 1989), a 200-750 m-wide zone of high strain, marks the southern boundary of Abitibi greenstone belt with

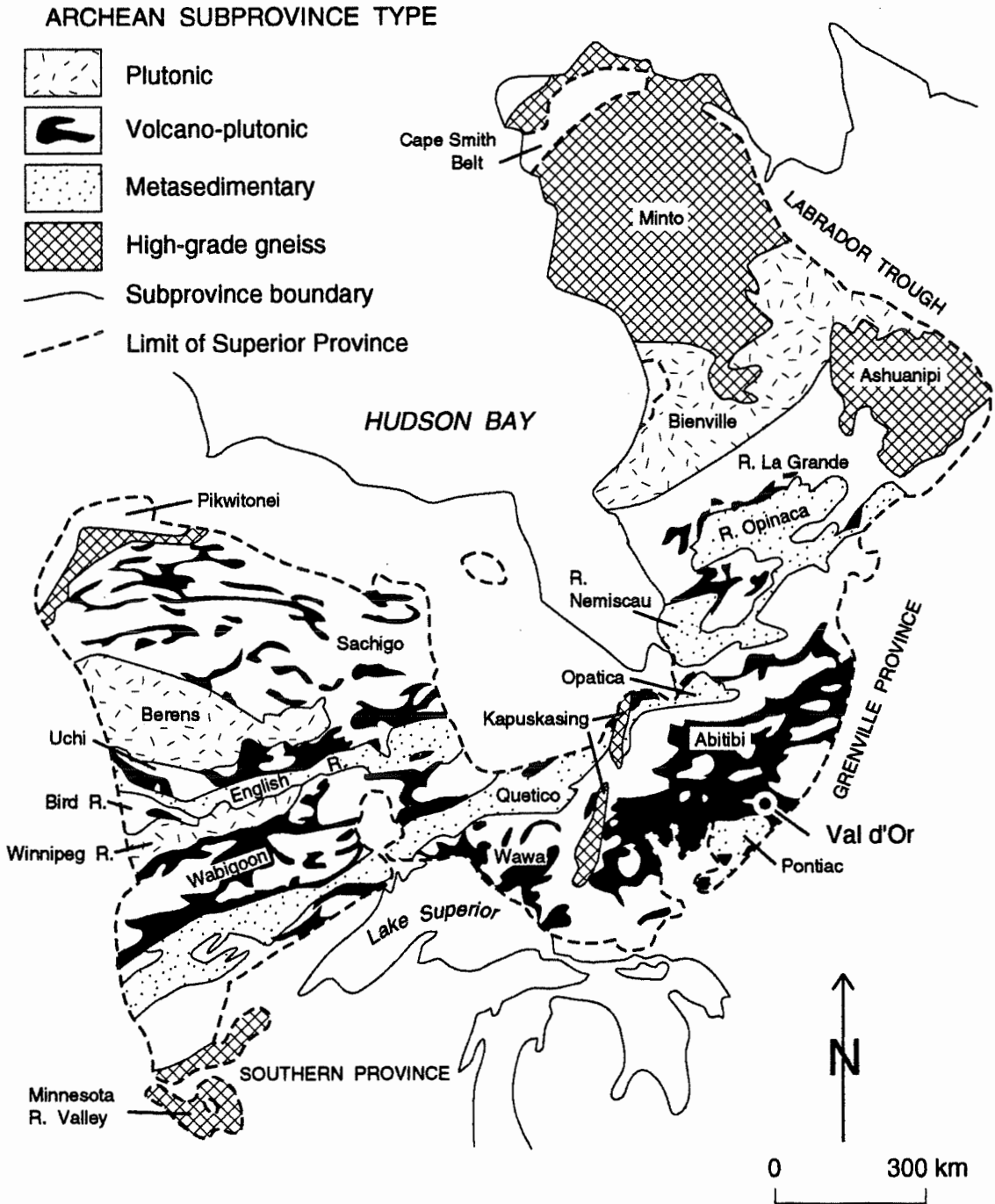


Figure 1. Subprovinces of the Superior Province (modified after Card, 1990).

the Pontiac Subprovince. The LLCTZ is well known for gold camps on its northern margin, i.e., within rocks on the Abitibi side of the tectonic zone, and it passes through the study area.

The Abitibi greenstone belt is characterized by an alternation of lozenge-shaped blocks (> 100 km E-W length, commonly 30-40 km N-S width; Hubert, 1990) of mafic to felsic volcanic rocks with intervening narrow linear belts of clastic sedimentary rocks generally striking northwest-southeast to east-west (Fig. 2). Whereas ultramafic flows are rare in the north, they are widespread and voluminous in the south. Intrusions vary from intermediate synvolcanic plutons and intermediate to mafic synvolcanic sills to syn- to post-tectonic felsic to mafic, commonly porphyritic stocks and dikes. More than 40 percent of the northern sector of the belt is underlain by large tonalite-trondhjemite-granodiorite plutons whereas less than 20 percent of the southern zone is underlain by such plutons (Dimroth et al., 1982).

The bedding and tectonic fabric of rocks in the southern Abitibi are generally moderately to steeply dipping (45° to 90°); shallow-dipping fabrics do occur, such as in the core of the Blake River Group in the Rouyn-Noranda district (Hubert et al., 1984). Folds are generally east/west-trending and upright. In the northern sector of the Abitibi belt, a major folding event formed a series of east/west-trending synclinoria in the supracrustal rocks between linear domes of synvolcanic plutons (Chown et al., 1992). The regional penetrative deformation of the Abitibi Subprovince is considered to have

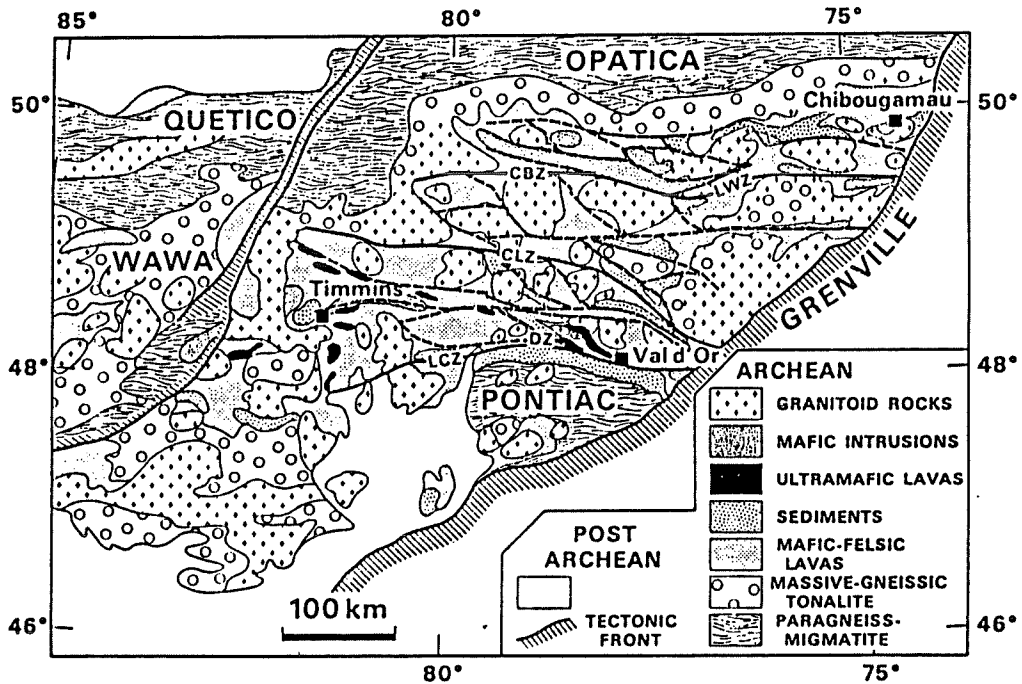


Figure 2. General map of the Abitibi Subprovince divided into lozenge-shaped blocks. CBZ = Casa Berardi Tectonic Zone, LWZ = Lac Waswanipi Tectonic Zone, CLZ = Chicobi Lake Tectonic Zone, DZ = Dumagami Tectonic Zone, LCZ = Larder Lake-Cadillac Tectonic Zone (from Hubert, 1990 as modified from Ludden and Hubert, 1986).

resulted from a north-south compressional event (Hubert, 1990).

Neighbouring "groups" (oldest terminology), "domains" or "assemblages" (current terminology) generally have mutual fault contacts or the contact relationship is unknown. Tectonic fabrics and mesoscopic features are increasingly recognized as domainal in distribution and type, and therefore, rigorous stratigraphic models are difficult to establish between domains (Jackson and Fyon, 1991; Desrochers et al., 1993).

The Abitibi Subprovince was subjected to a regional dynamic metamorphic event, except for late post-metamorphic granitic intrusions (Jolly, 1978). The majority of the subprovince rocks were metamorphosed to the greenschist facies, with local zones of prehnite-pumpellyite facies and lower amphibolite facies (Gunning and Ambrose, 1940; Jolly, 1978). Aureoles of amphibolite-grade contact metamorphism, commonly wider than 1 kilometre, are observed around late-tectonic granitic batholiths (Jolly, 1978; Imreh, 1984).

With the addition of precision age-dating in recent years, considerable improvement has been made to our understanding of Abitibi geology. Volcanic units and associated sedimentary assemblages in the northern Abitibi have ages ranging from approximately 2,730 to 2,711 Ma, with syntectonic plutons emplaced from approximately 2,703 to 2,690 Ma (Chown et al., 1992). In the southern part of the Abitibi, volcanic and associated sedimentary units and synvolcanic peridotitic to granodioritic intrusions

formed between approximately 2,750 and 2,700 Ma, with most assemblages being younger than 2,720 Ma (Corfu et al., 1989). North of the Porcupine-Destor deformation zone in Ontario, assemblages range in age from approximately less than 2,730 to 2,700 Ma whereas south of this deformation zone, many of the dated assemblages are younger than approximately 2,705 Ma (Jackson and Fyon, 1991). Regional folding in the southern Abitibi is estimated to have occurred from approximately 2,700 Ma to at least 2,686 Ma (Pilote et al., 1993), whereas regional greenschist metamorphism is estimated to have been active from $2,693 \pm 11$ to $2,684 \pm 7$ Ma (Wong et al., 1989, 1991; Hanes et al., 1989, 1992). Northeast-trending, Early Proterozoic tholeiitic dikes crosscut all lithologies and the dike swarm in the Senneterre district is dated at $2,214.3 \pm 12.4$ Ma (U-Pb, baddeleyite; Buchan et al., 1993).

Jackson and Fyon (1991) suggest from metamorphic, structural and geochronological data, that regional metamorphism of the southern Abitibi in Ontario pre-dated or shortly followed 2,690 Ma pre-Timiskaming deformation and emplacement of large granitoid complexes. Timiskaming assemblage rocks are, in part, younger than 2,680 Ma (Corfu et al., 1991) and are metamorphosed to the greenschist facies. Therefore, a second metamorphic event younger than 2,680 Ma is envisaged and is probably associated with post-Timiskaming deformation. Robert (1990a) notes also that for the Val d'Or district small syn- to late-tectonic porphyry intrusions which post-date regional tectonic and metamorphic events have greenschist-facies assemblages. Furthermore, a second metamorphism is observed to increase with depth in deep mines

such as in the Sigma mine of the Val d'Or mining camp (Robert and Brown, 1986a).

The locally-exposed, basal sequence of the Pontiac Subprovince is composed of komatiitic to basaltic volcanic rocks (Dimroth et al., 1982). A thick sequence (estimated to range from 2,200 metres (Holubec, 1972) to 1,000 metres (Dimroth et al., 1982) in thickness) of essentially greywacke and argillite, with rare occurrences of conglomerate and iron formation was deposited on the basal sequence. Dimroth et al. (1982) suggest that these sediments are distal submarine-fan deposits composed of Bouma-cycle sequences. The central to southern portion of the subprovince is characterized by late- to post-kinematic intrusions of granodiorite, monzonite and granite with carapaces of tonalite-granodiorite gneisses injected into the metasediments and/or ultramafic/mafic rocks (Hubert, 1990; Feng and Kerrich, 1992; Benn et al., 1992b). Deposition of sediments is bracketed between 2,695 and 2,686 Ma (Davis, 1991) whereas magmatism generally spanned 2,694 Ma to 2,645 Ma, with the youngest magmatic event in the Pontiac Subprovince dated at $2,632 \pm 3$ Ma (Machado et al., 1991; Feng and Kerrich, 1992).

The Pontiac rocks have been affected by two metamorphic events: 1) a greenschist-grade dynamic metamorphic event, and 2) a subsequent static metamorphic event. The effect of this second event is rapidly increasing metamorphic grade (greenschist- to amphibolite-facies) southward from the LLCTZ (Jolly, 1978; Imreh, 1984). The late- to post-kinematic intrusions did not create contact metamorphic

aureoles, probably because they intruded rocks that had already been metamorphosed to the amphibolite facies (Larouche, 1979).

1.2 LOCAL GEOLOGY

This section concerns the geology between the towns of Cadillac and Louvicourt. However, emphasis is given to the geology of the Val d'Or mining camp.

1.2.1 Historical Development

The Val d'Or mining camp is located in the southeast part of the Abitibi greenstone belt. The first stratigraphic nomenclature and structural interpretation encompassing this area was made by Gunning and Ambrose (1940) (Fig. 3). Based on field observations, they interpreted the stratigraphic sequence to form a synclinal fold, named the Malartic syncline, that was the major regional structure of the district. Despite questions raised by Norman (1941, 1942, 1943a, 1943b) on the validity of this regional structure as well as the stratigraphic correlations made by Gunning and Ambrose (1940), this original interpretation and nomenclature persisted without modification until the 1970s.

Only slight modifications were introduced to this first interpretation by Latulippe (1966, 1976). Although the regional synclinal structure was maintained, Latulippe (1976) demonstrated that the synclinal fold was not symmetrical and suggested a new

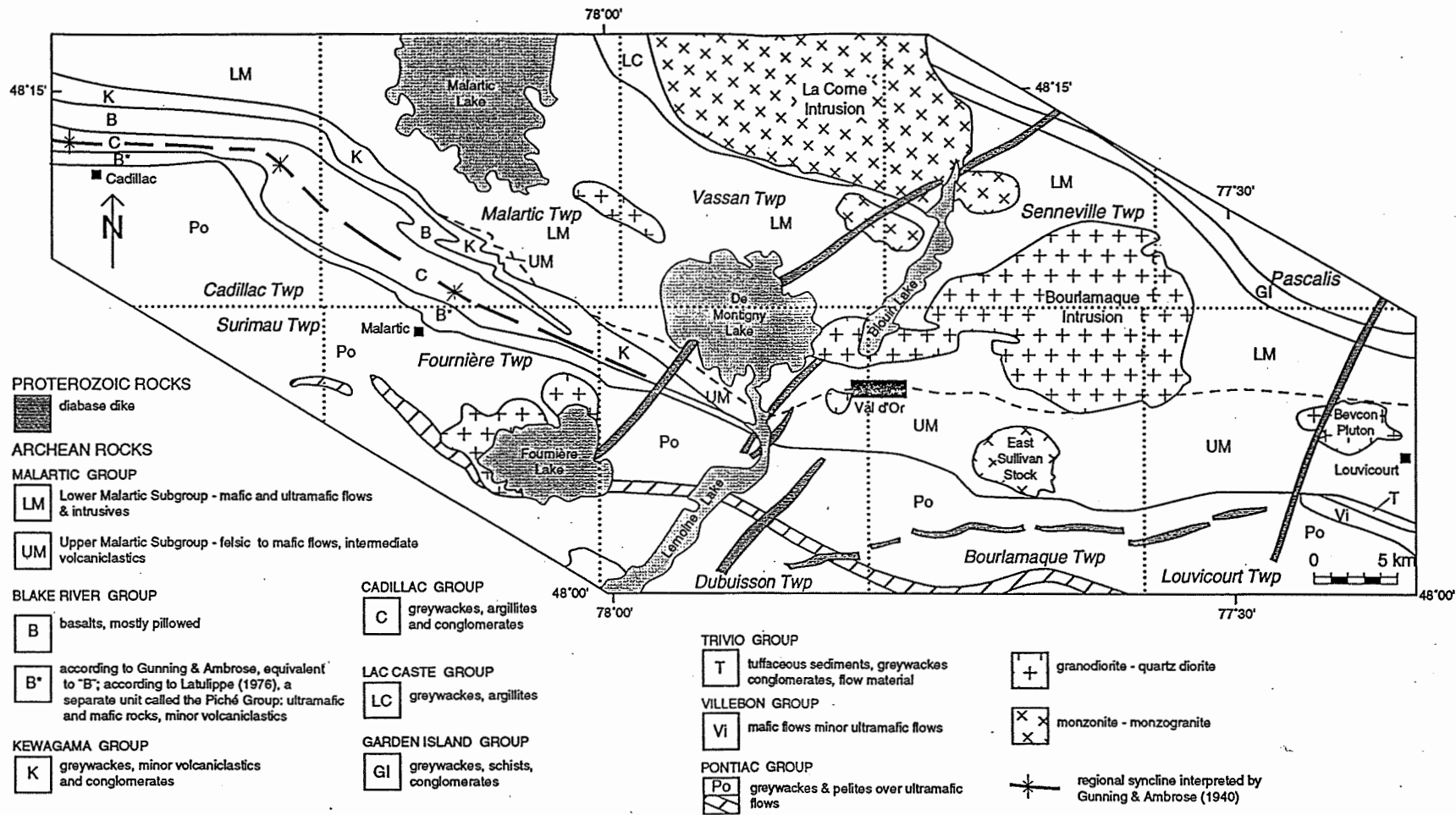


Figure 3. General geologic map of the Val d'Or region illustrating the regional syncline interpreted by Gunning and Ambrose (1940) and the division (broken line) of the Malartic Group into upper and lower subgroups (Latulippe 1976). The dotted lines represent township boundaries. The Bourlamaque and Louvicourt townships comprise the study area.

correlation of stratigraphic units between the northern and southern limbs of the fold. The changes included the correlation of the Malartic Group instead of the Blake River Group with the Piché Group and the division of the Malartic Group of Gunning and Ambrose (1940) into upper and lower sub-groups (Fig. 3).

A new interpretation of the lithostratigraphy and structure of the Val d'Or-Malartic area was made by Imreh (1976). By this time, it was recognized that a systematic revision was needed for the Val d'Or district because 1) the early maps were based on reconnaissance mapping, and 2) extrusive ultramafic rocks, an important rock type in this area, had been improperly mapped as intrusive bodies before the early 1970s. Imreh (1984) provides a new regional lithostratigraphic and structural interpretation which includes the Val d'Or district (Fig. 4). This report invokes an east/west-trending anticline, the La Motte-Vassan anticline, as the major regional structure whose southern flank is composed of the main lithologies defined by Gunning and Ambrose (1940) for the Malartic-Val d'Or districts. Imreh also divides the Malartic Group into five formations, based on geochemical and physiological characteristics of the rocks: the La Motte-Vassan, Dubuisson, Jacola, Val d'Or, and Héva formations. This synthesis of lithology, structure, and geochemistry enabled Imreh (1976, 1984) and co-workers (see Dimroth et al., 1982, 1983a, 1983b) to put forth a model for the geotectonic evolution of this area. In its simplest form, this model suggests that the rocks of the Val d'Or district were formed by deep-water, fissural-type volcanism upon which a central volcanic complex was formed as a product of crustal subduction.

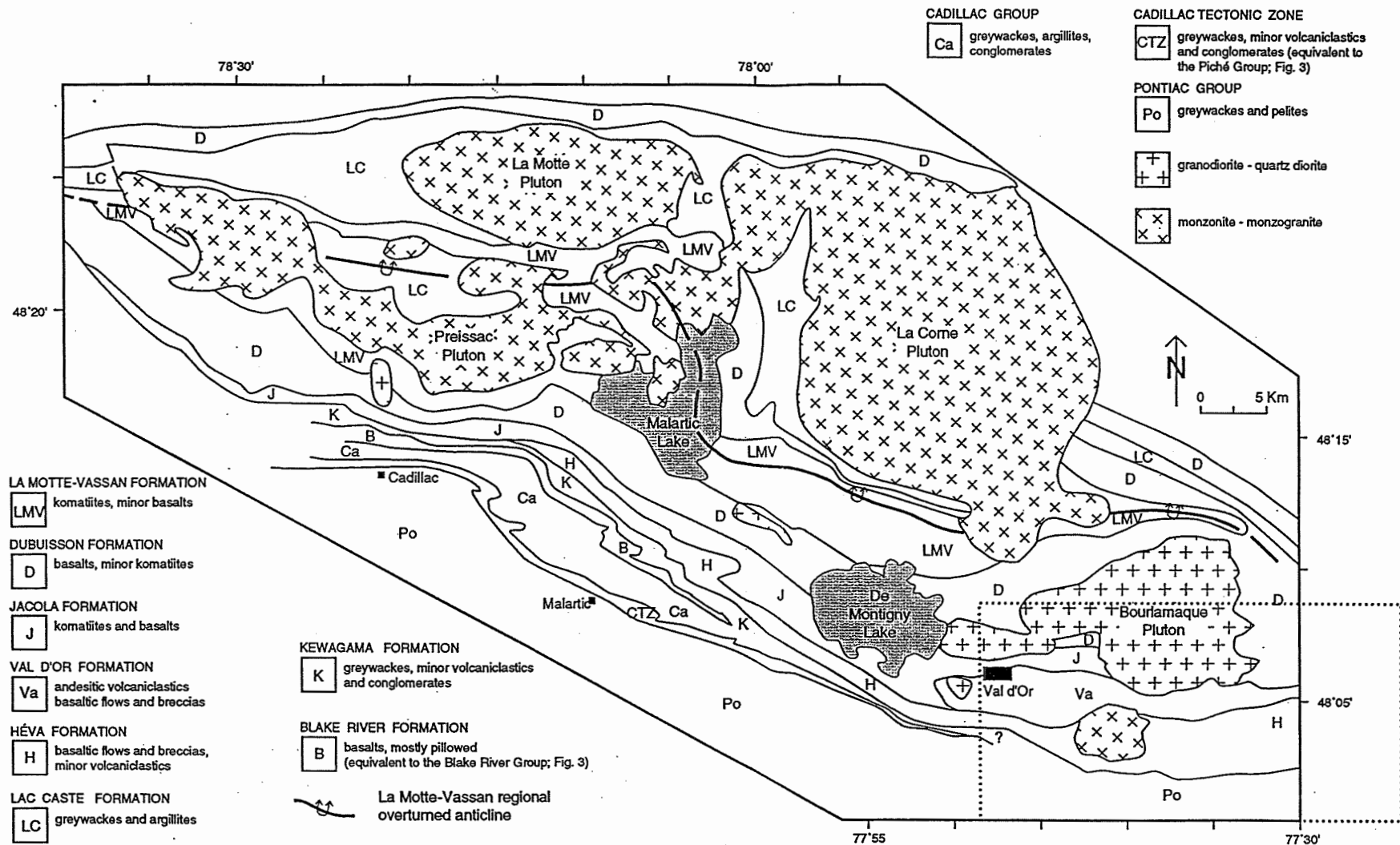


Figure 4. Geologic map of the Val d'Or region interpreted by Imreh (1984). The La Motte-Vassan overturned anticline is the dominant, regional structure and the Malaric Group as defined by Gunning and Ambrose (1940) and Latulippe (1966, 1976) is divided into the La Motte-Vassan, Dubuisson, Jacola, Val d'Or and Héva formations. The dotted line outlines the study area.

The structural and stratigraphic interpretations of this model have been debated extensively since their introduction to the geologic community. Structural analyses by Babineau (1985) show that the Malartic-La Motte district (west-northwest of Val d'Or) had a complicated structural story. This work shows that stratigraphic correlations are impossible between structural domains in the Lower Malartic Group, and questions the existence of a regional anticlinal structure where the stratigraphic section is composed of simple homoclinal sequences.

As field work progressed eastward from the town of Malartic to Val d'Or (Desrochers et al., 1993), the stratigraphic and structural interpretations of Imreh (1976, 1984) continued to be questioned. Babineau (1985) and Desrochers et al. (1993) identify distinctly new lithotectonic domains in the Malartic—Val d'Or district (Fig. 5), and Desrochers et al. (1993) suggest that the Malartic Group as used by Gunning and Ambrose (1940) and Latulippe (1966, 1976) consists of an amalgamation of fragments of oceanic plateau upon which was superimposed extension-related calc-alkalic volcanism (Figs. 6a and 6b).

In order to explain the various hypotheses of geodynamic evolution for the Val d'Or district used in this work, the stratigraphic units introduced by Gunning and Ambrose (1940) and their contemporaries are described below so that the various lithologies may be identified and geographically located. However, descriptions and discussions are also presented of the subsequent modifications made to unit divisions and

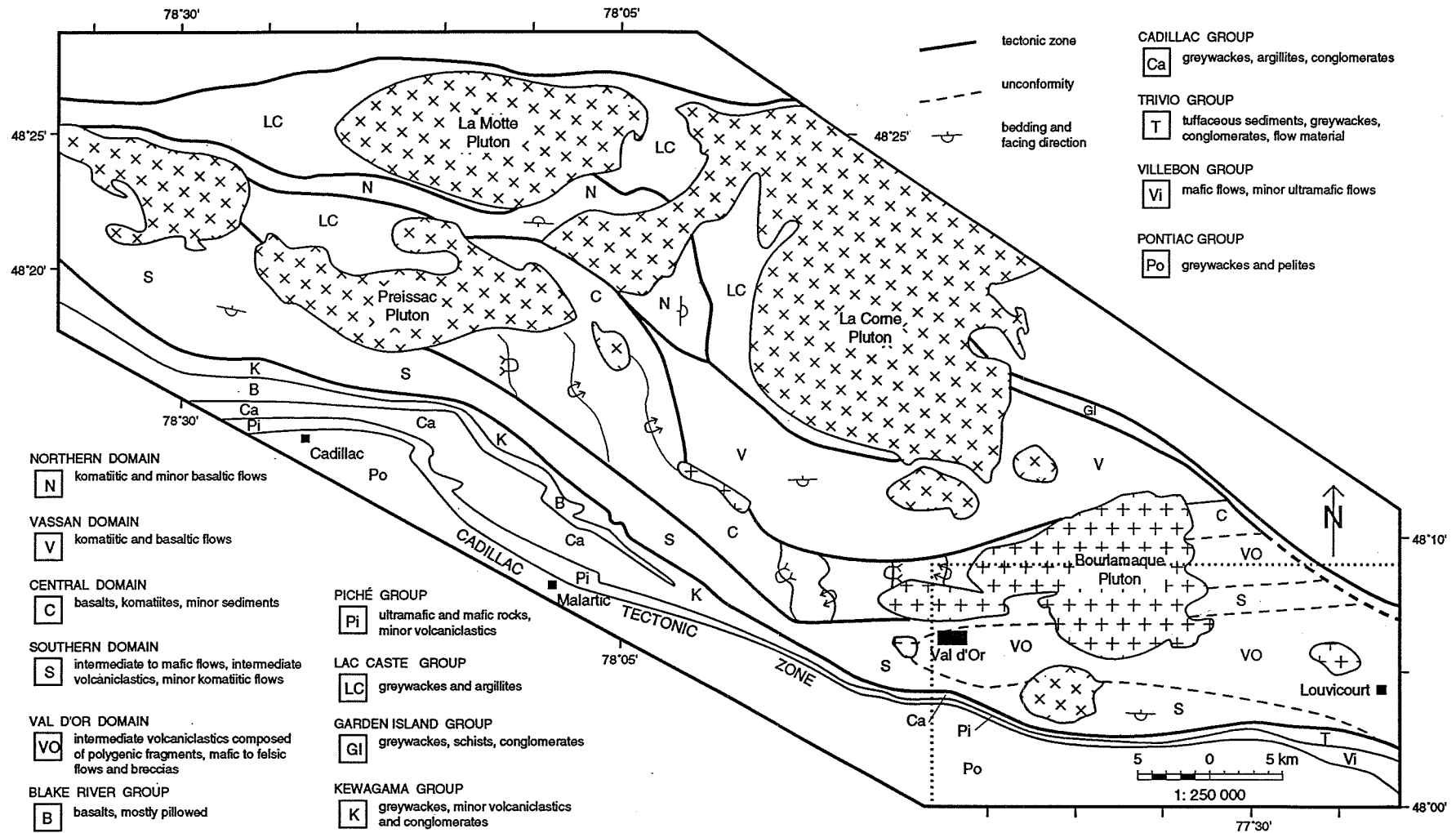


Figure 5. Tectonostratigraphic map of the Val d'Or region highlighting the five lithotectonic domains of the Malartic Composite Block (modified after Desrochers et al., 1993). The dotted line outlines the study area.

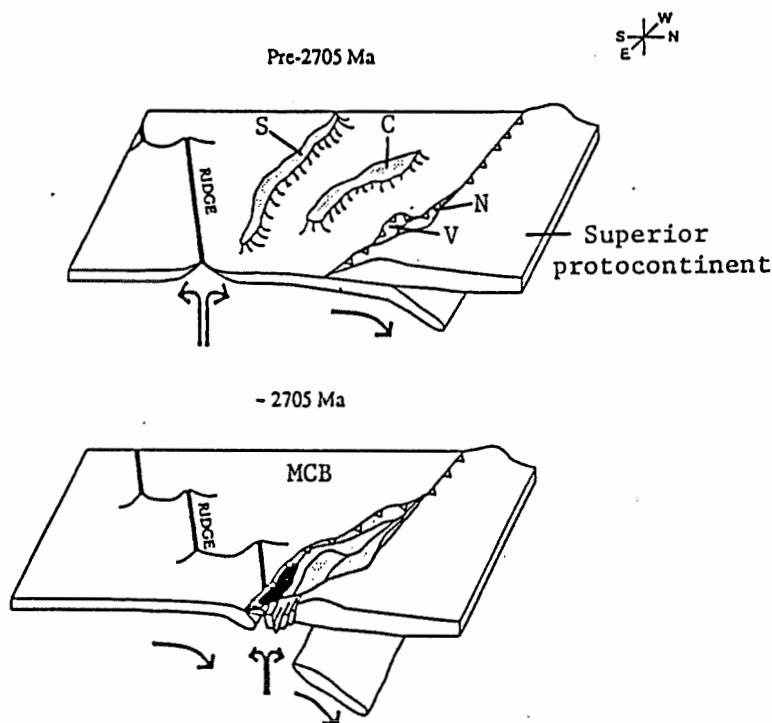


Figure 6a. Model for the formation of a Malartic Composite Block (shaded = MCB). Top: Progressive collage of oceanic plateaux (N = Northern, V = Vassan, C = Central, S = Southern domain) prior to 2,705 Ma on the Superior protocontinent. Bottom: Back-stepping of the subduction zone and ridge subduction resulting in calc-alkalic volcanism (Black = Val d'Or domain) on top of accreted plateaux at 2,705 Ma (modified after Desrochers et al., 1993).

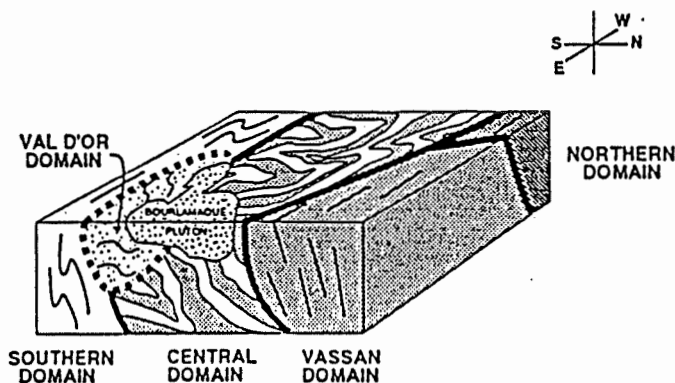


Figure 6b. Block diagram of assembled Malartic Composite Block. Thick lines represent fault zones bounding domains, dotted lines represent unconformities, and thin lines indicate bedding attitudes (from Desrochers et al., 1993).

of the consequential interpretations.

1.2.2 Group Descriptions (Figs. 3 and 4)

The **Lac Caste Group** is a lenticular unit of argillite and greywacke (Dimroth et al., 1982) transformed locally into staurolite-biotite schist and amphibolite indicative of amphibolite-facies metamorphism (Jolly, 1978). To the northwest of the study area, in Vassan Township, the group is composed essentially of greywacke. The primary bedding is strongly transposed, but where a few fold hinges are still identifiable, measured polarities indicate that stratigraphic tops are to the east (Desrochers and Hubert, 1991). It is possible that this group and the Garden Island Group (see below) to the east constitute a single sedimentary sequence that was truncated by the Lacorne batholith (Bell and Bell, 1931; Dimroth et al., 1982). $^{207}\text{Pb}/^{208}\text{Pb}$ minimum ages on detrital zircons from these sediments give an upper limit of 2691 ± 8 Ma for their deposition (Feng and Kerrich, 1991).

The **Garden Island Group** (Bell and Bell, 1931), located between the volcanic Malartic and Kinojevis groups, is composed of well-bedded greywacke, slaty schist, tuffaceous beds, local lenses of conglomerate and a few discrete beds of magnetite-facies iron formation (Sharpe, 1968; Marquis and Goulet, 1987). These sediments are thought to represent flysch-type sedimentation near an active volcanic centre (Marquis and Goulet, 1987). In Louvicourt Township, graded bedding in this unit indicates stratigraphic tops to the south (Sharpe, 1968), whereas in Pascalis Township (just north

of Louvicourt Township), south-southeast-trending beddings face northeast (Robert, 1990a). The important increase in exposed width of the Garden Island Group to the east from 750 metres to 6 kilometres is thought to be due to the repetition of lithologies in the hinge zone of a major antiform associated with Kenoran deformation (Marquis and Goulet, 1987). Because the contacts with the northern and southern volcanic units are sheared, the exact relationship of the sediments with the neighbouring volcanic rocks is unknown and the inferred antiform requires confirmation. Metamorphism increases to the south and east such that the greywacke becomes staurolite- and/or garnet-bearing micaschist (Marquis and Goulet, 1987). These sediments may be post-volcanic because the conglomerate lenses contain volcanic clasts in addition to granitic clasts. No geochronology has been done on these sediments to determine their absolute age.

The **Trivio Group** is composed of tuffaceous sediments, greywacke, arkose, graphitic phyllite, conglomerate, tuff, chert and lava (Sharpe, 1968). Marquis and Goulet (1987) identified magnetite-facies iron formation in the eastern part of the group, and correlated the Trivio and Garden Island groups, based on detailed structural and geophysical studies of the iron formation present in the two groups. To the west, the group is correlated to the Cadillac Group, based on similarities in composition and nature of sedimentary units from the Malartic and Louvicourt areas (Robert, 1989).

In the western half of Louvicourt Township, the LLCTZ marks the contact between the Trivio and Pontiac Groups (Sharpe, 1968; Robert, 1990a). This fault zone

is extended east to the south side of Lake Trivio located in the southeast quarter of Louvicourt Township, based on discontinuities in stratigraphy, metamorphism and structural style (Norman, 1945, 1947; Sharpe, 1968).

Gaudreau et al. (1986) and Marquis and Goulet (1987) observed several changes in facing directions and interpreted tight folds in the Trivio Group east of Louvicourt Township. Vogel (1972) also interpreted an important synclinal fold in this sedimentary unit in Villebon Township. Although no geochronology has been done on these sediments, sedimentation was probably partially contemporaneous with volcanism, as suggested by thin horizons of crystal and lapilli tuff (Gaudreau et al., 1986) with locally intercalated lava flows (Sharpe, 1968). If this group may be correlated with the Garden Island Group, the Garden Island Group may also be partially synchronous with volcanism, despite the lack of intercalated volcanic material.

The **Cadillac Group**, a thin unit east of Val d'Or, is nevertheless a regionally important sedimentary unit. It is composed essentially of greywacke and argillite with lenticular intercalations of polymictic conglomerate, tuff, volcanoclastic sandstone and iron formation (Gunning, 1937; Gunning and Ambrose, 1940). In the Bousquet region 40 kilometres west of Val d'Or, the group is composed of arkosic sandstone, mudstone, pebbly sandstone, immature volcanic-pebble conglomerate in a dark biotite matrix, polymictic conglomerate with feldspar porphyry and fuchsite-bearing pebbles, magnetite-facies iron formation, and rare beds of rhyolitic tuff (Gorman, 1986). Tuff intercalated

with Cadillac sediments probably indicates a distal volcanic event, presumably synchronous with the erosional event that produced Cadillac clastic units (Landry, 1991). Sandstone, siltstone, and mudstone together with minor amounts of conglomerate lenses and felsic dikes are the dominant Cadillac Group lithologies east of Val d'Or (Robert, 1989). The youngest detrital zircons from these sediments in the Val d'Or area indicate that the upper age limit on deposition is $2,688 \pm 3$ Ma (Davis, 1991).

On a local scale, zones of repetition of Cadillac and Piché lithologies have been recognized in drill core. However, contacts are generally sharp, range in dip from vertical to steeply dipping to the north. Gorman (1986) and Landry (1991) determined that the Cadillac Group overlies the Piché Group in the Bousquet region (see below).

The **Kewagama Group** is composed chiefly of greywacke, minor tuffaceous greywacke, and schist with minor amounts of conglomerate (Gunning and Ambrose, 1940). Despite generally sheared contacts between the Kewagama and Malartic groups (Babineau, 1985), a basal conglomerate, containing volcanic and intrusive clasts suggests that the Kewagama Group overlies the Malartic Group (Norman, 1942). East of Malartic, the Cadillac and Kewagama groups converge, and the nature of the contact between these two groups is unknown because of a lack of outcrop. However, U-Pb dating of detrital zircons indicate that the upper limit of deposition for both Kewagama and Cadillac sediments was approximately 2,688 Ma ago (Davis, 1991). Although Robert (1989) correlates the Cadillac Group sediments with Trivio Group sediments, it

is possible that Trivio sediments may be correlated with Kewagama sediments because of the uncertain relationship between the Cadillac and Kewagama groups and because both the Trivio and Kewagama groups border the southern edge of the Malartic Group. The upper age limit on deposition for the Kewagama sediments is $2,688 \pm 3$ Ma, i.e., equivalent to the age for Cadillac sediments.

The **Piché Group**, a long, narrow unit rarely measuring more than one kilometre in thickness, extends from Bousquet Township to Louvicourt Township over a distance of more than 70 kilometres. West of the town of Malartic, the group consists essentially of silicified mafic and intermediate volcanic rocks and of volcanoclastic rocks. East of Malartic, mafic and ultramafic lavas dominate with numerous intrusions of dioritic and syenitic dikes, sills, and plutons (Latulippe, 1976; Gorman, 1986; Sansfaçon, 1986). East of Val d'Or, the group is composed of a northern schistose unit derived from intermediate to felsic volcanoclastic rocks and a southern schistose unit derived in part from ultramafic flows, as indicated by locally preserved spinifex textures (Robert, 1989). The Piché Group is older than the overlying Cadillac sediments, as indicated by north-facing younging directions (Gorman, 1986; Landry, 1991). Some interflow sediments are preserved, suggesting that volcanism and sedimentation were in part contemporaneous (Gorman, 1986; Landry, 1991). Landry (1991) suggests that the Piché Group may overlie the Pontiac Group because 1) the younging directions in both groups are to the north, and 2) the sedimentary Pontiac and volcanic Piché rocks are interdigitated locally (Comline, 1979). Robert (1989) also observed repetitions of Piché and Pontiac rocks in

drill core from the Orenada mine area in Bourlamaque Township.

The Piché Group may be traced into the dominantly volcanic Villebon Group (see below) to the east, based on the composition and nature of the units and on additional information from a vertical gradient magnetic map (Geological Survey of Canada, 1981) and from drill cores (Robert, 1989).

For a good part of its length, the Piché Group hosts the LLCTZ. Deformation in the unit generally decreases westward. The heterogeneous nature of the deformation is exemplified by local domains of low strain. Two main foliations, S_1 and S_2 , are found within the LLCTZ (Robert, 1989). S_1 is the most penetrative, strikes east-west, dips steeply to the north, and is folded locally by asymmetric F_2 folds. S_2 is a spaced crenulation foliation of S_1 . Robert (1989) interprets the LLCTZ as a zone of dextral transpression composed of a significant shortening component and a transcurrent shearing component.

The **Villebon Group** outcrops largely in Villebon Township southeast of Louvicourt Township. The mafic and minor ultramafic volcanic flows which characterize this unit are locally strongly epidotized and serpentized and/or amphibolitized. A large anticlinal structure, in which the Villebon Group occupies the centre, suggests that the Villebon Group is older than the Pontiac Group (Vogel, 1972). However, contacts with the Trivio and Pontiac groups are strongly sheared such that the

true stratigraphic relation between these units is uncertain.

The **Pontiac Group** consists mainly of metamorphosed greywacke and mudstone (transformed to quartz-biotite schist) and isolated lenticular horizons of conglomerate (Sharpe, 1968; Rocheleau et al., 1990). Mafic tuff and black shale containing trace amounts of sphalerite, chalcopyrite and pyrrhotite are intercalated locally with the terrigenous sediments (Sansfaçon, 1986). Sedimentary structures and bed thicknesses suggest that the greywacke and mudstone are turbidites (Lajoie and Ludden, 1984; Sansfaçon, 1986). Thin units of ultramafic and mafic rocks (mostly extrusive flow rocks) outcrop locally and are the basement rocks for the sediments. Sedimentary and structural measurements indicate that stratigraphic tops are to the north (Robert, 1990a). An F_1 folding event formed a system of south-verging recumbent folds in these metasedimentary rocks (Dimroth et al., 1983b) and an F_2 folding event formed north/south-oriented recumbent folds that are west-verging (Hubert, 1990). In the Val d'Or area, the youngest detrital zircons from Pontiac sediments show that the upper age limit on deposition for these sediments is $2,686 \pm 3$ Ma (Davis, 1991).

The **Blake River Group** west of the study area apparently represents the eastern attenuation of an extensive, volcanic unit of the Rouyn-Noranda region to the west (Péloquin et al., 1990). Correlation of this narrow belt of rocks with the voluminous unit to the west is historical and may not be factual. In the Val d'Or-west area, the group is composed of mafic to felsic volcanic and volcanoclastic rocks with associated

diorite dikes. Minor amounts of greywacke and conglomerate are also present.

The **Malartic Group** (Gunning and Ambrose, 1940) is a regionally important lithological unit consisting of a wide variety of volcanic and plutonic rocks. The lozenge-shaped group is bounded on all sides by relatively narrow, metasedimentary groups (Lac Caste, Garden Island, Trivio, and Kewagama) interpreted to have been deposited as turbidity-current sediments (Lajoie and Ludden, 1984). The presence of interdigitated tuffs with the sedimentary rocks suggests that volcanism persisted during collisions between sub-province terranes, resulting in periodically emergent regions subject to erosion.

Latulippe (1966, 1976) divided the Malartic Group into upper and lower sub-groups, based on the predominant rock types characterizing each sub-group, and supported by distinctive petrological and geochemical differences (Alsac, 1977; Alsac and Latulippe, 1979). The **Lower Malartic Group** is composed dominantly of komatiitic and basaltic volcanic rocks and their intrusive counterparts. Rocks of this sub-group have komatiitic and tholeiitic geochemical signatures and have a tendency to be depleted in potassium. In contrast, the **Upper Malartic Group** is composed of relatively abundant intermediate volcanoclastic rocks, intercalated with mafic to felsic volcanic rocks and intruded by synvolcanic mafic to intermediate sills. Two rhyolitic units, representing the last major volcanic event of the Upper Malartic Group, have been dated at $2,705 \pm 1$ and $2,706 \pm 3$ Ma (U-Pb analyses of zircon; Wong et al., 1991; Pilote et al.,

1993). A portion of the Upper Malartic Group characterized by relatively abundant volcanoclastic material was named "the Central Pyroclastic Belt" by Sharpe (1968). The rocks of this sub-group have calc-alkalic and tholeiitic signatures, and they too have low potassium contents.

1.2.3 Structure

Lithological contacts in the Malartic Group are generally subvertical and strike northwest-southeast to east-west. Most rocks exhibit a weak to moderate foliation running parallel to lithological units. Younging directions are dominantly to the south, and the group has long been considered a south-facing homoclinal sequence. East of Val d'Or, the structural trend runs east-west to eastnortheast-westnorthwest, whereas west of Val d'Or, the structural grain is northwest-southeast and two superimposed generations of folds have been identified in the Malartic Group, as in the Kewagama and Cadillac groups (Bouchard, 1979, 1980; Babineau, 1985; Tourigny, 1984). Abundant shear zones of various dimensions are characteristic of the district. The strikes of shears generally lie parallel to the local structural trend and their dips are generally steep. The most prominent example is the LLCTZ (Robert, 1989).

1.2.4 Metamorphism

The metamorphic history of the rocks in the Val d'Or area is complex. Whereas most rocks are metamorphosed to the greenschist facies due to a regional dynamic metamorphic event, there are small syn- to late-tectonic feldspar porphyritic intrusions

post-dating regional deformation and regional dynamic metamorphism. These intrusions have also been metamorphosed to the greenschist facies (Robert, 1990a), suggesting a second metamorphic event. This metamorphic overprint increases in grade with depth (Robert and Brown, 1986a; Grant, 1986; Morasse et al., 1993). Although attempts have been made to date regional greenschist metamorphism, the age of this metamorphism is not well constrained; ages vary from $2,684 \pm 7$ Ma (U/Pb technique on metamorphic rutile; Wong et al., 1991) to $2,693 \pm 10$ Ma (Ar/Ar technique on metamorphic magnesio-hornblende; Hanes et al., 1992). Robert (1991a) interprets the older age to represent greenschist-facies dynamic metamorphism which accompanied deformation, and the younger age to represent a possible thermal, middle greenschist-facies metamorphism.

1.2.5 Major Intrusions

The Bourlamaque pluton is an aerielly extensive (≈ 170 km²) body which intruded the Malartic Group (Campiglio and Darling, 1976; Campiglio, 1977). The pluton is dioritic in composition, has a calc-alkalic signature like some rocks of the Upper Malartic Group, and is considered to be a pre-tectonic intrusion, lacking a contact metamorphic aureole and displaying a weakly developed regional foliation. Geochronology places its age at $2,699.8 \pm 1.0$ Ma (U-Pb/zircon) (Wong et al., 1991), and therefore, regional deformation has an upper age limit of approximately 2,700 Ma. Post-folding intrusions range in age from $2,694 \pm 2$ Ma (U-Pb/zircon) for feldspar porphyry dikes at the Sigma mine (Wong et al., 1991) to $2,685 \pm 3$ Ma (U-Pb/zircon) for a Lamaque plug (Jemielita et al., 1989), and 2,680-2,685 Ma (U-Pb/zircon and titanite) for the Camflo stock

(Zweng and Mortensen, 1989; Jemielita et al., 1989; Zweng et al., 1993). These ages bracket regional deformation between 2,700 and 2,694 Ma. However, it should be noted that the Kewagama and Cadillac sediments which have an upper age limit of deposition of approximately 2,688 Ma are also deformed, indicating that either the regional D₂ deformation actually lasted to at least 2,688 Ma or a later second pulse of regional deformation occurred.

The other significant intrusions of the district are the granodioritic Bevcon pluton (considered to be pre- to syn-tectonic; Sauv   et al., 1993) and the monzonitic East Sullivan stock (Taner, 1986) and the reversely graded, gabbro to leucomonzogranite Lacorne batholith (Bourne and Danis, 1987), both characterized by a contact metamorphic aureole and considered to be post-tectonic. The Lacorne batholith has a ²⁰⁷Pb/²⁰⁶Pb minimum age of 2,675 ± 24 Ma (Feng and Kerrich, 1991).

1.2.6 Interpretations of Local Geology

Several authors have contributed to the understanding of the local geology, and the following is a summary of the evolution of their interpretations.

As noted above, Gunning and Ambrose (1940) interpreted a regional isoclinal syncline, called the Malartic syncline, passing through the centre of the Cadillac Group in Cadillac and Malartic townships and continuing along the contact between the Pich  

and Cadillac/Kewagama groups in Fournière and Dubuisson townships west of Val d'Or (Fig. 3). On the north limb of the fold, the Cadillac sediments overlie successively the Blake River, Kewagama and Malartic groups. On the south limb of the fold, the Cadillac Group overlies successively highly-faulted volcanics assumed to be part of the Blake River Group and the sedimentary rocks of the Pontiac Group. The Blake River Group was correlated with intensely-deformed volcanic strata now known as the Piché Group (Latulippe, 1976), and the Kewagama Group was correlated with the Pontiac Group.

However, Norman (1941, 1942, 1943a, 1943b) argued against the existence of this regional synclinal structure. Norman doubted that the groups were conformable, noting, for example, that the contacts between the Blake River and Kewagama groups were sheared, perhaps as a result of faulting. He recognized the lack of symmetry of the fold, and questioned whether sufficient evidence was available to support the correlation of the highly-faulted Piché Group with the Blake River Group.

Despite objections to the existence of this regional fold, the stratigraphic and structural interpretations by Gunning and Ambrose (1940) persisted until the 1970s when Latulippe (1976) divided the Malartic Group into lower and upper subgroups, based on predominant rock types and petrological and geochemical characteristics. Like Norman, Latulippe also recognized that the Malartic syncline was asymmetric but he supported the existence of a regional fold. Unlike Gunning and Ambrose (1940), Latulippe correlated

the Piché Group with the Malartic Group.

Imreh (1976, 1984) brought forth a new model, envisaging a major regional structure, the La Motte-Vassan anticline (Fig. 4) which diminished the importance of the Malartic syncline as a regional feature. According to Imreh, the fold axis of the La Motte-Vassan anticline runs in a more or less east-west direction through the lowermost part of the Lower Malartic Group. The southern limb of the anticline is regarded as a south-facing, homoclinal sequence. Imreh (1976, 1984) also divided the Malartic Group into five lithostratigraphic formations based on physical and geochemical characteristics. The divisions, from north to south are, the La Motte-Vassan, Dubuisson, Jacola, Val d'Or and Héva formations (Fig. 4).

The **La Motte-Vassan Formation** is composed essentially of ultramafic, komatiitic flows with rare intercalations of tholeiitic basalt. In contrast, the **Dubuisson Formation** is composed mostly of tholeiitic basalt flows with minor komatiitic intercalations.

The **Jacola Formation** is characterized by an assemblage of, from bottom to top, komatiite, basalt, and various types of basaltic breccia. Where the sequence is incomplete, it is commonly the ultramafic section which is missing. The upper one-third of the formation is considered the lateral equivalent of the Val d'Or Formation in and east of the town of Val d'Or.

The **Val d'Or Formation** is composed of basaltic flows and flow breccias with important intercalations of andesitic volcanoclastic rocks. The rocks of this formation are characterized by a calc-alkalic nature.

The **Héva Formation** overlies both the Jacola and Val d'Or formations. Imreh (1984) informally subdivides the Héva Formation into lower and upper units. Between Lake Malartic and Val d'Or, the lower Héva Formation is composed of a basal basalt covered by vesicular pillow basalt and lateral and vertical facies of volcanoclastic material. A strong iron-enrichment trend on an AFM diagram characterizes the pillowed basalts of this unit (Imreh, 1984). West of Val d'Or, the lower Héva Formation is principally andesitic with basaltic facies. Flow breccia is by far the most prominent facies. A few pyroclastic lenses of decametre to kilometre scales are also present. East of Val d'Or, mafic volcanics continue and are grouped with the upper Héva Formation. Brecciated facies are more common than massive flows, and pillowed flows are subordinate. Primary magnetite characterizes the brecciated and massive flows. Minor, local intercalations of andesitic volcanoclastics are also present; this volcanism has a predominantly calc-alkalic signature.

Based on the physical and chemical characteristics of the five formations, Imreh (1984) and others (see, for example, Dimroth et al., 1982, 1983a, 1983b) modelled the paleovolcanic evolution of this area in terms of modern volcanism as follows:

The La Motte-Vassan and Dubuisson formations, having komatiitic and tholeiitic signatures, were the products of fissural-type volcanism. This abyssal-plain, deep-water volcanism was characterized by a lack of vesicularity and interpillow hyaloclastic material and by the absence of cracked or broken pillows.

After abyssal plain volcanism, transitional fissure-type volcanism of the Val d'Or central volcanic complex produced the Jacola Formation with its mafic and ultramafic volcanics. The limited regional dimensions of this formation, the tendency toward bifurcating units, and the limited lateral extension of the Jacola flows suggest that the paleoenvironment was that of an island arc.

The transitional-type volcanism of the Jacola Formation evolved laterally to the east (Val d'Or Formation) and to the south (Héva Formation) to volcanism typical of central complexes. The Val d'Or and Héva formations, typical of this volcanism, are composed of volcanoclastic rocks and felsic- to intermediate-type vesicular flows. The lithogeochemical evolution is seen to mature from west to east as the magmatism changes from tholeiitic, to tholeiitic and calc-alkalic, to calc-alkalic compositions. This chemical evolution is thought to confirm and complete the physical evolution of an island arc.

The structural interpretation of this regional anticline was not widely accepted. The most convincing evidence against such a structure, as well as the stratigraphic

continuity of the formations is the structural analysis in the La Motte region (northwest of Val d'Or) by Babineau (1985) in which three distinct structural domains were identified without the possibility of stratigraphic correlations between domains.

The major-element AFM subdivisions (Irvine and Baragar, 1971) used by Imreh are probably insufficient alone to classify the volcanic stratigraphy, given the intense alterations (i.e., seawater alteration, hydrothermal alteration, metamorphism(s), metasomatism) that have affected most rocks in the Val d'Or district. Trace and rare-earth element data may be helpful to more reliably characterize rock units because of their relative immobilities during alteration (Condie, 1976; Ludden et al., 1982). See Chapter 2 for geochemical data and interpretations of rocks in the study area.

Despite the dubious existence of the La Motte-Vassan anticline, the formational divisions of Imreh (1984) continue to be used albeit with certain inconsistencies. For example, Gaudreau et al. (1986), who mapped and geochemically analyzed (for major and selected trace elements) rocks in the eastern half of Louvicourt Township and in the neighbouring Vauquelin Township, continue to use Imreh's subunits, but the widths of the Val d'Or and Héva Formations do not match the formational limits defined by Imreh (1990) for the western sector of Louvicourt Township.

Desrochers et al. (1993) have recently proposed a new geotectonic model for the Val d'Or-Malartic district. Their interpretations of the terrane between the towns of

Malartic and Val d'Or also identify other structural domains besides those defined by Babineau (1985) in the La Motte region. In brief, the rocks belonging to the Malartic Group have been divided into five tectonostratigraphic domains (the Northern, Vassan, Central, Southern and Val d'Or domains; Fig. 5) which constitute a Malartic Composite Block (MCB) (Desrochers et al., 1993). According to these authors, the Northern, Vassan, Central and Southern domains represent the amalgamation of allochthonous oceanic fragments between which no stratigraphic relationships may be established due to faulting along domain boundaries (Figs. 6a and 6b). The Val d'Or domain would represent autochthonously superimposed extension-related calc-alkalic volcanism resulting from the subduction of an oceanic ridge. This scenario is analogous to Phanerozoic models (Skulski et al., 1991; Babcock et al., 1992) applied to parts of the west coast of North America where extension-related volcanic centers are interpreted to overlie accreted exotic terranes. The following domain descriptions and interpretations are taken from Desrochers et al. (1993).

The **Northern domain** consists of subvertical east/west- to north/south-striking komatiitic flows and minor basalts with younging directions to the north and to the east, respectively. Two subparallel east/west-trending penetrative foliations are developed here, one dipping moderately to steeply to the south (S_1) and one inclined vertically (S_2).

The **Vassan domain** is also a steeply dipping east-west homoclinal sequence, but its younging directions are to the south. It is composed of extensive komatiitic flows

with some intercalations of basalt and komatiitic basalt, overlain by basaltic flows with minor komatiitic intercalations. This domain displays tectonic features similar to those of the Northern domain, and due to their lithological similarities, both domains may have been part of one stratigraphic succession which was disrupted during the tectonic assembly of the MCB.

The **Central domain** consists of basaltic, komatiitic, and thin terrigenous sedimentary layers. These rocks are folded about northwest/southeast-trending D_1 fold traces and are refolded by east/west-trending D_2 folds (Babineau, 1985). The D_1 axial planes are inclined variably to the northeast or to the southwest, whereas the D_2 folds are upright. A penetrative schistosity developed during D_1 and was reoriented by an east-west crenulation cleavage associated with D_2 . The resulting superimposed fold pattern is truncated by the fault contacts with the adjacent Northern, Vassan and Southern domains. Since northwest/southeast-trending D_1 folds are restricted to this domain and are truncated at its boundaries, the D_1 event must have taken place prior to the amalgamation of the Central domain with the neighbouring Northern, Vassan and Southern domains.

The **Southern domain** is a south-facing homoclinal sequence composed of overturned, steeply north-dipping, east/west- to northwest/southeast-trending strata. The domain consists of basaltic flows and intermediate volcanoclastic intercalations with minor komatiitic flows, deformed into a series of asymmetric Z-shaped folds plunging steeply

to the east. The D_1 event overturned the strata which were subsequently overprinted by an east-west cleavage (S_2) axial to the Z-shaped folds.

The **Val d'Or domain** is composed of basaltic to dacitic flows and volcanoclastic sequences trending northeast-southwest in the western part (Desrochers et al., 1991) and northwest-southeast in the eastern part (Chartrand, 1991). The main schistosity varies from $N250^\circ$ to $N280^\circ$ and transposes the lithological contacts into a series of S-shaped folds in the west and into Z-shaped folds in the east. The Bourlamaque pluton and the volcanic rocks of the Val d'Or domain clearly truncate D_1 structures of the Central and Southern domains. Therefore, the rocks of the Val d'Or domain must have been emplaced after the D_1 event recorded in the other four domains.

According to Desrochers et al. (1993), the Northern, Vassan, Central and Southern domains form an amalgamated terrane that have each been affected by a D_1 deformation event recorded in each domain. This observation would suggest that the domains were once separate undeformed entities, and that during their juxtaposition, they developed D_1 fabrics which are variably oriented for each domain as a result of the direction of collision of each domain. D_1 deformation is not recognized in the Val d'Or domain. A predominant east-west foliation is present in the rocks of all five domains, and represents a D_2 deformational event post-dating the amalgamation of the MCB, and the calc-alkalic volcanism represented by the Val d'Or domain. Thus, the Val d'Or domain volcanic rocks and the contemporaneous Bourlamaque pluton (see sections 2.2

and 2.3.3.2) are thought to have been emplaced after the D_1 tectonic assembling event, and presumably to have been erupted through the accreted mafic-ultramafic domains creating an unconformity. The composition of the calc-alkalic volcanics suggests an origin as a result of a rift subducted beneath the amalgamated (Northern, Vassan, Central and Southern domains) terrane (Figs. 6a and 6b).

The geotectonic model of Desrochers et al. (1993) for the Malartic-Val d'Or district offers a plausible and attractive explanation of the stratigraphic and structural evolution of this region. However, it is not yet clear that the Southern and Val d'Or domains can be extrapolated east of Val d'Or, i.e., into the Bourlamaque and Louvicourt townships covered in the present study. For example, the terrane east of the town of Val d'Or defined by Desrochers et al. (1993) as Southern domain equivalent may be composed of another domain or even several domains. Another example of the fine tuning that needs to be made to this model concerns the interpretation of the Val d'Or domain boundary between the Bourlamaque pluton and the metasedimentary Garden Island Group. Field maps of Imreh (1990), Sharpe (1968), Gaudreau et al. (1986) and a M.E.R.Q. compilation map (Gaucher and associates, 1982) do not indicate abundant pyroclastic material, the criterion used by Desrochers (pers. commun., 1993) to define this portion of the Val d'Or domain.

Thirdly, the southern limit of the Val d'Or domain follows in part the limit between the Val d'Or and Héva formations as defined by Imreh (1990) and in part a Val

d'Or—Héva limit at a higher stratigraphic position as defined by Gaudreau et al. (1986). Also, the structural differences suggested by Desrochers et al. (1993) between Val d'Or domain rocks and Southern domain rocks have not been confirmed south of the Bourlamaque pluton. The southern boundary of the Val d'Or domain will be better defined when those structural criteria applied west of Val d'Or are also extended eastward.

Fourthly, another example of fine tuning is underlined by a geochemical study by Hébert et al. (1991). This study shows that the Vicour sill is differentiated and of tholeiitic affinity within the Val d'Or Formation (itself calc-alkalic, and therefore considered to be Val d'Or domain equivalent), and may be comagmatic with the tholeiitic volcanic rocks of the overlying Héva Formation. If the eastern extension of the Southern domain is essentially equivalent to the Héva Formation as defined by Imreh (1984) and Gaudreau et al. (1986), it is difficult to explain the chemical affinity between two rock suites proposed to have had different geotectonic origins.

The present author also suggests that subduction of an oceanic ridge may not be necessary to explain the Val d'Or domain volcanism. Normal subduction of young, hot oceanic crust under the amalgamated fragments of oceanic plateau accreted to a Superior protcontinent could also have caused melting of the mantle wedge and the amalgamated domains and formation of overlying calc-alkalic volcanic complexes. This simpler (hence possibly more plausible) scenario may be similar to the modern geotectonic settings of

the Indonesian region (Fig. 7) where numerous microplate interactions are taking place (Karig, 1970, 1971, 1972, 1974; Hamilton, 1979, 1988; Honza, 1991).

Despite the need for fine-tuning, the Desrochers et al. (1993) model clearly provides an attractive alternative to previous models invoking a regional syncline (Gunning and Ambrose, 1940; Latulippe, 1976) or a regional anticline (Imreh, 1976, 1984). In addition to its explanation of discordant structural styles, it incorporates many modern ideas on oceanic plate accretion found along the west coast of North America as well as in present-day situations (such as in the Indonesian region). Also, it offers a good working hypothesis for the formation of other major tracts of the Abitibi greenstone belt, including the field area of the present study.

The emplacement of the MCB is consistent with an evolutionary model suggested for the southern Abitibi greenstone belt by Jackson and Fyon (1991). Their compilation of information on environments of formation for assemblages in the western Abitibi suggest (1) that similar tectonic processes operated at different times, based on the repetition of assemblages with similar rock associations at different times, and (2) that different tectonic processes operated at the same time, based on the juxtaposition of coeval assemblages that are different in terms of lithologic associations. Jackson and Fyon (1991; page 470) note that in the Indonesian region (Fig. 7), "island-arc assemblages are being produced above subduction zones while oceanic crust is being generated at spreading centres. Some volcanism is being superimposed on both older

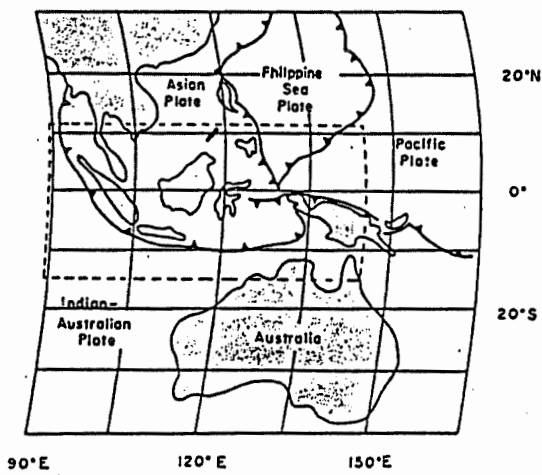
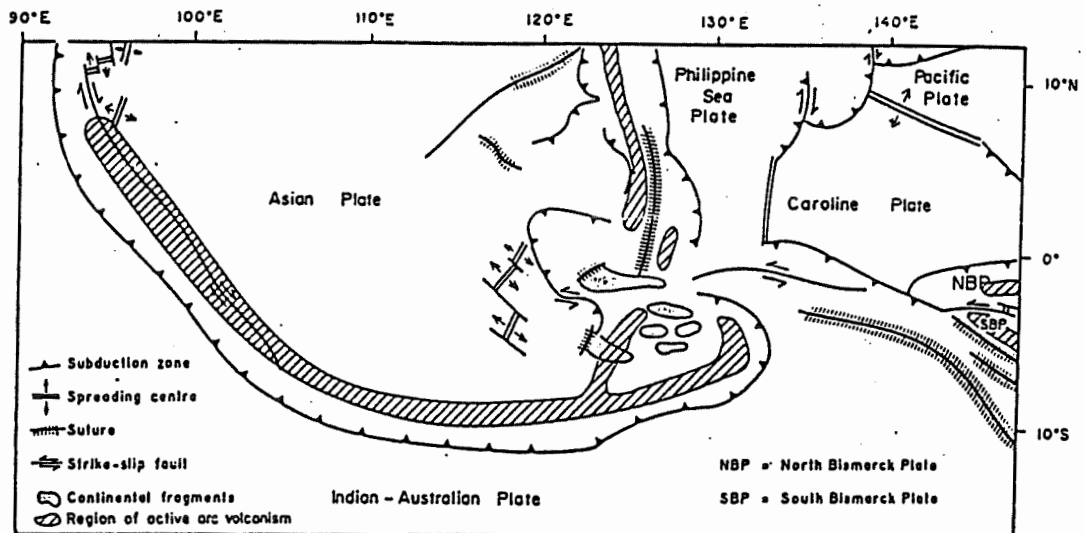


Figure 7. Schematic diagram of the tectonic interplay in the Indonesian region (from Jackson and Fyon, 1991 as modified from Hamilton, 1988).

continental fragments and on previously collided (sutured) island-arc complexes." They consider that this region, displaying numerous diverse microplate interactions, is a potential analogue for the southern Abitibi greenstone belt. They propose that the southern Abitibi microplate interaction occurred between two large converging bodies, the 2.8-3.5 Ga Minnesota River Valley gneiss terrane to the south (Sims et al., 1980) and the Uchi Subprovince (Stott and Corfu, 1991; Corfu and Stott, 1993) and previously accreted material to the north.

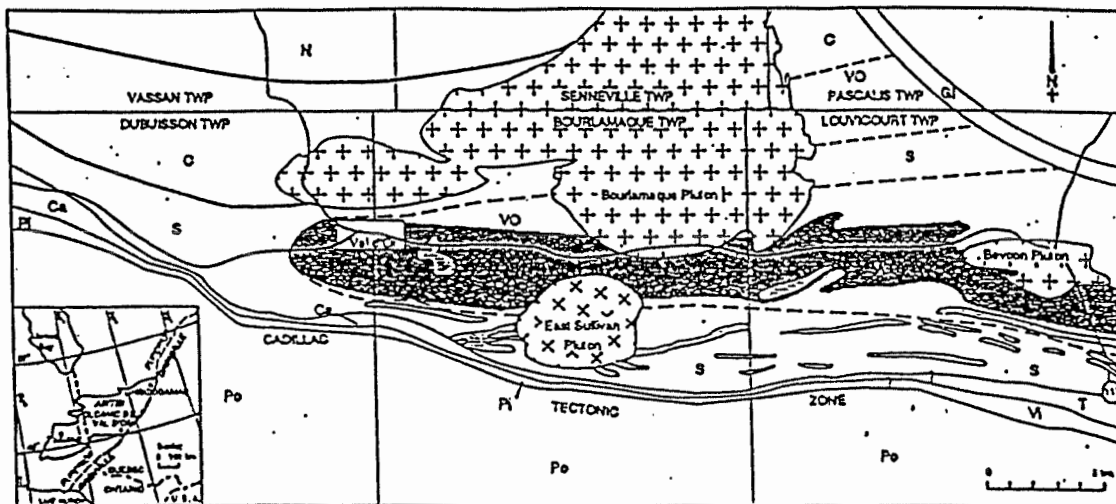
Applied to the MCB, microplate collision would have been responsible for the uplift of this composite terrane and the resultant fault-bounded sedimentary basins surrounding the MCB. With this microplate collision model in mind, it is possible that the Piché Group and the laterally-equivalent Villebon Group are part of the Pontiac Subprovince that was accreted to the south side of the sedimentary basins. Conversely, these groups may represent attenuated remnants of oceanic crust caught between the colliding Pontiac Subprovince and the MCB with the bordering sedimentary basins. Jackson and Fyon (1991) suggest that the Pontiac metasedimentary belt represents an approximately 2,600-2,700 Ma remnant of a rapidly formed, major early collisional accretionary wedge of turbiditic sediments. As collision continued, the MCB and surrounding lithologic units were deformed. It is hypothesized, based on structural and geophysical interpretations (Dimroth et al., 1983b; Green et al., 1990; Jackson et al., 1991) and by analogy with the Wawa Subprovince (Langford and Morin, 1976; Devaney and Williams, 1989) that the southern Abitibi greenstone belt was thrust over the Pontiac

Subprovince. The LLCTZ would then be a crustal-scale shear zone generally marking the suture between the Pontiac Subprovince and the MCB.

1.3 PECULIARITIES OF THE BOURLAMAQUE AND LOUVICOURT TOWNSHIPS GEOLOGY.

The majority of the rock units described in section 1.2.2 are present in Bourlamaque and Louvicourt townships. Although each rock unit is important to the understanding of the district geologic evolution, the Val d'Or domain and the Bourlamaque pluton hold special significance to the Archean VMS mineralization found in these two townships. Of specific interest in the Val d'Or domain is "the Central Pyroclastic Belt" (CPB), a band of abundant volcanoclastic rocks that was first defined by Sharpe (1968) in Louvicourt Township and that has been further defined in neighbouring townships by Chartrand (1991) (Fig. 8). The CPB is of particular metallogenic interest because it hosts the VMS deposits of this area (see Chapter 3). The following description of the CPB is taken largely from the compilation and field work done by Chartrand (1991), Chartrand and Moorhead (1992) and Moorhead and Chartrand (1993).

The CPB is composed of three volcanoclastic bands intercalated with flow rocks and essentially mafic sills. Strata generally trend east-west to eastnortheast-west-southwest; however, bedding with northeast-southwest trends has been observed



- | | |
|--|---|
| <p>V VASSAN DOMAIN
Kornatites, basalts.</p> <p>C CENTRAL DOMAIN
Basalts, komatites, minor sediments.</p> <p>S SOUTHERN DOMAIN
Intermediate to mafic flows, intermediate volcanics, minor komatitic flows.</p> <p>VO VAL D'OR DOMAIN
Intermediate volcanics composed of polygenic fragments, mafic to felsic flows and breccias.</p> <p>CENTRAL PYROCLASTIC BELT</p> <p>Ca CADILLAC GROUP
Gneisses, siltstones, conglomerates.</p> <p>PI PICHÉ GROUP
West of Val d'Or: mafic to ultramafic flows, east of Val d'Or: ultramafic to felsic schists (flow and volcanoclastic material).</p> | <p>T TRIVIO GROUP
Tuffaceous sediments, gneisses, conglomerates, flow material.</p> <p>VI VILLEBON GROUP
Mafic flows, a few ultramafic flows.</p> <p>Po PONTIAC GROUP
Gneisses, pelites.</p> <p>GI GARDEN ISLAND GROUP
Gneisses, schists, conglomerates.</p> <p>Mafic to intermediate silt or intrusion.</p> <p>Synvolcanic granodiorite-quartz diorite intrusion.</p> <p>Post-tectonic monzonitic intrusion.</p> |
|--|---|

Figure 8. General geologic map of the Val d'Or-east district (modified after Sauvé et al., 1986 and Desrochers et al., 1993) with the location of the Central Pyroclastic Belt as defined by Sharpe (1968) and Chartrand (1991).

immediately east of Val d'Or (Desrochers, 1992, pers. commun.) and north-south oriented bedding has been noted east (Lacroix, 1986; Hubert, 1993, pers. comm.) and southeast of the Bourlamaque pluton. The majority of the polarity determinations indicate a south-facing sequence slightly overturned to the north. S_0 generally parallels the regional, penetrative schistosity, S_2 , which formed during the main phase of deformation. S_2 is oriented east-west to eastnortheast-westnorthwest, dips subvertically, and overprints S_1 . Kink bands oriented northeast or northnorthwest are evidence of a still later phase of deformation. Rare occurrences of S_0 oriented at an oblique angle to S_2 suggest the possibility of juxtaposed mesoscopic structural panels. Alternatively, the Bourlamaque pluton may have caused local rotation of strata during its intrusion into the Val d'Or domain volcanic pile.

The compositions of flow rocks vary from basaltic to rhyolitic (Girault, 1986); andesitic compositions are the most common. Basaltic and andesitic lavas are generally massive or pillowed, and are commonly overlain by flow breccia. Massive lava is commonly fine- to medium-grained with local amygdale-rich horizons, whereas highly vesicular (up to 50 %) pillows and pillow fragments characterize pillowed and brecciated flows. Plagioclase-phyric horizons are also present locally. Contacts between pillow lavas and flow breccias are gradational. Flow contacts may be identified by the presence of 1) thin, highly amygdaloidal zones, 2) finely brecciated lava, or 3) rare, thin horizons of finely laminated tuff. Pillow lava is commonly formed of bun-and-mattress-shaped pillows less than 2 m long. Flow breccia is composed of isolated pillows and lobate

pillow fragments in a hyaloclastic matrix.

Dacitic to rhyolitic lavas tend to form small (a few hundred metres long by several dekametres wide), lenticular masses composed of 5 to 40 metre-thick flows. These felsic lavas have homogeneous textures, and consist of aphanitic to fine-grained, massive aphyric rock. Quartz and feldspar phenocrysts and quartz-feldspar spherulites are abundant locally. Individual flows and masses may be mantled by aprons of hyaloclastite and lobe breccia.

Lenses and layers of pyroclastic rock are interstratified with effusive rocks. In general, the proportion of pyroclastic to effusive rocks increases as compositions change from mafic to felsic. Polygenic tuff breccia, lapilli tuff, and crystal (feldspar and quartz) tuff are the most common pyroclastic rocks. Bed thicknesses range from several decimetres to several metres, and beds may be ungraded, normal, or reversely graded. Pyroclasts are composed of pumice, scoria, aphyric, spherulitic and porphyritic felsic-intermediate lava, amygdaloidal and porphyritic mafic lava, whole and fragmented crystals, and chert. The angularity of fragments is commonly high, although fragments are variably flattened and stretched parallel to the regional deformation. Less commonly, ash tuff and cherty pyritic tuff are interbedded with the lava and coarser-grained pyroclastic rocks, generally marking the end of volcanic episodes. Most massive sulphide bodies occur along these cherty, tuffaceous "marker" horizons which are interpreted to be exhalites. All marker beds are confined to the CPB.

In the following chapter, a literature review is given of prior geochemical data for Val d'Or district rocks. Also, new geochemical data on rocks from the CPB and surrounding lithotectonic units are presented and discussed in order to further characterize these rocks using trace and rare-earth element analyses in addition to major element data.

CHAPTER 2

GEOCHEMICAL DATA FOR ROCKS OF THE VAL D'OR DISTRICT

2.1 INTRODUCTION

Archean volcanic rocks are variably metamorphosed and altered, and as a consequence, their major-element oxide compositions have been affected to some degree by additions and/or subtractions of various elements. On the other hand, some trace elements, such as high-field-strength elements (HFSE: Zr, Y, Ti, Hf, Nb, Ta) and rare-earth elements (REE), are relatively immobile and alteration resistant and therefore, they are more reliable indicators of geochemical affinity and may aid in modelling volcanic paleo-environments.

Research of the literature has revealed a paucity of published geochemical data, especially HFSE and REE data, for rocks from the Val d'Or district. Thus, modelling of the paleo-environment for the Val d'Or district (e.g., Imreh, 1984; Rocheleau et al., 1990) has been based mainly on major-element oxide data plotted on AFM (Irvine and Baragar, 1971) and/or AFTiM (Jensen, 1976) diagrams. Also, interpretations are commonly impeded by the lack of sample locations and sample descriptions. Thus, more reliable information was gathered for the present study by sampling least-altered rocks for trace elements and REEs as well as for major-element oxide analyses. As part of this metallogenic study, a number of geochemical samples were taken in the Val d'Or

region so that 1) the geochemical nature of the various stratigraphic units of the region could be confidently identified and 2) paleo-volcanic models for the district could be supported or modified.

In this chapter, a review is given of prior geochemical data available for Val d'Or district rocks and of paleo-volcanic models based on these data. Following this review, new major-element, trace-element and REE data from the Val d'Or district are presented, and comparisons are drawn where possible, with prior data from the sector.

2.2 LITERATURE REVIEW OF THE GEOCHEMISTRY OF ROCKS IN THE VAL D'OR REGION.

The first published petrological and geochemical studies of the volcanic rocks of the Malartic Group in the Val d'Or district (Alsac et al., 1971, Alsac, 1977; Alsac and Latulippe, 1979) supported the first division of this stratigraphic unit into lower and upper groups, established on the predominant rock types characterizing each sub-group (Latulippe, 1966). Based on the major-element geochemistry plotted on AFM diagrams, the rocks of the Lower Malartic Group are characterized by tholeiitic and komatiitic signatures whereas rocks from the Upper Malartic Group are characterized by calc-alkalic and tholeiitic signatures.

However, several problems were encountered while examining the geochemical

data found in the report of Alsac (1977). For example, not all samples identified on the location map have corresponding analyses in the table, and samples in the table are not fully described (e.g., pillowed or massive, amygdaloidal or not, porphyritic or aphyric). In addition, only major-element oxide analyses were systematically done, and Yb and Y are the only relatively alteration-resistant elements given.

Spitz and Darling (1975) used major-element oxide analyses to study the petrochemical nature of altered volcanic rocks surrounding the Louvem VMS copper deposit (see Fig. 26 for deposit location). Their work identified the calc-alkalic nature of the volcanic rocks using olivine-nepheline-quartz and AFM diagrams, despite the presence of corundum in all norm calculations (refer to section 2.3.2 for further discussion on the relevance of corundum). Their investigations revealed that the peraluminous character of these rocks was due not to a gain in Al but rather to a depletion of alkali elements. This depletion around the VMS deposit may be explained by local hydrothermal alteration. Spitz and Darling (1975) also examined the analyses of Alsac et al. (1970) and Descarreaux (1972) for Louvicourt Township volcanic rocks and for Upper Malartic rocks, respectively, and they concluded that 60-70% of these volcanic mafic to felsic rocks have a peraluminous character. They suggested that the entire Upper Malartic Group was affected by widespread hydrothermal alteration and that this alteration is more intense locally around mineralized sites.

Subsequently, a paleo-volcanic evolution model for the Val d'Or district was

proposed by Imreh (1984), based on his extensive field work and geochemical sampling. Although a great number of geochemical analyses were done (available on computer diskette in 1992 from the M.E.R.Q), lithological descriptions are lacking, and no trace-element or REE analyses were done on rocks from the Val d'Or-east sector.

In this synthesis, Imreh illustrated the chemical characteristics of the different stratigraphic formations by plotting major-element oxide data on AFM diagrams. In summary, the La Motte-Vassan Formation is characterized by komatiitic rocks and minor tholeiitic basaltic rocks; the Dubuisson Formation is characterized by tholeiitic basaltic rocks and minor komatiitic rocks; the Jacola Formation is characterized by both komatiitic and tholeiitic rocks, the least evolved basalts falling between the tholeiitic and calc-alkalic domains; the Val d'Or Formation has a calc-alkalic nature; and the Héva Formation is tholeiitic west of Val d'Or and calc-alkalic east of Val d'Or. According to Imreh's model, the La Motte-Vassan and Dubuisson formations are products of abyssal plain volcanism whereas the Val d'Or and Héva formations are products of central volcanic complexes that formed upon the abyssal plain volcanic rocks. The Jacola Formation represents volcanism transitional between the abyssal plain and central complex volcanism.

Gaudreau et al. (1986) provides CO₂, loss on ignition (LOI), major-element and selected trace-element data, including Zr and Y of samples from the eastern half of Louvicourt Township and the neighbouring Vauquelin Township to the east. Lava and

fragmental rocks were sampled and their analyses were plotted on AFTiM diagrams to categorize the rocks according to Imreh's geochemical and stratigraphic formation divisions. Some data have been chosen by the author according to rejection criteria described in section 2.3.2, and these analyses are discussed in section 2.3.2.1 in conjunction with the author's data and other data from Girault (1986) (see below) who sampled various lithologies in Bourlamaque and Louvicourt townships for geochemical analyses.

Based on Gaudreau et al.'s work and an M.E.R.Q. interim report by Rocheleau et al. (1987) on the district extending east of Louvicourt Township to the Grenville Front, Rocheleau et al. (1990) elaborated a paleo-environment model similar to that of Imreh (1984). In Rocheleau et al. (1990), AFTiM diagrams are used to determine the geochemical affinity of the rocks from the various stratigraphic formations and environment-of-formation hypotheses are drawn from extended trace-element abundance diagrams. Unfortunately, representative analyses for examination are lacking as well as extended trace-element abundance diagrams.

According to Rocheleau and co-workers, ocean floor basalts were generated in an extensional zone (resulting in the Dubuisson Formation), upon which island arc-type volcanism occurred (resulting in the Jacola, Val d'Or, and Héva Formations). The Héva Formation at the top of the volcanic sequence represents an extensional phase characterized by the emplacement of tholeiitic magma. According to Rocheleau et al.

(1990), this geologic sequence is comparable to the model proposed by Crawford et al. (1981) for the Mariana arc in the southwest Pacific Ocean.

Girault (1986) deals with the petrography and geochemistry of the volcanic rocks in Bourlamaque and Louvicourt townships, and followed Imreh's geochemical and stratigraphic formation divisions. Interpretations of the geochemistry of these Archean rocks are based on diagrams constructed according to Winchester and Floyd (1976, 1977) and Pearce and Cann (1973) for Phanerozoic and Recent rocks. In addition, fractionation vectors from Pearce and Norry (1979) diagrams are used to suggest sources and fractionation types for rocks in this sector. CO₂ and LOI data are unfortunately absent, making it difficult to evaluate the degree of carbonatization or hydration, and although REE data are also lacking, useful trace elements such as Zr, Y, and Nb are provided. However, Nb concentrations may be questionable because of the difficulties in analyzing accurately this element at low concentrations (Girault, 1986). Data from Girault (1986) have been chosen by the author according to rejection criteria described in section 2.3.2., and are discussed in section 2.3.3.1 in conjunction with the author's data and pertinent data from Gaudreau et al. (1986).

Rare-earth element and trace-element data for the Bourlamaque intrusion and volcanic rocks from the Val d'Or and Dubuisson formations have been published by Tessier et al. (1990). A tholeiitic affinity was assigned to the Dubuisson Formation rocks, whereas a calc-alkalic affinity and cogenetic relationship was given to Val d'Or

Formation and Bourlamaque intrusive rocks. These geochemical affinities are based on composite sample profiles rather than individual profiles on REE diagrams. Examination of Tessier (1986) on which Tessier et al. (1990) is based reveals that REE analyses could not be unambiguously correlated with major-element oxide data due to sample number repetitions, that individual REE profiles for each rock type had anomalous spikes crossing one another, suggesting mobilization due to alteration of certain REEs, that samples were not described and, therefore, fragmental rocks from the Val d'Or Formation may have been analyzed (for petrogenetic analysis, it is preferable to sample flow rocks than a mixture of matrix and clasts from fragmental rocks), and that no map locates samples of Bourlamaque intrusive and Val d'Or Formation rocks. (Consultation with the authors of Tessier et al. (1990) confirmed the nonexistence of a sampling location map).

Additional REE data of the Bourlamaque intrusion have also been published by Taner and Trudel (1989). Unfortunately, major-element oxide analyses do not have complementary REE analyses. Also, the published REE data are averaged results for various deformation facies, and there is no sampling location map. Therefore, these data also have little comparative value.

Desrochers et al. (1993) review geochemical analyses for ultramafic to felsic rocks in the Malartic Group west of Val d'Or (Parent, 1985) and show that the komatiites and tholeiites of the Northern, Vassan, and Central domains are characterized by light

REE depletion, and that the komatiites, Fe-enriched tholeiites and rhyodacites of the Southern domain were fractionated from a depleted tholeiite parent. Desrochers et al. (1993) compare these data to those of Phanerozoic tholeiitic and komatiitic assemblages formed in oceanic plateau environments (cf., Storey et al., 1991), and they also suggest that the Galapagos oceanic spreading centres (cf., Perfit and Fornari, 1983) have tholeiitic to rhyodacitic fractionation trends that are equivalent to those of the Southern domain rocks. They conclude that these geochemical data are consistent with lavas extruded in an oceanic environment where thick crust may have formed as a result of a high thermal flux in the mantle and crust.

Desrochers et al. (1993) also examined geochemical data (light REE-enriched patterns of Tessier (1986) and Tessier et al. (1990)) of Val d'Or domain rocks and the Bourlamaque pluton east of Val d'Or. Desrochers et al. suggest that these calc-alkalic rocks were derived from a light REE-enriched source that underwent high-pressure fractionation at the base of a mafic crust thickened and stabilized by abundant tonalitic injections during subduction of oceanic lithosphere (cf., Laflèche et al., 1992).

The combination of structural and geochemical data lead Desrochers et al. to suggest that the Northern, Vassan, Central and Southern mafic domains represent accreted oceanic plateau material and that the younger, calc-alkalic Val d'Or domain represents extension-related volcanism that erupted through the accreted mafic domains (Figs. 6a and 6b). Their suggestion that extension may have been the result of ridge

subduction in a regime of oblique convergence is based on Phanerozoic models (e.g., Skulski et al, 1991; Babcock et al., 1992) applied to regions of the west coast of North America where extensional volcanic centers are interpreted to overlie accreted exotic fragments.

In summary, most petrogenetic and paleo-volcanic environment modelling for the Val d'Or district rock units have been based on AFM and/or AFTiM diagrams, and little HFSE and REE data exist for these rock units. Referenced trace-element data are commonly unpublished or not located on a base map, and samples are commonly not described. Thus, subsequent to this literature review, the author felt it was important to obtain for the rocks in the study area new geochemical data including pertinent trace-element and REE data that would be complementary to the prior geochemical data. These new data are presented in the next section.

2.3 NEW GEOCHEMICAL DATA FOR VAL D'OR DISTRICT ROCKS

2.3.1 Introduction

Sampling of rocks in the field, and in drill core when necessary, was done during the 1991 and 1992 summer field seasons in order to analyze various flow and intrusive rocks for major, trace and rare-earth elements. Sampling was focussed on mafic to felsic flow rocks in the Val d'Or and Southern domains in Bourlamaque and Louvicourt townships and on mafic flow rocks in the Central and Vassan domains in neighbouring

townships. In addition, sill-like intrusions in the Val d'Or and Southern domains and the Bourlamaque and Bevcon intrusions were sampled to characterize their possible relationships to extrusive magmatism, and relatively late-tectonic feldspar±quartz porphyries in both domains were sampled for comparison to similar porphyries discussed in the literature. Mafic and ultramafic rocks of the Central and Vassan domains are relatively scarce in the northern part of Bourlamaque and Louvicourt townships; therefore, samples were collected in Dubuisson and Vassan townships where these lithologic units are relatively more abundant and accessible. Few samples of komatiitic rocks were taken because of their low trace-element contents and hence difficulties in detecting accurate trace-element concentrations.

2.3.2 Characterization of Least-Altered Samples.

Gélinas et al. (1977), Gélinas et al. (1982) and Ludden et al. (1982) evaluate the major, trace and rare-earth element geochemistries of mafic and intermediate flow rocks, and give guidelines to selecting least-altered samples. Rocks having the following characteristics are classified as least altered, and are presumed to give reliable information about major-element behaviour: (1) no abnormal normative minerals such as corundum in the calculated norm, (2) a cut-off value of 3.8 wt.% for H₂O and CO₂ combined, (3) no limpid albite (an indicator of spilitization) in mafic rocks, and (4) chlorite-epidote-actinolite assemblages.

For the evaluation of trace-element and REE behaviours in mafic flows, Ludden

et al. (1982) examined least-altered, chlorite-epidote-actinolite-bearing samples and rarely chlorite-epidote-bearing samples, and although they used broader volatile cut-off limits (i.e., $\text{CO}_2 < 2.5 \text{ wt. \%}$; $\text{H}_2\text{O} < 4 \text{ wt. \%}$; $\text{CO}_2 + \text{H}_2\text{O} < 5 \text{ wt. \%}$) than Gélinas et al. (1977), the intent was the same, i.e., to eliminate highly hydrated or carbonated samples. For least-altered samples, Ludden et al. (1982) concluded that HFSEs (Zr, Y, Ti) and REEs are immobile. Highly altered samples were also examined for comparison, and Ludden and co-workers found that HFSE ratios remained unchanged whereas REEs may be leached and redeposited by carbonate-rich and K-rich metasomatic fluids.

The CIPW norm was calculated for each analysis using the program NEWPET, and the volatile content of the analyses was examined to evaluate the degrees of alteration. Except for one mafic flow rock, all extrusive volcanic rocks from the Val d'Or domain contain corundum in the normative calculation. Normative corundum in sub-alkalic rocks indicates extensive alteration resulting in peraluminous compositions due to depletion in CaO, Na₂O and K₂O.

It is not uncommon to have small quantities of corundum in the norms of Phanerozoic andesites (Chayes, 1970; Gill, 1982). These rocks commonly contain aluminum-rich micas or garnet. Compilation work by Chayes (1970) on the incidence of normative corundum in some common volcanic rocks (rhyolites to basalts) illustrates an inverse relationship between the relative frequency of corundum and CaO, a direct relationship with SiO₂ and an insignificant relationship with Al₂O₃. Its presence has

generally been taken as evidence of the assimilation of aluminous sediments or metamorphic rocks in the formation of andesites in orogenic environments (Chayes, 1970). In comparison, a laboratory experiment by Kushiro and Yoder (1972) suggests that andesites and dacites with excess alumina may be formed from direct partial melting of mantle peridotite under hydrous conditions at a minimum of 10 kilobars and from subsequent fractional crystallization involving the removal of clinopyroxene. The importance of hydrous conditions and pressures around 10 kilobars is corroborated by work done by Ujike (1975).

The peraluminous character of Val d'Or domain rocks has already been noted by other workers (see section 2.2). Figure 9 reaffirms the observation by Robert (1980) concerning the rocks surrounding the Manitou-Barvue deposit (see Fig. 26 for deposit location) that there is no obvious correlation between the quantities of normative corundum and alumina. Descarreaux (1973), Spitz and Darling (1973, 1975, 1978) and Robert (1980) recognize that the study area has been affected by a major hydrothermal alteration event associated with volcanogenic massive sulphide formation as well as greenschist-facies metamorphism. The Val d'Or domain rocks could have been originally rich in alumina and were subsequently enriched in alumina by alkali depletion as a result of intense hydrothermal alteration. Without unequivocal evidence to the contrary, the peraluminous nature of these rocks is assumed to be the result of important hydrothermal alteration.

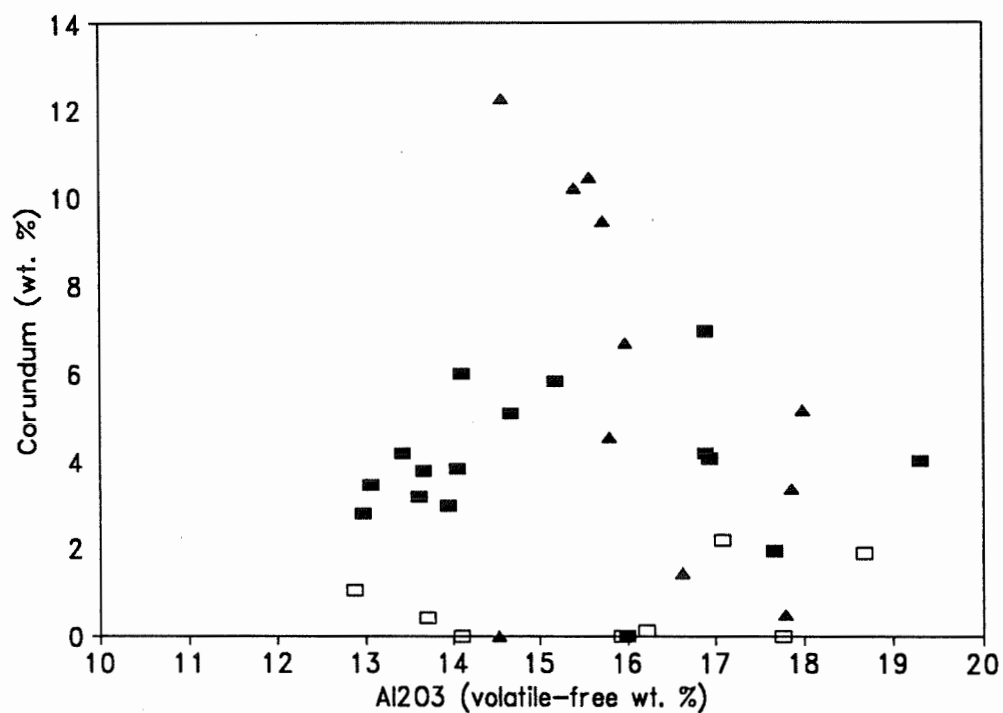


Figure 9. Binary diagram of normative corundum versus Al₂O₃ for flow and intrusive rocks of the Val d'Or domain. Solid boxes = flow rocks (author's data); triangles = intrusive rocks (author's data); open boxes = flow rocks (data from Girault, 1986 and Gaudreau et al., 1986).

Despite the apparent intense alteration of Val d'Or domain rocks, trace-element and REE analyses were done on these rocks with low volatile contents, presuming that typically immobile, alteration-resistant elements would still indicate geochemical affinities. Samples from the other domains did not have corundum in the normative calculations, and samples were selected based on low volatile contents.

All analyses were done at the Centre de Recherches minérales in Ste.-Foy, Quebec, and the sampling methods and the analytical techniques and their precision are explained in Appendix 1. Major-element oxide, trace-element and REE analyses and the norms for all samples are given in Appendix 2, and Figure A2.1 gives the sample locations of the analyzed rocks presented here. Brief macroscopic and microscopic descriptions of all analyzed rocks are found in Appendix 3.

In the following section, the geochemical characteristics of the new flow-rock data and of a group of data on Val d'Or domain flow rocks from Girault (1986) and Gaudreau et al. (1986) are discussed. The previously published data are included to increase the quantity of trace-element data on rocks from the study area. Also, geochemical data representing Southern, Central and Vassan domain rocks were selected from Desrochers (1994) to compensate for the lack of outcrops of these units in the study area. Finally, the geochemical data of intrusive rocks from the Val d'Or and Southern domains are discussed and compared to the flow data to establish their possible relationship to extrusive magmatism.

2.3.3 Evaluation of Geochemical Data

2.3.3.1 Geochemical Data of Flow Rocks

Flow rocks from the Vassan, Central and Southern domains (see Tables A2.1 and A4 in the Appendices) show that these rocks have reasonably low H₂O and CO₂ contents and that their normative compositions are corundum-free. Rocks from the Val d'Or domain (see Table A2.3) shows that all samples except one (sample No. 3867-91, a drill core sample) have corundum in their normative compositions, suggesting that these rocks were subjected to extensive alteration. Although the CO₂ contents of Val d'Or domain rocks are higher than those for samples from the Vassan, Central and Southern domains, all CO₂ values except two are less than 2.5 wt. % (cf. section 2.3.2). LOI values for Val d'Or domain rocks are relatively high indicating significant H₂O contents: four of the 16 analyses have LOI values greater than 4 wt. %, and only nine of the 16 samples have combined H₂O and CO₂ contents less than 5 wt. % (cf. section 2.3.2).

Microscopic observations of samples collected by the author (see Appendix 3) determined that actinolite is present in all except one sample from the accreted Southern, Central and Vassan domains, whereas actinolite is not observed in any samples from the Val d'Or domain. The lack of actinolite in the mafic to intermediate flow rocks and the presence of albite in several rocks are additional evidence of the intense alteration of the Val d'Or domain rocks. Therefore, the rock names given in Tables A2.1, A2.2, A2.3 and A2.4 are considered appropriate field names, rather than names based solely on SiO₂ contents.

Figure 10 shows that all of the flow rocks are subalkalic. The AFTiM plot (Jensen, 1976) (Fig. 11a) indicates that rocks from the Southern, Central and Vassan domains have tholeiitic to komatiitic affinities, and on the AFM plot (Irvine and Baragar, 1971) (Fig. 11b), the transitional evolution from komatiitic to tholeiitic affinities is underlined by the iron enrichment. Although a few samples from these domains fall in the calc-alkalic fields, indicating relatively high potassium or aluminum contents (boxes: samples 91-3647-N, 91-3707-N, 91-3708-S, 90-33640-S, 90-33670-S), other diagrams (presented below) confirm their tholeiitic nature. As for the Val d'Or domain rocks, the majority of the analyses have calc-alkalic affinities, lacking any significant iron enrichment on the AFM diagram (exceptions are 5671-92, 5657-92, and 3867-91). However, REE profiles (presented below) confirm the calc-alkalic nature of the first two samples; no REE analyses were done for sample 3867-91, and the geochemical affinity of this sample is not clear from trace-element diagrams.

In summary, these AFTiM and AFM plots identify the tholeiitic and komatiitic nature of rocks from the Southern, Central and Vassan domains and the calc-alkalic nature of Val d'Or domain rocks, as already established by previous workers (e.g., Latulippe, 1976; Imreh, 1984). However, for some samples falling in zones atypical of their domainal characteristic on such diagrams, trace-element and REE data must be employed to confirm their true geochemical affinities.

Major-element oxide binary diagrams (Fig. 12) also confirm the geochemical

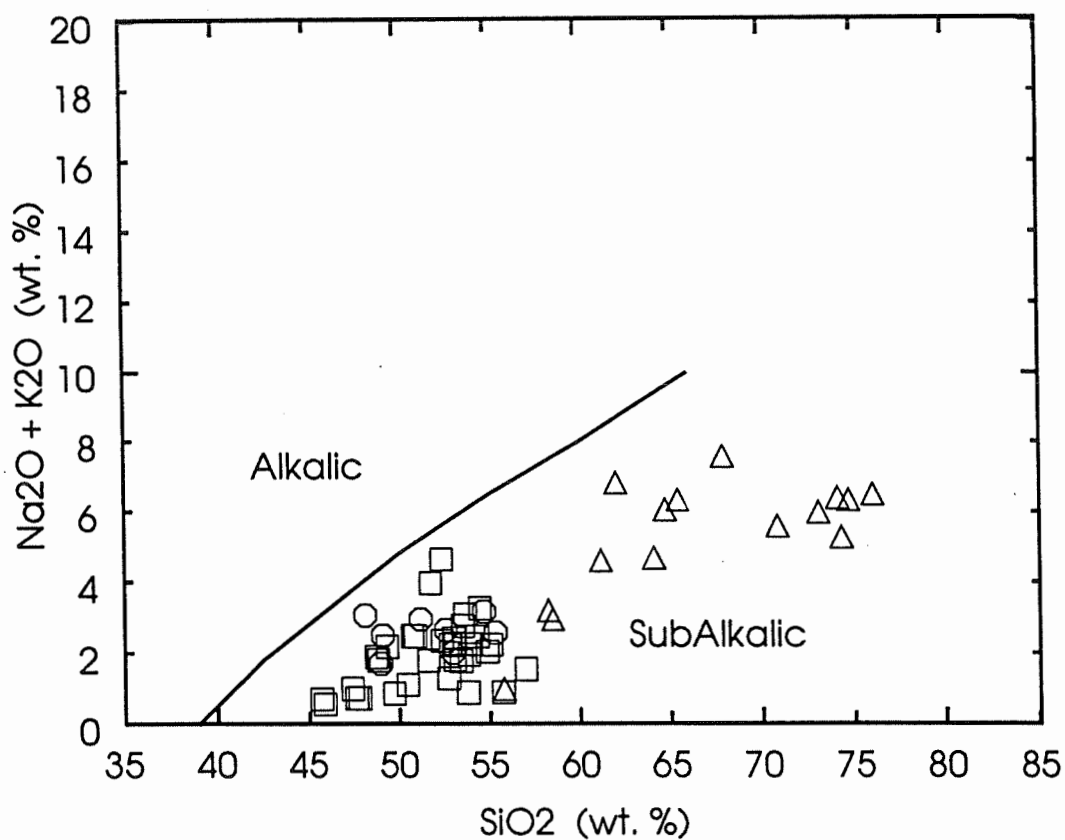


Figure 10. Alkalis-silica plot (Irvine and Baragar, 1971) for flow rocks of the Val d'Or district. Triangles = Val d'Or domain (author's data); circles = Southern and Vassan domains (author's data); and boxes = Southern, Central and Vassan domains (data from Desrochers, 1994).

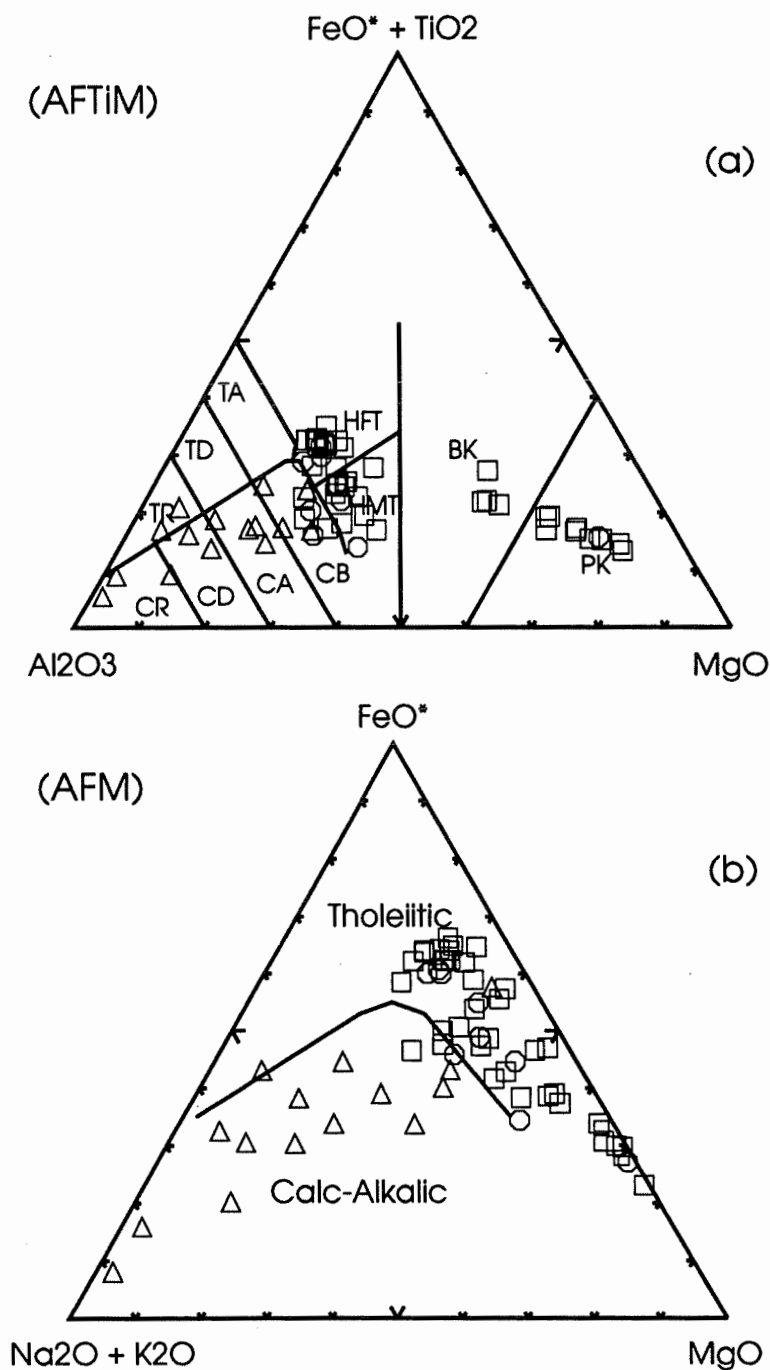


Figure 11. (a) AFTIM (Jensen, 1976) and (b) AFM (Irvine and Baragar, 1971) plots for flow rocks of the Val d'Or district. Triangles = Val d'Or domain (author's data); circles = Southern and Vassan domains (author's data); and boxes = Southern, Central and Vassan domains (data from Desrochers, 1994).

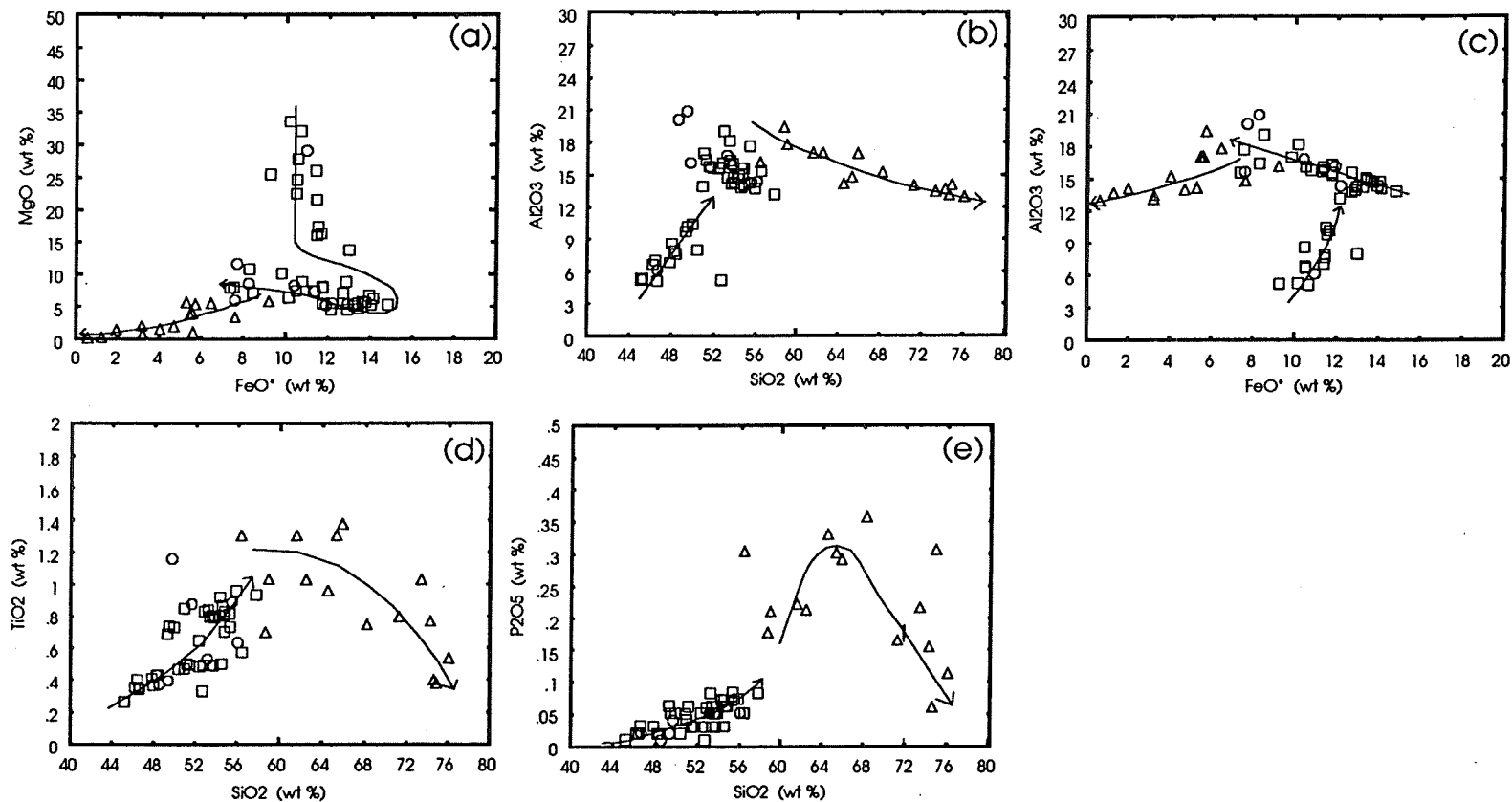


Figure 12. Binary major element oxide diagrams for flow rocks of the Val d'Or district. (a) = MgO vs FeO*, (b) = Al₂O₃ vs SiO₂, (c) = Al₂O₃ vs FeO*, (d) = TiO₂ vs SiO₂, (e) = P₂O₅ vs SiO₂. Triangles = Val d'Or domain (author's data); circles = Southern and Vassan domains (author's data); and boxes = Southern, Central and Vassan domains (data from Desrochers, 1994).

distinction (calc-alkalic versus tholeiitic and komatiitic) between the Val d'Or domain rocks and the Southern, Central and Vassan domain rocks. In Fig. 12a (MgO vs FeO*), komatiites have high MgO values which are interpreted to have decreased progressively as olivine crystallized and FeO* accumulated until magnetite began to crystallize, at which point FeO* tends toward zero. This geochemical evolution is characteristic of a tholeiitic trend. The calc-alkalic trend is lacking among relatively high MgO samples, but it is evident in the characteristic decrease toward zero MgO without any FeO* enrichment.

In Figure 12b (Al₂O₃ vs SiO₂), komatiites evolve to tholeiites with increasing Al₂O₃ and SiO₂ contents. Two samples (circles: 3834-91, 3865-91) with high Al₂O₃ contents are somewhat distinct from the main group of tholeiites and are called high-alumina magnesian basalt. (This type of basalt is common in the Jacola Formation; some of these basalts even contain calcic plagioclase phenocrysts which account for the high aluminum and calcium contents (Pers. commun., Sauvé, 1994)). Three other samples (boxes: 91-3684-S, 91-3691-S, 91-3674-S) are separated slightly from the main group of tholeiites; they correspond to those boxes in Figures 12d and 12e with the highest Al₂O₃ and TiO₂ contents, respectively. They also correspond to those samples identified by boxes in the calc-alkalic zone of the AFTiM plot (Fig. 11a). These samples may have been slightly enriched in aluminum.

In Figure 12c (Al₂O₃ vs FeO*), komatiites evolve to tholeiites, with FeO*

increasing with Al_2O_3 apparently due to olivine \pm clinopyroxene crystallization. The tholeiitic trend is marked by decreasing FeO contents (probably due to magnetite crystallization) and increasing Al_2O_3 contents. The calc-alkalic trend is characterized by decreasing Al_2O_3 contents with decreasing FeO* contents, probably as a result of plagioclase crystallization.

In Figure 12d (TiO_2 vs SiO_2), komatiites evolve to tholeiites as TiO_2 increases with increasing SiO_2 . Sample 5668-92, lying so far off the tholeiitic trend, must be rich in ilmenite or magnetite. The dog-leg trend (i.e., TiO_2 increasing with increasing SiO_2 , then TiO_2 decreasing with increasing SiO_2) of the Val d'Or domain rocks is representative of a calc-alkalic trend, with the onset of crystallization of Ti-bearing minerals such as ilmenite occurring at approximately 64 wt. % SiO_2 . A similar trend is also observed in Fig. 12e (P_2O_5 vs SiO_2), although P_2O_5 starts to decrease due to apatite crystallization at approximately 68 wt. % SiO_2 . TiO_2 and P_2O_5 do not start to decrease at the same SiO_2 content; this behaviour could be an argument against dilution due to silica (or magnesium) addition, suggesting that these three Val d'Or domain samples are related by crystallization. From the P_2O_5 - SiO_2 plot (Fig. 12e), the Val d'Or domain samples were classified into low- SiO_2 , medium- SiO_2 and high- SiO_2 groups, and the REE data from these groups are plotted in Figures 13a,b,c, respectively. The REE profiles of these rocks are similar to those of calc-alkalic island-arc type rocks (Jakeš and White, 1972). There is a general, small transition of increasing REE contents from the low- SiO_2 group (Fig. 13a) through the medium- SiO_2 group (Fig. 13b) to the high- SiO_2 group (Fig.

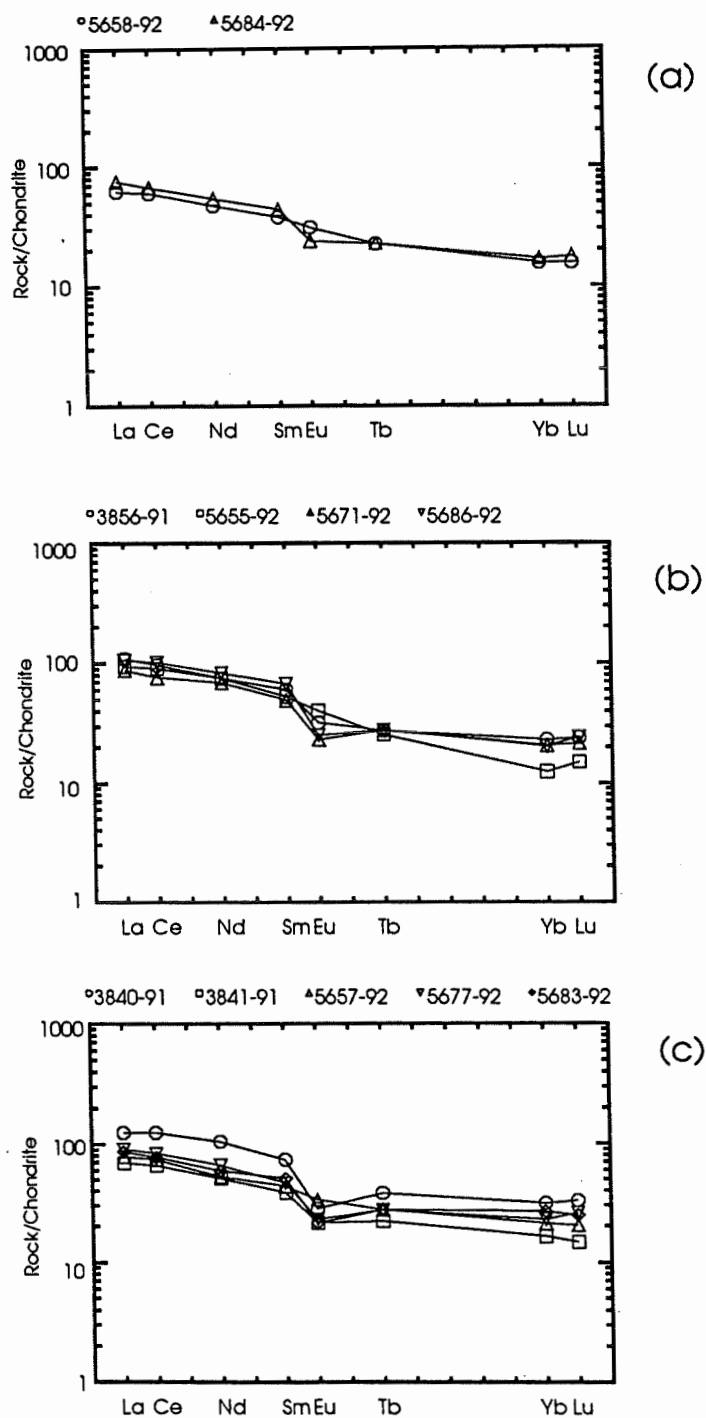


Figure 13. Rare-earth element profiles for Val d'Or domain flow rocks. (a) = low-SiO₂, (b) = medium-SiO₂, (c) = high-SiO₂ samples grouped according to their position in Figure 12e (P₂O₅ vs SiO₂). Elements normalized to the C1 chondrite (Sun and McDonough, 1989).

13c), suggesting that these groups are related by crystallization and that the "second stage" of SiO_2 increase is not due to silicification. Interestingly, the REE profile of sample 5684-92 (low- SiO_2 group) is similar to that of sample 3841-92 (high- SiO_2 group); also analysis 3856-91 is that of a pillowed flow which has a REE profile comparable to those of the high- SiO_2 group, implying that 3841-91 and 3856-91 are silicified.

The same transition is also observed in the extended trace-element abundance diagrams (Fig. 14). All samples exhibit a strong, negative niobium anomaly with respect to thorium and lanthanum, a characteristic typical of calc-alkalic rocks (Fig. 15). These rocks also have variably negative titanium and positive zirconium anomalies. Calc-alkalic rocks commonly have positive strontium anomalies but these samples exhibit variably negative strontium anomalies. Given that strontium is a mobile LILE known, these negative anomalies underline the high degree of alteration that affected the Val d'Or domain rocks.

Because HFSE are considered more resistant to alteration than major element oxides, a yttrium versus zirconium plot was constructed in order to further characterize the tholeiitic and calc-alkalic suites (Fig. 16). With regard to the steep positive trend formed by the komatiitic and tholeiitic samples of the Southern, Central and Vassan domains, two groups of basalts (low-Y (15-30 ppm) and high-Y (30-50 ppm)) and one group of komatiites (Y = 5-15 ppm) are recognized. Note that in the komatiite group, two samples (circles: 3865-91 and 3834-91) have MgO contents of less than 12 wt. %

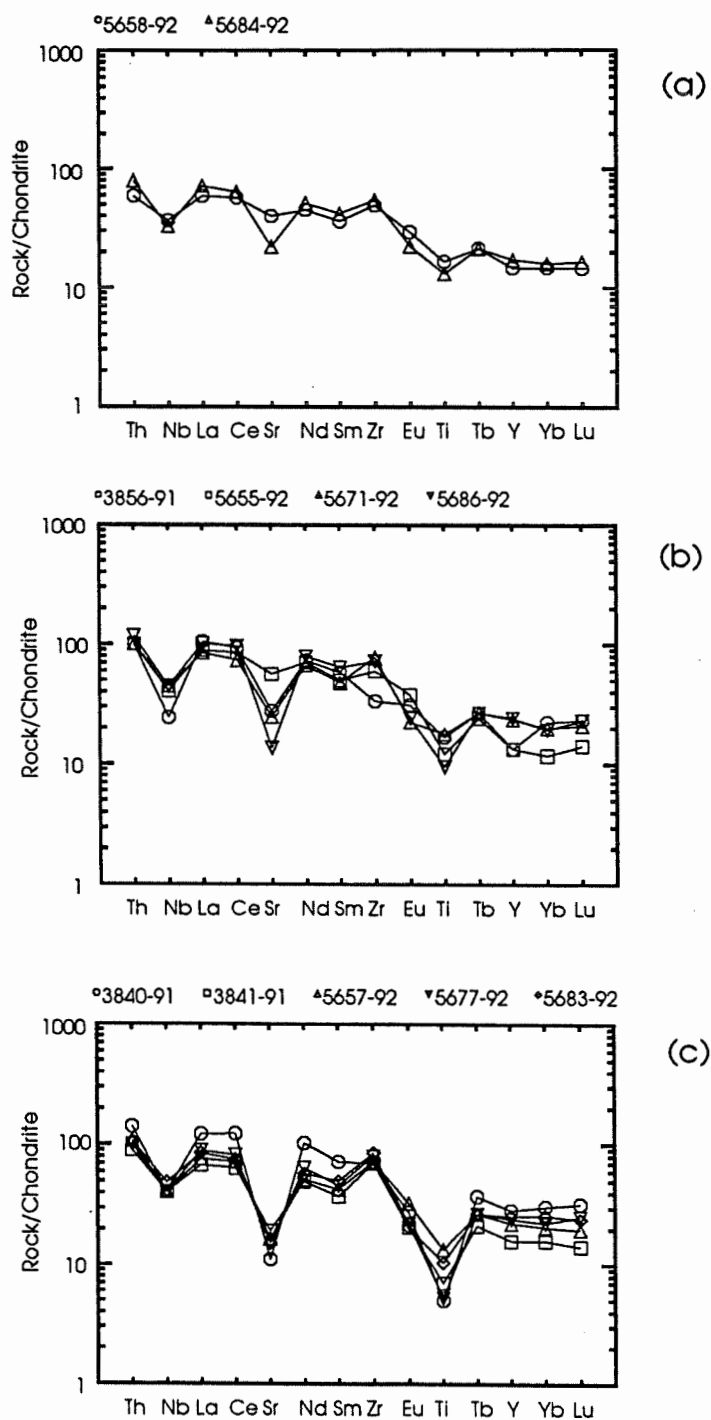


Figure 14. Extended trace-element abundance profiles for Val d'Or domain flow rocks. (a) = low-SiO₂, (b) = medium-SiO₂, (c) = high-SiO₂ samples grouped according to their position in Figure 12e (P₂O₅ vs SiO₂). Elements, normalized to the C1 chondrite (Sun and McDonough, 1989), exhibit decreasing incompatibilities from left to right.

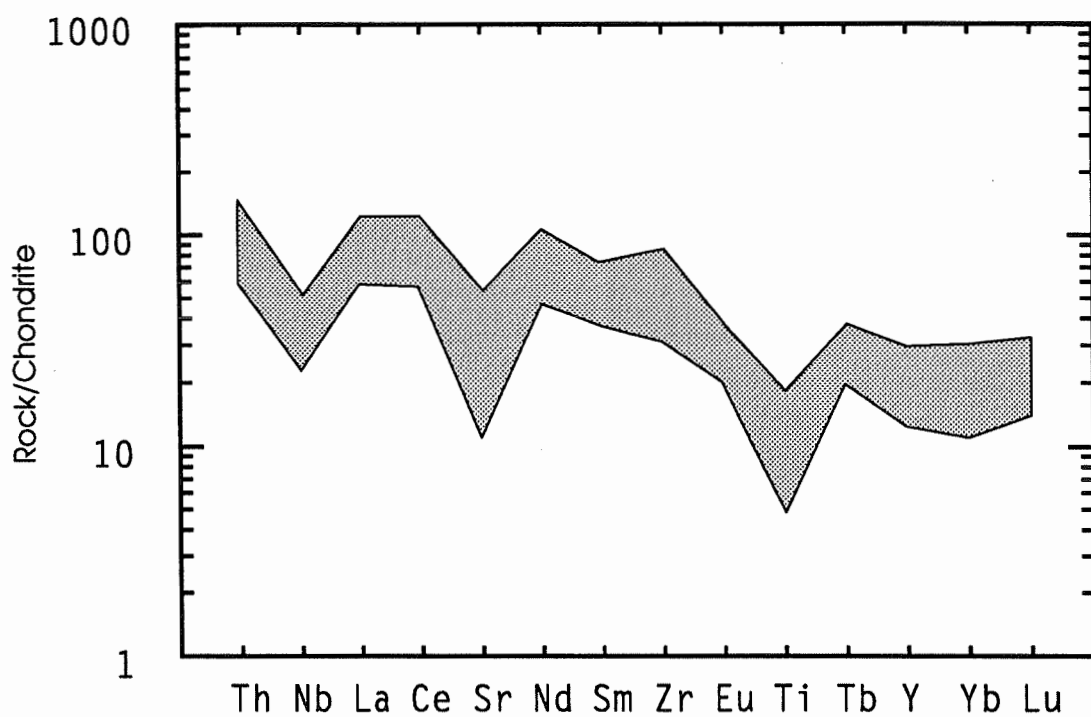


Figure 15. Field of composite extended trace-element abundance profiles for Val d'Or domain flow rocks. See Figure 14 for individual profiles.

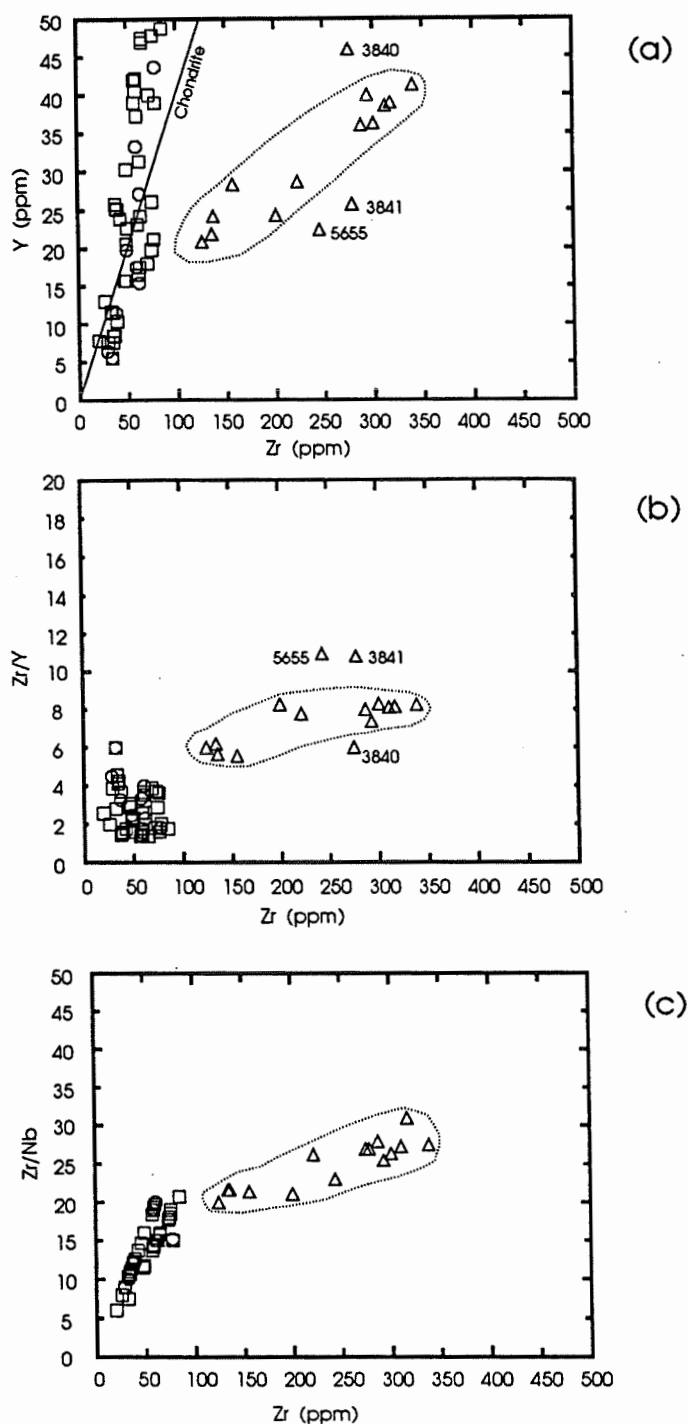


Figure 16 . Binary trace-element diagrams for flow rocks of the Val d'Or district. (a) = Y vs Zr, (b) = Zr/Y vs Zr, (c) = Zr/Nb vs Zr. Triangles = Val d'Or domain (author's data); circles = Southern and Vassan domains (author's data); boxes = Southern, Central and Vassan domains (data from Desrochers, 1994).

MgO. These magnesian basalt samples also have high Al_2O_3 values (see Figs. 12b and 12c and p. 66) and low Y values (≈ 6 and 11 ppm) compared to komatiitic basalts (15-20 ppm) and basalts (20-30 ppm) (J.N. Ludden, pers. commun., 1994), indicating that their Y contents have been modified.

Basalts typically have Y values varying from 15-30 ppm and a significant number of samples plot in this range (Fig. 16a). However, there is also a non-negligible number of samples with Y values between 30 and 50 ppm. These high-Y basalts plot distinctly to the left of the line representing the Y/Zr chondritic ratio, and it is difficult to explain firstly this non-chondritic behaviour and secondly, their high yttrium contents. One possible explanation is the accumulation of clinopyroxene in which yttrium is compatible.

Figure 16b (Zr/Y vs Zr) shows that the Southern, Central and Vassan domain flow rocks plot in a restricted part of the diagram, suggesting that these samples are not highly fractionated and that they may be genetically related. The average Zr/Y value for tholeiitic rocks of the Vassan, Central and Southern domain rocks is 2.3 which is comparable to the 2.9 average value for mafic flow rocks of tholeiitic units in the Rouyn-Noranda district (Gélinas et al., 1984).

Figures 17a (Ni vs Y) and 17b (Co vs Y) (where Ni and Co are compatible ferromagnesian elements controlled by olivine during fractional crystallization and Y is an incompatible HFSE) offer more substantial evidence that samples from the Southern,

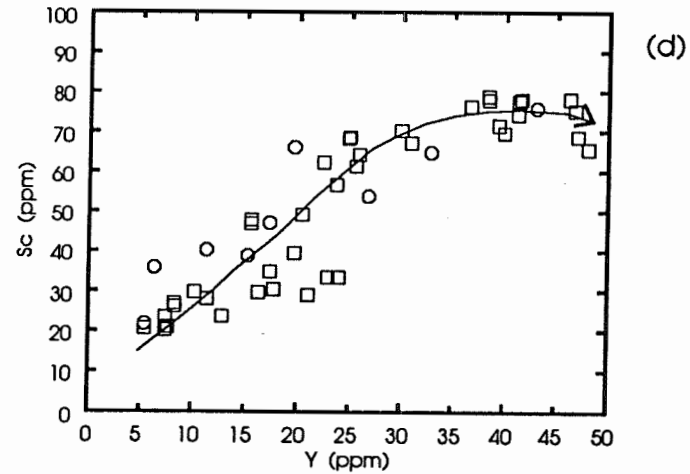
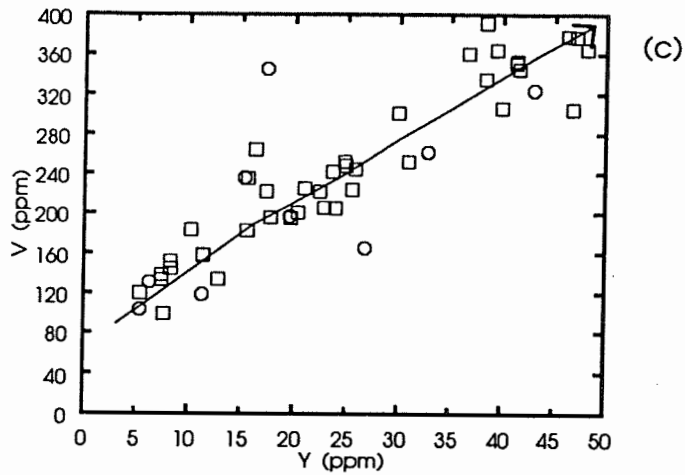
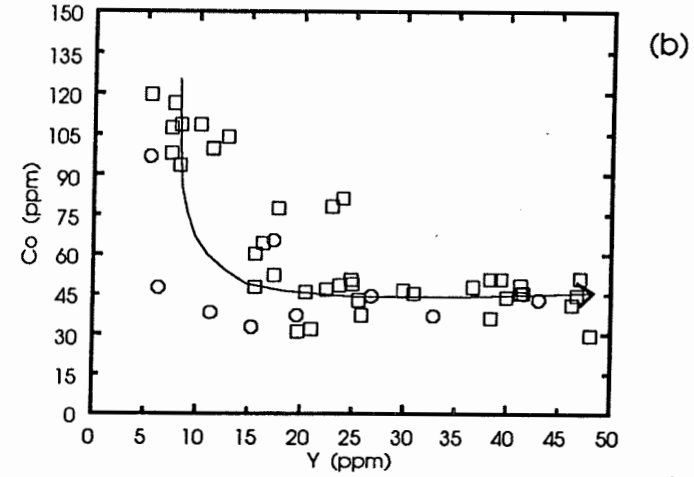
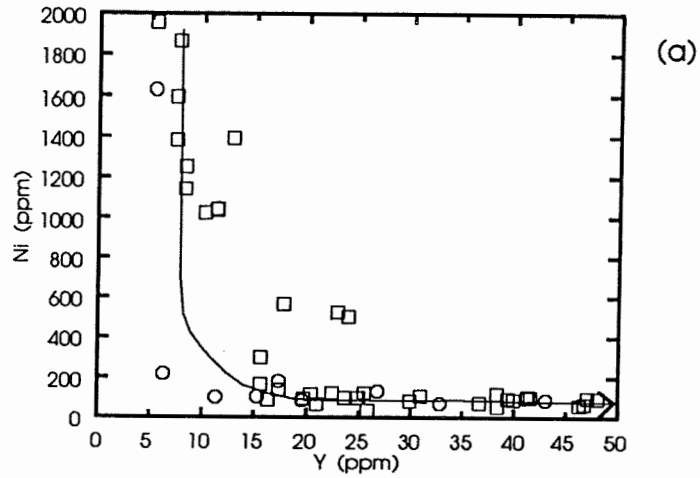


Figure 17. Binary trace-element diagrams for flow rocks of the Val d'Or district. (a) = Ni vs Y, (b) = Co vs Y, (c) = V vs Y, (d) = Sc vs Y. Circles = Southern and Vassan domains (author's data); boxes = Southern, Central and Vassan domains (data from Desrochers, 1994).

Central and Vassan domains (boxes and circles) are related by olivine fractionation and not by mixing of two magma sources or by contamination. This suggestion is reinforced in Figures 17c (V vs Y) and 17d (Sc vs Y) (where V and Sc are ferromagnesian elements controlled by clinopyroxene during fractional crystallization) where the same samples exhibit singular trends, implying a common source for the Southern, Central and Vassan domain rocks.

Contrary to the idea of a common source, Figures 18a and 18b show interesting and contrasting REE profiles for mafic and ultramafic rocks from the Southern, Central and Vassan domains. In Figure 18a, there are two, essentially flat REE profiles (average $[\text{La}/\text{Sm}]_N = 0.7$; average $[\text{La}/\text{Yb}]_N = 0.8$; average $[\text{Sm}/\text{Yb}]_N = 1.1$) which are approximately ten times chondrite level typical of tholeiitic mafic flow rocks. Although these two samples come from a restricted area in Louvicourt Township known to be dominated by tholeiitic rocks (in the vicinity of the Akasaba gold deposit; Lebel, 1987), flattish REE profiles have been also documented by Babineau (1982) and Parent (1985) in the Val d'Or-west/Malartic area. The other profile (3864-91) represents a komatiite sample from the Central domain. In Figure 18b, the REE profiles of other mafic and probably ultramafic samples 3834-91 and 3865-91 are characterized by depleted, flat LREEs (average $[\text{La}/\text{Sm}]_N = 1.0$) and unusually enriched HREEs (average $[\text{La}/\text{Yb}]_N = 0.5$; average $[\text{Sm}/\text{Yb}]_N = 0.5$). Although there are possible analytical problems in analyzing low concentrations of neodymium, the apparent enrichment of HREE is not considered to be an analytical problem at the Centre de Recherches Minérales (Sainte-

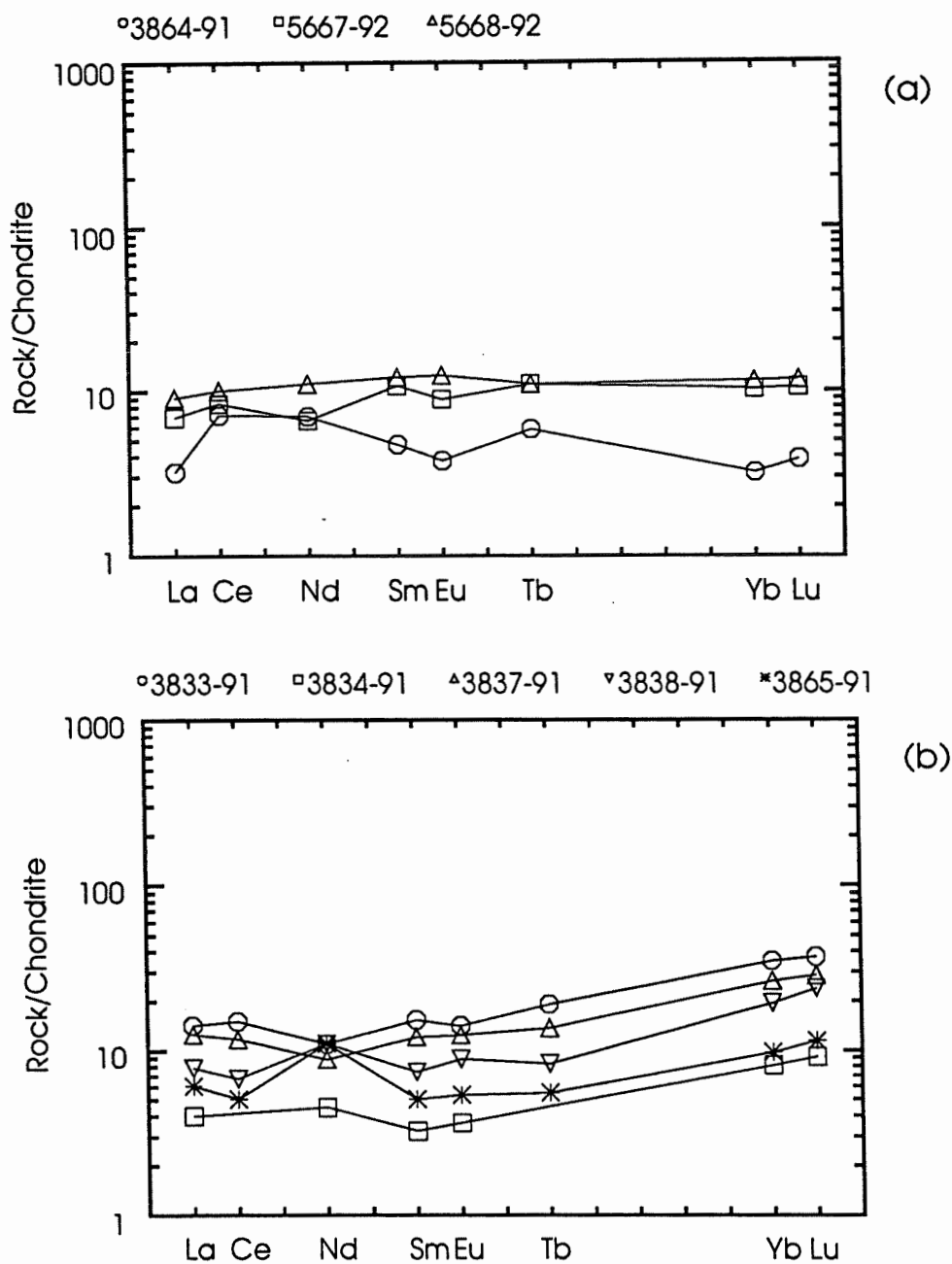


Figure 18. (a) Relatively flat rare-earth element profiles and (b) heavy rare-earth element enriched profiles for flow rocks from the Vassan (sample 3864-91), Central (3833-91, 3834-91, 3837-91) and Southern (3838-91, 3865-91, 5667-92, 5668-92) domains. Elements are normalized to the C1 chondrite (Sun and McDonough, 1989).

Foy, Quebec) because similar profiles for mafic flow rocks from the same area have been noted by Roy (1983) based on analyses done at l'École Polytechnique, Montreal.

Although alteration, resulting in leached LREEs and/or enriched HREEs, cannot be totally ruled out, these two REE patterns could indicate that the mafic flows were derived from two different source regions. Because no common mantle minerals (e.g., olivine, orthopyroxene, clinopyroxene, garnet, spinel) preferentially concentrate LREEs relative to HREEs (Hanson, 1980), the rocks with LREE-depleted patterns (Fig. 18b) may be derived from a mantle source that is itself depleted in LREEs. HREE-enriched/LREE-depleted profiles were also noted by Roy (1983), not only in the mineralized zone of the Kiena mine (just west of Val d'Or), but also in a relatively fresh basalt 300 metres from the mine. This sample, exhibiting undeformed cooling textures, is composed of epidote, actinolite and chlorite and has less than 2 % LOI ($\text{CO}_2 = 0.2$ %). Roy (1983) acknowledged the possibility that alteration is related to mineralization and contributed to a local redistribution of REEs without involving an enrichment or selective alteration of the REEs. In addition, Roy did not observe redeposition of LREEs elsewhere in the mine. Finally, Roy found no correlation between CO_2 and selective alteration of LREEs and he suggested a primary magmatic origin for the HREE-enriched profiles, supported 1) by small differences in the absolute values of the REEs caused by magmatic differentiation (observable on a La versus Yb diagram); and 2) by relatively fresh, undeformed and unmineralized basalts with HREE-enriched profiles similar to those of mineralized rocks from the Kiena mine.

Extended trace-element abundance profiles (Figs. 19a and 19b) support the tholeiitic affinity of the Southern, Central and Vassan domain rocks which share the characteristic of having positive niobium anomalies with respect to thorium and lanthanum, a trait common to mid-Atlantic ridge basalts (MORB) (Sun et al., 1979). These rocks also have positive zirconium anomalies and variable titanium anomalies. As in the calc-alkalic rocks of the Val d'Or domain, strontium has been mobilized, creating positive anomalies atypical of MORB.

In Figure 16a (Y vs Zr), the Val d'Or domain flow rocks have a positive, gently sloping trend, originating in the Y range of normal basalts (≈ 20 ppm). The range of Zr values indicates the degree of fractionation of these calc-alkalic rocks. There does not appear to be any correlation between the P_2O_5 - SiO_2 groupings and the Y-Zr values of these samples. For example, although samples 3856-91, 5655-92, 5671-92 and 5686-92 are all "medium- SiO_2 " samples on the P_2O_5 - SiO_2 diagram (Fig. 12e), they plot in disparate zones in Figure 16a, suggesting either that Y and Zr have been mobilized in some samples or that alteration truly accounts for the "second stage" of SiO_2 increase with decreasing P_2O_5 . All geochemical data from Girault (1986) for flow, pyroclastic and intrusive rocks in Bourlamaque and Louvicourt townships are plotted on a P_2O_5 - SiO_2 diagram (Fig. 20a) showing P_2O_5 decreasing at 68 wt.% SiO_2 , similar to the trend observed in Figure 12e for data from this study. Unfortunately, TiO_2 data from Girault (1986) do not define a clear trend on a TiO_2 - SiO_2 diagram (Fig. 20b) so as to determine at what SiO_2 wt.% titanium decreases.

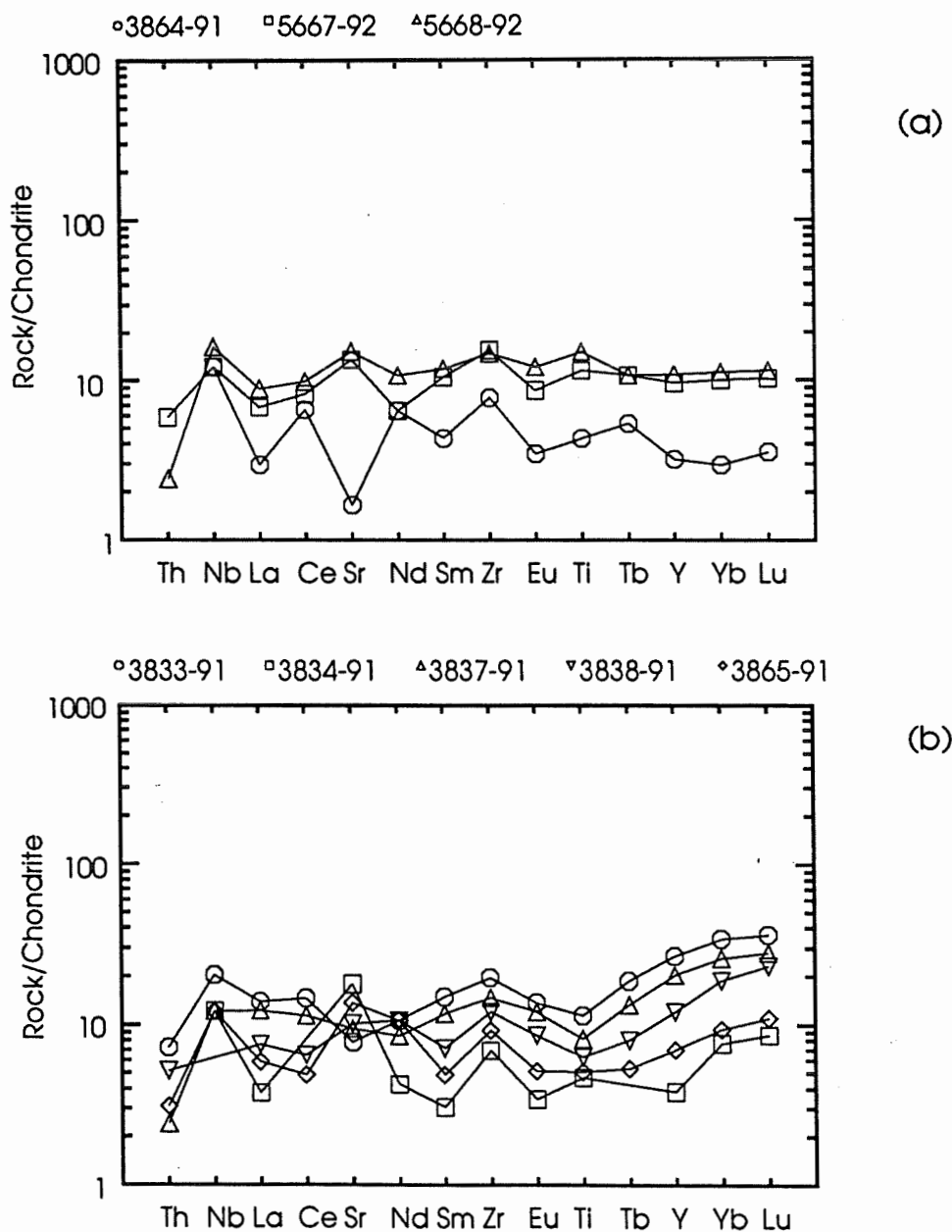


Figure 19. Extended trace-element abundance profiles for flow rocks grouped according to (a) relatively flat REE and (b) HREE-enriched profiles in Figure 18. Samples are from the Vassan (sample 3864-91), Central (3833-92, 3834-91, 3837-91) and Southern (3838-91, 3865-91, 5667-92, 5668-92) domains. Elements, normalized to the C1 chondrite (Sun and McDonough, 1989), exhibit decreasing incompatibilities from left to right.

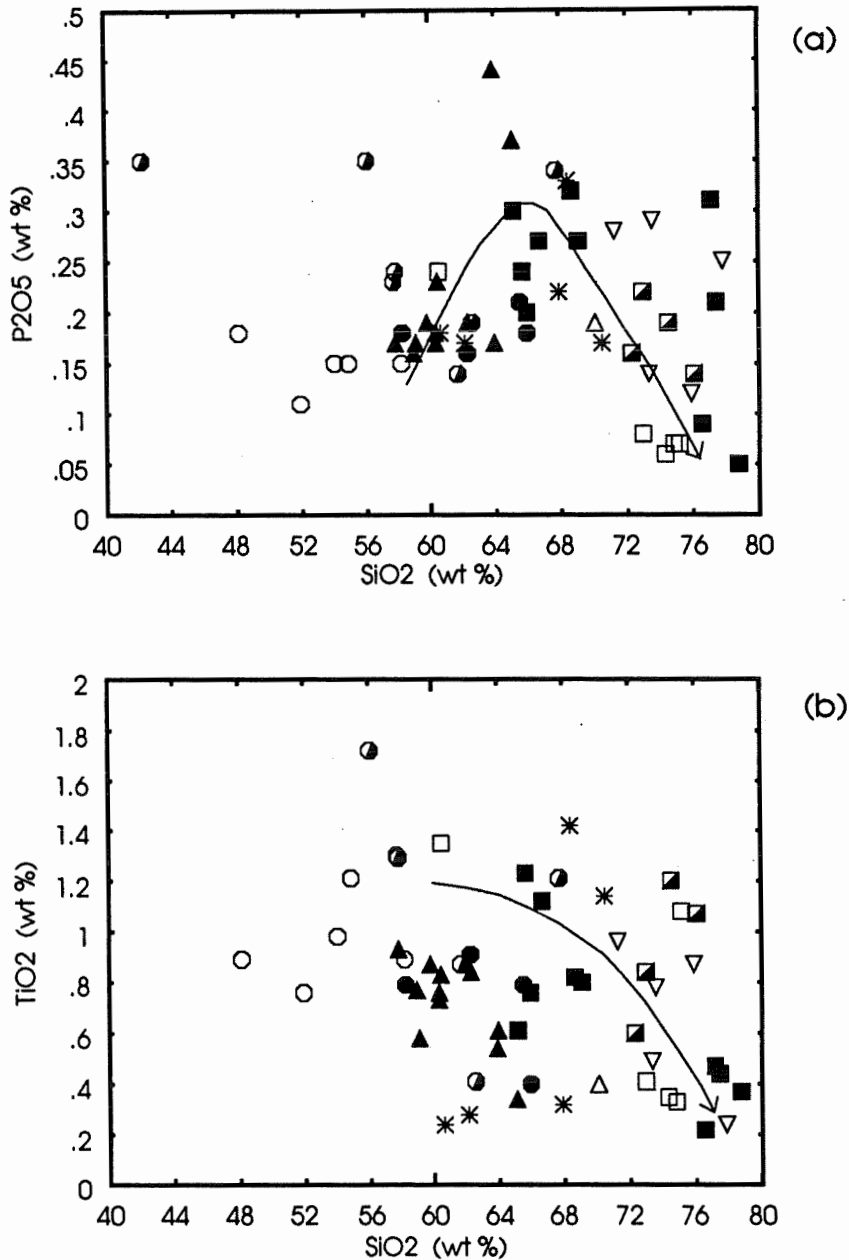


Figure 20. (a) P₂O₅ vs SiO₂ and (b) TiO₂ vs SiO₂ plots for selected rocks sampled by Girault (1986) in the Val d'Or domain. Trends taken from Figures 12d and 12e. Open circle = basalt, half-filled circle = andesite, filled circle = porphyritic lava, open box = rhyolite, half-filled box = rhyolitic pyroclastic block, filled box = dacite, filled upright triangle = diorite sill, open inverted triangle = albite microgranite, asterisk = tuff.

On the Zr/Y versus Zr diagram (Fig. 16b), all Val d'Or domain samples (except 5655-91, 3840-91 and 3841-91) form a trend suggesting a fractional crystallization relationship between these samples. In comparison, on a Zr/Nb versus Zr plot (Fig. 16c), all Val d'Or domain points fall along the zirconium fractionation trend. These observations suggest that the Y values of samples 5655-92, 3840-91 and 3841-91 have been modified so that the Zr/Y values of these samples do not fall along the zirconium fractionation trend. In addition, Finlow-Bates and Stumpfl (1981) state that as a result of several successive hydrothermal alterations related to volcanogenic massive sulphide formation, elements such as Y, Nb and Sc may become extremely mobile. The Val d'Or domain is host to several volcanogenic massive sulphide deposits (see Chapter 3) and has undoubtedly been affected by several hydrothermal events. Therefore, it is possible that Y contents in some samples have been significantly modified.

The most mafic samples from the Val d'Or domain have an average Zr/Y value of 5.9 which is comparable to the 5.4 average value for mafic effusive rocks of calc-alkalic units in the Rouyn-Noranda district (Gélinas et al., 1984). The central eight samples (Fig. 16b) representing intermediate to felsic samples (Table A2.4) have an average Zr/Y value of 8.1 which falls in the range of 6 to 11 for FII felsic rocks associated with Archean volcanogenic massive sulphide deposits (Leshner et al., 1986).

Least-altered geochemical analyses of flow rocks from Bourlamaque and Louvicourt townships were chosen from Girault (1986) and Gaudreau et al. (1986) based

on their volatile contents and normative mineral compositions. These analyses (see Appendix 5, with sample locations given in Figures A5.1 and A5.2) are used in conjunction with data from this study to characterize the Val d'Or domain rocks.

Samples taken by Girault (1986) in Bourlamaque and Louvicourt townships were analyzed for major-element oxides and selected trace-elements such as Zr and Y. CO₂ and LOI information is not available, and the CIPW norms were calculated to evaluate the degree of alteration of the samples. Analyses with no normative corundum were chosen, as well as three mafic flow analyses with less than 2.5 % normative corundum for comparison (Appendix 5).

Five of the nine analyses for Val d'Or Formation flow rocks in Gaudreau et al. (1986) have acceptable LOI and CO₂ values (LOI ≤ 3.8 % and CO₂ ≤ 0.5 %) and are retained. Of these five samples, two do not have normative corundum, and the most felsic sample has only 0.4% normative corundum (Appendix 5).

On a Y versus Zr diagram (Fig. 21), a cluster of Girault's (1986) data, representing samples from a relatively restricted geographic location in the Val d'Or domain (see Fig. A5.1), falls close to the Y/Zr chondritic ratio trend. Three analyses from Gaudreau et al. (1986), representing samples from another geographically restricted location (see Fig. A5.2), also plot in this Y-Zr space. The other points fall far right of this line. Comparison of these data to those of this study (Fig. 16a) suggests: 1) a

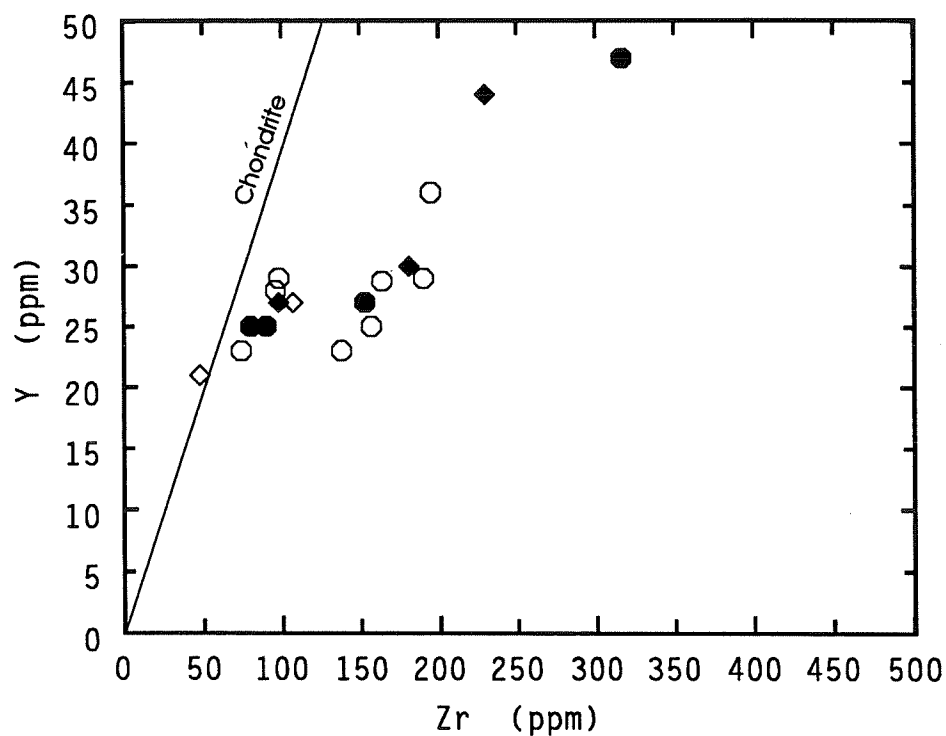


Figure 21. Y versus Zr plot for flow rocks of the Val d'Or domain (data from Girault, 1986 and Gaudreau et al., 1986). Empty diamonds = no normative corundum, full diamonds = with normative corundum (data from Gaudreau et al., 1986); empty circles = no normative corundum, full circles = with normative corundum (data from Girault, 1986).

tholeiitic character for the cluster of points near the Y/Zr chondritic ratio line, 2) a calc-alkalic character for the data points right of the chondritic ratio line, and 3) a relatively immobile character for Zr and Y in these samples because of the coincidence of corundum- and non-corundum-bearing analyses for rocks of tholeiitic and calc-alkalic affinity. Girault's and Gaudreau et al.'s data from restricted geographic areas may suggest 1) that tholeiitic and calc-alkalic rocks are interstratified in the Val d'Or domain, 2) that there are isolated areas of tholeiitic rocks in the Val d'Or domain as windows of underlying Southern domain rocks, following the geotectonic model of Desrochers et al. (1993), or 3) that the current boundaries of the Val d'Or domain need to be better defined.

2.3.3.2 Geochemical Data of Intrusive Rocks

A limited number of intrusive rock samples (6 from the Bourlamaque intrusion; 1 from the Bevcon pluton; 4 from feldspar ± quartz porphyritic rocks; and 11 from mafic intrusions) were taken for comparison from the Val d'Or and Southern domains in Bourlamaque and Louvicourt townships. Twenty-two samples were analyzed for major-element oxides and trace elements and 12 of these samples were analyzed for REE (Tables A2.5 and A2.6). Macroscopic and microscopic descriptions of these rocks are found in Appendix 3. The CO₂, LOI, and corundum data indicate that the majority of these samples have been affected by extensive alteration. However, a greater number of intrusive samples (8 out of 22 or 36 % of the samples), in comparison to the flow rocks (1 out of 16 or only 6 % of the samples), do not have corundum in the norm.

Note that only two of the eight samples without corundum come from the Val d'Or domain, underlining again the widespread alteration of Val d'Or domain rocks.

Excluding the porphyritic rocks, the difference between intrusions from the Southern and Val d'Or domains is highlighted by their distinct trends on a Y versus Zr diagram (Fig. 22). The Southern domain intrusions plot in the same area as the tholeiitic extrusive rocks of the Southern, Central and Vassan domains near the Y/Zr chondritic ratio line (Fig. 16a). Conversely, the Val d'Or domain intrusive rocks plot in the same area as the flow rocks of the same domain. Three of the four porphyritic rocks have relatively low Y values, similar to the quartz-feldspar porphyries from the Lamaque mine (Daigneault et al, 1983) (Fig. 23), and consequently, they do not plot with either the Val d'Or or Southern domain rocks. The other porphyritic sample plots near the calc-alkalic trend, similar to the feldspar porphyries of Daigneault et al. (1983) (Fig. 23).

The REE patterns in Figure 24a for the Bourlamaque intrusion, the Bevcon pluton and the Dunraine sill (a large, mafic sill in Louvicourt Township east of the Dunraine VMS deposit — see Figure 26) suggest a calc-alkalic character for these rocks. They have enriched LREEs ($\text{average(La/Sm)}_N = 2.1$; $\text{average(La/Yb)}_N = 4.3$), weak to negligible europium anomalies, and flat HREE profiles ($\text{average (Sm/Yb)}_N = 2.2$). These patterns are similar to those of Val d'Or domain rocks (Fig. 13), despite the slightly more fractionated LREEs for the intrusions. The profiles for these rocks in the extended trace-element abundance diagrams (Fig. 25) are similar to those for flow rocks

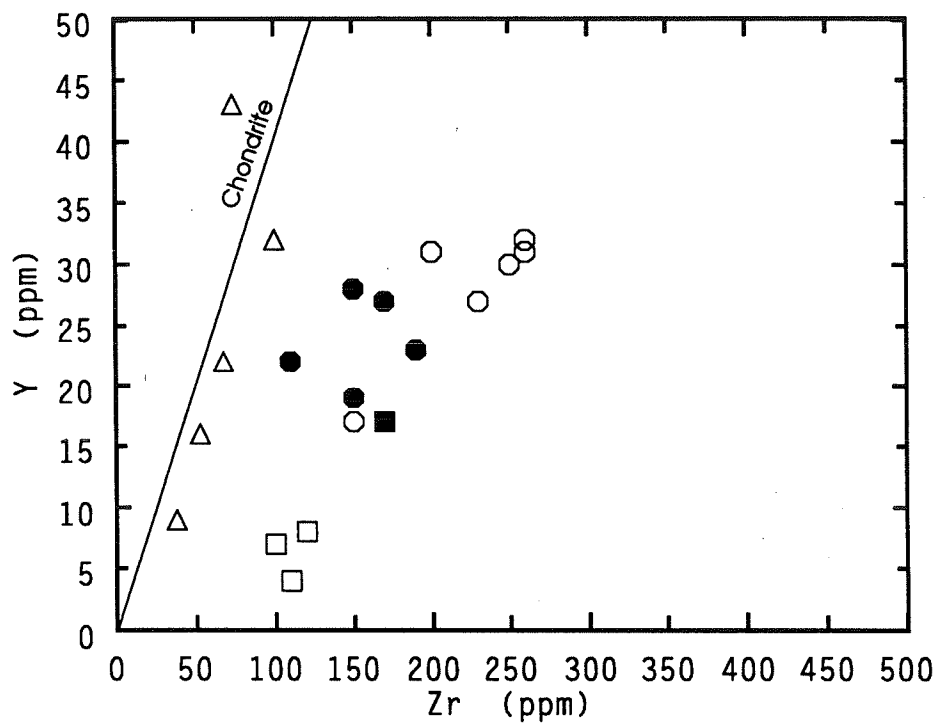
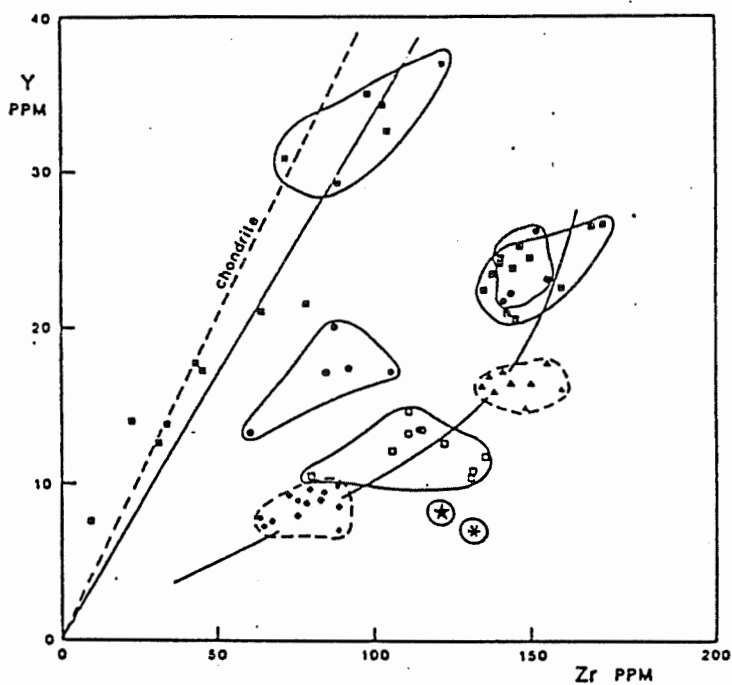


Figure 22. Y versus Zr plot for intrusive rocks of the Val d'Or and Southern domains. Triangles = Southern domain; empty boxes = feldspar±quartz porphyries; full box = feldspar porphyry; empty circles = Val d'Or domain; full circles = Bourlamaque intrusion. Samples not plotted: 5669-92 (triangle: 73 ppm Y, 160 ppm Zr) and 3880-91 (full circle: 34 ppm Y, 1,000 ppm Zr).



- | | |
|----------------------------|---------------------|
| ◆ Quartz feldspar porphyry | ▲ Feldspar porphyry |
| ★ East quartz tonalite | * West tonalite |
| □ Main tonalite | ▣ Main diorite |
| ● No. 5 diorite | ■ No. 4 diorite |

Figure 23 . Y versus Zr plot of porphyries and plugs of the Lamaque mine, Val d'Or (modified after Daigneault et al., 1983).

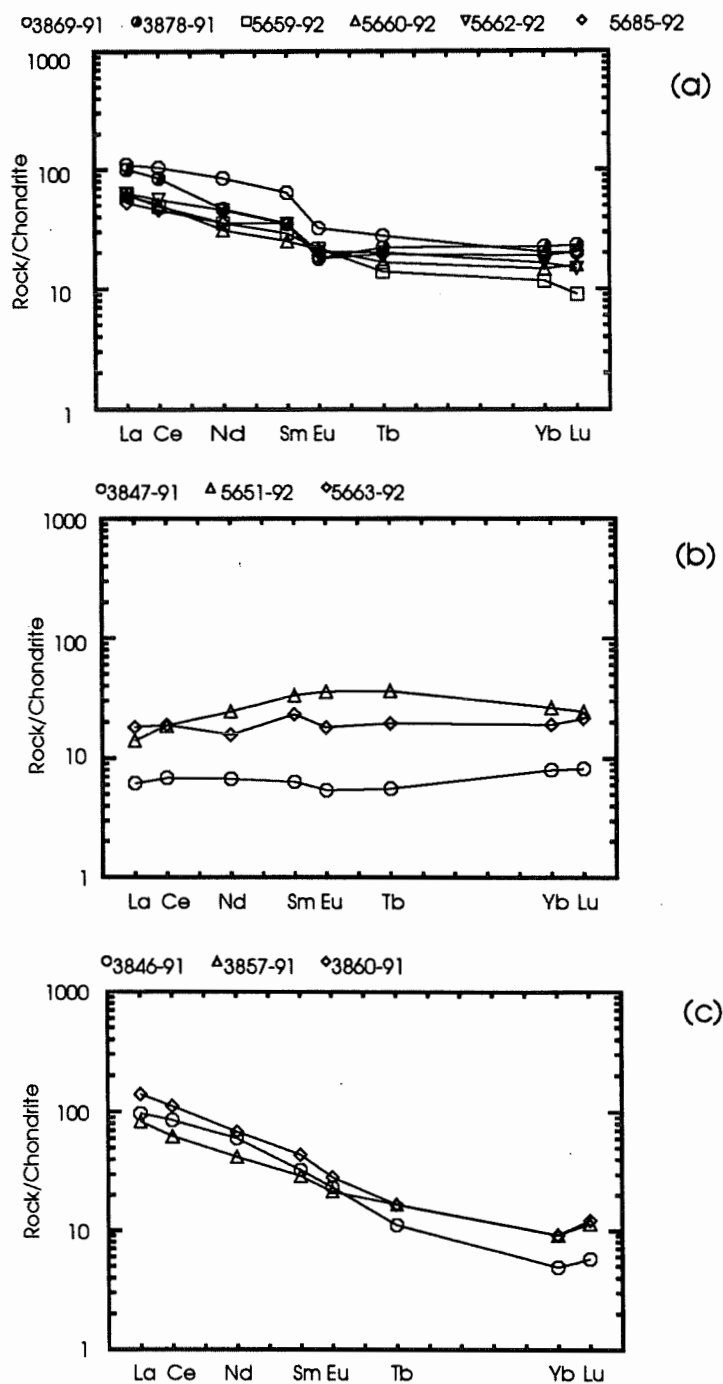


Figure 24. Rare-earth element profiles for intrusive rocks from the (a) Val d'Or and (b) Southern domains; and (c) for two feldspar±quartz porphyries (samples 3846-91; 3857-91) and one gabbroic intrusion (3860-91) from the Val d'Or and Southern domains. Elements are normalized to the C1 chondrite (Sun and McDonough, 1989).

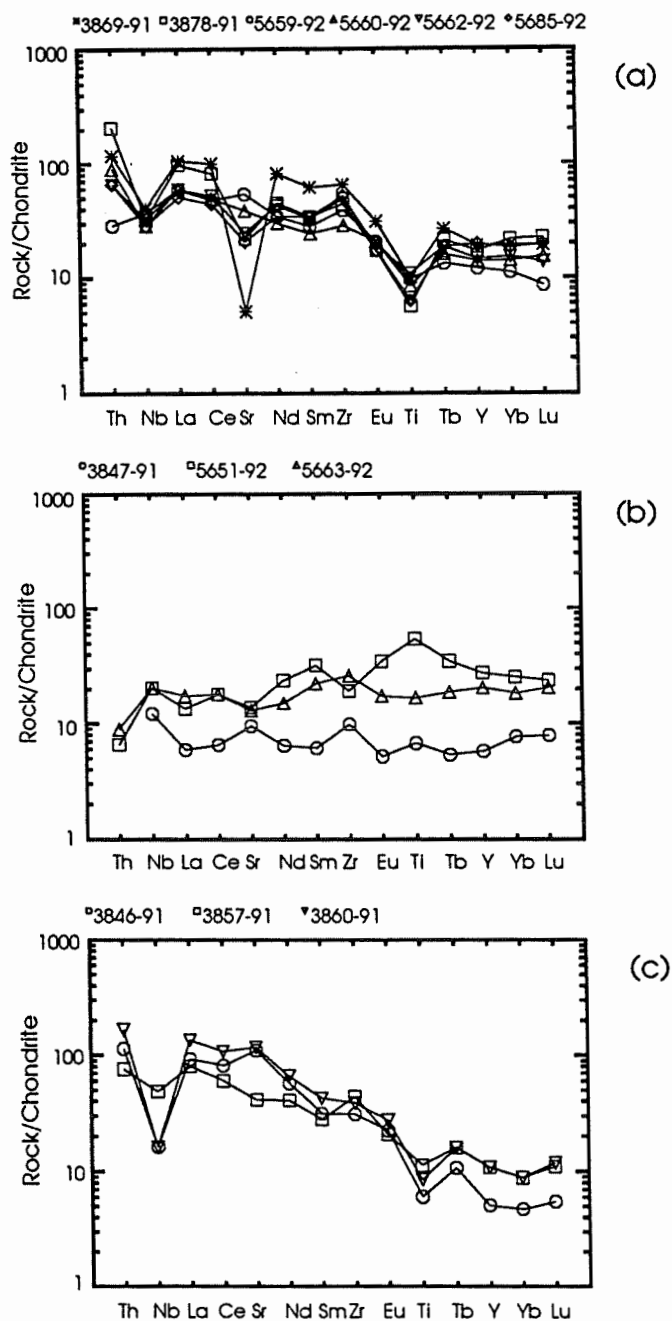


Figure 25. Extended trace-element abundance profiles for intrusive rocks from the (a) Southern and (b) Val d'Or domains; and (c) for two feldspar±quartz porphyries (samples 3846-91; 3857-91) and one gabbroic intrusion (3860-91) from the Val d'Or and Southern domains. Elements, normalized to the C1 chondrite (Sun and McDonough, 1989), exhibit decreasing incompatibilities from left to right.

from the Val d'Or domain (Fig. 14). The similarity of the REE and extended trace-element abundance patterns suggests a cogenetic relationship between these intrusions and Val d'Or domain flow rocks.

These data are comparable to rocks belonging to Group I as defined by Burrows and Spooner (1989). Group I is composed of Bourlamaque intrusion samples and porphyry samples from the Sigma and Lamaque mines (# 5 and # 8 in Fig. 34). According to Burrows and Spooner, these rocks have calc-alkalic characteristics typical of modern island-arc calc-alkalic suites, such as lack of Fe enrichment, Nb and Ti troughs, relatively flat HREE patterns and low Ni and Cr contents. They explain these geochemical characteristics by partial melting of the mantle overlying a subducted slab with high-level fractionation leaving gabbroic cumulates. They judge that their Bourlamaque intrusive data resemble that of recent volcanics in Deception and Bridgeman Islands located on a back-arc spreading axis in the Bransfield Strait, Antarctic peninsula (Tarney et al., 1982). The geochemical characteristics of these recent volcanics are transitional between oceanic basalts and calc-alkalic rocks.

The three mafic intrusions (no corundum in the norm) from the Southern domain have relatively flat REE patterns (Fig. 24b). The patterns of two samples (5663-92 and 3847-91) in the extended trace-element abundance diagram (Fig. 25b) are similar in shape with positive Nb anomalies and negligible Ti anomalies, whereas sample 5651-92 crosses the profile of sample 5663-92 and has a pronounced positive Ti anomaly in

addition to a positive Nb anomaly. These REE and extended trace-element abundance patterns are similar to those for tholeiitic flow rocks from the same region of the Southern domain (Figs. 18a and 19a).

Figure 24c shows REE patterns for one mafic intrusion and two feldspar ± quartz porphyritic rocks. The mafic intrusion (sample 3860-91) and one of the porphyritic rocks (3857-91) come from the same outcrop zone in the Val d'Or domain, whereas the other porphyritic rock comes from the Southern domain. These REE patterns are more fractionated than those for the calc-alkalic rocks, with $(La/Sm)_N$ varying from 2.8 to 3.2, $(La/Yb)_N$ varying from 9.1 to 20, and $(Sm/Yb)_N$ varying from 3.2 to 4.8. The extended trace-element abundance diagram patterns (Fig. 25c) for these rocks, having variably negative Nb and weakly negative Ti anomalies, are generally steep between Nb and Ti and flat between Ti and Lu. These REE and extended-trace element abundance profiles are similar to those of both Groups II and III as determined by Burrows and Spooner (1989). Group II rocks consists of feldspar ± quartz porphyries and albitite dikes from the Hollinger-McIntyre mines (Timmins region, Ontario), which are considered to be post-tectonic but pre-metamorphic (Robert et al., 1983). Group II rocks have enriched LREE abundances, fractionated middle to heavy REEs associated with increased Sr contents, and loss of Eu anomalies relative to Group I. Burrows and Spooner suggest that these rocks were derived from a relatively deep source with plagioclase on the liquidus and probably garnet stable in the residue which resulted in depletion of heavy REEs and relatively high $(La/Yb)_N$ ratios. They equate their geochemical data with those

of typical Archean tonalite-trondhjemite-granodiorite magmas studied by Bickle et al. (1983) and Martin (1986).

Group III rocks of Burrows and Spooner (1989) is composed of rocks from the main, east and west plugs at the former Lamaque mine (see Fig. 34 for location). These intrusions show fractionated LREEs but relatively high and unfractionated HREEs and no Eu anomaly. To explain these trends, Burrows and Spooner suggest a simple fractional crystallization process (hornblende-orthopyroxene-plagioclase), with later perturbations in the REE patterns caused by apatite and titanite crystallization. These rocks have Nb and Ti negative anomalies typical of subduction-related magmas (Thompson et al., 1984).

2.4 SUMMARY AND CONCLUSION

Normative corundum is present in almost all CIPW norm calculations for extrusive and intrusive rocks of the Val d'Or domain, indicating widespread and intense alteration. However, corundum-absent and corundum-bearing rocks behave similarly on a Y versus Zr plot (Fig. 21), suggesting that despite alteration, HFSEs such as Y, Zr, and Nb retain their immobile character in the majority of the rocks sampled.

It has been shown that AFM and AFTiM diagrams for the extrusive flow rocks of the Val d'Or district reliably identify the affinities of these rocks. However, for

altered rocks, such as those in the study area, trace element and REE data can offer more precise information about the geochemical nature of the rocks because these elements commonly retain their immobile character in altered rocks.

Major element oxide diagrams indicate that the flow rocks of the Vassan, Central and Southern domains have komatiitic to tholeiitic affinities. Although the majority of these samples have chondritic Y/Zr ratios, a small group of basalts have high Y contents, suggesting either a slight mobility of Y or, more likely, a control of Y by clinopyroxene in these samples. All of these rocks share common positive Nb and Zr anomalies. Ni-Y, Co-Y, V-Y and Sc-Y plots suggest that flow rocks from these domains are magmatically related. However, contrasting REE profiles, i.e., flat REEs versus LREE-depleted/HREE-enriched profiles, suggest that the mafic flow rocks of the Central and Southern domains come from two distinct mantle sources: a depleted tholeiitic mantle source, and a depleted tholeiitic mantle source which is also LREE-depleted. Although these data are consistent with an oceanic plateau environment (Desrochers et al., 1993), the author suggests that further characterization is needed of HREE-enriched rocks, as well as mapping of their extent in the field and their physical relationship to those rocks with more typical flat-REE tholeiitic profiles.

Regardless of the ubiquitous and intense alteration that affected Val d'Or domain rocks, magmatic trends, based on major-element behaviour, are still evident, and trace-element and REE data (negative Nb and Ti and positive Zr anomalies, LREE-enriched)

are suggestive of a calc-alkalic affinity for these rocks. Intrusive and extrusive rocks of this domain have similar geochemical characteristics suggesting a cogenetic relationship. Also, given that the geochemical data of intrusive and extrusive rocks of the Val d'Or domain are similar to those of Group I as defined by Burrows and Spooner (1989), the geochemical and geotectonic interpretation of Group I rocks may apply to all Val d'Or domain rocks. The implications of this calc-alkalic affinity to the interpretation of a geotectonic environment suitable for VMS-type mineralization is commented upon in Chapter 3.

CHAPTER 3

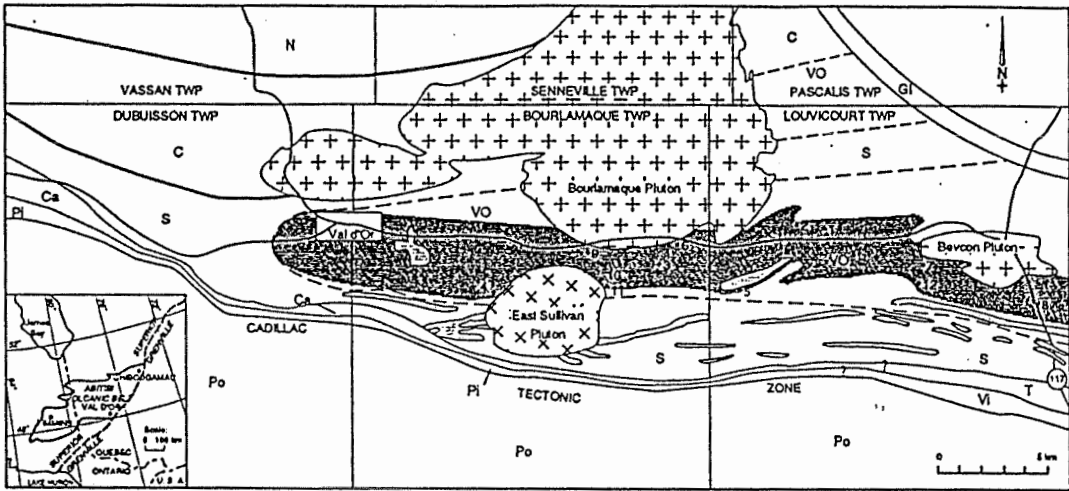
VOLCANOGENIC MASSIVE SULPHIDE MODELLING

FOR THE BOURLAMAQUE AND LOUVICOURT TOWNSHIPS

3.1 VOLCANOGENIC MASSIVE SULPHIDE MINERALIZATION IN THE STUDY AREA.

In this chapter, a summary is presented of the characteristics at the mine scale of the known VMS deposits and prospects located in the Central Pyroclastic Belt (refer to section 1.3) and a discussion covers the Mattabi-subtype classification (Morton and Franklin, 1987) of these deposits. This examination is followed by a review of the mechanics of the heat-driven convection-cell model for the genesis of VMS deposits. Then, modern analogues to the Archean VMS deposits are presented. Finally, the Bourlamaque and Louvicourt townships are taken as a test area in which an attempt is made to identify the required elements for VMS formation.

Figure 26 shows the location of the major and minor base-metal sulphide deposits in the Central Pyroclastic Belt, and Table 1 summarizes their characteristics, emphasizing the importance of felsic fragmental rocks as host lithologies for these deposits. Mineralization occurs as stratiform lenses, and at the Louvicourt, Louvem and Manitou-Barvue deposits, stockwork zones have also been identified. Broad conformable alteration zones extending laterally in the footwall of the massive sulphide mineralization



- | | |
|---|--|
| <p>V VASSAN DOMAIN
Komatiites, basalts.</p> <p>C CENTRAL DOMAIN
Basalts, komatiites, minor sediments.</p> <p>S SOUTHERN DOMAIN
Intermediate to mafic flows, intermediate volcanics, minor komatiitic flows.</p> <p>VO VAL D'OR DOMAIN
Intermediate volcanics composed of polygenic fragments, mafic to felsic flows and breccias.</p> <p>CP CENTRAL PYROCLASTIC BELT</p> <p>Ca CADILLAC GROUP
Greywackes, siltstones, conglomerates.</p> <p>PI PICHÉ GROUP
West of Val d'Or: mafic to ultramafic flows, east of Val d'Or: ultramafic to felsic schists (flow and volcanoclastic material).</p> | <p>T TRIVIO GROUP
Tuffaceous sediments, greywackes, conglomerates, flow material.</p> <p>VI VILLEBON GROUP
Mafic flows, a few ultramafic flows.</p> <p>Po PONTIAC GROUP
Greywackes, pelites.</p> <p>GI GARDEN ISLAND GROUP
Greywackes, schists, conglomerates.</p> <p>M Mafic to intermediate siltstone or intrusions.</p> <p>++ Synvolcanic granodiorite-quartz diorite intrusion.</p> <p>xx Post-tectonic monzonitic intrusion.</p> |
|---|--|

Figure 26. Location map of major and minor base-metal sulphide deposits in the east Val d'Or region, Quebec; modified after Sauvé et al. (1986), Chartrand (1991) and Desrochers et al. (1993). Numbers correspond to deposits described in Table 1.

Table 1. Summary of characteristics of major and minor base metal sulphide deposits in the Val d'Or district (modified after Chartrand (1991) and the author's compilation) (See following page for superscript explanations).

NAME	LOUVICOURT	LOUVEM	Manitou-Barvue
Status	to open in 1994	Past Producer	Past Producer
Symbol in Fig. 26.	1	2	3
Size (Mt) ¹	15.7 ³	1.599	11.222
Cu ² (t x 1000)	534 ³	18	33
Zn ² (t x 1000)	345 ³	60	300
Au ² (kg)	14,130 ³	1,170	9,265
Ag ² (kg)	486,700 ³	31,375	1,104
Host Rocks	Felsic lapilli and ash tuff, cherty exhalite, felsic hyaloclastite and breccia.	Coarse- to fine-grained volcanoclastic rock.	Rhyolitic tuff.
Morphology	Several tabular lenses of massive and semi-massive sulphide; underlying Cu-stockwork zones.	Several tabular lenses of massive and semi-massive sulphide; a few Cu-stockwork zones.	Cylindrical Cu-stockwork zone, rotated parallel to stratigraphy; stratiform Zn zone hosting several massive sulphide lenses.
Ore Mineralogy and Zonation ⁴	Py-Cp-Sp dominant, Cu/Zn decreases upward & outward; Au-rich.	Py-Po-Sp-Cp dominant; deposit as a whole is Cu/Zn zoned.	Py-Sp-Cp dominant, some Gn; deposit as a whole is zoned.
Alteration	Intense Mg-chloritization associated with stockwork sulphides; sericitization, Fe carbonatization, and silicification; some chloritoid and garnet.	Cu-stockwork zones are Mg-chloritized; sericitization, carbonatization and silicification; minor chloritoid in ash tuff.	Cu-stockwork zone is Mg-chloritized; sericitization and silicification associated with Zn mineralization; Fe carbonatization noted.
References	Bubar et al. (1989); Mannard and Bubar (1991); The Northern Miner (1994).	Raymond (1983); Spitz & Darling (1973).	Robert (1980).

Table 1. Summary of characteristics of major and minor base metal sulphide deposits in the Val d'Or district (modified after Chartrand (1991) and the author's compilation) (continued).

NAME	EAST SULLIVAN	DUNRAINE	QUEBEC-MANITOU
Status	Past Producer	Past Producer	Deposit
Symbol in Figure 26.	4	5	6
Size (Mt) ¹	14.952	0.255	0.487
Cu ² (t x 1000)	141	4	6.4
Zn ² (t x 1000)	73	0	N.A.
Au ² (kg)	3,683	46	N.A.
Ag ² (kg)	119,000	887	N.A.
Host Rocks	Felsic lapilli tuff and tuff.	Felsic tuff, tuff breccia and flow breccia.	Tuff.
Morphology	16 massive and semi-massive lenses and accumulations of veinlet sulphides.	Several semi-massive and veinlet zones.	En echelon stratiform masses over a distance of 550 m.
Ore Mineralogy and Zonation ⁴	Cp-Po dominant in central area of ore zone; Py-Sp dominant in peripheral ore zone.	Py-Cp dominant.	Disseminations and veinlets of Cp-Sp-Au-Ag-Py.
Alteration ⁴	Cp-Po orebodies associated with chloritization, Sp-Py orebodies associated with sericitization; silification, chloritoid common; some garnet.	Chloritization dominant.	Sericitization and chloritization.
References	Assad (1958).	Latulippe (1976).	M.E.R.Q. microfiche deposit # 32C/4-77.

¹- Mt: million metric tonnes; values compiled from Couture (1991) except for the Louvicourt and Quebec-Manitou (from the M.E.R.Q. microfiche #32C/4-77) deposits.

²- Values compiled from Couture (1991).

³- Values from The Northern Miner (1994).

⁴- Py: pyrite; Cp: chalcopyrite; Sp: sphalerite; Po: pyrrhotite; Gn: galena; Mn: magnetite.

N.A.- Not applicable.

Table 1. Summary of characteristics of major and minor base metal sulphide deposits in the Val d'Or district (modified after Chartrand, 1991 and the author's compilation) (end).

NAME	ABITIBI COPPER	BRITT	LAVALIE
Status	Deposit	Prospect	Prospect
Symbol in Figure 26.	7	8	9
Host Rocks	Felsic volcanic rocks.	Volcaniclastic rocks.	Sheared tuff and tuff breccia.
Morphology	Stratiform, lensoid deposit; 105-120 m long, 18.28 m wide, up to 244 m deep.	Stratiform mass measuring a few tens of meters long and up to 6 m wide.	Stratiform mass.
Ore Mineralogy and Zonation ¹	Cp-Sp-Au-Mn-Py-Po disseminated.	Cp-Au-Sp-Py.	Disseminated Py-Sp-Ag-Au.
Alteration	Unknown.	Chloritization noted in the area.	Sericitization noted in the area.
References	M.E.R.Q. microfiche deposit # 32C/3-29.	M.E.R.Q. microfiche deposit # 32C/3-36.	M.E.R.Q. microfiche deposit # 32C/4-70.

NAME	ANNAMAQUE	VANKIRK	KENCOURT
Status	Prospect	Prospect	Prospect
Symbol in Figure 26.	10	11	12
Host Rocks	Tuff.	Tuff between andesitic flows.	Volcaniclastic rocks.
Morphology	Unknown.	Stratiform mass.	Stratabound.
Ore Mineralogy and Zonation ¹	Massive and disseminated Py-Po-Cp-Sp.	Disseminated Cp-Au-Ag-Py.	Disseminations of Cp-Sp-Mn.
Alteration	Unknown.	Unknown.	Unknown.
Reference	M.E.R.Q. microfiche deposit # 32C/4-71.	M.E.R.Q. microfiche deposit # 32C/4-72.	M.E.R.Q. microfiche deposit # 32C/3-26.

¹- Py: pyrite; Cp: chalcopyrite; Sp: sphalerite; Po: pyrrhotite; Gn: galena; Mn: magnetite.

are recognized at the Louvem and Louvicourt deposits. Chloritization and sericitization are typical alterations associated with all deposits. In addition, iron carbonate is noted at the Louvicourt, Louvem and Manitou-Barvue deposits, and chloritoid (iron aluminosilicate) is found at the Louvicourt, Louvem and East Sullivan deposits. Chalcopyrite and sphalerite are the common, abundant ore minerals, accompanied mainly by pyrite with or without pyrrhotite. Silver, gold and galena may be present in minor amounts.

Several geochemical studies on rocks in the study area (see section 2.2) suggest that the rocks of the Central Pyroclastic Belt were affected by intense, hydrothermal alteration which resulted in widespread alkali depletion and peraluminous signatures for these rocks. New geochemical data presented in section 2.3 are in accord with this suggestion.

Spitz and Darling (1978) observed at the Louvem mine that the longitudinal orebody and the associated, symmetrical alteration at the Louvem mine are generally conformable with the enclosing, fragmental strata. Alteration changes from dominantly chloritic to the west to dominantly pyritic toward the east. Noting a zinc deposit in the same fragmental layer east of the copper deposit (i.e., further downstream in the subsurface hydrothermal system), Spitz and Darling (1978) suggested, by analogy with chloritic alteration pipes underlying pyritic volcanogenic deposits, that fluid flowed from west to east longitudinally along the fragmental layer.

3.2 VOLCANOGENIC MASSIVE SULPHIDE CLASSIFICATION

As described below, the VMS deposits of the Val d'Or mining camp may be classified with the copper-zinc compositional group as defined by Franklin et al. (1981), and they are similar to the Mattabi-subtype deposits, following the two-fold classification of Archean VMS deposits proposed by Morton and Franklin (1987).

Mattabi-subtype deposits (see Noranda-subtype, following page) are characterized by 1) relatively abundant felsic fragmental volcanic rocks, 2) relatively broad, poorly-defined alteration pipes, 3) large, well-developed, semi-conformable alteration zones, and 4) iron carbonate and/or chloritoid in the alteration pipes and/or alteration zones. Although not a cited characteristic of Mattabi-subtype mineralization, Franklin (1986) also noted that several deposits of this class had relatively high Pb/Zn ratios in comparison to other Cu-Zn deposits.

Based on the trace-element geochemistry of ore-associated versus barren felsic metavolcanic rocks from the Superior Province, Leshner et al. (1986) classify felsic samples from the Mattabi mine and surrounding Sturgeon Lake area as FII rhyodacites and rhyolites characterized by gently sloping REE patterns ($[La/Yb]_N = 2-6$), with variable Eu anomalies ($Eu/Eu^* = 0.35-1.4$), moderate Zr/Y values (6-11) and intermediate abundances of high field strength elements (HFSE) and Sr. Preliminary investigations into ore-associated felsic metavolcanic rocks outside of the Superior

Province suggest that the majority of these rocks are FII type (Lesher et al., 1986).

It was first thought that the volcanic rocks of Mattabi-subtype deposits were emplaced at relatively shallow water depths, i.e., less than 500 metres (D.A. Groves, 1984; D.A. Groves et al., 1984). In this Mattabi-subtype environment, low hydrostatic pressures would have allowed more widespread hydrofracturing of the rocks by ascending fluids, perhaps also explaining the relatively diffuse nature of their alteration pipes (Morton and Franklin, 1987). In addition, the abundance of fragmental rocks expected to have good permeabilities would tend to favour the formation of a broad, gradational alteration zone (Franklin, 1986). Thus, initial detailed studies of several Mattabi-subtype deposits have suggested that the volcanoclastic rocks formed in relatively shallow subaqueous and/or subaerial environments as a result of hydrovolcanic eruptions (Morton and Franklin (1987) and references therein). However, further studies by Morton et al. (1991) show that the bedded ash-flow tuff hosting the Mattabi massive sulphide deposit was erupted and deposited at water depths of 500 to 800 metres, as explained below.

Conversely, the **Noranda-subtype** of VMS deposits are characterized by 1) relatively high abundances of mafic and felsic flows and hyaloclastite, 2) well-developed alteration pipes, and 3) poorly defined semi-conformable alteration zones consisting of patches and lenses of highly altered rocks. Contrary to Mattabi-subtype deposits, Noranda-subtype deposits contain little to no carbonate, and Gibson et al. (1986) suggest that the volcanic rocks were formed at water depths greater than 500 metres.

3.2.1 Significance of Water Depth

It is apparent that a particularly crucial factor in the two-fold classification of VMS deposits by Morton and Franklin (1987) is the relative depth of water at which the deposits formed, which may play a major role in determining 1) the morphologies of the massive deposits and their stockworks, 2) the alterations associated with deposits, and 3) the host-rock lithologies to some extent.

Although Morton and Franklin's classification is widely accepted, the nature of the fragmental rocks of Mattabi-subtype deposits and the estimation of water depth are disputed. Eruption and deposition of the bedded Mattabi ash-flow tuff are considered to have occurred in submarine caldera complexes at water depths of 500 to 800 metres (Morton et al., 1991), based on the presence of well-vesiculated and variably-quenched pumice and on the need for ambient water pressures significantly lower than the critical pressure of water in order that subaqueous pyroclastic eruptions may occur (McBirney, 1963).

The strongest supporting arguments given by Morton et al. (1991) for the subaqueous eruption and emplacement of the Mattabi ash-flow tuff are 1) the lateral and vertical homogeneity of the tuff units, 2) the lack of interbedded epiclastic material, 3) the small percentage of lithic fragments present, and 4) the pronounced geochemical zonation exhibited by individual flow units, a characteristic inherited from the magma and not from the flow movement. However, Yamada (1984) states that some subaqueous

pyroclastic flow deposits are exogenous in that they formed elsewhere and were subsequently transported to the present environment (e.g., they may have erupted on land or in shallow water and may have flowed into a deep-water environment). As an example, Car and Ayres (1991) have interpreted a thick, dacitic Precambrian debris flow from the Lake of the Woods area in Ontario as a subaqueous debris flow deposit. For many researchers (e.g., Cas, 1992; Fisher, 1984; Yamada, 1984), the recognition of subaqueously-erupted pyroclastic flow deposits is debatable. Cas (1992) concludes that much of the volcanoclastic material hosting VMS deposits are in fact autobreccias and hyaloclastites which may represent huge volumes of debris.

Furthermore, work by Chartrand (1991) in the Central Pyroclastic Belt east of Val d'Or suggests that the amount of pyroclastic material has been over-estimated and that flow breccia and quench-fragmented hyaloclastite are at least locally important. Chartrand also suggests that massive sulphide bodies in the Val d'Or camp are associated with felsic cryptodomes, their associated autobreccia and hyaloclastite. These observations, in addition to the fact that mapping in this area is frustrated by deformation, suggest that subaqueously-erupted pyroclastic flow deposits in the Val d'Or camp are difficult to confirm. Therefore, the pyroclastic units in the Mattabi mine area could also be re-interpreted as subaerial pyroclastic flows that were deposited subaqueously. In either case, the VMS mineralization was deposited in a subaqueous environment.

The Scuddles VMS deposit in the Golden Grove belt of the western Yilgarn craton, Australia (Fig. 27), is an Archean deposit having many similarities to Matabi mineralization except for the interpreted water depth (Barley, 1992; Whitford and Ashley, 1992). Mineralization occurs as two massive Zn-Cu sulphide lenses underlain by a stratabound stockwork of pyrite-chalcopyrite mineralization. Host rocks in the stockwork zone are intensely altered to iron-rich chlorite and carbonates, and overlie a more widespread zone of pervasive stratabound quartz-chlorite-sericite-carbonate-sulphide alteration. Mineralization occurs in calc-alkalic pyroclastic and epiclastic sedimentary rocks interpreted to have been deposited in a deep ($> 1,000$ m) submarine environment, based on a detailed reconstruction of the mineralized volcano-sedimentary sequence (Clifford, 1987). Despite the many geochemical and physical similarities between the Scuddles and Matabi deposits, the interpreted water depth for the Scuddles deposit exceeds that expected for the Matabi classification of Morton and Franklin (1987), suggesting that water depth is perhaps not as crucial as initially proposed.

Additional constraints on the depth of VMS emplacement may be gathered from the mechanisms of sulphide precipitation. Boiling, commonly causing ore-fluid temperatures to decrease, is thought to be an important cause of sulphide precipitation in stockwork deposits below the seafloor (Franklin et al., 1981; Henley and Ellis, 1983; Drummond and Ohmoto, 1985). Figure 28 shows the relationship between temperature and water column depth for boiling aqueous liquids. In addition, for a given temperature, increasing salinity decreases the depth of boiling. To prevent boiling and

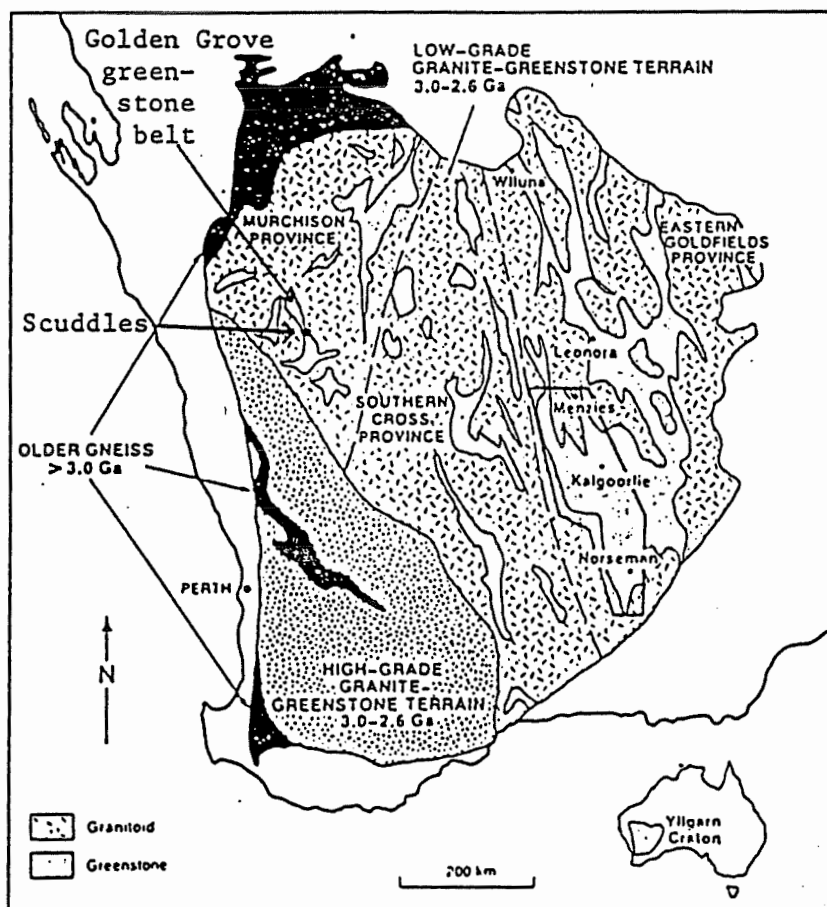


Figure 27. General geologic map of the Yilgarn Craton, Australia with location of the Scuddles VMS deposit in the Golden Grove greenstone belt (modified after Swager et al., 1992).

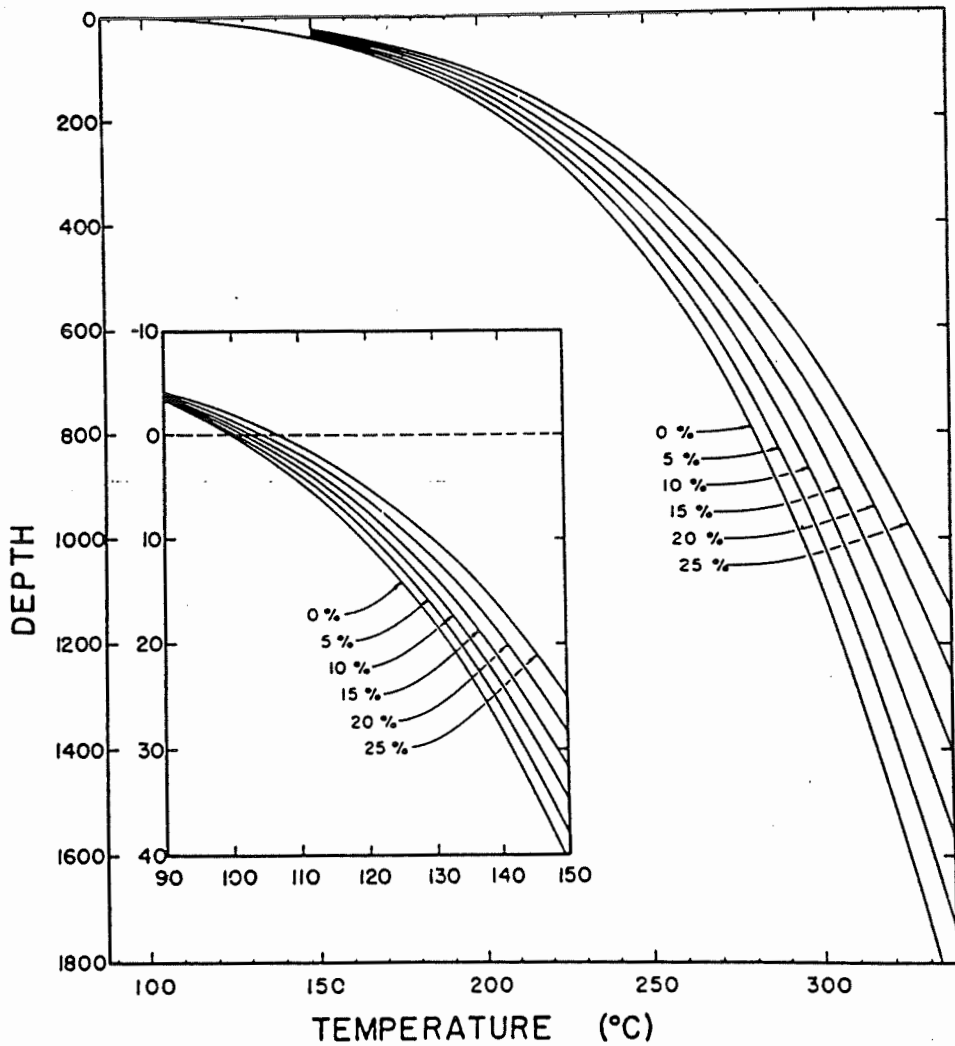


Figure 28. Boiling point curves for H_2O liquid (0 wt. percent salts) and for brines of constant composition given in wt. percent NaCl. The insert expands the relations between $100^\circ C$ and $150^\circ C$. The temperature at 0 metres for each curve is the boiling point for the liquid at 1.013 bars (1.0 atm) load pressure which is equivalent to atmospheric pressure at sea level. The uncertainty is contained within the width of the lines (original curves from Haas, 1971).

promote massive sulphide accumulation on the seafloor, a sufficient hydrostatic pressure must be present, requiring a minimum water column of approximately 500 metres (Drummond and Ohmoto, 1985). This water depth matches the general water depth below which explosive volcanism is not thought to occur and hence massive ores may form directly above the exhalative vent.

It is also noteworthy that the degree of vesicularity of flow rocks may be used erroneously to interpret and estimate the depth of extrusion (Moore, 1965, 1979; Moore and Schilling, 1973). Although some studies (e.g., Dimroth et al., 1978; Staudigel and Schmincke, 1984) have attributed upward-increasing vesicularity in pillow piles to the growth of the lava pile in increasingly shallower, lower-pressure water conditions, highly vesicular textures have been noted in deep abyssal basalts such as in the Hokuroku district, in the Mariana trench, in the East Scotia Sea and in the Shikoku basin (Dudás, 1983). The water content of the extruded magma may need to be taken into consideration. Calculations indicate, for example, that vesiculated Kuroko basalts could have formed at water depths up to 4,000 metres at total H₂O contents of 2.3 wt. % (Dudás, 1983). For comparison, vesiculated Kuroko basalts erupted at water depths of 1,000 and 500 metres would have needed total H₂O contents of only 0.81 wt. % and 0.38 wt. %, respectively.

Irrespective of this consideration, there are basic factors such as subvolcanic intrusions and tensional rift-type environments, and secondary aspects such as deep,

penetrating faults, "caps" to the hydrothermal reaction zones, implied sources of fluids and metals, chemical reactions causing alteration, and mechanisms for precipitating sulphides which are common to both the Noranda-subtype and Mattabi-subtype deposits as well as to modern seafloor VMS deposits. These features are discussed further in the following section.

3.3 HYDROTHERMAL CONVECTION-CELL MODEL

3.3.1 Introduction

Current ideas on ancient VMS formation are influenced greatly by studies of modern seafloor hydrothermal emanations which have greatly advanced our understanding of hydrothermal sulphide accumulation and geochemistry. Supported largely by these studies, and by geochemical and isotopic studies on fossil VMS deposits, the hydrothermal convection-cell model is the most widely accepted explanation for both modern and ancient massive sulphide deposition. Other models, such as magmatic hydrothermal (Urabe and Sato, 1978; Henley and Thornley, 1979; Sawkins, 1982; 1986; Stanton, 1991; Urabe and Marumo, 1991) and the stratal aquifer (Lydon, 1988) model have their own merits and may better describe and explain certain VMS deposits, as described below.

In brief, the **magmatic hydrothermal model** suggests that metal-bearing fluids are degassed from a crystallizing magma chamber and mix with abundant convecting

seawater (Henley and Thornley, 1979; Sawkins, 1982, 1986; Stanton, 1991). Metalliferous fluids are thought to be released during a particular stage of crystallization and differentiation in a subvolcanic magma chamber. Stanton (1991) has examined the incorporation of base metals as well as Ba and Sr into various silicate minerals and suggests that progressive crystallization and magmatic differentiation are important processes that supply metals to ore-forming environments. The contribution of some base metals from country rocks, due to leaching by convecting modified seawater, is acknowledged, but is not considered the major source of metals.

As described by Lydon (1988), the **stratal aquifer model** suggests that ore fluids originate from pore fluids in porous rock units (i.e., aquifers) and they are prevented from rising to the seafloor surface by impervious units (i.e., caprocks). The low water-rock ratio of the aquifer results in high metal concentrations in the hydrothermal solution caused by leaching of the aquifer rocks. Progressive burial of the aquifer results in pore-fluid temperatures rising along the geothermal gradient which may be abnormal due to extensional tectonics and pressures rising above hydrostatic or possibly exceeding lithostatic pressures. Large quantities of over-pressured fluids rise quickly to the surface via fracture zones, possibly created by tectonic activity.

Lydon (1988) reminds us that it may be erroneous to explain all VMS deposits with one model. By the same token, it may be difficult or impossible to classify all Cu-Zn deposits as Noranda-subtype or Mattabi-subtype deposits. Nevertheless, the

convection-cell model explains most characteristics of VMS deposits. The following discussion is a summary of the required elements of the convection-cell model for VMS formation (Fig. 29): an oceanic environment, a heat source, an extensional fracture system, a cap to the hydrothermal reaction zone, a source of fluids and metals, chemical reactions causing alteration, and mechanisms for precipitating and accumulating sulphides. These elements are readily formed in a rifting oceanic crust environment.

3.3.2 Oceanic Environment

A tensional crustal regime is a favourable environment in which isolated rift basins may form and VMS accumulation may occur. More specifically, an island arc, a back arc, a propagating rift or a subducting rift scenario are all possible environments in which such rifting may occur and where VMS mineralization may be preserved.

3.3.3 Heat Source

A large focussed heat source is needed to supply sufficient heat to generate buoyant, convecting fluids. These fluids must be sufficiently hot to cause alteration reactions leading to acidic conditions favourable to the leaching of base metals, particularly copper and zinc, from the country rocks. The heat source is generally considered to be that of primitive magmas and their derivatives which rise along the axes of rifting oceanic crust. The high-level intrusions which directly circulate the ore-forming fluids are considered to be sill-like subvolcanic bodies.

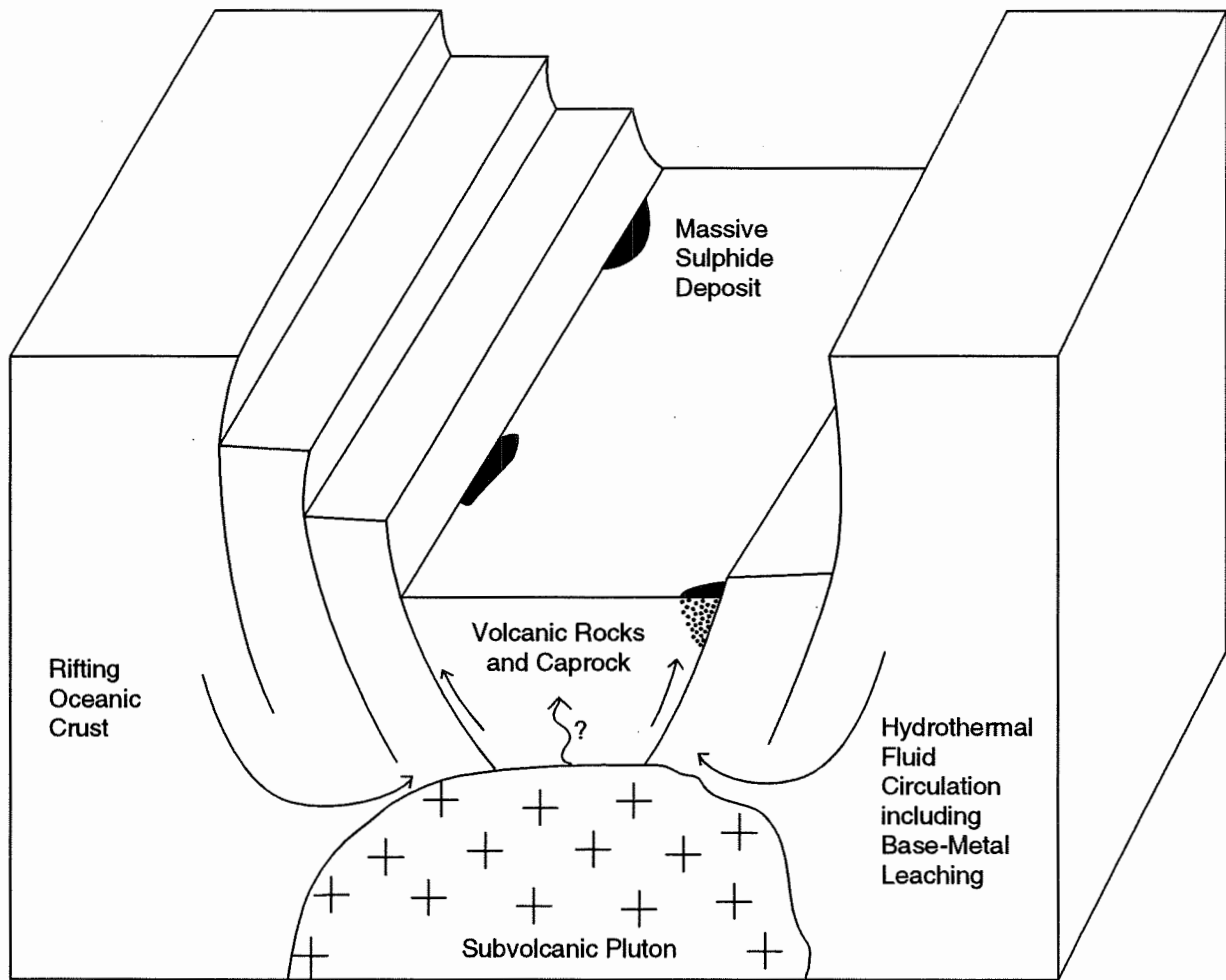


Figure 29. Schematic representation of the hydrothermal convection-cell model. Caprock = sediments, ashflow material, silicification ± epidotization or carbonatization.

Franklin (1990) has summarized the prevalent characteristics of subvolcanic intrusions associated with VMS deposits; in addition to their sill-like configurations, they occur 2 to 3 kilometres stratigraphically below the base-metal deposits, they have minor metamorphic halos, some felsic intrusions have minor porphyry copper-type occurrences, and their REE patterns, including characteristic negative Eu anomalies, are similar to those of their coeval felsic volcanic rocks.

Studies of modern seafloor-spreading centres have been imaged by geophysical (gravity) techniques revealing relatively shallow intrusive heat sources beneath the ridges. Intermediate- to fast-spreading ridges are thought to be underlain by relatively shallow magma chambers, whereas slow-spreading ridges are thought to be underlain by relatively deep-seated magma chambers (Rona, 1984). Periodic replenishment of the magma chamber may explain episodic spreading and volcanic activity and the resultant hydrothermal activity at ridge centres. Cathles (1983) suggests that cooling by convection of multiple small magmatic pulses resulted in the formation of individual ore lenses in the Hokoroku basin, Japan. In that case, mineralization is thought to have formed in less than 5,000 years and probably in less than approximately 100 years (Cathles, 1981). However, recent work on the world-class Kidd Creek VMS deposit in Ontario suggests that it may have taken as much as five million years to form this deposit (Hannington et al., 1994).

According to Cathles (1981), there are three sources of heat to drive hydrothermal

circulation. The principal source is thermal conduction from the intrusion, first to the country rock and later to fluids circulating through the intrusion at temperatures less than approximately 350-400°C. Also, venting magmatic volatiles may contribute heat, and the heat of radioactive decay within the intrusion is acknowledged, although it would be a minor source of heat in the time frame of a VMS system.

3.3.4 Extensional Fracture System

Whereas downward-moving fluids would readily percolate throughout the fractured country rock towards the subvolcanic intrusive heat source, upward-moving hydrothermal fluids are focussed along principal, marginal rift faults (Kappel and Franklin, 1989). Fault and fracture zones are important to enable hot (approximate maximum temperature of 350-400°C; Cathles, 1991) aqueous fluids to be released by more or less continuous flow by buoyant rise to the surface. According to Mottl (1983), adiabatic cooling by movement up rift fault structures would result in only a 10°C drop in the temperature of the hydrothermal fluid.

3.3.5 "Cap" on the Hydrothermal Reaction Zone

A cap on the hydrothermal reaction zone is an important feature of the VMS convection-cell model. It inhibits cooling of the heat source by rapid inflow of seawater, holds fluids at depth, and allows convecting fluids to attain elevated temperatures necessary for the solubility of base metals (approximately > 300°C for Cu, and lower temperatures for Pb-Zn; Lydon, 1988). As documented by Kappel and Franklin (1989)

for sulphide deposit-bearing ridge crests in the northeast Pacific Ocean, a thick layer of sediment or ash-flow material may provide the necessary impermeability layer and thermal insulation. Lower semi-conformable alteration zones have been recognized under several fossil VMS deposits and are thought to have acted as barriers between cold, down-welling seawater and metalliferous fluids rising from reservoir zones (i.e., the source of metals and sulphur for the ore-bearing fluids) (Franklin et al., 1975; MacGeehan, 1978; MacGeehan and Maclean, 1980; Cathles, 1983; Gibson et al, 1983; Galley and Franklin, 1991). These widespread alteration zones, characterized by abundant silicification \pm epidotization in Noranda-subtype deposits and by carbonatization in Mattabi-subtype deposits, are thought to be the products of early-forming alteration, subsequently crosscut by chloritic alteration limited around actual vent-stockwork sites (Franklin et al, 1975; Gibson et al., 1983). Because these alteration zones may be metal-depleted (MacGeehan and MacLean, 1980; Gibson et al., 1983), they may have been a part of the metal source zone. Focussed discharges of metalliferous fluids would occur where the rising fluids breached these alteration zones along rift-related fault zones.

3.3.6 Source of Fluids and Metals

Based on 1) oxygen and hydrogen isotope data for hydrothermal minerals and water from fluid inclusions in minerals associated with fossil VMS deposits and 2) the discovery and characterization of hydrothermal fluids venting at actively spreading mid-ocean ridges, the consensus is that the main source of fluids for hydrothermal emanations

on the seafloor is seawater that has circulated by heat convection and has reacted with the country rock (for reviews see Large, 1977; Franklin et al., 1981; Cathles, 1981, 1983; Lydon, 1988; Franklin, 1990). Metals are considered to be leached from the country rocks by the convecting hydrothermal fluids. Some contribution of fluids from a magmatic source is suggested by studies of the Galapagos VMS deposits (Perfit and Fornari, 1983; Perfit et al., 1983) and isotopic studies of the Kuroko deposits (Ohmoto and Rye, 1974; Hattori and Muehlenbachs, 1980; Pisutha-Arnond and Ohmoto, 1983). According to Elder's rule (1977) as used by Cathles (1981), the total mass of convecting hydrothermal fluid would approximately equal the mass of the heat source.

Leaching of metals from rocks is achieved essentially by the Mg, Ca, or Na metasomatism (resulting in a decrease in pH) of primary minerals containing trace amounts of metals in their crystalline structure and, to a lesser degree, by scavenging metals loosely bound to mineral surfaces or held to mineral surfaces by coatings with high adsorption capacities (Lydon, 1988). Based on measurements of seafloor fluid emanations and experimental data, modified seawater in basaltic terranes must reach temperatures of at least 385°C, and in a few cases, at least a few degrees above 400°C, to become significantly cupriferous (Franklin, 1986 and references therein). Increased salinities may enhance the ability of a solution to leach metals and the reactive capacity of a pore solution (meaning a solution is not in chemical equilibrium with a rock and is therefore able to alter the rock surface with which it has contact; Lydon, 1988). Low water/rock ratios favour high metal concentrations in pore fluids by means of simple rock

hydration (see Lydon, 1988).

Magmatic fluids may also be a significant source of metals. By analogy to porphyry copper deposits, Henley and Thornley (1979) suggest that, whereas some ore metals may be derived by leaching of country rocks, magmatic fluids may be a source of base metals, sulphur and carbon dioxide. They propose a hybrid model in which these components may be transported by a buoyant magmatic plume which then mixes with convecting seawater-derived fluids. Sawkins (1982; 1986), Stanton (1991) and Urabe and Marumo (1991) also propose hybrid models similar to the Henley and Thornley model.

Both Sawkins (1982, 1986) and Stanton (1991) suggest that leaching of oceanic basalt cannot be the principal mechanism to generate metalliferous fluids for VMS deposits. Firstly, Sawkins questions the ability of hydrothermal convection cells to maintain optimum effective water/rock ratios and temperatures to leach base metals from the altered rocks. Secondly, Sawkins suggests that fluids circulating through faults and fractures would create altered selvages that would not allow subsequent fluids to interact with unaltered rocks, unless these rocks were repeatedly fractured. In this case, Sawkins would expect more repetitive alteration patterns in the paragenesis of Kuroko-type deposits. Thirdly, Sawkins argues that the uniformity of Pb isotope data for Kuroko ores (Sato, 1975), similar to Pb isotopic data for coeval igneous rocks, could not be maintained by fluids leaching diverse basement formations within the Kuroko region.

However, Campbell et al. (1981) suggest, based on an evaluation of strontium and lead isotope data of the Kuroko ores, that little circulation of hydrothermal fluids affected the basement rocks in the Kuroko region.

Stanton notes the clustering of VMS deposits in time, and associates these groupings to a brief, clearly-defined event (magmatic crystallization and differentiation) rather than a prolonged process such as alteration by modified seawater and metal leaching. Secondly, Stanton stresses that basalts contain comparable or more abundant amounts of zinc than andesites, dacites and rhyolites and that the zinc in basalts may be leached fairly readily from olivine. However, zinc-rich deposits are not commonly found in Cyprus-type basaltic environments, but they are prominent in andesite-rhyolite, calc-alkalic sequences. Also, Stanton notes that basalts contain trace amounts of lead, and following the leaching model, basalt-associated orebodies should contain lead, whereas they are essentially devoid of lead. Finally, Stanton notes that basalts contain nickel and cobalt in the same order of abundance as copper and zinc, and that nickel and cobalt, like zinc, are located in olivine, an easily altered mineral. Based on the leaching hypothesis, Stanton would expect basalt-associated Cyprus-type deposits to contain nickel and cobalt sulphides as major constituents, which is not the case.

3.3.7 Ore-Metal Transport

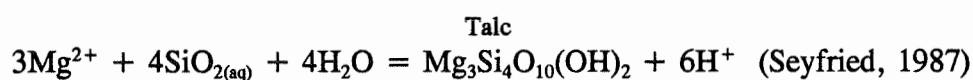
Laboratory experiments on ore and gangue mineral solubilities (see Barnes (1979) and Franklin et al. (1981) for summaries) and direct analyses of modern seafloor

emanations (see Franklin, 1986 and references therein) have recognized that the dominant characteristics of base metal-bearing fluids, such as temperatures, pressures ("...at temperatures approaching the two-phase boundary of seawater..., pressure can have an important effect on mineral solubility and correspondingly H^+ production...": Seyfried and Janecky, 1985), salinities, fluid densities, water/rock ratios, fugacity of oxygen, and fugacity of sulphur, play important roles in modifying the fluid and the environment in which it circulates.

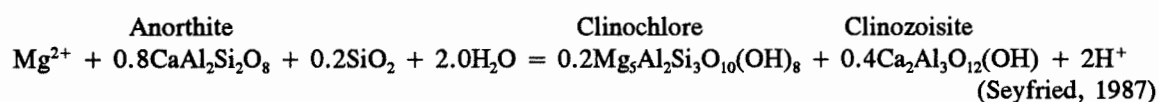
Under the chemical and physical conditions expected for base-metal transport and deposition for ancient Cu-Zn-type deposits, optimal conditions for Cu-Zn transport require that the ore metals be transported as sulphide (HS^- and possibly H_2S) complexes in alkaline solutions with pH greater than 6, or possibly as chloride complexes in acidic solutions (Franklin et al, 1981; Lydon, 1988). Whether the metals are transported as bisulphide or chloride complexes depends largely on such factors as pH and the Cl:S ratio. Based on actively-venting fluids on the modern seafloor (see Rona (1988) for review) and fluid-inclusions studies of certain fossil deposits (Spooner and Bray, 1977; Pisutha-Armond and Ohmoto, 1983), ore-forming solutions have temperatures up to approximately 400°C, salinities up to two to three times that of modern seawater (i.e., 7-10 equiv. wt. % NaCl), and are reduced such that the activity of H_2S is much greater than the activity of SO_4^{2-} .

3.3.8 Chemical Reactions Causing Alteration

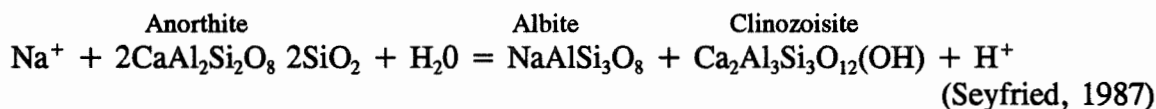
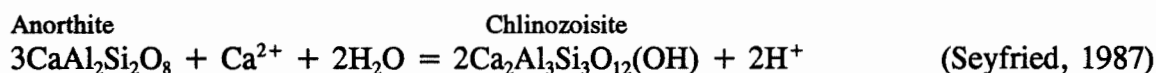
Experiments examining the reactions between basalt and low temperature (approximately $\leq 150^\circ\text{C}$) seawater-derived solutions (see Seyfried (1987) for review and references) show that Mg^{2+} is removed from seawater and deposited as Mg-rich alteration minerals, according to reactions of the type:



At temperatures of 150-350°C and seawater/rock mass ratios less than 50, the acidic character of the fluid is short lived due to the replacement of aqueous Mg^{2+} by Ca^{2+} , and at very-low seawater/rock mass ratios by Na^+ and K^+ as a result of the dissolution of primary silicate phases. In moderate- to high-temperature fluids (250-450°C), Mg^{2+} may still be removed from solution and create acidic conditions according to reactions of the following type:



However, at high-temperatures (approximately $\geq 350^\circ\text{C}$), Ca^{2+} and Na^+ are lost from solution and become fixed in hydrous alteration phases, resulting in acidic fluid conditions. Calcium-fixation reactions in relatively SiO_2 -poor systems and sodium-fixation reactions (spilitization) in relatively SiO_2 -rich systems, rather than Mg-fixation reactions, provide the most likely mechanisms of forming acidic solutions, according to reactions of the following types:



Generally, VMS-forming hydrothermal fluids are oversaturated in silica in comparison to cold seawater. Mixing of cold seawater with venting hydrothermal fluids (\pm boiling) will result in rapidly falling temperatures and silica precipitation (Franklin, 1990). Pronounced silicification is commonly found in zones below Noranda-subtype VMS deposits, forming semi-conformable footwall alteration zones (MacGeehan and Maclean, 1980; Gibson et al., 1983).

Carbonate alteration in Mattabi-subtype VMS deposits is thought to have formed prior to metal deposition (Franklin et al., 1975; 1977). An early low-density CO_2 -rich aqueous hydrothermal phase may have risen quickly because of its low density, altering the rocks in its path, and leaving behind a dense, residual metal-rich brine that would have subsequently risen slowly through the footwall rocks (Franklin, 1986).

3.3.9 Alteration Pipes

Various alteration assemblages found in alteration pipes are summarized in Figure 30 (from Lydon, 1988). Generally, these pipes have chloritic cores and sericitic or illitic margins (or chloritic cores and sericitic tops just underneath the sulphide mound). Magnesium enrichment of cores is commonly observed. The chlorite to sericite

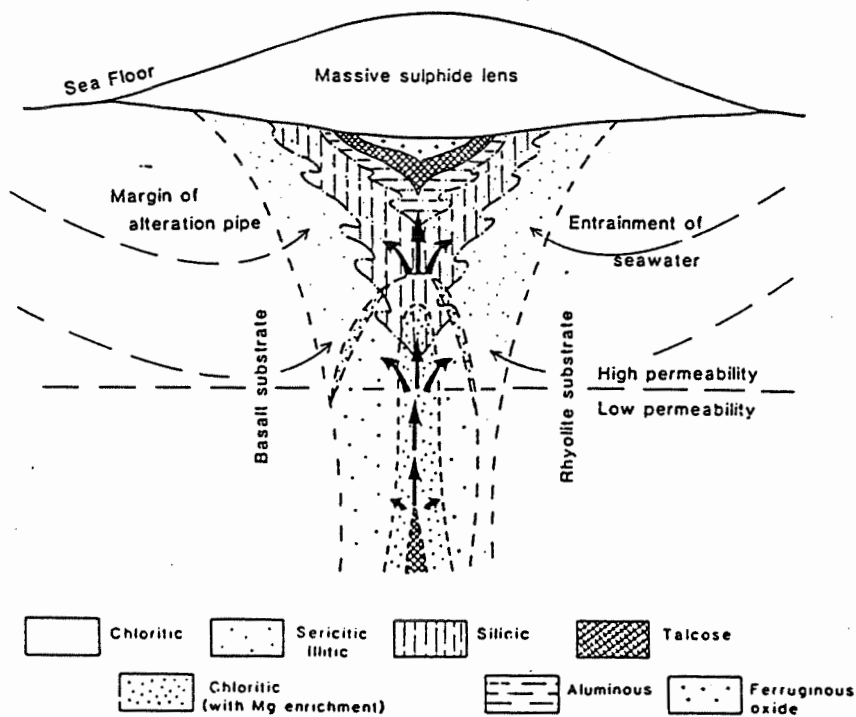


Figure 30. Composite representation of the various alteration assemblages that have been reported for alteration pipes of VMS deposits (from Lydon, 1988).

transition in alteration pipes is interpreted to represent a decreasing geothermal gradient, as does the Cu/Zn zonation (Riverin and Hodgson, 1980; Lydon and Galley, 1986).

Potassium is added to the alteration pipe rock in the form of sericite. It is derived either from seawater and the ore fluid, or was released during chloritization of the core of the alteration pipe. Magnesium in the uppermost parts of the alteration pipe and peripheral zones is most likely contributed by entrained seawater, whereas magnesium in Mg-rich cores and in sulphide vein selvages comes from ore fluids, implying either a minor addition by entrainment originally from seawater or by leaching of feldspar-free lithologies (e.g., completely chloritized/epidotized basalt, argillaceous sediments or ultramafic rocks). Siliceous, aluminous, carbonaceous, talcose or ferruginous oxide assemblages may occur in footwall rocks immediately below the exhalite massive sulphide accumulations.

3.3.10 Mechanisms for Precipitating and Accumulating Sulphides

The most important mechanism for causing base-metal sulphide precipitation is the abrupt temperature decrease resulting from 1) mixing of the hot hydrothermal fluids with cold seawater, or 2) subsurface boiling of hydrothermal fluids (Henley and Ellis, 1983; Drummond and Ohmoto, 1985).

The most important requirement for initiating sulphide accumulation is a porous barrier over a hydrothermal discharge site (Franklin, 1986; Lydon, 1988). This barrier

defocuses the discharge of hydrothermal fluids and provides a site for the meeting and mixing of cold seawater and hot venting fluids, which results in rapid cooling of the fluids and initiates near-vent sulphide accumulation. Study of modern seafloor VMS accumulations reveals that anhydrite (CaSO_4) commonly acts as the porous barrier, which 1) impedes direct venting of hydrothermal fluids onto the seafloor, 2) provides a surface upon which hydrothermal precipitation may occur, and 3) filters sulphide particles suspended in the hydrothermal fluid. Although calcium is leached from oceanic lithologies by convecting hydrothermal fluids, sulphur isotope studies show that the sulphate in anhydrite related to VMS deposits comes from the seawater (Styrt et al., 1981). Thus, anhydrite precipitates from seawater at the sharp thermal gradient between hot, venting hydrothermal fluids and cold, ambient seawater. This mineral is absent or rare in ancient VMS deposits, and is thought to have been dissolved by later ore fluids (Lydon, 1988). If anhydrite was not present in the Archean (i.e., pre-oxygenation time; Roscoe, 1973), then a layer of fragmental rocks ("millrock"; Sangster, 1972) over the discharge vent probably acted as a porous barrier in ancient VMS deposits. The fragmental rocks were either of magmatic, phreatic, or hydrothermal explosive origin or were talus accumulations, and promoted advective, convective or adiabatic cooling of the hydrothermal fluids in the seafloor mound. Repeated episodes of hydraulic fracturing beneath the seafloor surface created hydrothermal breccia pipes, a porous medium in which fresh seawater could circulate and sulphide minerals could accumulate as a stockwork body.

3.4 MODERN ANALOGUES

Our understanding of polymetallic massive sulphide precipitation and accumulation and related hydrothermal fluid chemistry has advanced greatly since the discovery of this type of deposit at many seafloor spreading sites, especially along the East Pacific Rise (see Rona (1984, 1988) for a review). However, sulphide deposits along the East Pacific Rise or the Mid-Atlantic Ridge are associated with mafic, oceanic-spreading centres, and much of the modelling of ancient VMS deposits suggests that these deposits formed instead in island arc/back-arc environments. Therefore, the East Pacific Rise and the Mid-Atlantic Ridge deposits are not the most appropriate modern analogues for ancient VMS deposits. Fouquet et al. (1991) underline this distinction (p.780): "Although the basic ore-forming processes in back-arc environments are similar to those described at MOR spreading centres, specific properties of the fluids and deposits are largely controlled by the physicochemical properties of the crust which in turn reflects the tectonic setting. Both mineralogical and geochemical compositions of sulphides and fluids indicate the differences between back-arc and ocean-ridge environments." Complex interactions between island arcs, back arcs, ridges and trenches in the southwest Pacific Ocean have been described by Karig (1970, 1971, 1972, 1974) and Hamilton (1988), and deep exploration by bathyspheres since the late 1980s have proven successful in finding examples of sulphide accumulations on the seafloor in back-arc environments in this region. Four modern examples analogous to Archean VMS deposits are discussed below.

The Okinawa Trough is an active intracontinental back-arc basin located between the Ryukyu Island chain and the east coast of China (Fig. 31). It hosts the Jade deposit considered to be a modern analogue of Kuroko-type VMS deposits (Halbach et al., 1989, 1993). The area is characterized by valleys and ridges composed of rocks with calc-alkalic island-arc affinities. The extending oceanic crust is cut by normal faults which act as conduits for fluid circulation and for rising volcanic intrusions. The Jade hydrothermal field is located in a caldera-like structure where four types of sulphide mineralization have been identified: 1) massive sulphides composed of sphalerite, argentiferous galena and pyrite with minor amounts of chalcopyrite; 2) massive sulphides composed of sphalerite, chalcopyrite and pyrite; 3) stockwork mineralization composed of sphalerite, Ag- and Sb-bearing tennantite, galena, enargite and lesser amounts of pyrite and chalcopyrite; and 4) sulphide-bearing sediments composed of sphalerite, pyrite and barite with quartz, calcite, illite and chlorite as detrital components. $\delta^{34}\text{S}$ values from pyrite (+4.3 to +10.7) are similar to those of Kuroko sulphides (+5 to +8), and based on these isotopic results and chemical metal analyses, Halbach et al. (1989, 1993) suggest that the Jade hydrothermal field of the Okinawa Trough is similar, in its nascent state, to Au-poor, high-temperature black ores and stockwork mineralization of Kuroko-type deposits.

Similarly, the Lau back-arc basin, located between a remnant (Lau ridge) and an active volcanic arc (Tofua volcanic arc) east of Fiji, hosts active hydrothermal activity along the felsic to mafic Valu Fa Ridge (Fig. 32). Fouquet et al. (1991, 1993) suggest

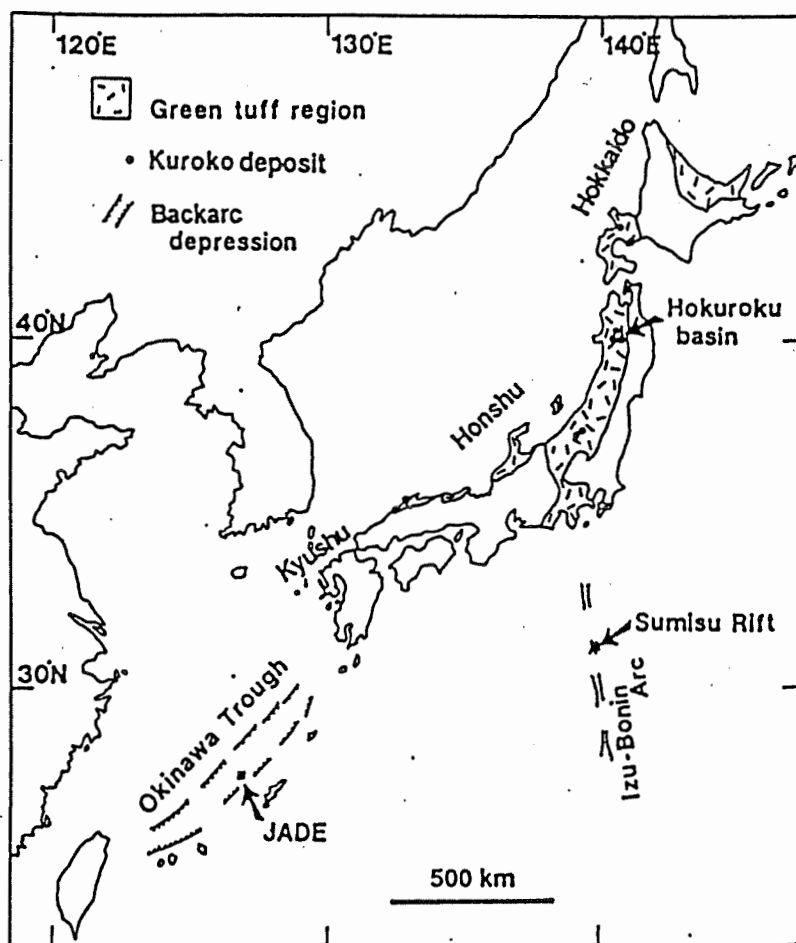


Figure 31. Location map of the Okinawa Trough and the Jade deposit (from Urabe and Marumo, 1991).

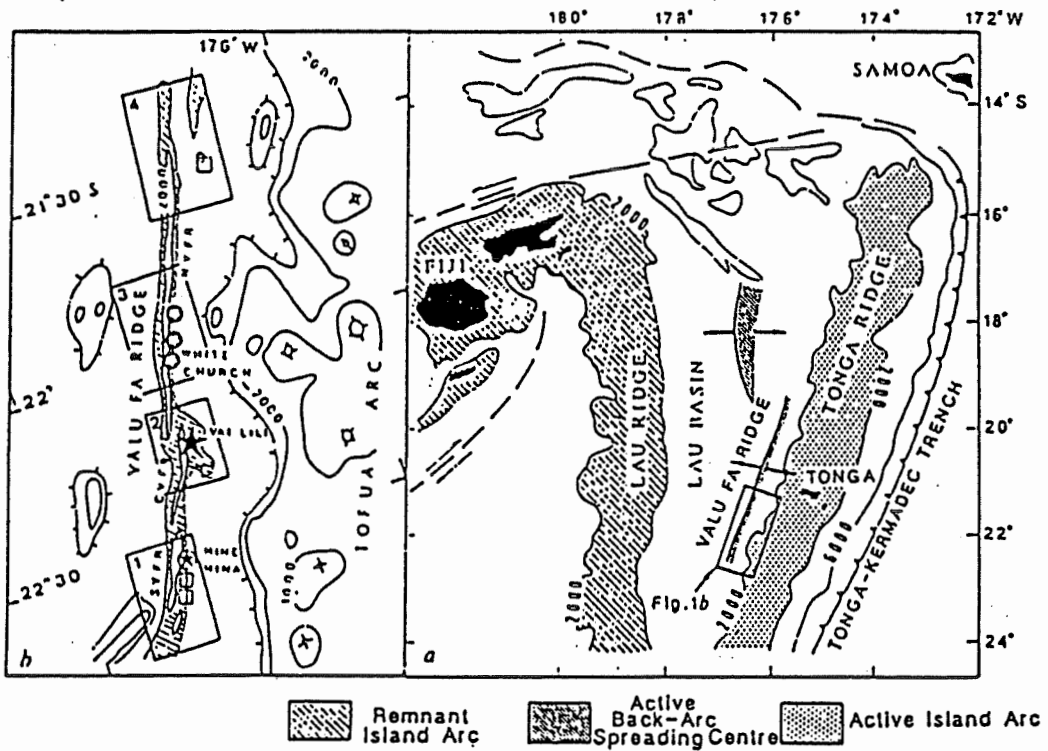


Figure 32. General map (a) of the Lau back-arc basin, and (b) location of hydrothermal fields along the Valu Fa Ridge (from Fouquet et al., 1991).

that the Lau back-arc basin deposits are intermediate between typical mid-ocean-ridge mineralization and Kuroko-type massive sulphide mineralization. The substrata consist of highly vesicular and highly brecciated basaltic andesites to dacites, favouring good fluid circulation and seafloor and subsurface mineralization. Analyses of emanating hydrothermal fluids show 1) that the fluids are acid (pH as low as 2); 2) that these fluids have temperatures up to 400°C; 3) that the fluids contain high concentrations of trace metals; and 4) that primary gold is present in the accompanying mineral deposits. The sulphide deposits consist of chimneys, sulphide mounds and stockworks. A cross-section from top to bottom of a massive sulphide deposit in the Vai Lili hydrothermal field shows broken copper/zinc chimneys, immature porous zinc sulphides (with minor amounts of galena), massive zinc-rich chimneys, massive copper-rich sulphides, and stockwork mineralization consisting of centimetre-thick chalcopyrite veins with veins of silica, barite and sphalerite. This cross-section is similar to the normal sequence of mineralization in typical Kuroko-type deposits where the outer portion of the deposit is "black ore" (barite, sphalerite, pyrite, galena) and the core is "yellow ore" (pyrite, chalcopyrite). Given that the Okinawa Basin is a nascent back arc presently forming within continental crust, Fouquet et al. (1991, 1993) conclude, based on sulphide compositions and the presence of a differentiated series with island-arc affinities, that the Lau Basin is intermediate between oceanic and continental back-arc environments.

The eastern Manus basin is a back-arc extensional structure located north of the New Britain subduction trench and volcanic arc east of Papua New Guinea where

polymetallic sulphide deposits are actively forming (Fig. 33) (Binns et Scott, 1993). This area is noted for the oblique intersection of its spreading segments and transform faults and for its hydrothermal activity and extensive sulphide deposits associated with dacitic to rhyodacitic volcanism. Andesitic to rhyodacitic lavas define a calcic fractionation lineage, and relatively shallow-level fractionation is implied by the calcic nature of plagioclase phenocrysts. Elevated Sr and Ba contents and depleted Nb abundances suggest affinities with arc magmatism. A sample of altered dacite is enriched in K, Ba, Mg and Cr (relative to immobile Al), depleted in Si, Fe, Na, and Ca (relative to Al) and is extremely depleted in Mn and Li. Ferruginous oxide deposits and altered lavas with disseminated pyrite and native sulphur were noted by Sakai (1991) in a basaltic andesite caldera. Binns and Scott (1993) observed blue-grey crusts, interpreted to be Fe-Mn-Si oxides in the PACMANUS hydrothermal field (Fig. 33). Although dredging of hydrothermal deposits was unsuccessful during their studies, small chips recovered from camera equipment were found to be composed of crystalline anhydrite, disseminated sulphides and friable massive sulphides, chalcopyrite being the dominant sulphide mineral. Binns and Scott (1993) conclude that the PACMANUS site in the eastern Manus back-arc basin may be analogous to ancient VMS-hosting environments.

The Franklin Seamount is a basaltic andesite volcano with rare occurrences of sodic rhyolite located near the western propagating tip of a seafloor spreading axis in the Woodlark basin, located between the Solomon Islands and the southeast tip of Papua New Guinea (Fig. 33) (Binns et al., 1993). Major faults associated with the Woodlark

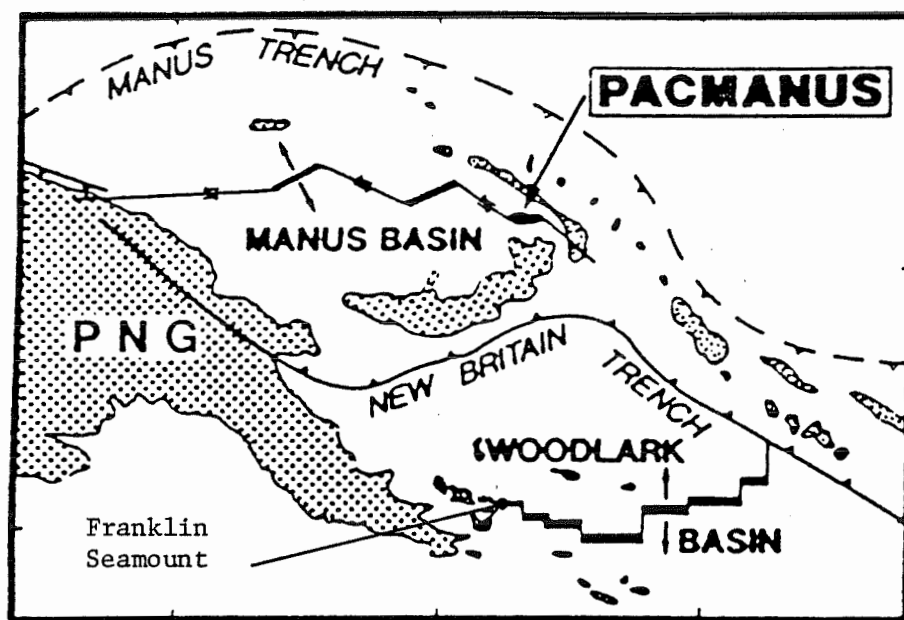


Figure 33. General location map of the Manus and Woodlark basins east of Papua New Guinea (PNG) (modified after Binns and Scott, 1993).

spreading axis are present on both sides of the Franklin volcanic ridge, providing conduits for deep seawater circulation in the volcanic pile. Fe-Mn-Si oxide mounds and spines are found on and near the Franklin Seamount, and inactive gold-rich and silver-rich barite-silica chimneys with sparsely disseminated sulphides are also seen and may underlie the Fe-Mn-Si accumulations. Although no massive sulphide accumulations were found, geochemical analysis of venting fluids suggests that sulphide stockworks probably occur within the underlying pile. Binns et al. (1993) suggest that this propagating seafloor spreading axis, where seafloor hydrothermal activity is associated with volcanism in a continental margin environment, probably represents a more realistic environment for ancient VMS accumulation than mid-ocean ridges and mature back-arc basins.

Many other sites of massive sulphide deposition in oceanic-ridge environments have been documented (see Rona and Scott, 1993), but only a small number of sites, characterized by the above four sites of recent sulphide accumulation in back-arc or propagating rift environments, have mineralization associated with felsic volcanism. Despite this small number of modern analogues to ancient VMS deposits, these modern examples are very helpful in establishing the probable environments of Archean VMS deposition. Firstly, they underline the complexities of crustal tectonics in creating a favourable environment for sulphide accumulation. Secondly, as Binns and Scott (1993) point out for the eastern Manus back-arc basin environment, there may be less deep fluid circulation in this type of environment than in mid-oceanic ridge environments,

decreasing the opportunity for increasing fluid temperatures and leaching metals from the surrounding rocks. With this in mind, Binns and Scott intend that future research at this site will address the importance of magmatic devolatilization and basement fluid-rock interaction inferred for some ancient VMS deposits (e.g., Sawkins, 1982, 1986; Stanton, 1991; Urabe and Marumo, 1991).

3.5 CASE STUDY: BOURLAMAQUE AND LOUVICOURT TOWNSHIPS

In this following section, the required and secondary elements of VMS formation in Bourlamaque and Louvicourt Townships of the east Val d'Or mining district are discussed in order to apply the general VMS model (above) to the actual field area.

The first question to answer is whether an adequate subvolcanic heat source existed in the district. The obvious choice is the apparently synvolcanic Bourlamaque pluton (Fig. 26), a large (170 km²; Campiglio and Darling, 1976) dioritic intrusion with no metamorphic halo. The calc-alkalic character of this intrusion and of the Val d'Or domain rocks suggest that they are comagmatic (Tessier et al., 1990; Chapter 2 of this report). However, their reported ages do not concord well (2,699.8 ± 1.0 Ma for the Bourlamaque intrusion; 2,704.9 ± 1.1 Ma and 2,706 ± 3 Ma for the Val d'Or domain; Wong et al., 1991 and Pilote et al., 1993); i.e., their ages do not agree within the precision of zircon age dating of ≈ 2.7 Ga old rocks.

Unfortunately, there is some uncertainty over the sampling for age-dating of the Bourlamaque pluton. Moreover, recent mapping and precision-age dating of the Flavrian pluton in the Noranda district has demonstrated that synvolcanic intrusions are typically compositionally heterogeneous and probably composed of multiple injections of subvolcanic magma over many millions of years. The Bourlamaque-Val d'Or system may also have had a prolonged subvolcanic and volcanic history. Based on major element and selected trace element (Li, V, Cr, Co, Ni, Cu, Zn, Rb, Sr) geochemistry, Campiglio and Darling (1976) and Campiglio (1977) suggested that two, possibly three sill-like injections formed the Bourlamaque pluton. The shape of the intrusion also suggests that it is composed of more than one intrusive phase. Campiglio and Darling (1976) and Campiglio (1977) propose that the central portion of the intrusion was the first intrusive pulse, followed by the more differentiated northern portion of the intrusion. The southern border of the central portion is the most mafic and may represent a separate intrusion or a zone of contamination of the central intrusion. The most pertinent, precise geochronology sample comes from the most western extremity of the northern (i.e., late) portion of the intrusion (Wong et al., 1991) and may represent a late phase of the Bourlamaque intrusion.

A synvolcanic pluton of the size of the Bourlamaque pluton would clearly have been an adequate heat source to generate a convection-cell system, based on simple calculations of the type made by Cathles (1981). These calculations suggest that an intrusion approximately ten times smaller than the Bourlamaque intrusion could have

generated hydrothermal convection cells capable of depositing the Cu and Zn tonnage in all of the known VMS deposits of the Val d'Or-east camp. This difference in intrusion size implies that the Bourlamaque pluton had the potential of forming many more VMS deposits than those presently known in this district.

The geotectonic model for the Val d'Or mining district of Desrochers et al. (1993) envisages the emplacement of the calc-alkalic Bourlamaque intrusion and comagmatic Val d'Or domain rocks in an extensional regime due to the subduction of an oceanic ridge beneath the Malartic Composite Block (MCB; see Chapter 1 and Figs. 6a and 6b) accreted to a Superior protocontinent. In this scenario, the ridge retains its oceanic extensional characteristic, resulting in 1) the melting of mantle-wedge material and MCB material and 2) the unconformable emplacement of the Bourlamaque intrusion and Val d'Or domain rocks. On the contrary, as mentioned in section 1.2.6, if the Val d'Or domain rocks formed as a result of subduction of simply oceanic crust underneath the MCB accreted to a Superior protocontinent, local tensional environments would still exist even though the overall force is compressional. This scenario is similar to the aborted rift model for Kuroko massive sulphide deposits of the Green Tuff Belt (Cathles et al., 1983). It is also akin to the preliminary stage of an intracontinental back-arc basin (Halbach et al., 1989, 1993). Furthermore, a simple back-arc spreading axis environment has been suggested for the formation of the Bourlamaque intrusion and its overlying coeval volcanic units, the Val d'Or domain (see section 2.3.3.2; Burrows and Spooner, 1989), in agreement with the general model for the formation of VMS deposits.

Concrete evidence supporting a rift environment, such as basin-bounding faults and the preservation of talus-type sediments, has not yet been recognized probably due in large part to the deformation of the CPB. Compilation maps of the district do identify abundant, major and minor shear zones parallel to the more or less east-west tectonic grain of the district; however, they are apparently overprinted syntectonic features, not synvolcanic. Nevertheless, certain characteristics of the Val d'Or domain may be used as support for a rift environment: 1) the recognition by Desrochers et al. (1993) of a distinct calc-alkalic Val d'Or domain and its unconformable relationship to the accreted tholeiitic-komatiitic domains, which implies from its character, a rifting event of the type suitable for VMS deposits; 2) the restriction of known VMS deposits in the Val d'Or-east mining camp to the Val d'Or domain; and 3) the peraluminous nature restricted to Val d'Or domain rocks commonly associated with Archean VMS deposits, suggesting that these rocks and their VMS deposits formed in an isolated environment.

So far, the number of discovered VMS deposits in the Val d'Or-east area is significant, although relatively limited compared to the Rouyn-Noranda camp. Documentation of these deposits is also limited, and the most-recently discovered and largest deposit, the Louvicourt deposit, is yet to be studied and described. However, Mg-chlorite-rich alteration pipes at the Louvicourt, Louvem and Manitou-Barvue deposits are evidence, by analogy to modern settings, that focussed discharge did occur along local fracture zones, but the presence of cross-cutting feeder dikes or faults remains unknown (again due largely to later deformation).

Also largely due to the limited information on these deposits, the type of subvolcanic caprock expected above the hydrothermal reaction zones and heat source remains speculative. All descriptions note the type of alteration associated with the kinds of mineralization; however, no systematic structural or geochemical work has been done to characterize lateral changes in alteration. Consequently, it is not known if these deposits formed their own caps of silica or carbonate alteration, or if their volcanic piles acted as caprocks.

The general lack of detailed experimental studies on these deposits leaves us with little solid evidence to suggest the actual sources of ore fluids and metals, nor the characteristics of the hydrothermal fluids that circulated. It may only be repeated that, according to the most favourable hypothesis for VMS formation, seawater was the major source of fluids and that modified seawater leached metals from the rocks through which it convected. A small amount of ore-bearing fluids may also have come from the Bourlamaque magmatic source.

As for fluid characteristics, their compositions were probably similar to the optimal conditions defined in section 3.3.7 for leaching, transporting, and precipitating base-metal sulphides (< 400°C, saline, reduced, alkaline, sulphide- and chloride-bearing, aqueous solutions). The hydrothermal fluids that convected through the Val d'Or domain rocks are known to have formed chlorite alteration associated with copper mineralization, and sericite ± silica alteration associated with zinc mineralization. Carbonate ±

chloritoid \pm garnet provide supporting evidence for a Mattabi-subtype classification.

Although four mines are closed, the Louvicourt mine, the most recent and largest VMS deposit of the camp, is to start production in 1994 and should operate for at least 12 years (The Northern Miner, 1994). Over the life time of this mine, it will hopefully be possible to undertake studies to characterize the hydrothermal fluids responsible for the mineralization and related alteration, and to better define the characterization of this deposit and the other apparent Mattabi-subtype deposits in the district.

3.6 CONCLUSION

The hydrothermal convection-cell model is the most widely accepted explanation for modern and ancient volcanogenic massive sulphide accumulations, although some researchers continue to suggest that magmatic devolatilization was the major source of metals (see Section 3.3). Evaluation of the Val d'Or-east terrane and its known VMS deposits suggests that the deposits are similar to Mattabi-subtype deposits. However, the author suggests that the Mattabi-subtype/Noranda-subtype classification of ancient VMS deposits may need further definition with respect to depth of water, host-rock association and type of sulphide accumulation (massive sulphides \pm stockwork zones). With the relatively recent discovery of modern analogues in the southwest Pacific and the recognition of the tectonic complexities surrounding these sites, the author foresees further characterization of tectonic environments favourable to hosting VMS

accumulations and the application of this classification to ancient VMS deposits.

CHAPTER 4

ARCHEAN MESOTHERMAL LODGE-GOLD MODELLING

4.1 INTRODUCTION

In the broadest sense, gold mineralization in Archean greenstone belts may exist in synvolcanic and/or syn- to late-tectonic settings. Synvolcanic gold mineralization may be found in porphyry copper, skarn, epithermal, volcanogenic massive sulphide (VMS) and/or banded iron-formation environments. Only a few Precambrian deposits have characteristics similar to Phanerozoic porphyry copper (Kirkham, 1972; Griffis, 1979; Gaál and Isohanni, 1979; Goldie et al., 1979; Guha, 1984; Guha et al., 1988; Symons et al., 1988; Hodgson, 1990; Tessier, 1990; Fraser, 1993), skarn (Mueller, 1988) and epithermal (Guha, 1984 and Guha et al., 1988) deposits. Some VMS deposits, such as the Horne mine in the Rouyn-Noranda camp (Kerr and Mason, 1990), may host appreciable quantities of gold. As for banded iron-formation, although they may host important quantities of gold mineralization, it is still debated whether gold deposition was contemporaneous with iron-formation precipitation or was added later, such as during deformation. The pertinence of these types of synvolcanic gold mineralization to the Bourlamaque-Louvicourt townships study area is addressed in section 4.2.

Syn- to late-tectonic gold mineralization, the most abundant type of gold mineralization in Archean greenstone belts, includes the quartz vein deposits (e.g., Sigma

mine; Robert et al., 1983; Robert and Brown, 1984, 1986a, b) and the pyritic deposits (e.g., Bousquet district; Marquis et al., 1990a,b). The timing of the introduction of gold to the pyritic deposits may be in part synvolcanic (Tourigny et al., 1989, 1993).

A compilation of the major gold deposits in Bourlamaque and Louvicourt townships is given in Table 2 with locations in Figure 34. In addition to these 21 gold deposits, there are 28 significant gold showings which do not figure in this table (Bellemare and Germain, 1987). This compilation illustrates the dominance of syn- to late-tectonic quartz-vein gold deposits and the lack of known pyritic gold deposits in the study area.

The principal characteristics of these two deposit types are described in section 4.3. Following these descriptions, current mesothermal models used to explain Archean lode-gold mineralization (meteoric, orthomagmatic, metamorphic, mantle degassing-granulitization fluids) are characterized and compared, and Phanerozoic examples of mesothermal lode-gold mineralization are also briefly discussed because several characteristics of these young deposits appear to be analogous with Archean mesothermal lode-gold deposits. The current mesothermal models are then applied to the study area in order to evaluate what processes best explain the formation of auriferous fluids, migration and gold deposition in this area.

Table 2. Summary of characteristics of gold deposits in Bourlamaque and Louvicourt townships, Val d'Or-east district.

NAME	SIGMA-2	BRAS D'OR	FERDERBER
Status	Active Mine	Closed Mine	Closed Mine
Symbol in Figure 34.	1	2	3
Size (Mt x 1,000) ¹	165	862	866
Au (kg) ²	516	5,446	5,699
Host Rocks	Granophyric part of a differentiated gabbroic sill.	Bourlamaque diorite-quartz diorite intrusion.	Bourlamaque diorite-quartz diorite intrusion.
Morphology ³	Subhorizontal quartz lenses and bleaching of surrounding wallrock.	Discontinuous gold-bearing Qz-Tm-Cb-phyllsilicates veins in a shear zone.	Qz-Tm-Py-mica lenses in a E-W shear zone.
Ore Mineralogy ³	Qz-Tm ± Cb-Py-Po ± Cp-Au in lenses. Asp in bleached wallrock. Au associated with Py and Asp, occurs as inclusions and veinlets cross-cutting sulphide grains.	Py-Cp-Au. Gold closely associated with Py, and concentration increases when Cp is present too.	Py-Cp-Au. Gold is more common within Py when Cp is abundant and Au is generally in contact with both Py and Cp at "triple phase" grain junctions.
Alteration ³	Sericitization, albitization, silicification, and minor carbonatization.	Silicification and carbonatization.	Sericitization, chloritization, carbonatization, and low red hematite alteration.
Reference	Hébert et al. (1991); Couture (1991).	Belkabir (1990); Couture (1991).	Vu (1990); Couture (1991).

¹-Metric tonnes; values compiled from Couture (1991).

²- Values compiled from Couture (1991).

³- Qz: quartz; Tm: tourmaline; Cb: carbonate; Py: pyrite; Po: pyrrhotite; Cp: chalcopyrite; Au: gold; Ag: silver; Asp: arsenopyrite; Sh: scheelite; Gn: galena; Bi: bismuthinite; Te: tellurides; Mn: magnetite; Ep: epidote.

Table 2. Summary of characteristics of gold deposits in Bourlamaque and Louvicourt townships, Val d'Or-east district (continued).

NAME	L.C. BÉLIVEAU	SIGMA	BEVCON
Status	Closed Mine	Active Mine	Closed Mine
Symbol in Figure 34.	4	5	6
Size (Mt x 1,000) ¹	35	19,786	3,170
Au (kg) ²	120	112,793	12,671
Host Rocks	Diorite dikes	Andesitic flows, porphyritic diorite, feldspar porphyry dikes.	Bevcon granodioritic pluton and one mineralized lens in volcanic rocks.
Morphology ³	A series of en echelon Qz-Tm-Py-Au veins.	Subhorizontal and vertical Qz-Tm-Cb-Ch veins; dike stringers.	Numerous, narrow, lenticular Qz-Cb-Tm veins.
Ore Mineralogy ³	Py-Cp-Po-Au-Te; Au is closely associated with Py and Cp.	Py-Po-Sh-Au.	Au-Ag-Py-Cp-Sh disseminated in quartz veins.
Alteration	Carbonatization.	Cryptic: white mica, calcite, apatite added and epidote destroyed; Visible: paragonite, quartz, calcite, apatite, tourmaline added.	Carbonatization, albitization, tourmalinization, sericitization.
Reference	Lacroix (1986); Couture (1991).	Robert and Brown (1984); Robert and Brown (1986b); Couture (1991).	MERQ microfiche deposit # 32C/3-32; Sauvé et al. (1986); Couture (1991).

¹- Metric tonnes; values compiled from Couture (1991).

²- Values compiled from Couture (1991).

³- Qz: quartz; Tm: tourmaline; Cb: carbonate; Py: pyrite; Po: pyrrhotite; Cp: chalcocopyrite; Au: gold; Ag: silver; Asp: arsenopyrite; Sh: scheelite; Gn: galena; Bi: bismuthinite; Te: tellurides; Mn: magnetite; Ep: epidote.

Table 2. Summary of characteristics of gold deposits in Bourlamaque and Louvicourt townships, Val d'Or-east district (continued).

NAME	BUSSIERES	LAMAQUE	SIMKAR
Status	Closed Mine	Closed Mine	Closed Mine
Symbol in Figure 34.	7	8	9
Size (Mt x 1,000) ¹	225	23,803	308 ⁴
Au (kg) ²	1,296	141,389	1,605 ⁴
Host Rocks	Bourlamaque granodioritic intrusion.	Granodiorite and diorite plugs and volcanic rocks.	Diorite dike crosscut by several porphyritic dikes.
Morphology ³	Two-metre-wide quartz vein.	Qz-Tm-Cb veins and veinlets.	Discontinuous zone of Qz-Tm veins, 488 m long following a shear zone.
Ore Mineralogy ³	Py-Cp-Au-Ag disseminated in Qz vein.	Py-Au-Sh-Cp-Gn-Sp-Bi disseminated in veins and veinlets.	Au-Cp-Sp-Sh-Py-Po disseminated in Qz veins.
Alteration	Carbonatization, sericitization, albitization.	Carbonatization, albitization, silification.	Silicification, pyritization.
Reference	M.E.R.Q. microfiche deposit # 32C/4-36; Couture (1991).	M.E.R.Q. microfiche deposit # 32C/4-57; Daigneault et al. (1983) Couture (1991).	M.E.R.Q. microfiche deposit # 32C/4-81; Dussault (1993).

¹- Metric tonnes; values compiled from Couture (1991).

²- Values compiled from Couture (1991) except for the Simkar mine (Dussault, 1993).

³- Qz: quartz; Tm: tourmaline; Cb: carbonate; Py: pyrite; Po: pyrrhotite; Cp: chalcopyrite; Au: gold; Ag: silver; Asp: arsenopyrite; Sh: scheelite; Gn: galena; Bi: bismuthinite; Te: tellurides; Mn: magnetite; Ep: epidote.

⁴- Values taken from Dussault (1993).

Table 2. Summary of characteristics of gold deposits in Bourlamaque and Louvicourt townships, Val d'Or-east district (continued).

NAME	D'OR VAL	MID-CANADA (& Orenada #4)	AKASABA
Status	Closed mine	Closed mine	Closed mine
Symbol in Figure 34.	10	11	12
Size (Mt X 1,000) ¹	132	75 (19)	263
Au (kg) ²	320	345 (25)	1,236
Host Rocks	Bourlamaque granodiorite intrusion	Brecciated and fractured basic lava, chlorite schist, fractured diorite, siliceous and basic volcanic rocks.	Mafic lapilli tuff.
Morphology ³	Several Qz-Tm veins.	Deposit composed of several zones; disseminated and vein- type mineralization.	Au and Po disseminated in lower part of tuff, forming two large lenses; a few auriferous Qz-Ep veinlets crosscut the deposit and the underlying basalt unit.
Ore Mineralogy ³	Au-Ag-Cp-Py-Te disseminated in qz veins.	Au-Asp-Cp-Ag-Py- Mn-Po. Au closely associated with Asp.	Au-Po-Py-Cp-Mn.
Alteration	Not mentioned.	Carbonatization, albitization, tourmalinization, As mineralization.	Epidotization, biotitization, magnetite, pyrrhotite.
Reference	M.E.R.Q. microfiche deposit # 32C/4-82.	M.E.R.Q. microfiche deposit # 32C/4-89; Robert et al. (1990); Couture (1991)	Sauvé (1985); Couture (1991).

¹- Metric tonnes; values compiled from Couture (1991).

²- Values compiled from Couture (1991).

³- Qz: quartz; Tm: tourmaline; Cb: carbonate; Py: pyrite; Po: pyrrhotite; Cp: chalcopyrite; Au: gold; Ag: silver; Asp: arsenopyrite; Sh: scheelite; Gn: galena; Bi: bismuthinite; Te: tellurides; Mn: magnetite; Ep: epidote.

Table 2. Summary of characteristics of gold deposits in Bourlamaque and Louvicourt townships, Val d'Or-east district (continued).

NAME	NEW HARRICANA	AUMAQUE	BIDLAMAQUE
Status	Deposit	Deposit	Deposit
Symbol in Figure 34.	13	14	15
Size	In 1981, reserves defined by drilling were 60,000 t grading 5.48 g/t Au.	In 1984, probable reserves were 172,000 t grading 8.57 g/t Au.	Erratic Au and Cu values; 36,288 t grading 7.89 g/t Au.
Host Rocks	Volcanic rocks underlying a granodioritic porphyry dyke.	Sheared tuff and agglomerate.	Sheared felsic volcanic rocks.
Morphology	Quartz veins.	Quartz veins.	Quartz veins.
Ore Mineralogy ¹	Au-Py-Cp disseminated in Qz veins.	Au-Ag-Cp-Sp-Py disseminated in Qz veins.	Au-Cp-Ni-Sh-Py-Po-Tm disseminated in Qz veins.
Alteration	Chloritization	Chloritization, carbonatization, sericitization.	Not mentioned.
Reference	M.E.R.Q. microfiche deposit # 32C/4-56.	M.E.R.Q. microfiche deposit # 32C/4-63.	M.E.R.Q. microfiche deposit # 32C/4-66.

¹- Qz: quartz; Tm: tourmaline; Cb: carbonate; Py: pyrite; Po: pyrrhotite; Cp: chalcopryrite; Au: gold; Ag: silver; Asp: arsenopyrite; Sh: scheelite; Gn: galena; Bi: bismuthinite; Te: tellurides; Mn: magnetite; Ep: epidote.

Table 2. Summary of characteristics of gold deposits in Bourlamaque and Louvicourt townships, Val d'Or-east district (continued).

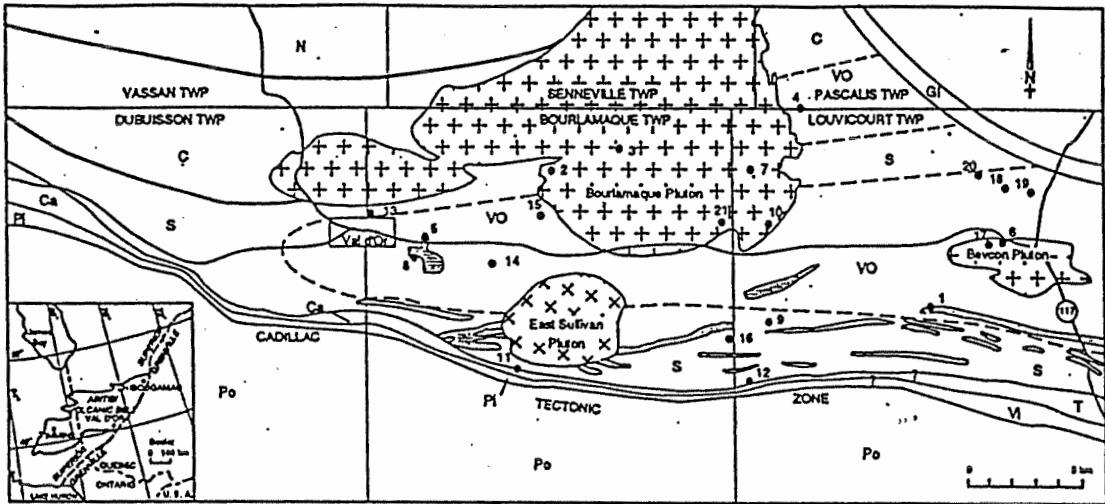
NAME	EL SOL	BUFFADISON	ADELMONT
Status	Deposit	Deposit	Deposit
Symbol in Figure 34.	16	17	18
Size	In 1983, possible reserves of 45,000 t grading 11.32 g/t Au.	In 1986, reserves of 530,581 t grading 4.11 g/t Au.	In 1987, possible reserves before dilution of 500,000 t grading 5.14 g/t Au.
Host Rocks	Diorite sill.	Bevcon granodiorite pluton.	Sheared diorite.
Morphology ¹	Qz veins.	Multiple Qz-Tm-Cb veins.	Qz-Cb veins.
Ore Mineralogy ¹	Au-Py disseminated in veins.	Au-Ag-Py-Cp-Sh disseminated in veins.	Au-Py in veins.
Alteration	Not mentioned.	Not mentioned.	Silicification.
Reference	M.E.R.Q. microfiche deposit # 32C/4-91.	M.E.R.Q. microfiche deposit # 32C/3-31.	M.E.R.Q. microfiche deposit # 32C/3-34.

¹- Qz: quartz; Tm: tourmaline; Cb: carbonate; Py: pyrite; Po: pyrrhotite; Cp: chalcopyrite; Au: gold; Ag: silver; Asp: arsenopyrite; Sh: scheelite; Gn: galena; Bi: bismuthinite; Te: tellurides; Mn: magnetite; Ep: epidote.

Table 2. Summary of characteristics of gold deposits in Bourlamaque and Louvicourt townships, Val d'Or-east district (end).

NAME	NORCOURT	MONIQUE	WRIGHTBAR ZONE D.
Status	Deposit	Deposit	Deposit
Symbol in Figure 34.	19	20	21
Size	In 1987, 467,205 t grading 6.17 g/t Au.	In 1986, probable and possible reserves of 728,000 t grading 6.10 g/t Au.	In 1988, potential reserves of more than 300,000 t grading 7.89 g/t Au.
Host Rocks	Diorite.	Veins crosscutting intrusions.	Shear zone in Bourlamaque granodiorite intrusion.
Morphology	Quartz veins.	Quartz veins.	Qz-Tm-Ch-Cb veins.
Ore Mineralogy ¹	Au disseminated in quartz veins.	Au-Py.	Au-Cp-Py.
Alteration	Not mentioned.	Not mentioned.	Not mentioned.
Reference	M.E.R.Q. microfiche deposit # 32C/3-35.	M.E.R.Q. microfiche deposit # 32C/3-58.	M.E.R.Q. microfiche deposit # 32C/4-98.

¹- Qz: quartz; Tm: tourmaline; Cb: carbonate; Py: pyrite; Po: pyrrhotite; Cp: chalcopyrite; Au: gold; Ag: silver; Asp: arsenopyrite; Sh: scheelite; Gn: galena; Bi: bismuthinite; Te: tellurides; Mn: magnetite; Ep: epidote; Ch: chlorite.





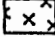
- | | |
|--|--|
| <p>V VASSAN DOMAIN
Komatiites, basalts.</p> <p>C CENTRAL DOMAIN
Basalts, komatiites, minor sediments.</p> <p>S SOUTHERN DOMAIN
Intermediate to mafic flows, intermediate volcanics, minor komatiitic flows.</p> <p>VO VAL D'OR DOMAIN
Intermediate volcanics composed of polygenic fragments, mafic to felsic flows and breccias.</p> <p>Ca CADILLAC GROUP
Greywackes, siltstones, conglomerates.</p> <p>PI PICHÉ GROUP
West of Val d'Or: mafic to ultramafic flows, east of Val d'Or: ultramafic to felsic schists (flow and volcanoclastic material).</p> <p>T TRIVIO GROUP
Tuffaceous sediments, greywackes, conglomerates, flow material.</p> | <p>VI VILLEBON GROUP
Mafic flows, a few ultramafic flows.</p> <p>Po PONTIAC GROUP
Greywackes, pebbles.</p> <p>GI GARDEN ISLAND GROUP
Greywackes, schists, conglomerates.</p> <p> Mafic to intermediate sills or intrusions.</p> <p> Synvolcanic granodiorite-quartz diorite intrusion.</p> <p> Post-tectonic monzonitic intrusion.</p> |
|--|--|

Figure 34. Location map of major gold deposits in Bourlamarque and Louvicourt townships; modified after Sauvé et al. (1986) and Desrochers et al. (1993). Numbers correspond to deposits described in Table 2.

4.2 ENVIRONMENTS OF SYNVOLCANIC GOLD MINERALIZATION

4.2.1 Porphyry Copper Deposits

Although technically plutonic, porphyry copper deposits are listed among synvolcanic deposits because of their high crustal (subvolcanic) position and timing. In general, porphyry copper deposits are large and low-grade (at least 20 million tonnes containing a minimum of 0.1 % Cu, according to Lowell, 1974), intrusion-related deposits that can be mined using mass mining techniques. The intrusions are generally felsic and differentiated, were emplaced at less than approximately four kilometres from the surface, and are almost invariably porphyritic. Local portions of the intrusions are suggested to be the source of heat causing circulation of hydrothermal fluids from both magmatic and groundwater sources.

Large-scale patterns of alteration and mineralization resulted from hydrothermal circulation. The complete sequence is rarely developed or preserved. However, a completely developed alteration and mineralization pattern would include potassic alteration (intense hydrolysis) which coincides with low-grade ore in the core of the deposit centred on the intrusion, mantled by a higher-grade ore shell (disseminations, fracture fillings, and quartz vein fillings of chalcopyrite, bornite, molybdenite, pyrite) associated with pyrite-phyllitic alteration which is in turn mantled by a less intensely altered argillic-propylitic zone containing veins of Au, Ag, Cu, Zn, and Pb (Lowell and Guilbert, 1970; Guilbert and Lowell, 1974).

Porphyry copper deposits are found mainly in island arc and continental margin settings, emphasizing the relationship between subduction, magmatism, and porphyry copper deposits. According to their setting, these deposits may be characterized as plutonic, volcanic or "classic" (Cenozoic deposits in the southwest United States) (McMillan and Panteleyev, 1980). Plutonic porphyry copper deposits occur in batholithic settings with mineralization principally occurring in one or more phases of plutonic hostrock. Volcanic types occur in the roots of volcanoes, with mineralization overprinted on both the volcanic rocks and associated co-magmatic plutons. Classic types occur in and around high-level, post-orogenic stocks that intrude unrelated host rocks. Mineralization may occur entirely within the intrusive rock, entirely in the country rock, or in both.

As already stated in the Introduction of this chapter, only a few Precambrian deposits with characteristics similar to porphyry copper deposits have been described (Kirkham, 1972; Griffis, 1979; Gaál and Isohanni, 1979; Goldie et al., 1979; Guha, 1984; Symons et al., 1988; Guha et al., 1988; Hodgson, 1990; Tessier, 1990; Fraser, 1993). Primary features may be obscured by deformation and metamorphism (Kirkham, 1972; Griffis, 1979), and any sulphide and metal zonation that might have been present is at least affected by later deformation and metamorphism (Kirkham, 1972). Kirkham (1972) also suggests that classic porphyry copper deposits associated with post-orogenic stocks have probably been eroded away to a large extent due to their emplacement at high levels in the crust.

As for the suitability of the Bourlamaque-Louvicourt townships study area for porphyry mineralization, we first note that there are three types of porphyry copper deposits according to metal concentrations: 1) copper-bearing, 2) copper-molybdenum-bearing, and copper-gold-bearing (McMillan and Panteleyev, 1980; Titley and Beane, 1981). In the Bourlamaque-Louvicourt townships study area proper, there is only one copper-molybdenum occurrence (the Savard-2 showing; microfiche deposit # 32C/4-29; Bellemare and Germain, 1987) associated with a quartz porphyry crosscutting the Bourlamaque intrusion (Campiglio, 1977). However, in Pascalis Township, just north of Louvicourt Township, porphyry copper-type mineralization has been recognized in the Perron mine located along the eastern border of the Bourlamaque intrusion (Tessier, 1990). This occurrence is similar to porphyry copper-type Cu-Au mineralization in the McIntyre mine in Ontario (Hodgson, 1990). Molybdenum and tungsten analyses of the Bourlamaque pluton by Campiglio (1977) gave values at or below the 1 ppm detection limit for both elements; these are "normal" values for diorites (Vinogradov, 1962). In spite of certain characteristics of the Bourlamaque intrusion common to plutons associated with plutonic porphyry copper deposits (batholithic size, inferred depth of emplacement between 2 and 4 kilometres (see Section 3.3.3), calc-alkalic composition and co-magmatic with surrounding rocks (see sections 2.2 and 2.3.3.2), expected breccias are absent and more importantly, there is no apparent alteration and/or metal zonation associated with this intrusion.

Small (0.2 to 10 km²), calc-alkalic intrusions co-magmatic with surrounding volcanic rocks are commonly found associated with volcanic-type porphyry copper deposits. In the study area, similar intrusive bodies may have generated porphyry-type mineralization; however, Cu±Mo±Au mineralization and zoned alteration are unknown in association with these relatively small intrusions. Furthermore, as suggested above by Kirkham (1972) for classic porphyry copper deposits, volcanic-type if not also pluton-type porphyry copper deposits in our study area may have been eroded away. Solomon (1990) suggests that porphyry copper-gold deposits of island arc systems form in emergent, essentially compressional island arc regimes, a tectonic setting incompatible with Kuroko-type, volcanic-hosted massive sulphide deposits which typically develop in extensional back-arc basins. Based on this suggestion and the known occurrences of synvolcanic massive sulphide deposit in the study area (Chapter 3), island-arc porphyry copper-gold systems are not likely to have formed during synvolcanic time in our study area.

4.2.2 Gold Skarn Deposits

The following summary on skarns and gold skarn deposits is taken mainly from Meinert (1992). A rock may be defined as a skarn by the presence of a wide variety of calc-silicate and associated minerals, usually including garnet and pyroxene. The majority of skarns are found in lithologies containing some carbonate, but they may occur in shale, sandstone, granite, basalt, and komatiite. Skarns form during regional

and contact metamorphism and typically comprise a variety of metasomatic processes involving fluids of magmatic, metamorphic and evolved meteoric and/or marine origin.

Most high-grade gold-bearing skarn deposits are associated with reduced (ilmenite-bearing) diorite-granodiorite plutons and dike/sill complexes. Such skarns are dominated by iron-rich pyroxene. Most gold is present as electrum and is strongly associated with bismuth- and telluride-bearing minerals. Gold is considered to have been transported by hot (> 700 °C), highly saline (up to 30 wt. % NaCl equivalent) fluids.

The vast majority of skarn deposits are associated with magmatic arcs related to subduction beneath continental crust. Some economic gold skarns appear to have formed in back-arc basins associated with oceanic volcanic arcs (Ray et al., 1988). These deposits are characterized by their association with gabbroic and dioritic plutons, abundant endoskarns, widespread sodium metasomatism, and the absence of Sn and Pb, reflecting the primitive, oceanic nature of the crust, wallrocks and plutons.

Several Archean gold-silver deposits in the Southern Cross greenstone belt of western Australia have prominent calc-silicate alteration and are classified as skarn deposits (Mueller, 1988). Replacement of mafic or ultramafic amphibolites and silicate-facies banded iron formation during the retrograde phase of contact metamorphism resulted in the formation of strongly Ca- and K-metasomatized skarn deposits.

Given that the majority of skarns are associated with lithologies having some carbonate, it is unlikely that skarns and gold-bearing skarn deposits formed in the Bourlamaque-Louvicourt townships study area which lacks carbonates. Secondly, the indicator minerals, garnet and pyroxene, are non-existent or present in only trace amounts in this region. Therefore, the presence of skarn deposits in the Bourlamaque-Louvicourt townships study area is improbable.

4.2.3 Epithermal Precious Metal Deposits

The analogy has been drawn between active geothermal systems and epithermal precious metal (EPM) deposits (Henley and Ellis, 1983; Henley, 1985). Epithermal mineralization occurs from surface to a maximum depth of approximately 1,000 metres. Low-grade, and local high-grade ("Bonanza-type"; Romberger, 1992), finely-disseminated gold (\pm silver) mineralization commonly characterizes EPM deposits and occurs in both volcanic and sedimentary rocks.

Romberger (1986a) has summarized the principal characteristics of epithermal precious metal deposits. The simplest model involves heat supplied by a subvolcanic intrusion whose emplacement was guided by local fault zones and fracture systems. Meteoric water heated by a magmatic source leaches metals from all material through which the solutions pass. The mineralized fluids rise by open subvertical fracture systems, precipitating metals as a result of physicochemical changes (e.g., boiling, cooling, oxidation) occurring at high levels in the system.

The host rocks commonly serve as "chemical sinks" for materials dissolved in the hydrothermal solutions. Chemical exchange between the host rocks and convecting mineralized fluids is evident because of the various alterations associated with mineralization. Silicification is the most important type of alteration; other types include decalcification and argillization.

In general, disseminated gold deposits have little or no obvious crustal-scale structural control. However, at the deposit scale, the style of fracturing and hence mineralization varies according to the host rock. For example, argillaceous sedimentary rocks will yield as well as fracture at depth due to direct stresses, and they commonly host disseminated precious metal deposits. In contrast, volcanic rocks emplaced at or near the surface may develop well-developed open fractures as a result of brittle failure. Therefore, precious metal deposits in volcanic rocks commonly show a strong structural control, where veins acted as feeder systems for disseminated mineralization.

On a regional scale, faults and fracture systems localize igneous activity. In turn, on a local scale, this igneous activity creates smaller-scale fracturing, thus furnishing the permeability necessary for the circulation of ore solutions and the filling of open spaces with mineral constituents.

Gold (\pm silver) mineralization in EPM deposits shows a close association with pyrite. Realgar (AsS), orpiment (As₂S₃), cinnabar (HgS) and arsenopyrite (FeAsS) are

also common. Gold is thought to have been transported as bisulphide complexes (e.g., $\text{Au}(\text{HS})_2^-$; Seward, 1973; Shenberger and Barnes, 1989) in solutions with salinities of 3 wt. % NaCl equivalent on average, and at temperatures in the 200 to 300°C range (Romberger, 1986b).

Gold precipitation may occur principally as a result of a decrease in temperature, boiling, oxidation, or H_2S activity. Boiling of a gold-bearing hydrothermal fluid results in a loss of volatiles (CO_2 , CH_4 , H_2S , H_2) to the gas component of the fluid which increases the fugacity of oxygen and decreases the activity of HS^- of the remaining liquid, and consequently, destabilizes Au-transporting thiocomplexes such as $\text{Au}(\text{HS})_2^-$. Boiling also decreases the fluid temperature, accelerating gold precipitation. Mixing of hydrothermal fluids with cool, oxidized near-surface fluids has similar effects as boiling: heat is lost, decreasing sulphide complex activities, oxidizing these sulphide complexes, and hence favouring gold precipitation. Hydrothermal fluids may also be oxidized if they circulate through an oxide-bearing rock, again causing a decrease in sulphide complex activities. Drummond and Ohmoto (1985) show that a decrease in H_2S activity is more efficient than oxidation for precipitation of gold in a boiling hydrothermal system.

Because of the shallow environment of deposition for EPM mineralization, this type of ore deposit has probably been eroded away, if it ever formed in the study area during Archean times. However, there is a possibility that, during folding and faulting, a section of upper crust with EPM mineralization may have been isolated and preserved

at depth. Nevertheless, minerals characteristic of shallow environments of deposition, such as realgar, cinnabar, and orpiment, have not been detected in the study area.

4.2.4 Volcanogenic Massive Sulphide Deposits

Volcanogenic massive sulphide (VMS) deposits are typically mined for their copper, zinc and/or lead contents. However, some VMS deposits contain non-negligible amounts of gold \pm silver in addition to their base-metal contents (Chartrand and Cattalani, 1990; Large, 1992). And in some cases, gold is a major economic metal, as in the case of the Horne mine in Rouyn-Noranda (Kerr and Mason, 1990).

Huston and Large (1989) and Large et al. (1989) studied the presence of gold in several Australian VMS deposits, whereas Hannington et al. (1986) and Hannington and Scott (1989) examined gold mineralization in VMS deposits from active hydrothermal vents on the seafloor. These studies discuss the important geochemical parameters of fluid chemistry affecting the transport and precipitation of gold in VMS environments. The following is a brief summary of the comparison between Huston and Large (1989) and Large et al. (1989) and Hannington et al. (1986) and Hannington and Scott (1989). VMS formation has been discussed in Chapter 3, and the reader is referred to that section for a summary of this topic.

Huston and Large (1989) and Large et al. (1989) identified two distinct spatial and mineralogical associations of gold and base metals in VMS deposits, based mainly

on their study of Australian gold-bearing VMS deposits: 1) a gold-zinc(-lead-silver-barite) association, typically of zinc-lead-rich deposits, with gold concentrated at the top of the massive sulphide bodies; and 2) a gold-copper association in which gold is concentrated in the central and lower portions of the massive sulphide bodies and in the cores of stringer zones. Although some deposits may exhibit both associations, one commonly dominates over the other.

Huston and Large (1989) and Large et al. (1989) reviewed these metal associations elsewhere. For example, the Millenbach deposit (Knuckey et al., 1982) in Abitibi has a gold-copper association and the Corbet deposit (Knuckey and Watkins, 1982) exhibits a gold-zinc association. In the Kuroko district of Japan, the majority of the deposits has a gold-zinc association, although the Nurukawa deposit, Akita prefecture (Yamada et al., 1987) in the Hokuroko district is a good example of a gold-copper association. Also, recent sulphide chimneys at seafloor spreading centres exhibit gold-zinc associations and lack the gold-copper association (Hannington et al., 1986). Huston and Large (1989) and Large et al. (1989) suggest that the gold-copper association has not been detected in modern sulphide deposits because of the small sample population and possibly because of a lack of samples from the deeper chimney portion of these deposits where the gold-copper association would be expected to occur.

The transport of gold in VMS-forming systems may be constrained in part from our understanding of gold transport in other hydrothermal systems. For example, several

studies have suggested that the thiocomplex $\text{Au}(\text{HS})_2^-$ is the most important species for gold transport in epithermal gold and Archean lode-gold environments (Seward, 1973, 1984; Phillips and Groves, 1983; Henley, 1984, 1985; Cathles, 1986; Shenberger and Barnes, 1989), although chlorocomplexes, thioarsenates, thioantimonates, and tellurium species are also recognized as possible gold complexes (Seward, 1984; Romberger, 1986b).

However, Huston and Large (1989) and Large et al. (1989) suggest that chlorocomplexes may be especially important in massive sulphide environments whose higher salinities and lower pHs, in comparison to Archean lode-gold and epithermal gold conditions, would favour chlorocomplexes. Based on thermodynamic data for gold, copper, and zinc, geochemical calculations by Huston and Large (1989) and Large et al. (1989) suggest that the gold-copper and gold-zinc associations may be explained by two different complexing species. For the gold-copper association, they suggest that gold is transported as a AuCl_2^- complex in relatively high-temperature fluids ($> 300^\circ\text{C}$) with low pH (< 4.5), low H_2S concentrations ($< 10^{-2.5}$ m), high salinities ($>$ seawater), and moderate to high oxygen fugacities (pyrite or magnetite \pm hematite stable). Conversely, for the gold-zinc association, they suggest that gold is transported as the $\text{Au}(\text{HS})_2^-$ complex in relatively low-temperature fluids ($150\text{-}300^\circ\text{C}$) with moderate to alkaline pH (> 4.5), high H_2S concentrations ($> 10^{-2.5}$ m), low salinities ($<$ seawater), and moderate oxygen fugacities (pyrite field only).

Hannington et al. (1986) and Hannington and Scott (1989) observed in sulphide chimneys from various, modern seafloor sites the gold-zinc but not the gold-copper association. They suggest, based on geochemical data from several sulphide chimney settings, that gold mineralization from fluids with high concentrations of H_2S , temperatures greater than $350^\circ C$, and $pH \geq 3.6$ indicates gold transported as bisulphide complexes. Hannington et al. (1986) and Hannington and Scott (1989) acknowledge that gold may be removed from source rocks as $AuCl_2^-$ species, but that more gold would precipitate from the $Au(HS)_2^-$ species than from the $AuCl_2^-$ species. Hannington and Scott (1989) accept the two-fold gold association of Huston and Large (1989) and Large et al. (1989), but, they state that (p.503) "the enrichment of gold in pyrite-chalcopyrite assemblages at some H_2S -rich vent sites (e.g., TAG field) cautions us not to exclude the possibility of gold mineralization from $Au(HS)_2^-$ in the Cu-rich, pyrite-chalcopyrite ores of some ancient deposits (e.g., HW mine, *British Columbia*). In general, a Cu-Au association by itself is insufficient proof for chloride complexing of gold." (Italicized words added by the author).

In conclusion, gold mineralization may be present in the stockwork or massive sulphide body of VMS deposits and may be associated with either lead-zinc or copper mineralization. Although the transport and precipitation mechanisms for gold in base-metal environments are not yet clear, bisulphide complexes are generally accepted as important species for transporting gold in geological situations pertinent to VMS environments.

Although gold and silver accompany base-metal mineralization of the VMS type in the study area (see Table 1, pages 97-99), little information exists on the association of precious metals with base metals. Assad (1958) mentions that gold is a minor metallic mineral at the East Sullivan deposit, occurring in native form as small particles in pyrite associated with other metallic minerals. At the Manitou-Barvue Zn-Cu-Ag deposit, silver and minor gold are found in a series of stratiform lenses of massive pyrite and sphalerite, and minor amounts of gold and silver are found in the cupriferous stockwork zone (Popov, 1976). For the Louvem mine, Raymond (1983) briefly mentions the presence of minor amounts of gold, silver and galena with zinc mineralization, and at the recently discovered Louvicourt deposit, gold mineralization is associated with Zn mineralization (I. Rougerie, 1993, pers. commun.).

The Akasaba gold deposit located in the south-central part of Louvicourt Township (deposit #12 of Fig. 34) exhibits features akin to a synvolcanic environment. It consists of disseminated gold in a lapilli tuff accompanied by pyrrhotite, chalcopyrite, magnetite, and pyrite (Sauvé, 1985). The deposit is also characterized by abundant epidote alteration and relatively rare carbonate alteration. Sauvé (1985) hypothesizes that the emplacement of this deposit is fundamentally synvolcanic. Its mineralogy, configuration and emplacement near the top of the volcanic pile, if the paleoenvironment of Imreh (1984) is followed, suggest that the Akasaba deposit is in fact synvolcanic.

4.2.5 Banded Iron-Formation-Hosted Gold Deposits

It is widely agreed that Archean banded iron-formation is a chemical or possibly biochemical submarine precipitate attributed to a volcanic exhalative source (Goodwin, 1973). The classic oxide, carbonate and sulphide facies of iron formation represent deposition in progressively deeper water, respectively. Although oxide-facies iron-formation is the most readily recognized type, gold mineralization is typically associated with sulphide-facies iron-formation (Phillips et al., 1984; Groves et al., 1987), and some gold is associated with sulphidization of oxide and/or carbonate facies iron formation (Macdonald and Fyon, 1986).

There is poor agreement on the timing and source of gold mineralization in iron-formation. Three genetic models (syngenetic, multistage or remobilization, and epigenetic) are commonly used to explain iron-formation-hosted gold deposits. The syngenetic model states that gold is concentrated during the deposition of iron formation on the seafloor (Ridler, 1970; Hutchinson et al., 1971; Fripp (1976a,b); Franklin and Thorpe, 1982; Kerswill, 1986). Fripp (1976a,b) suggests that convecting heated seawater leached gold from country rocks and deposited the metal contemporaneously with the banded iron-formation on the seafloor. The multistage model invokes syngenetic concentrations of gold in iron formation followed by remobilization and further concentration of that gold during later metamorphic and/or tectonic events (Rye and Rye, 1974; Anhaeusser, 1976; Saager et al., 1987; Oberthür et al., 1990; Ladeira, 1991). For example, Saager et al. (1987) and Oberthür et al. (1990) note an increase in metamorphic

grade from greenschist facies in the Bar 20 mine to amphibolite facies in the Vubachikwe mine, both hosted by iron formations in the Gwanda greenstone belt, Zimbabwe. This trend is also accompanied by increased grain sizes for quartz, arsenopyrite and gold "which unquestionably points to ore emplacement prior to the peak of regional metamorphism" (page S133; Oberthür et al., 1990). The epigenetic model proposes that gold emplacement took place at some time after the deposition of the iron-formation (Fyon et al., 1983; Macdonald, 1983; Macdonald and Fyon, 1986; Phillips et al., 1984; Groves et al., 1987; Fisher and Foster, 1991). Fyon et al. (1983) and Macdonald (1983) stress the strong structural control on gold mineralization in banded iron-formation and present evidence of selective replacement (i.e., sulphidation) of oxide and/or carbonate minerals in banded iron-formation by later, gold-bearing sulphides. For example, the Carshaw and Malga iron-formations of the Timmins area clearly have anomalous gold contents (up to 6 ppm) where sulphidized along cross-cutting fractures (Fyon et al., 1983), whereas unaltered, undeformed and non-sulphidized banded iron-formation have normal background levels of gold (< 10 ppb) (Macdonald and Fyon, 1986). In addition, several characteristics suggest that Archean banded iron-formation-hosted gold deposits were formed by processes similar to those involved in lode-gold deposition (Groves et al., 1987).

In conclusion, although the epigenetic model seems presently to be the favoured model to explain gold mineralization in iron-formation, there seems to be some evidence

of syngenetic gold being remobilized by later events, and hence the multistage model may also locally apply.

Although two units of magnetite-facies iron-formation occur in the Garden Island and Trivio groups in the neighbouring Vauquelin and Pershing townships (Marquis and Goulet, 1987), no iron-formation has been noted in these geologic groups in the study area. In addition, there is no mention by Marquis and Goulet (1987) of gold mineralization associated with the banded iron-formations east of the Bourlamaque-Louvicourt townships study area.

4.3 SYN- TO LATE-TECTONIC GOLD MINERALIZATION ENVIRONMENTS

4.3.1 Quartz-Vein Gold Deposits

Classic quartz-vein gold deposits are considered syn- to late-tectonic as opposed to synvolcanic deposits. They occur mostly as mesothermal quartz-carbonate veins, disseminations, and replacements in shear zones, and less commonly as veins in extensional fractures, stockwork zones, and breccias. They are associated spatially with regional first-order fault zones (Eisenlohr et al., 1989; Poulsen and Robert, 1989; Robert, 1990a) known traditionally as major east-west-trending "breaks" in the Abitibi. In the case of the regional Larder Lake-Cadillac "break" or tectonic zone (LLCTZ), gold deposits occur along and up to 15 kilometres north of this first-order crustal-scale structure. The lode-gold deposits themselves are more closely related to more local

second-order structures. Within the deposits, the mineralization typically occurs in third-order structures (Poulsen and Robert, 1989; Robert, 1990a), and is frequently hosted by or spatially associated with small felsic porphyry intrusions. Third-order structures may attain a few hundred to a few thousand metres in length, and they include individual shear zones, extensional fractures, and discrete fault systems. Shear zones may exhibit a mix of brittle-ductile behaviour, indicating either differences in host rock competency or variations in the more or less mesothermal depth of gold mineralization.

Mineralized veins are composed mainly of quartz with variable amounts of pyrite, arsenopyrite, chalcopyrite, carbonate, tourmaline, albite, chlorite, scheelite, tellurides, and native gold. Val d'Or-east gold veins are commonly characterized by abundant tourmaline, forming a distinctive "vein field" of mineralized quartz-carbonate-tourmaline-pyrite veins (Robert and Boullier, in press). The abundant tourmaline may indicate a plumbing system intersecting marine sediments (Pontiac sediments?) at depth (Robert, 1993, pers. commun.). Arsenopyrite is also commonly present in gold deposits located in or near sedimentary sequences.

Considerable information on the nature and timing of the mesothermal vein mineralization has been gained from studies of the vein genesis and mineral paragenesis. Wallrocks surrounding quartz veins are hydrothermally altered, and in the case of the Sigma mine, this alteration is both visible and cryptic (Figs. 35a and 35b; Robert and Brown, 1984, 1986b). The strongest and most common wallrock alterations in initially

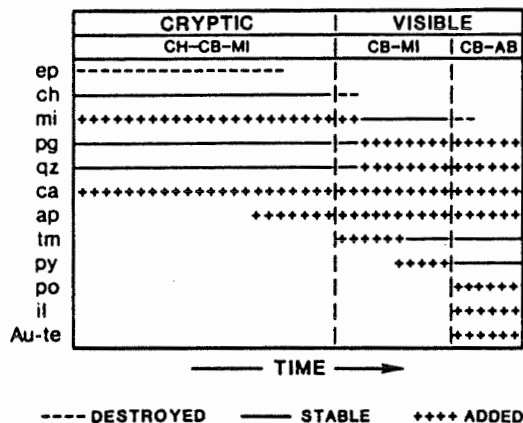


Figure 35a. Sequence of development of alteration zones and subzones around tension veins. Horizontal axis represents time as well as intensity of alteration. (CH: chlorite, CB: carbonate, MI: white mica, AB: albite, ep: epidote, ch: chlorite, mi: white mica, pg: plagioclase, qz: quartz, ca: calcite, ap: apatite, tm: tourmaline, py: pyrite, po: pyrrhotite, il: ilmenite, Au: gold, te: tellurobismuthite). (from Robert and Brown, 1986b).

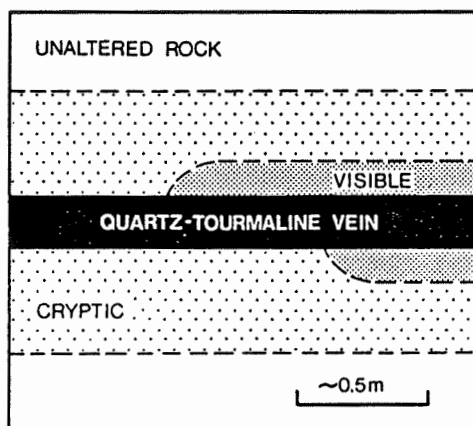


Figure 35b. A schematic representation of the distribution of cryptic and visible alteration zones around flat veins and dike stringers. Visible alteration may be absent and grade laterally to asymmetrical or to symmetrical alteration envelopes (from Robert and Brown, 1984).

greenschist-facies hostrocks include carbonatization, potassium metasomatism and pyritization, indicating additions of CO₂, K, and S. Pre-ore metamorphic minerals, such as chlorite, biotite, and epidote, are commonly destroyed in the wallrocks, with the most intense destruction adjacent to the veins where hydrothermal fluids circulated. Buff to beige visible alteration next to the veins is characterized by a carbonate-white mica outer subzone and a carbonate-albite inner subzone (Fig. 35a), whereas cryptic alteration is characterized by a greenish chlorite-carbonate-white mica assemblage.

Fluid-inclusion and light-stable isotope studies have aided in understanding the geochemical characteristics of the fluids responsible for Archean lode-gold mineralization. The following summary of the results of many fluid-inclusion and stable-isotope studies is based on an overview by Colvine et al. (1988; p.61-69).

Studies of fluids interpreted to have been trapped during gold precipitation indicate that the gold-bearing fluids 1) had low salinities (< 6 wt. % NaCl equivalent); 2) were aqueous with moderate- to high-CO₂ densities (0,7 to > 1,0 g/cm³) and possibly contained minor amounts of CH₄; 3) were neutral to slightly acid where sericite is stable; 4) had minimum fluid-inclusion trapping temperatures between 200 and 400°C and cluster around 350°C (actual trapping temperatures may have been higher); and 5) had trapping pressures between 1.5 and 4.5 kilobars, corresponding to depths of approximately 4 to 12 kilometres if lithostatic pressures are assumed.

Similarities between Canadian and Australian Archean gold deposits for carbon, sulphur, oxygen, and hydrogen isotopic data suggest that 1) a compositionally uniform fluid was involved in gold mineralization and its associated hydrothermal alteration; 2) a common fluid generation process occurred for most deposits; and 3) fluids were derived from a large reservoir external to the immediate depositional site. Under the optimal geochemical conditions, total dissolved carbon in auriferous hydrothermal fluids would have an approximate $\delta^{13}\text{C}$ value of -7 to 0 per mil; the median value of -3,5 per mil may be a more realistic estimate of the carbon isotope value for the ore-fluid, given the $\delta^{13}\text{C}$ variations at deposit sites. For the $\delta^{34}\text{S}$ content of total dissolved sulphur in the auriferous hydrothermal fluid, a general value of 0 per mil is suggested. $\delta^{18}\text{O}$ values for Abitibi vein quartz vary from +5 to +10 per mil (no matter what the host rock is) and Australian $\delta^{18}\text{O}$ values for vein quartz vary between +11 to +14 per mil. $\delta^{18}\text{O}$ values for hydrothermal fluids from which vein quartz precipitated range from +5 to +10 per mil (Abitibi and Australian data combined). There are few hydrogen isotopic data, in comparison to carbon, sulphur, and oxygen data, and the data are variable and difficult to interpret because of hydrogen's inherent mobile nature such that there is no general value or range for hydrogen isotopic data.

Because of the destruction of metamorphic minerals, the relative timing of fluid circulation and vein formation for most lode-gold deposits is considered to be post-peak metamorphism, although the Norseman lode-gold deposits in the Norseman-Wiluna Belt of the Eastern Goldfields Province in Australia developed prior to the peak of

metamorphism (Golding and Wilson, 1987). Geochronological studies on metamorphic minerals and minerals from mineralized veins associated with alteration envelopes from deposits in the Val d'Or district estimate peak metamorphism at ca 2,680 Ma (from hornblende using the $^{40}\text{Ar}/^{39}\text{Ar}$ method; Hanes, et al., 1992) and the majority of vein formation and gold mineralization at ca 2,580 to 2,630 Ma, based on various techniques (e.g., U-Pb, K-Ar, $^{40}\text{Ar}/^{39}\text{Ar}$, Rb-Sr, Sm-Nd, $^{207}\text{Pb}/^{206}\text{Pb}$ analyses) on various minerals (zircon, micas, scheelite, rutile, titanite, monazite) (Jemielita et al., 1989; Zweng and Mortensen, 1989; Wong et al., 1991; Hanes et al., 1992; Zweng et al., 1993; Corfu, 1993). However, recent geochronological work on gold deposits west of Val d'Or indicate that some gold mineralization is older and may have formed prior to peak-metamorphic conditions (minimum age — $2,686 \pm 2$ Ma: Morasse et al., 1993 and minimum age — $2,692 \pm 2$ Ma: Pilote et al., 1993) (see sections 4.4.4 and 4.6 for further discussions of these older ages).

4.3.2 Pyritic Gold Deposits

In addition to classic mesothermal quartz veins, gold in the Abitibi occurs in pyritic deposits (Robert, 1990b). Archean pyritic gold mineralization in the Abitibi is especially well-known in the Bousquet camp of the Cadillac area, including the Dumagami, Bousquet No.1 and No.2, Ellison, and Doyon deposits. They have been extensively studied (e.g., Valliant and Hutchinson, 1982; Valliant et al., 1982; Tourigny et al., 1989a,b; Marquis et al., 1990a,b) and their principal characteristics have been

summarized in Robert (1990b). The following description of pyritic gold deposits is based on a summary by Robert (1990b).

Archean pyritic gold deposits are characterized by high sulphide contents and are composed of lenses of disseminated to massive sulphides and zones of pyrite-rich veinlets. Several ages of disseminated pyrite are identified: synvolcanic, syntectonic, and late tectonic as alteration fringes around late-tectonic Fe-dolomitic veins. Regionally, they are located in or near major deformation zones within volcanic units known for VMS deposits (e.g., the Blake River Group in the southern Abitibi). On a local scale, the deposits are found dominantly in sericitized, felsic volcanic rocks, but they may also be found in mafic volcanic rocks. Contrary to quartz-vein deposits, they lack an association with small felsic porphyry intrusions.

Pyrite, the principal sulphide, is accompanied by variable amounts of chalcopyrite, pyrrhotite, sphalerite, arsenopyrite, galena, and magnetite. Quartz and carbonate constitute the main non-sulphide gangue minerals. Gold is typically intimately associated with pyrite±chalcopyrite, and is commonly accompanied by tellurides.

Metamorphic minerals such as andalusite, kyanite, chloritoid, and manganiferous garnet reflect a highly aluminous composition for the host rocks, caused either by seafloor hydrothermal alteration or by VMS-type hydrothermal alteration of footwall

rocks. A post-peak metamorphism alteration event, concordant with gold mineralization, is recognized in the transformation of andalusite to kaolinite, pyrophyllite, and diaspore.

It is generally agreed that the sulphide bodies of these pyritic gold deposits have a synvolcanic origin of the VMS-type. However, there is no clear consensus of the timing of gold emplacement. Valliant and Hutchinson (1982) and Valliant et al. (1982) proposed that the gold mineralization was purely synvolcanic (exhalative), Tourigny et al. (1989b, 1993) interpreted it to be entirely syntectonic in its final distribution, with a possibly initial synvolcanic emplacement in VMS-type mineralization, and Marquis et al. (1990a,b) regard it as syn- to late-tectonic in timing. The possibility of syntectonic remobilization of early synvolcanic gold has not been fully examined, and this question is being addressed by N. Teasdale, Ph.D. candidate at l'École Polytechnique, in his study of the Bousquet #2 deposit where primary volcanic features seem to have survived through syntectonic deformation.

4.4 MODELS FOR ARCHEAN MESOTHERMAL LODGE-GOLD MINERALIZATION

4.4.1 Introduction

Genetic models for Archean mesothermal lode-gold mineralization have been debated extensively over the last ten years, and as a result, our understanding has advanced considerably on such topics as fluid chemistry, hostrock alteration, and vein formation involved in the genesis of this deposit type. Concurrent with these advances,

our knowledge of tectonic and petrogenetic processes has broadened considerably, enabling a better understand of the development of greenstone-belts and craton formation.

The principal mesothermal lode-gold genetic models (the meteoric water, orthomagmatic, metamorphic dehydration, and mantle degassing-granulitization models) propose various fluid and solute sources and numerous reasons for gold deposition. The following section is a brief summary of these four genetic models and of the several characteristics of Bourlamaque and Louvicourt townships (Val d'Or-east sector) that are concordant with the principal elements of the mantle degassing-granulitization model. The evaluation of these models suggests that the mantle degassing-granulitization model, although not completely satisfactory, best explains Archean mesothermal lode-gold mineralization in the context of the greenstone-belt evolution of the study area.

4.4.2 Meteoric Water Model

In this model, it is hypothesized that epithermal and mesothermal gold deposits in the Canadian Cordillera were formed by the convection of descending meteoric waters (Fig. 36). Because of chemical and geological similarities between mesothermal gold deposits of the Canadian Cordillera (Late Jurassic to Late Tertiary) and Archean lode-gold deposits (Hodgson et al., 1982), proponents of the meteoric water model (Nesbitt et al., 1986, 1987, 1989; Nesbitt, 1988; Nesbitt and Muehlenbachs 1989a, b) suggest that deep circulating meteoric fluids were a major component of Archean mineralizing fluids.

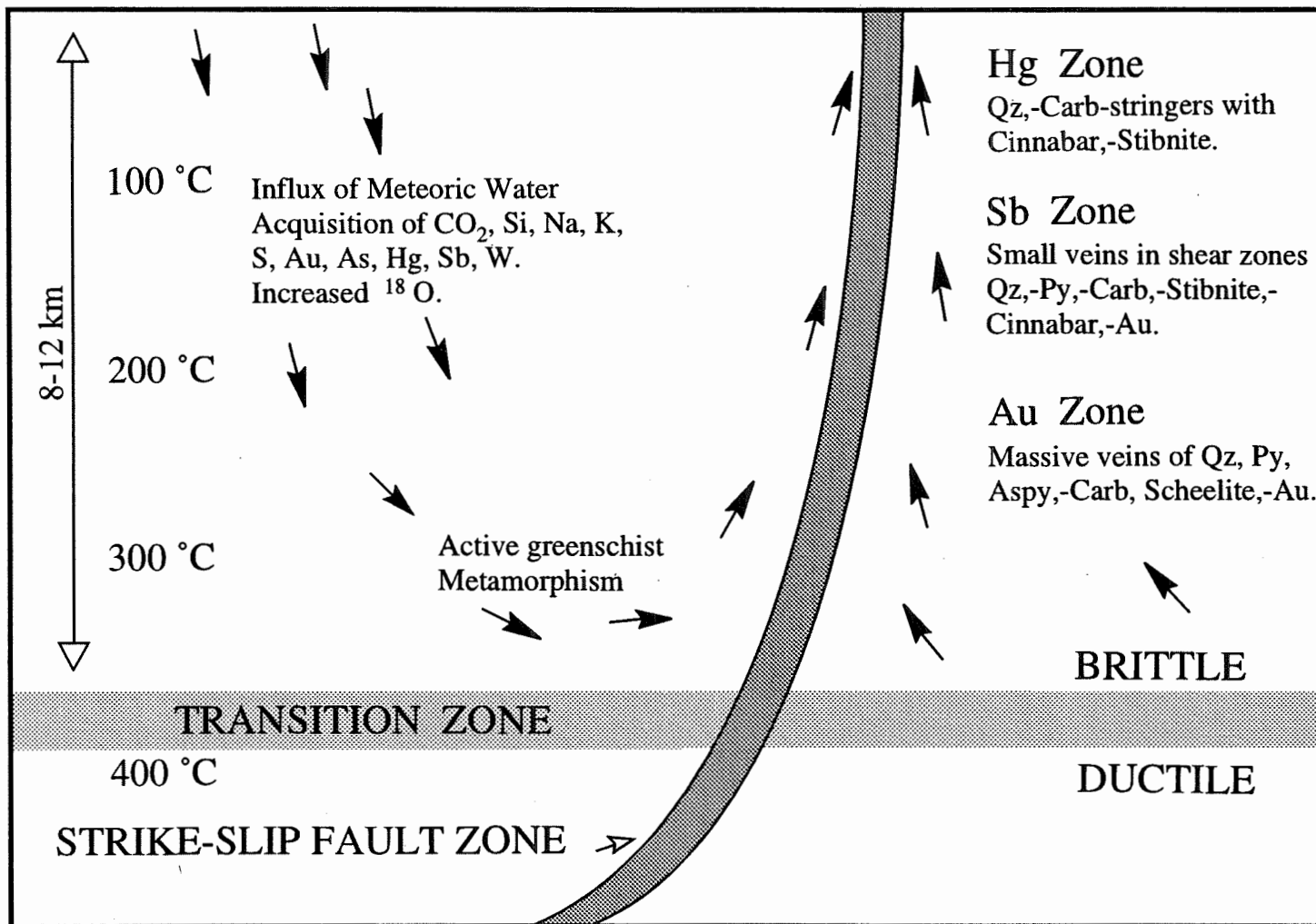


Figure 36. Schematic representation of the meteoric water model for epithermal and mesothermal gold deposits (modified after Nesbitt et al., 1989).

Mesothermal gold (\pm Sb \pm As \pm W) deposits of the Canadian Cordillera commonly have a spatial association with deep-reaching strike-slip faults. Antimony and mercury deposits in the Cordillera also seem to be spatially related to regional strike-slip faults. Nesbitt et al. (1986) suggest that the vertical zonation of Au, Sb, and Hg mineralization (Fig. 36) is spatially and genetically related to the upward circulation of meteoric fluids along these strike-slip faults. In this case, gold mineralization could be deposited in the vicinity of the brittle-ductile transition (8-12 km depth; 300°-350°C), antimony at shallower depths under lower fluid pressures, and mercury \pm antimony deposits near surface at 150°-200°C. The depth of gold deposition would correspond to pressures of 1 ± 0.2 kilobars for a hydrostatic pressure gradient needed to convect meteoric waters.

δ D data are used principally to support the model. Nesbitt et al. (1986) note lower δ D values (more negative) for Canadian Cordillera mesothermal deposits in comparison to California Mother Lode deposits, suggesting a trend toward decreasing δ D values with increasing latitudes. They conclude that the change in δ D values with latitude for these mesothermal deposits indicates that meteoric waters were responsible for the formation of the mesothermal deposits of the North American Cordillera.

This model has been criticized mainly because of the interpretations (Pickthorn et al., 1987; Kyser and Kerrich, 1990) of the fluid inclusion δ D data. Pickthorn et al.'s evaluation of the fluid inclusion δ D data led them to conclude that secondary rather than primary fluid inclusions were sampled by Nesbitt et al. (1986). Also, an extensive

hydrogen isotope study of Cordilleran mesothermal lode-gold deposits (Taylor et al., 1991) reveals that gold-depositing fluids were not of distinguishable meteoric origin and that secondary fluid inclusions of meteoric water origin dominate in quartz veins. In brief, the δD data of Nesbitt and coworkers appear to represent secondary meteoric and not primary mineralizing fluids. However, an isotopic study of a few lode-gold deposits from the Yilgarn block in Australia indicates tendencies for gold-bearing ore fluids toward isotopically heavy (positive) δD values and isotopically light (negative) $\delta^{18}O$ values, suggesting that a seawater or low-latitude meteoric component was involved in the formation of some Archean lode-gold deposits (Golding and Wilson, 1987; Groves et al., 1992; McNaughton et al., 1992).

Kyser and Kerrich (1990) also give several criticisms of the meteoric water model. The most important problem concerns the need for hydrostatic pressures for meteoric water circulation to the depths of mesothermal mineralization. Although Nesbitt (1988) and Nesbitt and Muehlenbachs (1989b) refer to several examples of meteoric and seawater circulation to depths of 10 to 15 kilometres, fluid inclusion and mineral barometer studies indicate that mesothermal gold-vein systems formed at pressures of 1.5 to 3 kilobars, corresponding to depths of 8 to 12 kilometres assuming lithostatic pressures, or to depths of 15 to 30 kilometres under hydrostatic pressures (Weir and Kerrick, 1984; Ho, 1987; Walshe et al., 1988). At these depths, the formation of veins in tensile fractures would require suprahydrostatic pressures, and flat veins would require supralithostatic pressures, not just the hydrostatic pressures available in a meteoric water

model (Kerrick and Allison, 1978). Also, Sibson et al. (1988) have shown that near-lithostatic pressures are needed for the reactivation of high-angle normal faults in which mesothermal lode-gold deposits commonly occur. Therefore, it is improbable that meteoric water convection, limited to hydrostatic fluid pressures, could account for quartz-gold vein deposits formed under mesothermal conditions. It should be noted, however, that significant pressure fluctuations between supralithostatic and hydrostatic conditions may occur if the system is alternately capped and breached (Robert, 1991b), explaining possibly breccia pipes and seawater or meteoric water signatures in some Archean lode-gold deposits.

4.4.3 Orthomagmatic Model

This model for Archean lode-gold deposits suggests that, as a magmatic body crystallizes, it exsolves hydrothermal fluids carrying metals, sulphur and gangue mineral constituents which may ultimately form quartz-gold vein deposits (Fig. 37). Geochemical and isotopic data are used to support this hypothesis (Burrows et al., 1986; Hattori, 1987; Cameron and Carrigan, 1987; Cameron and Hattori, 1987; Burrows and Spooner, 1987, 1989).

Hattori (1987), Cameron and Carrigan (1987) and Cameron and Hattori (1987) investigated several small felsic intrusions spatially related to quartz-gold vein mineralization, and they suggest, knowing that gold ore-forming fluids are CO₂-bearing and oxidizing (Kerrick, 1983; Roedder, 1984), that magmatic-hydrothermal fluids were

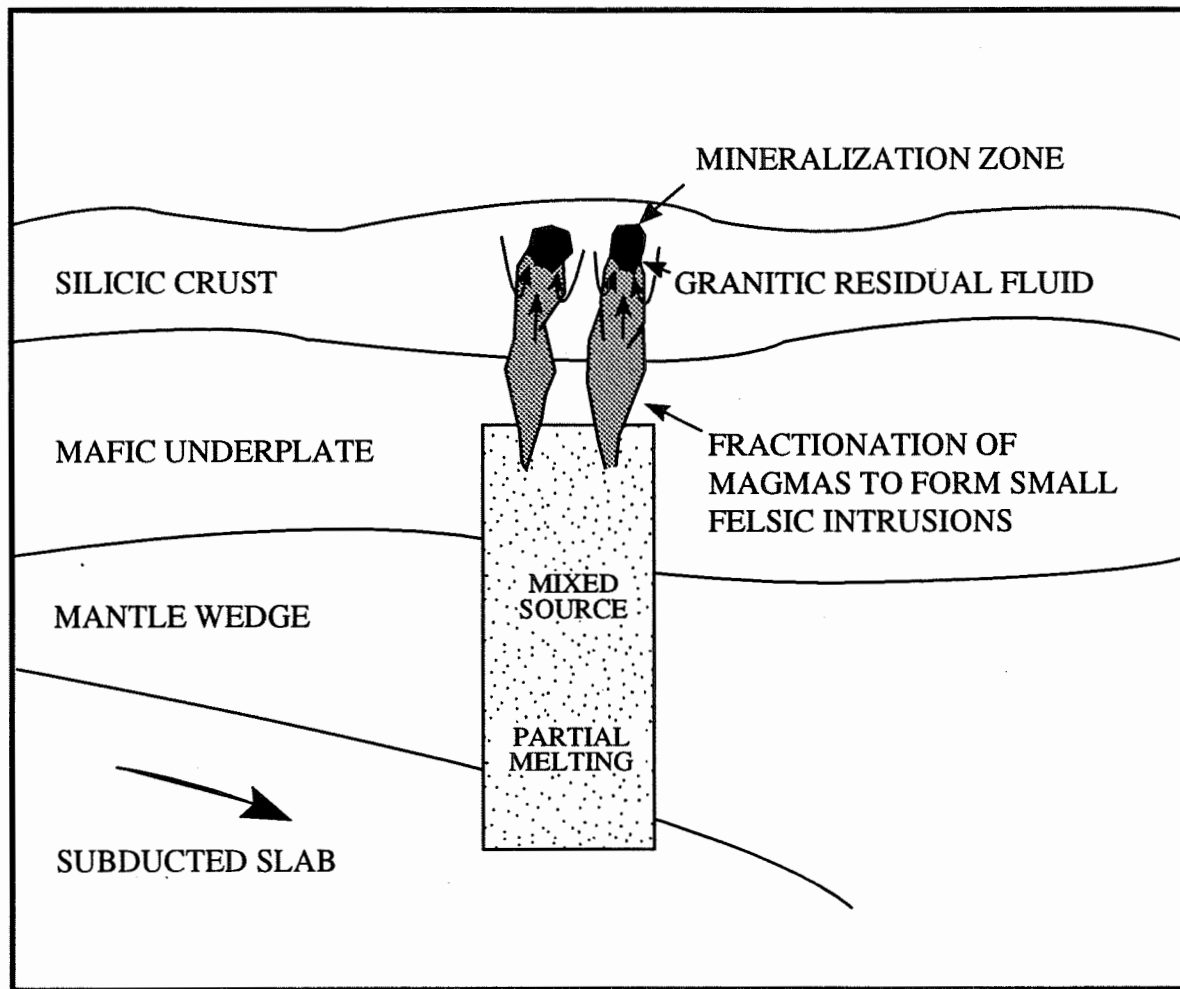


Figure 37. Schematic representation of the orthomagmatic model for Archean lode-gold deposits (modified after Rodgers and Greenberg, 1990).

the source of gold mineralization. They use the presence of sulphate minerals, hematite, and sulphides of various isotopic compositions in zones of intrusions lacking obvious alteration as evidence of intrinsically oxidizing conditions, and state that some small felsic stocks hosting lode-gold deposits are analogous of I-type granites which typically have higher oxygen fugacities than S-type granites (Ishihara, 1975, 1981).

Burrows and Spooner (1989) studied intrusions hosting lode-gold deposits in the Val d'Or and Timmins areas. Their geochemical analyses suggest that the dioritic intrusions of the Lamaque mine are the result of extensive fractional crystallization and that these intrusions have anomalous gold concentrations (7 ppb [range 0 to 31] geometric mean, in comparison to background gold levels of 1-2 ppb for barren intrusions: Kwong and Crocket, 1978; Saager and Meyer, 1984). Burrows and Spooner (1989) hypothesize that the Lamaque mine intrusions were derived periodically from a deep parental dioritic magma in which gold was progressively enriched through fractional crystallization into the most evolved late melt and possibly into a coexisting magmatic hydrothermal fluid.

Kyser and Kerrich (1990) give several reasons why the orthomagmatic model does not explain Archean lode-gold deposits; four of their more persuasive arguments are given here. Firstly, the common presence of pyrite+arsenopyrite±pyrrhotite±graphite in quartz-gold veins "constrains the fluid Eh to conditions at or below the QFM buffer such that the model of Cameron and Hattori (1987) is not general". Secondly, most compositionally uniform magmas differ from quartz-gold veins in that the magmas have

uniform initial Sr, Pb, and Nd isotope ratios, whereas the mineralized veins have variable initial Pb- (Franklin et al., 1983; Dahl et al., 1987) and Sr-isotope ratios (Kerrick et al., 1987). Thirdly, the spatial relationship between lode-gold mineralization and small intrusive bodies is aptly explained by rheological arguments: the intrusions are considered to have been relatively brittle in comparison to surrounding volcano-sedimentary sequences, and they therefore acted as anisotropic bodies, localizing hydraulic fracturing during post-magmatic syntectonic fluid flow and mineralization. Fourthly, the purely orthomagmatic origin for Archean lode-gold mineralization is disputed with geochronological data. For example, various intrusions and their spatially associated lode-gold mineralization and alteration in the Timmins and Val d'Or mining camps have been dated (Corfu et al., 1989; Zweng and Mortensen, 1989; Jemielita et al., 1990; Wong et al., 1991; Hanes et al., 1992; Zweng et al., 1993), showing that gold mineralization post-dates by approximately 60 to 100 million years the host intrusion, regional magmatism, and regional metamorphism, such that a direct genetic link between magmatism and lode-gold mineralization seems highly unlikely.

Nevertheless, Morasse et al. (1993) have recently proposed a hydrothermal magmatic origin for the gold mineralization at the Kiena mine west of Val d'Or. Their model is based on the dating of an intermineralization granodiorite dike at $2,686 \pm 2$ Ma (U-Pb method on zircon). The present author concurs that this date reflects the minimum age of auriferous mineralization at Kiena indicating an earlier gold event than for the majority of lode-gold mineralization so far dated. However, no supporting evidence has

yet been provided to show that magmatic fluids formed the gold mineralization at this mine. Secondly, Morasse et al. (1993) state that this gold mineralization is older than the regional tectonic and metamorphic effects of the Kenoran orogeny which they bracketed between 2,677 Ma and 2,645 Ma based on data and interpretations presented in various references (e.g., Stockwell, 1982; Dimroth et al., 1983a,b; Corfu et al., 1989; Card, 1990; Machado et al., 1991; Feng and Kerrich, 1991; W.G. Powell et al., 1992, 1993; Poulsen et al., 1992), and therefore they conclude that the metamorphic model for gold mineralization cannot be applied to the Kiena mineralization. However, important metamorphic dates ($2,693 \pm 11$ Ma from an $^{40}\text{Ar}/^{39}\text{Ar}$ age of magnesio-hornblende from the Sigma mine, Hanes et al., 1989, 1992; and $2,684 \pm 7$ Ma from a U-Pb age of rutile from a Colombière rhyolite, Wong et al., 1989, 1991) from the Val d'Or-east sector are omitted from Morasse et al.'s compilation. These dates overlap the minimum age of gold mineralization at Kiena, and therefore, Morasse et al. (1993) should not rule out the metamorphic model for gold mineralization.

In addition to Kyser and Kerrich's arguments, Perring et al. (1987) note certain problems with the strictly orthomagmatic model for Archean lode-gold mineralization. Firstly, if gold-bearing fluids originated from spatially-related porphyritic intrusions, the ore-fluid compositions should be varied and reflect variations in intrusive compositions, whereas Archean lode-gold fluids are noted for their narrow range in composition. Secondly, if intrusions spatially related to lode-gold mineralization were the source of mineralizing fluids, it would be difficult to reconcile the relatively small size of the

intrusions with the relatively massive amounts of lode-gold ore, unless batholithic equivalents are present at depth. Finally, there is no correlation between the volume of the porphyry bodies and deposit size. For example, porphyries are abundant at the >2 tonne Au Victory gold deposit in Australia, but they are scarce at the >50 tonne Au Golden Mile gold deposits.

4.4.4 Metamorphic Dehydration Model

This model envisages the focussed discharge along crustal-scale faults of low-salinity, low-density CO₂-H₂O-rich fluids derived by devolatilization of greenstone volcanic rocks during amphibolite-greenschist-facies metamorphism, synchronous with late-stage deformation and granitoid emplacement (Kerrick and Fryer, 1979; Groves and Phillips, 1987; Wyman and Kerrich, 1988; Kyser and Kerrich, 1990). Seismic pumping (Sibson, 1990) or crack-and-seal processes (Ramsay, 1980; Etheridge et al., 1984) may have helped to channel fluids into major fault zones, producing high fluid/rock ratios along the principal fluid channelways. Complex, large-scale convective cells (Etheridge et al., 1983) may have been important in maintaining these high fluid-rock ratios. It is postulated that metamorphic fluids, while being drawn into crustal-scale fault systems, scavenged gold from greenstone terranes (Fig. 38). The positive aspects and weaknesses of the metamorphic dehydration model are reviewed by Perring et al. (1987) and Kerrich (1989b); only key points are summarized here.

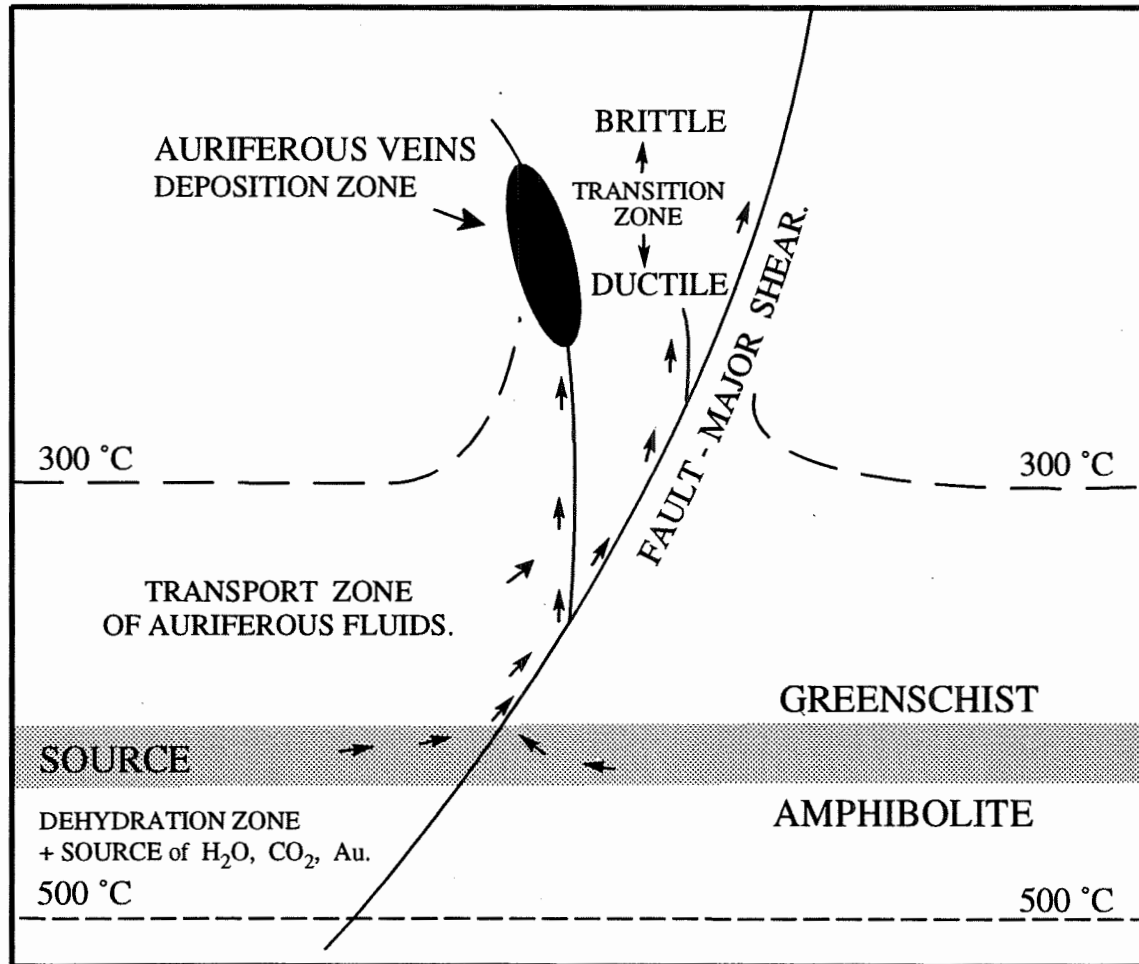


Figure 38. Schematic representation of the metamorphic dehydration model for Archean lode-gold deposits (modified after Kerrich and Fryer, 1979).

The metamorphic model is capable of explaining the widespread occurrence of gold deposits (D.I. Groves et al., 1984) because regional metamorphism is widespread and the resulting fluids are an expected integral part of greenstone belt development (Groves and Phillips, 1987). Consequently, lode-gold deposits occurring at some distance from major fault zones are explained by this model as well as the mesothermal gold deposits commonly related spatially to large-scale fault zones.

Metamorphic dehydration reactions (e.g., dehydration accompanying the passage from the greenschist to the amphibolite facies) are pervasive, and the fluid/rock ratio remains low because of the proportionately greater volume of rock compared to the volume of fluid produced. These characteristics, as well as the predictably low salinity, CO₂-rich nature of the fluids, would result in effective scavenging of gold from greenstone belt rocks (Ho, 1987). Calculations by Phillips et al. (1987) show that the giant Golden Mile lode-gold district of Kalgoorlie, Australia, could have formed from metamorphic fluids by the extraction of 1-2 ppb gold from a greenstone slab 8x8 kilometres in area and 5 kilometres thick. No special gold-enriched source rock is needed to produce giant gold deposits, nor are unreasonably large volumes of greenstone rocks involved. Moreover, Hodgson and MacGeehan (1982), Keays (1984) and Hodgson (1990) propose that metamorphic fluids could scavenge more gold from komatiitic and/or mafic rocks because of their relatively high gold contents compared to intermediate and felsic igneous rocks. The pronounced coincidence between the largest gold deposits and high gold productivity in greenstone belts and the presence of abundant komatiites in

these greenstone terranes suggests that this mafic to ultramafic rock type was a favourable gold source.

The general lack of vertical zonation of mineral assemblages, moderate fluid temperatures and relatively heavy (positive) $\delta^{18}\text{O}$ values in deposits is also consistent with large-scale, fluid-rock thermal equilibrium of the type inherent in prograde metamorphism (Groves and Phillips, 1987; Kerrich, 1989b). Furthermore, for large-scale fluid circulation along high-angle faults in greenstone belts, near lithostatic fluid pressures characteristic of lode-gold deposits would be consistent with metamorphic dehydration processes (Kerrich, 1989b).

However, this model has been disputed because hydrothermal alteration generally overprints regional metamorphic facies assemblages (Robert and Brown, 1986a,b) and precise geochronological data indicate that the majority of lode-gold mineralization significantly postdates metamorphism (Jemielita et al., 1990; Wong et al., 1991; Hanes et al., 1992). Nevertheless, Kerrich (1989b) and Kyser and Kerrich (1990) argue that in collisional environments where crustal thickening is essentially instantaneous in comparison to thermal relaxation, peak metamorphism at deep crustal levels postdates peak metamorphism at shallower depths by up to 40 Ma. This thermal relaxation could explain how late, metamorphic fluids formed at deep levels could overprint peak metamorphic assemblages formed earlier at shallow crustal levels. Also, R. Powell et al. (1991) argue that greenstone metamorphism did not entail major crustal thickening

because of the preservation of very shallow levels of greenstone belts, and that if crustal deformation is accompanied by mantle thinning (e.g., a low-pressure, high-temperature scenario), then peak metamorphic fluids at mid-crustal levels should have been released in prograde time into shallow crustal levels that had attained peak metamorphism and were in fact already retrograde.

Recent geochronological work on two intrusions crosscutting two examples of gold mineralization west of Val d'Or indicates that gold mineralization has a minimum age of $2,686 \pm 2$ Ma at the Kiena mine (U-Pb method on zircon: Morasse et al., 1993) and $2,692 \pm 2$ Ma at the Norlartie mine (U-Pb method on zircon: Pilote et al., 1993). These ages are similar to metamorphic ages determined for metamorphic minerals east of Val d'Or ($2,693 \pm 11$ Ma, from the $^{40}\text{Ar}/^{39}\text{Ar}$ method on magnesio-hornblende: Hanes et al., 1989, 1992 and $2,684 \pm 7$ Ma, from the U-Pb method on rutile: Wong et al., 1989, 1991). The similarity of ages may suggest a metamorphic relationship between mineralizing fluids and these gold deposits; however, the age of regional metamorphism has not been tightly constrained and therefore, the significance of these older ages for gold mineralization is still unclear.

Some deposits found in upper amphibolite facies rocks question the plausibility of metamorphic dehydration as the source of mineralized fluids formed under the greenschist to amphibolite transition. However, crustal thickening by thrust stacking, whereby high-grade rocks are superimposed on low grade rocks, may explain the

presence of lode-gold mineralization in high-grade rocks (Jaupart and Provost, 1985; Connolly and Thompson, 1989). As noted above, amphibolite-grade rocks could be thrust onto lower-grade rocks, inverting geothermal gradients, and therefore source regions do not necessarily have metamorphic grades higher than upper amphibolite facies (Kerrick, 1989a; Kyser and Kerrich, 1990).

Because of the spatial and temporal association between carbonate alteration and lode-gold mineralization, researchers have studied carbon isotopes of carbonate in an attempt to identify the source of gold and associated carbon. If carbon was leached from the crust by circulating metamorphic fluids, the $\delta^{13}\text{C}$ values of carbonate from the largest lode-gold deposits, formed probably by unusually extensive "plumbing" systems, should represent more closely average $\delta^{13}\text{C}$ crustal values ($\delta^{13}\text{C}_{\text{crust}} \approx -5$ per mil and $\delta^{13}\text{C}_{\text{C in carbonate}} \approx -4$ per mil; Kerrich, 1989b). However, $\delta^{13}\text{C}$ values of carbonate from these deposits converge around -3 per mil, a value representative of magmatic or mantle origins (Ohmoto and Rye, 1979). Therefore, carbon isotope data may not be used to distinguish between these two sources and do not point unequivocally to a metamorphic source.

4.4.5 Mantle Degassing-Granulitization Model

Proponents of this model (e.g., Colvine et al., 1988; Cameron, 1988) suggest that the driving force behind the formation of Archean lode-gold deposits is the advection of mantle CO_2 through lower crustal rocks, resulting in the formation of a dehydrated,

granulitic residue, based on the granulite formation model of Newton et al. (1980). Colvine et al. (1988) link Archean gold metallogeny to the late magmatic-tectonic-thermal history of the Kenoran orogeny. Some granulitization models invoke a source of heat or fluid external to the crust (Touret and Dietvorst, 1983; Bohlen, 1987; Frost and Frost, 1987); therefore, it is proposed that the mantle is able to supply large volumes of CO₂-bearing hydrothermal fluids to the lower crust.

Figure 39 summarizes the model of Colvine et al. (1988) of granulitization and the resulting formation of gold-bearing hydrothermal fluids. Mantle diapirism supplies magma, heat and volatiles to the base of the crust, which induces granulitization. CO₂, H₂O, incompatible elements, and gold are channelled into deep regional structures. Small, intrusive bodies may also be entrapped in the regional deformation zones. Gold, CO₂ and associated elements may have been extracted and transported to the depositional site by at least one or the other of two distinct processes: 1) rising, silicate magmas, formed by anatexis of the mantle or lower crust (Touret and Dietvorst, 1983), may exsolve gold and companion elements into a H₂O-CO₂-bearing magmatic fluid; and 2) hydrothermal fluids may transport gold, CO₂ and companion elements from the source to the depositional site without being incorporated into a magmatic medium (cf., Frost and Frost, 1987). Note that, at this time, fluid inclusion and stable isotope studies cannot distinguish between metamorphic and magmatic fluids formed in the lower crust.

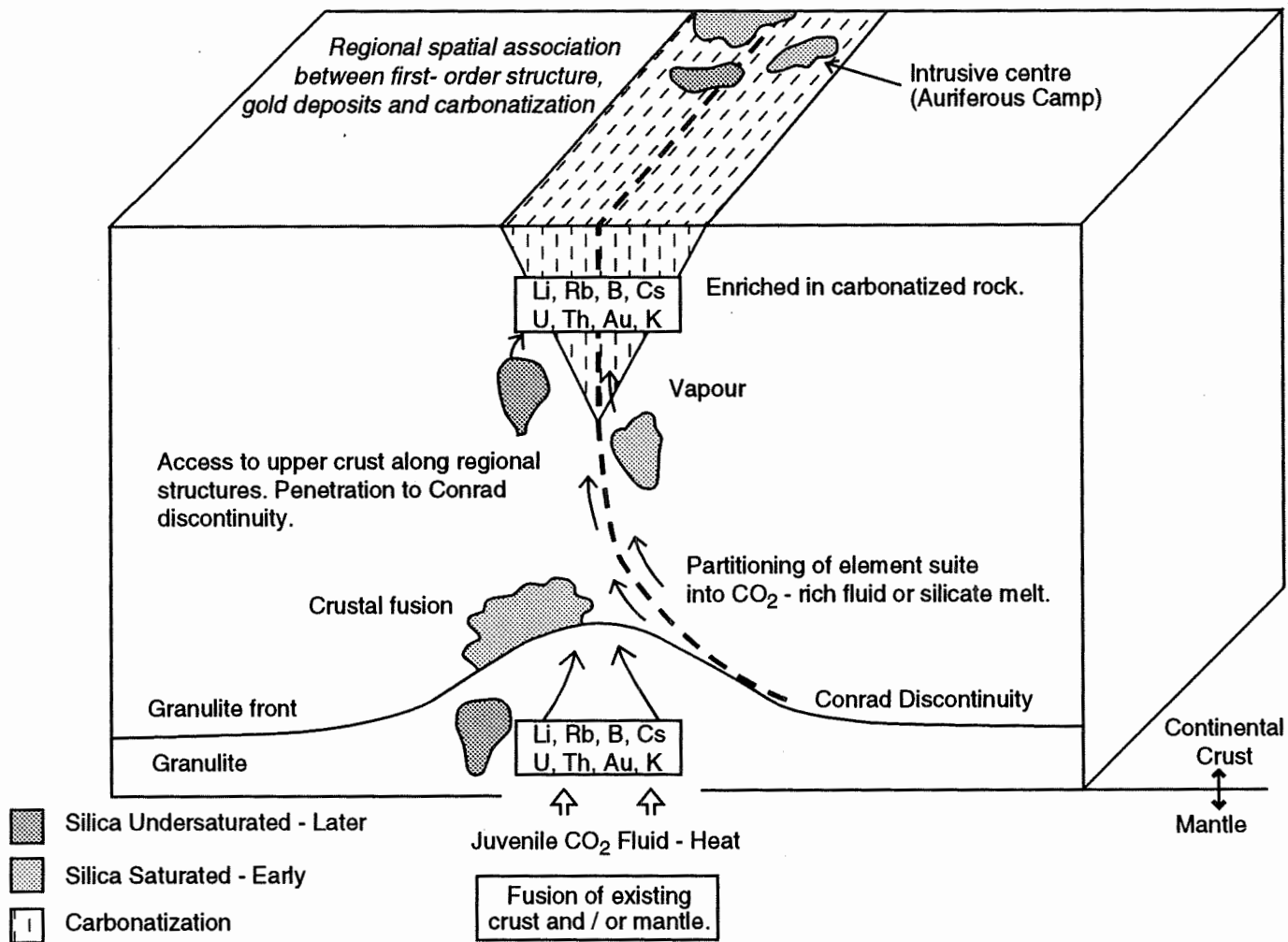


Figure 39. Schematic representation of the mantle degassing-granulitization model for Archean lode-gold deposits (after Colvine et al., 1988).

Groves et al. (1988, 1989) and Perring et al. (1989) offer variations of the mantle degassing-granulitization model. These researchers, in agreement with Colvine et al. (1988) and Cameron (1988), suggest that Archean lode-gold deposits are the result of mantle-crustal outgassing involving deep mantle magmatism responding to convergent tectonics. However, because of the "provinciality" of stable and radiogenic isotopes within gold camps and even among gold deposits related to the same fault system (Golding et al., 1987; Kerrich et al., 1987; Perring et al., 1987), these researchers argue that crustal-scale metamorphic devolatilization also contributed to fluid formation, in addition to mantle fluids; therefore, the ore fluids would be composed of mantle, lower crust, and greenstone components (Golding et al., 1987; Perring et al., 1987, 1989; Groves et al., 1988, 1989).

Other studies also suggest that gold-bearing hydrothermal fluids have a mantle-deep crustal origin. For example, Peterson and Newton (1989, 1990), based on their experimental work on the melting of a CO₂-H₂O-bearing biotite granite, show that CO₂-H₂O-bearing basaltic magmas may have intruded into the deep crust, resulting in the formation of lamprophyres and volatile-rich granites by melting of the crust. Later differentiation of these granites at depth may have resulted in the exsolution of large amounts of CO₂-H₂O fluids and other generations of lamprophyres. The resulting oxidizing fluids are capable of transporting gold and companion elements, and thus gold may be partitioned from cooling magmas into the CO₂-H₂O fluid, or scoured from the crust by these fluids.

In connection with the mantle degassing model, the spatial and temporal relationship between Archean lode-gold mineralization and lamprophyres of mantle origin sparked the suggestion that lamprophyres were in fact the source rocks of gold (Rock and Groves, 1988a,b). Although stable isotope work showed that there was no direct relationship between lamprophyres and gold-bearing fluids, Rock et al. (1989) propose that lamprophyres may have supplied, in part, gold-bearing fluids from deep sources and that these fluids were reworked in an evolving metamorphic fluid. Conversely, Wyman and Kerrich (1988, 1989) have argued that lamprophyres do not constitute a preferential source reservoir of gold, and that lamprophyres and Archean lode-gold mineralization result from independent processes. They contend that the temporally- and spatially-related lamprophyres were derived from mantle lithosphere and asthenosphere depths, whereas gold-mineralizing systems are restricted to crustal environments.

Perring et al. (1987), Kerrich (1989b), and Kyser and Kerrich (1990) have covered the many strengths and weaknesses of this mantle degassing-granulitization model as an explanation for Archean lode-gold mineralization. The main observations supporting this model include: 1) many low- and medium-pressure granulites are depleted in certain incompatible elements (K, Rb, Cs, U, Th, Y, heavy REEs), and these elements are enriched in gold-quartz vein deposits, suggesting a source-sink relationship (Fyon et al., 1989 and references therein); and 2) a secular conjunction exists between "depleted" Archean granulites and Archean mesothermal lode-gold deposits (Kyser and Kerrich, 1990 and references therein).

In addition, age dating suggests that late, post-peak metamorphic fluid activity in the lower crust (e.g., the Kapuskasing Structural Zone) was contemporaneous with brittle deformation, host rock alteration and lode-gold mineralization at high crustal levels (Corfu, 1987; Krogh et al., 1988; Krogh, 1990). Consequently, fluids resulting from granulitization of the upper mantle/lower crust zone could have been the source of Archean lode-gold mineralization, widely considered to have occurred after peak metamorphism and associated deformation (Robert and Brown, 1986a,b). In addition, Sr and Pb isotopes indicate a lower crustal component in the gold mineralizing fluids (Kerrick, 1986; Dahl et al., 1987); the contamination of rising mantle-degassed fluids by lower crustal rocks would explain these isotopic data (Perring et al., 1987).

Finally, recent $^{40}\text{Ar}/^{39}\text{Ar}$ thermochronology carried out on hydrothermal micas related to gold-quartz veins and quartz-pyrite lodes at the Camflo mine, Malartic, Quebec (Zweng et al., 1993) supports the importance of mafic underplating to the lower crust during peak granulite formation (cf., Bohlen, 1987). The $^{40}\text{Ar}/^{39}\text{Ar}$ data indicate 1) that these micas are 70-170 Ma younger than the monzonitic host stock ($2,685 \pm 10$ Ma) and 2) that the $^{40}\text{Ar}/^{39}\text{Ar}$ ages of micas from the 1650 mine level are ≈ 10 to 15 Ma older than $^{40}\text{Ar}/^{39}\text{Ar}$ ages of micas from the 3475 mine level. Zweng et al. suggest that the younger ages represent closure temperatures arrived at during cooling and not recrystallization or reset ages. Also, based on their $^{40}\text{Ar}/^{39}\text{Ar}$ data, Zweng et al. calculated slow cooling and slow apparent uplift rates for the Camflo terrane. In their review of cooling and uplift rates, they explain that in areas of collision, rapid uplift is

the essential means of cooling of tectonically thickened crust. The Himalayas which have rapid rates of uplift also have rapid rates of cooling. However, metamorphic belts, formed of crust thickened by magmatic underplating where conduction is the prevalent means of cooling (cf., Wells, 1980), experience slow uplift rates, and therefore have slow cooling rates. Based on these $^{40}\text{Ar}/^{39}\text{Ar}$ data and other hydrothermal ages (see section 4.6 for further explanation), Zweng et al. suggest that their model of mafic magmatic underplating and slow cooling and uplift is consistent with the geochronology of granulite facies metamorphism in the Kapuskasing structural zone and with postpeak metamorphic ages for $\text{CO}_2\text{-H}_2\text{O}$ fluid inclusions in regional granulite terranes (cf., Percival and Krogh, 1983; Corfu, 1987; Krogh et al., 1988; Krogh, 1990) where decreasingly younger ages with depth are interpreted as indicating downward vertical accretion of the Archean crust.

Several important weaknesses are nevertheless found in the granulitization model. Firstly, many post-Archean and some Archean granulites are not markedly depleted in LILEs, especially those with sedimentary or volcanic protoliths. Therefore, Kyser and Kerrich (1990) propose that LILE depletion is not an inevitable or even commonly expected result of granulite-facies metamorphism.

Secondly, although Colvine et al. (1988) judge that $\delta^{13}\text{C}$ data for CO_2 , from which Archean gold-related hydrothermal carbonates precipitated, are most consistent with a magmatic reservoir (range -8 to -3 per mil), a metamorphic reservoir cannot be ruled

out. The difficulty surrounding the interpretation of $\delta^{13}\text{C}$ data stems from the fact that average igneous, metamorphic, and sedimentary carbon reservoirs have similar $\delta^{13}\text{C}$ values of approximately -5 per mil (Ohmoto and Rye, 1979). For this reason, carbon isotopic data must be interpreted cautiously because of their limited ability to distinguish between source reservoirs. Thirdly, although the presence of seemingly high-density CO_2 fluid inclusions in granulite facies minerals has been used as evidence for the granulite-facies metamorphic model (Newton et al., 1980), these apparently primary inclusions have commonly been related to a post-metamorphic P-T path (Lamb et al., 1987; Valley, 1988; Morrison and Valley, 1988). Fourthly, Vry et al. (1988) have shown that many granulites were internally buffered, rather than having been buffered by an external mantle CO_2 reservoir. And finally, for granulites resulting from continental crust dehydration, $\text{C}/^3\text{He}$ measurements indicate that the amount of CO_2 , estimated from mantle-derived He fluxes (He being the best tracer for mantle volatiles), entering the crust in tectonically active regions is not sufficient to produce granulites on a regional scale (O'Nions and Oxburgh, 1988).

Golding et al. (1987), Kerrich et al. (1987), and Perring et al. (1987) have identified "provincialities" of Sr, Pb, and C isotopic signatures for individual gold camps, as well as among gold mines related to the same fault systems, and they propose that these provincialities cannot be explained by a large, uniform mantle reservoir. Rather, greenstone-belt processes are invoked to explain the between-province isotopic variations. However, according to Colvine et al. (1988), it is not clear whether these provincialities

stem from source variations, or fluid-rock interactions enroute to or at the depositional site. In the case of carbon, provinciality may be a source characteristic and consequently, isotopic provincialities may not help in differentiating between magmatic or metamorphic reservoirs (Colvine et al., 1988 and references therein).

Finally, recent geochronological work on intrusive rocks crosscutting early, deformed, quartz-carbonate-pyrite-gold veins (Robert, 1994; Robert and Boullier, 1994) at the Kiena mine (Morasse et al., 1993) and the Norlartic mine (Pilote et al., 1993) west of Val d'Or indicates that gold mineralization at Kiena has a minimum age of $2,686 \pm 2$ Ma and that gold mineralization at Norlartic has a minimum age of $2,692 \pm 2$ Ma (see section 4.6 for further discussion of these and other dates). These dates are much older than those for minerals associated with undeformed, younger gold mineralization ($\approx 2,630$ to $2,580$ Ma; Corfu, 1993) and are not yet readily explained by the mantle-degassing-granulitization model.

In summary, Perring et al. (1987) note that a large number of small gold deposits are not associated with large-scale fault zones and their subsidiary fracture systems, and hence cannot be readily explained by mantle-degassed fluids channelled along major faults. For this reason, Perring et al. (1987) invoke crustal-scale processes such as metamorphic dehydration to explain the emplacement of gold deposits far from large-scale faults. However, no examples of such deposits are given nor the distances of these deposits from large-scale fault zones. Also, Perring et al. (1987) do not mention what

type of structural control, if any is present, for these deposits. Nevertheless, in an attempt to define the distance between lode-gold deposits and first-order shear zones and their subsidiary shear zones, we cite a maximum 15- to 20-kilometre distance between first-order shear zones and lode-gold deposits, as established by Eisenlohr et al. (1989) for the Yilgarn block in Australia and by Robert (1990) for the Val d'Or district.

4.4.6 Conclusion

Considering the difficulties cited above, meteoric fluids were probably not a major fluid component in Archean mesothermal lode-gold deposits, but some amount of descending meteoric fluid mixing with a dominant, ascending fluid cannot be ruled out. As for magmatic fluids, there is no apparent direct connection between intrusions and the gold mineralization they host, although there is an hypothesis that silica-undersaturated magmas (spatially and temporally associated with gold mineralization) are genetically associated with gold mineralization. Magmatic fluids may have originated from mantle and/or lower crustal sources; however, stable and radiogenic isotopes do not differentiate between these sources nor can they unequivocally distinguish metamorphic from magmatic fluids. Also, derivation of fluids from the mantle is inferred in some instances but it is unknown whether mantle devolatilization occurs by direct volatile streaming into the crust or by formation of volatile-rich intrusions that rise into the crust and exsolve their fluids there.

Stable isotopes of some elements such as H, C, and O are used to suggest fluid source, whereas radiogenic isotopes such as Sr and Pb are used to suggest metal source. While some isotopic evidence may point to one source of fluids, other isotopic evidence may strongly suggest another source of fluids. In reality, much of the data do not characterize unequivocally any one source. Strontium, lead and carbon isotope data for Archean gold deposits from large geographic regions show interdeposit variations and hence, define a "provinciality" in their distribution. This "provincial" clustering of data suggests laterally heterogeneous sources, thereby dismissing the notion of a single source reservoir for gold (for review see Kerrich et al., 1987; Colvine et al., 1988; Kerrich, 1989a). However, Colvine et al. (1988) argue that $\delta^{13}\text{C}$ "provinciality" may be a characteristic of the mantle (Deines and Gold, 1973); consequently, carbon "provinciality" cannot be used for or against metamorphic or magmatic fluid sources.

Given these divergent interpretations, all isotopic data must be examined together, and at present, they suggest that more than one source of fluids and solutes exists and they definitely indicate that one ultimate criterion will not answer the question of solute and fluid provenance for mesothermal gold deposits. In fact, one must consider the possibility that the fluids and their contained solutes and volatiles are not all necessarily from the same source (Kerrich, 1989a).

All of the models postulated to explain Archean lode-gold mineralization have weaknesses, as noted above, requiring that research continue to examine the multi-faceted

question of fluid-solute-volatile source-transport-deposition. However, the mantle degassing-granulitization model appears presently to be the most comprehensive model for explaining most Archean lode-gold mineralization. Furthermore, as proposed by Colvine et al. (1988), this model is seen as part of the cratonization of the Superior Province and may be seen then as an almost inevitable product of crustal-mantle processes in Archean terrane (Brown et al., 1990).

Because their model takes into account a broad spectrum of geologic data, including tectonic, metamorphic, geochemical (isotope, fluid inclusion, alteration) and geochronological data of Superior Province greenstone belts hosting lode-gold mineralization, Colvine et al. (1988) coined their genetic model a "holistic" model for Archean gold metallogeny. Although the model suggests an ultimate mantle origin for fluids and solutes, the proponents of this model recognize the present difficulty in unequivocally distinguishing between magmatic fluids from a mantle source and metamorphic fluids and do not rule out the importance of either one. However, despite the comprehensive nature of this model, the interpretation of its geochemical data has been criticized (Perring et al., 1987; Kerrich, 1989b; Kyser and Kerrich, 1990), mainly because the geochemical data do not point unequivocally to a mantle origin for the CO₂-H₂O fluids and its solutes. Also, recent dating of some gold mineralization as old as 2,686 Ma or older suggests that some gold mineralization may not be readily linked to mantle degassing and granulitization.

Finally, because "provincial-scale" variations of Sr, Pb, and C isotopic data in Archean mesothermal lode-gold deposits do not appear to indicate a unique source rock for gold (Kerrich, 1989a), the author suggests that for some lode-gold districts, the notion of amphibolite-facies metamorphic fluids scavenging gold from crustal rocks should be added to the mantle degassing-granulitization model. Also, the possible involvement of meteoric water or seawater in some greenschist to sub-greenschist facies deposits should not be overlooked, based on tentative stable isotope and fluid inclusion data for some Archean lode-gold deposits of the Yilgarn craton in Western Australia (Groves et al., 1992; McNaughton et al., 1992). In fact, it is increasingly evident that several sources of fluids may have interacted in the formation of some Archean mesothermal lode-gold deposits and that gold may have been leached by these fluids from a variety of subcrustal to crustal environments.

4.5 PHANEROZOIC ANALOGUES

Probably the best analogues for Archean lode-gold mineralization are mesothermal lode-gold deposits of the North American west coast. As reviewed by Nesbitt et al. (1986), Goldfarb et al. (1988), Nesbitt and Muehlenbachs (1988), Kerrich (1989b), Kerrich and Wyman (1990) and Wyman and Kerrich (1990), the western coast of North America is composed of a series of allochthonous, tectonostratigraphic terranes with oceanic and island-arc affinities, accreted to and subducted below the continental margin during Cretaceous to Eocene times (see Engebretson et al., 1985; Debiche et al., 1987;

Coney, 1989; Oldow et al., 1989; and Monger, 1993 for reviews of terrane accretion in the North American Cordillera). Mesothermal lode-gold deposits are found only in the allochthonous terranes of the Cordillera and are regionally associated with post-metamorphic, crustal-scale transcurrent faults thought to be suture zones between the accreted terranes. The deposits are commonly hosted by subvertical, reverse faults subsidiary to these major fault zones. Table 3 from Nesbitt and Muehlenbachs (1988) summarizes the characteristics of Canadian Cordillera mesothermal lode-gold deposits and illustrates the several structural, mineralogical, and geochemical attributes of these deposits that are similar to those of Archean mesothermal gold deposits (cf., Colvine et al., 1988; Groves et al., 1992).

In addition to the North American Cordilleran terranes, Kerrich and Wyman (1990) identify other Phanerozoic terranes (e.g., the Monte Rosa Lodes of the Italian Alps and the Ballarat Slate Belt of Southern Australia) hosting mesothermal gold deposits which share a similar geodynamic setting. This common geodynamic environment consists, again, of the accretion of allochthonous terranes to continental margins or arcs. Based on their evaluation of Archean and Phanerozoic mesothermal lode-gold terranes, Kerrich and Wyman (1990) suggest that a recurring sequence in these environments (transpressive deformation, uplift, shoshonitic magmatism and late-kinematic mineralization) would be consistent with thermal re-equilibration of tectonically thickened crust. Furthermore, given the tectonic, physical, and geochemical similarities of Archean and Phanerozoic mesothermal lode-gold deposits, they suggest that it was unlikely that

Table 3. Characteristics of Canadian Cordillera mesothermal lode-gold deposits (from Nesbitt and Muehlenbachs, 1988).

Size:	Largest 8×10^6 Tonnes. Most 3×10^6 Tonnes or less
Grades:	0.15-0.05 g/tonne
Au/Ag:	1 to >10
Tectonic Setting:	Typically associated with major, strike-slip fault zones
Age:	Late Jurassic to Tertiary, Post-peak metamorphism
Host Petrology:	Mafic to Felsic volcanics and plutons, clastic sedimentary units, serpentinites, limestones; Low to upper greenschist facies
Structure:	Vertical to subvertical quartz veins in highly deformed fault zones subsidiary to major faults; Substantial vertical continuity
Mineralogy:	Quartz, Ca-Mg-Fe carbonates, albite, muscovite, scheelite, pyrite, pyrrhotite, arsenopyrite, graphite, galena, sphalerite, chalcopyrite, native Au, Au-Ag tellurides
Paragenesis:	Stage 1 - Vein formation; quartz, carbonate, albite, muscovite, scheelite, and Fe, As sulfides Stage 2 - Late fractures with Au, galena, sphalerite, minor quartz and carbonate
Textures:	Massive to ribboned quartz veins, 0.1 to 5 meters in width, occasional replacement zones
Alteration:	Carbonate, sericite, silica, pyrite, mariposite, albite, chlorite, talc, graphite
Fluid Inclusions:	$T_H = 250-350^\circ\text{C}$, $X_{\text{CO}_2} = 0.1$ to 0.3 , occasionally up to pure CO_2 , <2 Eq. Wt. % NaCl, rare CH_4
Stable Isotopes:	$\delta^{18}\text{O}_{\text{Qtz}} = +13$ to $+17\%$; $\delta^{18}\text{O}_{\text{Carb}} = +14$ to $+18\%$ $\delta\text{D}_{\text{F.I.}} = -90\%$ in southern Cordillera and -160% in northern Cordillera
Associated Elements:	Ag, As, W, Pb, Zn, C, B, Sb, Hg, Te

Archean mesothermal lode-gold mineralization formed by processes unique to the Archean and instead "a singular genetic process restricted to a specific geodynamic environment may be applied to mesothermal deposits of all ages" (Wyman and Kerrich, 1990). In their model, subduction-related crustal underplating and deep, late metamorphism in a transpressive regime occurring over a 10 to 40 m.y. period would be a necessary precursor to mesothermal gold mineralization.

Despite the similarities between Archean and Phanerozoic mesothermal gold deposits and despite our preference for a mantle degassing-granulitization model, no consensus has yet been made on the origin of hydrothermal fluids or gold. Continued research and debate on geodynamic settings and fluid geochemistry will hopefully identify and refine the genetic model (or models?) that best explains mesothermal lode-gold mineralization throughout time. Surely, the current rapid evolution of ideas on the formation of Abitibi-type crust, resulting significantly from renewed research in the Abitibi, will resolve many of the outstanding questions in the near future.

4.6 GEOCHRONOLOGICAL AND GEOTECTONIC DEVELOPMENTS PERTINENT TO THE BOURLAMAQUE-LOUVICOURT TOWNSHIPS STUDY AREA

In this section, a summary is presented of the above-mentioned geochronological and geotectonic developments pertinent to the Bourlamaque-Louvicourt townships sector.

This overview is then followed by the application of the major characteristics of the mantle degassing-granulitization model and the favourable aspects of the metamorphic dehydration model to the study area in order to examine what processes and sources best explain fluid formation, migration and lode-gold deposition.

The geochronological studies of the Archean Sigma gold deposit (deposit #5 of Fig.34) by Wong et al. (1989, 1991) and Hanes et al. (1989, 1992) produced the first significant dates for the Val d'Or region. Volcanism of the Val d'Or Formation occurred at $2,704.9 \pm 1.1$ Ma (U-Pb zircon age) and a porphyritic diorite with similar deformation characteristics as the volcanic rocks gives an age of $2,703.7 \pm 2.5$ Ma (U-Pb zircon age). The calc-alkalic Bourlamaque pluton, geochemically similar to the Val d'Or Formation rocks, gives a U-Pb zircon age of $2,699.8 \pm 1.0$ Ma. Although the Bourlamaque age is not within reasonable error limits of the Val d'Or Formation age, there is a real possibility that a young phase of the Bourlamaque intrusion was dated (sampled only in the southwest apophysis) and that an older age could be obtained by dating the central-southeast part of the intrusion (Campiglio and Darling, 1976; Campiglio, 1977).

A feeling for post-volcanic events can be found in age dating of syn- to post-tectonic events. A feldspar porphyry dike postdating regional folding from the Sigma mine gives a U-Pb zircon age of $2,694.0 \pm 2.2$ Ma. Robert (1991) uses this age with the Bourlamaque intrusion date to bracket regional folding between 2,700 and 2,694 Ma;

it also places an upper age limit of 2,694 Ma on regional greenschist-facies metamorphism. However, it has been noted (F. Robert, pers. commun., 1993) that the youngest detrital zircons from the deformed Kewagama and Cadillac sediments have an upper age limit of sedimentation of approximately 2,688 Ma (Davis, 1991), suggesting that there was another pulse of regional deformation whose age limits are not yet defined.

With regard to the timing of regional greenschist metamorphism, an $^{40}\text{Ar}/^{39}\text{Ar}$ age of $2,693 \pm 11$ Ma was obtained on a metamorphic magnesio-hornblende from the Sigma mine (Hanes et al., 1992), whereas a U-Pb age of $2,684 \pm 7$ Ma was obtained on metamorphic rutile from the Val d'Or Formation (Wong et al., 1991). Although Wong et al. (1991) note that these two metamorphic dates are analytically indistinguishable, Robert (1991) interprets the apparently older age of 2,693 Ma to represent greenschist-facies, dynamic metamorphism which accompanied an early pulse of D_2 deformation, and the apparently younger age of 2,684 Ma to represent a static, middle greenschist-facies metamorphic event.

Lode-gold deposits are commonly hosted by or crosscut syn- to late-tectonic intrusions, and dating of these magmatic events may provide an upper age limit on gold mineralization. In the Val d'Or camp, the Lamaque mine (deposit #8 of Fig. 34) is a good example of lode-gold mineralization hosted by intrusions. Jemielita et al. (1989) obtained a U-Pb zircon age of $2,685 \pm 3$ Ma for a gold-hosting Lamaque plug, placing

an upper age limit on quartz-carbonate-tourmaline-pyrite veining of approximately 2,685 Ma.

On the other hand, ages of several apparently ore-related minerals suggest that mineralization post-dated metamorphism and deformation by a wide gap. Gold mineralization and associated hydrothermal alteration are superimposed on metamorphosed rocks (Robert and Brown, 1986b) at the Sigma mine, and hydrothermal rutile from Sigma gives a U-Pb age of $2,599 \pm 9$ Ma (Wong et al., 1991). This age is similar to a "plateau" date of $2,579 \pm 9$ Ma for muscovite from a gold-bearing quartz vein at the Sigma mine (Hanes et al., 1992), to a Sm-Nd age of $2,602 \pm 20$ Ma for scheelite separates from the Sigma mine and two other lode-gold deposits in the Val d'Or region (Anglin, 1990), and to a U-Pb age of $2,593 \pm 5$ Ma for hydrothermal rutile from the Lamaque mine (Jemielita et al., 1989). Based on all of these ages, Wong et al. (1991) and Hanes et al. (1992) conclude that gold mineralization associated with undeformed quartz-tourmaline-carbonate-pyrite veins in the Val d'Or mining camp took place approximately 80 to 100 million years after $\approx 2,693$ to 2,684 Ma regional metamorphism.

Further physical and mineralogical characterization of quartz-vein gold mineralization in the Val d'Or mining camp by Robert (1994) and Robert and Boullier (in press) has identified two generations of shear zone-related gold-quartz veins. In the western part of the camp, early quartz-carbonate-pyrite veins are associated with second-

order shear zones. The veins are commonly folded and boudinaged and cut by diorite and tonalite dikes. In the eastern part of the camp, younger quartz-tourmaline-carbonate-pyrite veins are associated with third-order shear zones, crosscutting all intrusive rocks (except Proterozoic diabase dikes) and modified only by weak effects of the dextral strike-slip reactivation of the LLCTZ. Based on the structural sites and physical distributions of these various veins, Robert (1994) suggests that all of the veins do not originate from the same hydrothermal event and that at least two generations of shear-zone-related, gold-bearing, quartz veins occurred in the Val d'Or district. At present, deformed quartz-carbonate-pyrite veins west of Val d'Or are older than approximately 2,686 Ma, based on U-Pb zircon ages of $2,692 \pm 2$ Ma and $2,686 \pm 2$ Ma of intrusions crosscutting deformed quartz-carbonate-pyrite veining at the Norlartic (Pilote et al., 1993) and Kiena (Morasse et al., 1993) mines, respectively. Quartz-tourmaline-carbonate-pyrite veins east of Val d'Or are younger than approximately 2,685 Ma, the age of magmatic zircon from the diorite-tonalite stock hosting the Lamaque mine (Jemielita et al., 1989).

SHRIMP ion-microprobe methods were used by Claoué-Long et al. (1990) on zircon to date the Bourlamaque intrusion and gold mineralization at four mines east of Val d'Or. This age-dating study, along with results in Claoué-Long et al. (1992), does not support the suggestion that lode-gold mineralization occurred significantly after regional metamorphism. For the Bourlamaque intrusion, a concordant set of data gives a weighted mean $^{207}\text{Pb}/^{206}\text{Pb}$ age of $2,711 \pm 12$ Ma. Hydrothermal zircon is reportedly

associated with auriferous quartz-tourmaline veins at the Dumont, Pascalis Nord (formerly Perron), Sigma, and Bevcon mines east of Val d'Or. Hydrothermal zircon from the Dumont mine gives an imprecise age of $2,694 \pm 70$ Ma, whereas hydrothermal zircon from the Pascalis Nord and Sigma mines give more precise, weighted mean $^{207}\text{Pb}/^{206}\text{Pb}$ ages of $2,697 \pm 17$ Ma (note: the age given on page 125 of Claoué-Long et al. (1990) differs slightly from the age of $2,697 \pm 19$ Ma given on page 121) and $2,682 \pm 8$ Ma, respectively. Two populations of morphologically different zircon from the Bevcon mine give weighted mean $^{207}\text{Pb}/^{206}\text{Pb}$ ages of $2,704 \pm 6$ Ma and $2,681 \pm 6$ Ma. According to Claoué-Long et al. (1990), their Bourlamaque date of $2,711 \pm 12$ Ma best evaluates the intrusion's age, in agreement with the $2,710 +5/-4$ Ma age determined by Taner and Trudel (1989) using very discordant U-Pb zircon analyses from an ultramafic xenolith containing zircon (possibly of metasomatic origin formed during crystallization of the intrusion). With regards to the gold mineralization, Claoué-Long et al. (1990) state that, although the Dumont and Pascalis Nord zircons may date the Bourlamaque intrusion or the hydrothermal event affecting the intrusion, the hydrothermal zircons from the Sigma mine and the younger population of hydrothermal zircons from the Bevcon mine have younger ages than the Bourlamaque intrusion and the Dumont and Pascalis Nord mines, which is taken to be "compelling evidence of their hydrothermal origin". Claoué-Long et al. suggest that two growth events of morphologically different zircon ($\approx 2,700$ Ma and $\approx 2,680$ Ma) occurred, linked to the kinematic development of the Val d'Or region, and that gold mineralization in the Val d'Or region was not due to a single hydrothermal event. They also argue that the much younger ages for gold

mineralization using micas, scheelite, rutile, and sphene record either reset isotopic systems or renewed hydrothermal mineral growth.

In opposition to the assertion of hydrothermal zircon, Corfu and Davis (1991) comment on a gamut of problems found in the article by Cloué-Long et al. (1990), the most important being discordant data obtained from what they judge to be metamict zircons. Therefore, Corfu and Davis question the hydrothermal origin of the analyzed zircons, arguing that they are more likely zircons from wallrocks and therefore give ages broadly coeval with magmatism in the Val d'Or camp. In rebuttal, Cloué-Long et al. (1992) submit electron backscatter images of gold-bearing zircon not included in their 1990 article, and they maintain, along with Kerrich and King (1993), that their age of gold mineralization ($\approx 2,680$ Ma) dates gold introduction with quartz-tourmaline-(zircon) in veins and that younger ages are consistent with renewed hydrothermal activity, remobilization of gold and rejuvenation of isotopic systems in non-robust minerals and possibly even in normally alteration-resistant zircon.

Recently, Feng et al. (1992) have proposed for the southern part of the Abitibi a model in which Archean mesothermal lode-gold mineralization is related to the collision of the Pontiac and Abitibi subprovinces at about 2,690 to 2,670 Ma, supporting the geochronological data and interpretations of Cloué-Long et al. (1990, 1992). The model is based on geobarometric, geochemical and geochronological data. In Feng and Kerrich (1990), geobarometric data are presented for various intrusions in the Pontiac

Subprovince and in the Abitibi's Southern Volcanic Zone (SVZ; Ludden et al., 1986). Pressure distributions indicate that the Pontiac and a block of terrane northwest of Val d'Or (the Lacorne block, as named by these authors; Fig. 40a) have similar high pressures, indicative of relatively-deep crustal levels, and of mineralization (Mo, Be, Li, U, Ni) at such levels (Fig. 40b). Feng and Kerrich (1990) interpret the Lacorne block as part of the Pontiac Subprovince and suggest that the Lacorne block was emplaced in the SVZ by differential uplift, caused by strike-slip faulting during oblique collisional tectonics in late Archean time. Further geochemical and geochronological work by Feng and Kerrich (1991), Feng and Kerrich (1992), and Feng et al. (1992) on sediments and intrusive rocks from the Lacorne block, the SVZ, and the Pontiac Subprovince also suggest that the Pontiac and Lacorne terranes have similar features. The sum of the geochemical and geochronological data lead Feng et al. (1992) to suggest a model (Fig. 41) whereby oceanic lithosphere was subducted separately under the Pontiac Subprovince and the Abitibi SVZ from 2,740 to 2,680 Ma ago, resulting in a first thermal event, accompanied by low-pressure, greenschist-facies metamorphism and the intrusion of abundant syntectonic batholiths. At about 2,670 to 2,630 Ma, the two terranes collided and the Pontiac Subprovince was locally thrust under the Abitibi SVZ, which caused a second thermal event and partial melting of the underthrust Pontiac metasediments, forming S-type collisional garnet-muscovite granites and associated pegmatites. Subsequent differential uplift exposed the entire Pontiac Subprovince and the Lacorne block. Feng et al. (1992) suggest that this second thermal event probably reset isotopic systems in non-robust minerals, resulting in the reported young ages (up to approximately

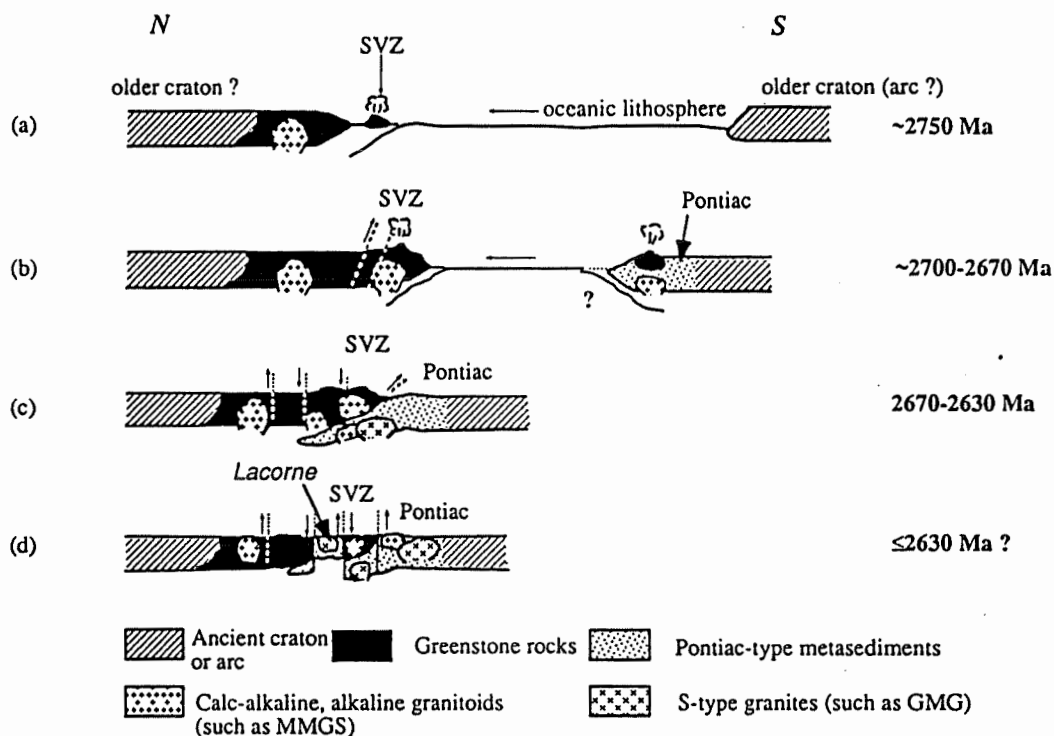


Figure 41. Simplified tectonic model for the evolution of the Abitibi Southern Volcanic Zone (SVZ) and the Pontiac subprovince. (a) Stage 1: oceanic subduction and arc (and/or back-arc) volcanism. (b) Stage 2: plutonism (such as tonalite-granodiorite-granite-quartz monzodiorite intrusions in the Abitibi SVZ, and monzodiorite-monzonite-granodiorite-syenite (MMGS) intrusions in the Pontiac subprovince), initial metamorphism, accretionary tectonics, and coeval alkaline magmatism and gold mineralization. (c) Stage 3: arc (continent)—continent (older arc?) collision, second metamorphism, emplacement of S-type, garnet-muscovite granite (GMG) intrusions, probably derived from the metasedimentary Pontiac subprovince, and reactivation of gold. (d) Stage 4: differential uplift, exposing the entire Pontiac subprovince, and the higher grade Lacorne block within the Abitibi SVZ (from Feng et al., 1992).

100 Ma younger than the early thermal-tectonic event) for gold mineralization, and that the primary gold event was coeval with late-kinematic events (2,690-2,670 Ma).

Although this model could be employed to explain the "early" dates for gold mineralization at the Kiena and Norlartic mines, it is difficult to understand how a thermal event could reset the isotopic systems in various minerals which give concordant "late" ages for gold mineralization related to undeformed quartz-tourmaline-carbonate-pyrite veins.

Uranium-lead analyses of detrital zircons from Pontiac, Cadillac and Kewagama sediments and their interpretations by Davis (1991) conflict with those of Feng and Kerrich (1991) for sediments in the Lacorne block. An upper age limit of $2,686 \pm 3$ Ma is given for deposition of Pontiac sediments in the Val d'Or area, $2,688 \pm 3$ Ma for Cadillac sediments, and $2,688 \pm 3$ Ma for Kewagama sediments. The majority of zircons analyzed are younger than 2,725 Ma, and were probably derived from rocks presently exposed in the Abitibi Subprovince, whereas approximately 20 % of the zircons fall in the age range of 2,840 to 2,760 Ma, implying erosion of an abundant older crust in the northern Superior Province. In contrast, detrital zircons from the Lacorne block were analyzed by the single zircon Pb-evaporation technique to obtain $^{207}\text{Pb}/^{206}\text{Pb}$ minimum ages (Feng and Kerrich, 1991). Ages range from $2,691 \pm 8$ Ma to $3,042 \pm 6$ Ma, with 60 % of the detrital zircons found to be older than 2,750 Ma. The upper

limit for sedimentation is set by the younger zircons which yield ages of $2,691 \pm 8$ Ma, $2,695 \pm 4$ Ma, $2,715 \pm 16$ Ma, and $2,719 \pm 4$ Ma.

Recent structural work by Desrochers et al. (1993) in the Malartic and Val d'Or region (Fig. 5) casts doubt on the existence of the Pontiac block. They suggest the segmentation of the volcanic pile in this region into four distinct mafic lithotectonic domains (the Northern, Vassan, Central and Southern domains; Fig. 5) that are overlain by a calc-alkalic sequence (the Val d'Or domain). According to these divisions, the Pontiac block would be composed of parts of the Northern, Vassan and Central domains (compare Figs. 5 and 40a). Desrochers et al. (1993) interpret the mafic domains to be accreted fragments of Archean oceanic plateaux that were deformed during their accretion, whereas the calc-alkalic sequence represents extension-related volcanism and plutonism, the whole package of five domains being deformed possibly as a result of ridge subduction in a regime of oblique convergence. This scenario has been suggested by Skulski et al. (1991) and Babcock et al. (1992) for two spreading centres on the Pacific coast of North America.

Finally, additional information on "young" dates from Zweng et al. (1993) continues the debate on the significance of these ages to gold mineralization. Zweng et al. (1993) provide geochronological data from the Camflo gold mine located near Malartic, Quebec. Uranium-lead age dating on magmatic zircon gave an age of $2,685 \pm 10$ Ma for the Camflo monzonitic stock, whereas hydrothermal titanite gave an age

of $2,621 \pm 4$ Ma and titanite and K feldspar samples gave a Pb-Pb isochron age of $2,621 \pm 7$ Ma. Zweng et al. suggest then that gold mineralization at Camflo occurred approximately 60 m.y. after crystallization of the Camflo stock. Zweng et al. also calculated $^{40}\text{Ar}/^{39}\text{Ar}$ ages of hydrothermal micas related to gold-quartz veining to be 70 to 170 m.y. younger than the titanite hydrothermal age. The younger $^{40}\text{Ar}/^{39}\text{Ar}$ ages are interpreted by Zweng et al. to represent closure temperatures arrived at during cooling, and not recrystallization or reset ages. Slow cooling would be expected from mantle-derived basalt underplating the lower crust during peak granulite formation.

Zweng et al. (1993) also provide a summary of other radiometric ages from other volcanogenic massive sulphide and lode-gold deposits in Abitibi. Firstly, their evaluation of hydrothermal mineral dates from the Sigma mine (Bell et al., 1989; Hanes et al., 1989, 1992; Wong et al., 1989, 1991; Anglin, 1990; Cloué-Long et al., 1990) suggests these dates represent cooling ages. Secondly, Zweng et al. reviewed various ages from the Kidd Creek massive sulphide deposit near Timmins, Ontario, that are much younger ($2,663 \pm 28$ Ma to $2,618 \pm 8$ Ma) than the ore-hosting rhyolite ($2,717 \pm 2$ Ma). Other researchers (see review in Zweng et al., 1993, p. 1718) suggest that these younger dates represent either a post-metamorphic hydrothermal event or the closing stages of regional metamorphism, and some authors note the similarity between a young fuschite average plateau age of $2,618 \pm 8$ Ma (Smith et al., 1991, 1993) from potassium metasomatic alteration at the Kidd Creek VMS mine and that of hydrothermal muscovite ($2,617 \pm 8$ Ma; Masliwec et al., 1986) related to gold mineralization at the nearby Hollinger mine,

suggesting that the fuchsite dates represent a later hydrothermal event (see also Smith et al., 1993; Schandl and Wicks, 1993; Vervoort et al., 1993).

Zweng et al. (1993) offer an alternative explanation of these young mica ages.

They suggest (p. 1718):

"that the young ($\approx 2,620 - <2,500$ Ma) K-Ar, $^{40}\text{Ar}/^{39}\text{Ar}$, Rb-Sr, and Sm-Nd ages for micas from pre-Kenoran plutons and massive sulphide deposits, as well as from post-Kenoran plutons and gold deposits, bracket the time when segments of the southern Abitibi subprovince cooled below the temperature required for daughter product retention. Since peak metamorphic temperatures were probably in excess of those required for daughter retention in muscovite and biotite, it is possible that post-Kenoran plutons and gold deposits were emplaced before regional postmetamorphic temperatures had dropped below those required for closure by each of the radiometric systems....A protracted cooling model can more easily account for the wide range of younger radiometric ages whereas scenarios employing multiple thermal and/or hydrothermal events must be cyclical in nature without the younger thermal pluses disturbing radiometric ages reset by older pulses."

4.7 APPLICATION OF THE MANTLE DEGASSING-GRANULITIZATION MODEL TO THE BOURLAMAQUE-LOUVICOURT TOWNSHIPS STUDY AREA.

In synthesis, gold mineralization in the mantle degassing-granulitization model, as applied to the Superior Province, is interpreted as an integral part of crustal cratonization, brought on by the addition of mantle diapiric masses to the lower crust. This underplating results in the granulitization of the lower crust by the addition of heat, magma, and volatiles, especially CO₂, to the lower crust. Compositionally variable magmas are generated by partial melting of the heterogeneous upper and lower crusts. Fluids and silicate magmas migrate upwards via crustal-scale zones of weakness represented by deep-reaching "breaks" such as the LLCTZ. Given that granulitization occurs slowly at depth, fluid and magmatic migration toward the surface may postdate and overprint upper-crustal thermal-tectonic activities where metamorphism and deformation have already passed their peaks.

Examination of the Bourlamaque-Louvicourt townships sector and its lode-gold deposits reveals several characteristics consistent with the key elements of the mantle degassing-granulitization genetic model. An adequate crustal-scale "plumbing" system needed to channel rising gold-bearing hydrothermal fluids is represented in the study area by the LLCTZ and its subsidiary shear zones. Robert (1990a) groups the brittle-ductile shear zones into three groups (Fig. 42). The first-order shear of the Val d'Or district

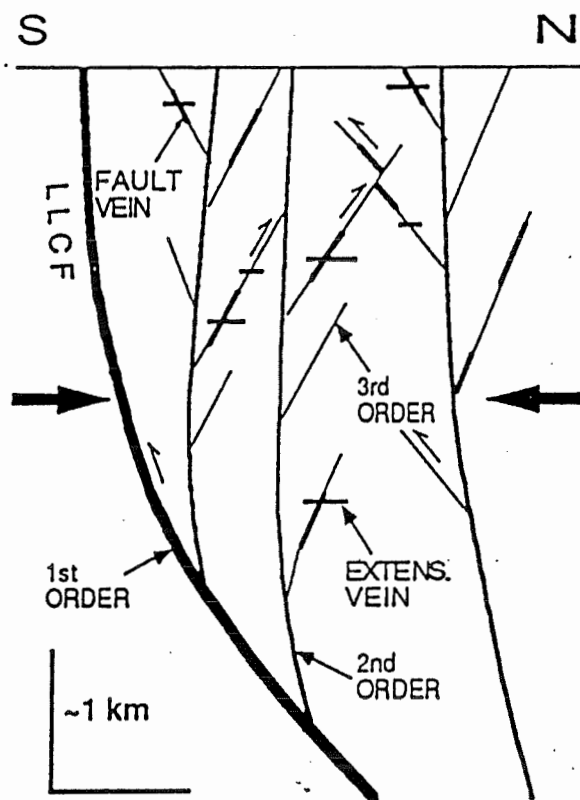


Figure 42. Schematic cross-section through the Val d'Or district showing relationships between veins and different orders of shear zones (LLCF: Larder Lake-Cadillac Fault (from Robert and Boullier, 1994).

is the LLCTZ, a major, crustal-scale shear zone separating the Pontiac Subprovince and the Malartic Composite Block (MCB; Desrochers et al., 1993) in the study area, and this shear zone probably represents a suture zone between the MCB and the Pontiac Subprovince, considered to have been thrust to the north underneath the Abitibi subprovince (Dimroth et al., 1983a,b; Hodgson et al., 1990). Measuring approximately 200-750 metres wide, the high-strain zone dips steeply to the north in Quebec and steeply to the south in Ontario, and has a strike length greater than 200 kilometres, extending from the Kirkland Lake area in Ontario to just east of the study area. Geophysical imaging (Green et al., 1990; Jackson et al., 1990) indicates that this steeply-dipping fault zone has a maximum crustal depth of approximately 15 kilometres and may become listric to the north (Green et al., 1990). Second- and third-order shear zones constitute a subsidiary shear system to the LLCTZ. The second-order shear zones are generally 5 to 10 kilometres long and less than 300 metres wide, lie subparallel to the LLCTZ, and host early, quartz-carbonate-pyrite veins (Morasse et al., 1993; Pilote et al., 1993; Robert and Boullier, in press). Third-order shear zones, typically hosting later quartz-tourmaline-carbonate-pyrite veins (Robert and Boullier, in press), are less than 2 kilometres long and are generally only several metres wide. The distinguishing characteristic of third-order shears is their oblique dips to the general structural trend.

Of course, granulitization is an intense metamorphism, and attempts have been made to date metamorphism and lode-gold mineralization in the Val d'Or region. An $^{40}\text{Ar}/^{39}\text{Ar}$ age of metamorphic hornblende $2,693 \pm 11$ Ma (Hanes et al., 1992) from the

Sigma mine probably represents greenschist-grade, dynamic metamorphism, concordant with the bracketed time period for regional deformation (2,700-2,684 Ma). A U/Pb age on metamorphic rutile of $2,684 \pm 7$ Ma from the Colombière rhyolite of the Val d'Or Formation (Wong et al., 1991) probably represents thermal, middle greenschist-facies metamorphism (Robert, 1990a; Robert, 1991) which affected the small syn- to late-kinematic porphyritic intrusions and has been observed to increase with depth in some of the deep mines of the Val d'Or region (Grant, 1986; Robert, 1990a; Morasse et al., 1993). The $2,694 \pm 2$ Ma age of the non-foliated porphyritic dike from the Sigma mine is considered by Wong et al. (1991) to be an upper age limit on regional-greenschist facies metamorphism.

With regard to geochemical affinities to the mantle degassing-granulitization model, several characteristics of lode-gold mineralization in the study area are consistent with this genetic model. Important quantities of carbonate accompany all three orders of shears, as wallrock alteration and as an important vein constituent. Fluid inclusion work by Robert and Kelly (1987) on secondary fluid inclusions from Sigma mine veins identified three types of inclusions: 1) high-salinity Na-Ca-Cl aqueous inclusions (25-35 wt. % salt) with small amounts of CO₂, 2) CO₂-rich inclusions containing small amounts of H₂O and CH₄, and 3) homogeneous, low-salinity H₂O-CO₂ fluids (< 10 equiv wt. % NaCl) with CO₂ contents commonly ranging from 15 to 30 mole percent CO₂. Robert and Kelly (1987) interpret the ore-bearing fluid to have been similar to the third type of fluid inclusions, entrapped at minimum temperatures between 285° and 395°C. That

fluid then experienced unmixing, possibly as a result of extreme fluid pressure fluctuations (Guha et al., 1991) and resulted in daughter fluids similar to types 1 and 2. In conclusion, CO₂ is recognized as an important, hydrothermal-fluid component, possibly originating from a mantle/deep-crustal source.

Based on alteration studies and mass-balance calculations of vein wallrocks from the Sigma and Lamaque mines, hydrothermal fluids related to gold mineralization are seen to have caused considerable enrichments in CO₂, Ca, Na, K, B, S, P, Au, REE, Ti, Zr, Y, Hf, U, Ta, Nb, and Th and important depletions in Mg, Fe, Al, Rb, and H₂O in visibly altered zones next to veins (carbonate-white mica outer subzones and carbonate-albite inner subzones; see Figs. 35a and 35b) (Ludden et al., 1984; Robert and Brown, 1986b). The laterally more extensive cryptic alteration zones, characterized by chlorite-carbonate-white mica assemblages (see Figs. 35a and 35b), are enriched in CO₂, K, Rb, and S, depleted in REE and U, and slightly depleted in Sr; Th, Ta, and Hf behave inconsistently. Like K and Rb, Li and Cs are commonly enriched in gold-bearing veins systems and their associated wallrocks (Kerrick, 1983). However, the Sigma-Lamaque studies did not include Li and Cs analyses, and consequently, it cannot be confirmed if they are enriched, as K and Rb are, in wallrock alteration zones associated with the auriferous Sigma and Lamaque quartz-carbonate veins. Overall, these enrichments and depletions are in agreement with the mantle degassing-granulitization model (Fig. 39).

Tourmaline is common and relatively abundant in the gold mines of the study area (Table 2) and in the Val d'Or-east camp in general (Robert, 1990b; Robert and Boullier, 1994). The characteristic presence of tourmaline in veins and associated wallrock may indicate a fundamental difference (boron-rich) in fluid composition and genesis (Guha et al., 1991) and may imply that a local source rock has affected the mineral assemblages in these gold deposits. Generally, boron is highly enriched in ocean sediments and in the altered portions of subducted oceanic crust, indicating its high concentration in ocean water and its strongly adsorptive behaviour during sedimentation (Morris et al., 1990 and references therein). Boron-beryllium analyses of subduction rocks of four island arcs suggest that boron is not subducted to depth, nor is it stored in the sub-arc mantle. It is possible that convection may circulate boron-enriched, sub-arc material to back-arc environments. In the Bourlamaque-Louvicourt townships study area, the Pontiac Subprovince is an obvious source of abundant sediments, and it is thought to have been thrust under the Abitibi (Dimroth et al., 1983a,b; Hodgson et al., 1990). It is possible then that fluid-rich sediments of the Pontiac Subprovince were thrust underneath this part of the Abitibi and contributed boron-rich fluids to the gold-mineralizing system.

After pyrite, the principal sulphide in lode-gold deposits located in or proximal to sedimentary units is arsenopyrite (Robert, 1990b), and in the Val d'Or district this relationship is best exemplified among gold deposits west of Val d'Or. This relationship would suggest the local importance of sediments (e.g., shales) to supply appreciable amounts of arsenic. In the Val d'Or-east study area, the Orenada deposit (deposit #11

of Fig. 34), located southwest of the East Sullivan stock in Piché Group volcanics next to the Pontiac Subprovince, contains up to 20 % arsenopyrite as wallrock alteration (Robert et al., 1990). The Sigma-2 deposit (deposit #1 of Fig. 34) also contains abundant arsenopyrite. However, the latter deposit is hosted by the granophyric portion of the differentiated gabbroic Vicour sill located approximately 3 to 4 kilometres geographically north of the Pontiac sediments. Also, the mineralized veins and surrounding wallrocks contain a relatively small amount of carbonate, an observation consistent with the fluid inclusion study of Kheang and Perrault (1987). If Pontiac sediments were thrust or subducted beneath the study area (Dimroth et al., 1983a,b; Hodgson et al., 1990), it is not yet clear why there is not more arsenopyrite in all Val d'Or-east deposits. The abundance of arsenopyrite at the Sigma-2 mine may indicate a sedimentary source of arsenic still more local than the scale of the vein field described by Robert (1994) for the gold mineralizing fluids of Sigma-2.

The Akasaba gold deposit (deposit #12 of Fig. 34) is another atypical deposit of the study area, if not of the whole Val d'Or mining camp. As already described in section 4.2.4.1, it consists of disseminated gold in a lapilli tuff accompanied by pyrrhotite, chalcopyrite, magnetite, and pyrite (Sauvé, 1985). The deposit is also characterized by abundant epidote alteration and relatively rare carbonate alteration. Sauvé (1985) hypothesizes that the emplacement of this deposit is fundamentally synvolcanic. Its mineralogy, configuration and emplacement near the top of the volcanic

pile, if the paleoenvironment of Imreh (1984) is followed, suggest that the Akasaba deposit is in fact plausibly synvolcanic.

Although lode-gold deposits may be hosted by volcanic, igneous or sedimentary rocks, the majority of the gold deposits in Bourlamaque and Louvicourt townships are hosted by intrusions. Generally, three categories of intrusion can be distinguished by their relative ages: 1) synvolcanic, pre-kinematic gabbro-diorite-tonalite intrusions, ranging from small stocks (such as those at the Sigma and Lamaque deposits) to the large plutons of the Bourlamaque and Bevcon intrusions; 2) syn- to late-kinematic, diorite-tonalite-syenite dikes and small stocks that are commonly porphyritic; and 3) large, late- to post-kinematic intrusions such as the peraluminous monzonite of the East Sullivan stock (Robert, 1990b).

In the Bourlamaque-Louvicourt townships study area, pre-kinematic and syn- to post-kinematic intrusions commonly host lode-gold deposits. A pre-kinematic porphyritic diorite at Sigma is dated at 2704 ± 3 Ma (U-Pb zircon age), whereas the apparently synvolcanic Bourlamaque intrusion probably has an age of $2,699.8 \pm 1.0$ Ma (U-Pb zircon age) (Wong et al., 1991) (although it would not be surprising if a geochronological date of the main body of the intrusion was more concordant with the age of volcanism ($2,704.9 \pm 1.1$ Ma; Wong et al., 1991)). Feldspar \pm quartz porphyritic dikes are commonly associated spatially with lode-gold mineralization and are relatively abundant in the southern part of the volcanic terrane in the study area. A non-foliated

feldspar porphyry dike at Sigma has an age of $2,694 \pm 2$ Ma (U-Pb zircon age; Wong et al., 1991) and most dikes of this type seem to have been injected after the major period of deformation. However, schistose porphyry dikes are observed spatially related to non-foliated ones and may vary laterally from foliated to non-foliated (Sauvé et al., 1986). These observations suggest that porphyry dikes are probably late- to post-kinematic in age, with the major regional deformation being bracketed between approximately 2,700 and at least 2,688 Ma (age of deformed Cadillac and Kewagama sediments).

A summary of geochronological data pertinent to the study area has been presented in section 4.6 where the reader may review details on this subject. In summary, gold mineralization related to quartz-tourmaline-carbonate-pyrite veins in the Val d'Or-east sector is younger than 2,685 Ma, the age of the diorite-tonalite stock of the Lamaque mine and may be as young as approximately 2,579 Ma. Wong et al. (1991) and Hanes et al. (1992) conclude that this mineralization postdates syn- to post-tectonic magmatism and regional metamorphism by up to ca 100 Ma, and they disregard the possibility that their data represent cooling or reset ages, giving several arguments against these hypotheses (p.334 in Wong et al., 1991 and p.1858-1859 in Hanes et al., 1992). These "later" (circa 2,600 Ma) dates suggest a correlation between lower crustal magmatism and metamorphism (as recorded in the Kapuskasing Structural Zone; Corfu, 1987; Krogh et al., 1988; Krogh, 1990) and hydrothermal gold mineralization at mid-crustal levels, in agreement with the mantle degassing-granulitization model. Wong et

al. (1991) note the existence in the Central Superior Province of gold mineralization, synchronous with late magmatic activity (in the age range of 2,720-2,700 Ma), and they acknowledge the possibility of ca 2,700 Ma gold deposits in the southern Abitibi. Although not in the study area proper, two examples of gold mineralization have been dated as having minimum ages of 2,686 Ma (Morasse et al., 1993) and 2,692 Ma (Pilote et al., 1993). Further characterization of these two sites of "early" gold mineralization are needed to determine the significance of these ages with respect to initial gold emplacement and the cratonization of the Superior Province in general.

In conclusion, several characteristics of the Bourlamaque-Louvicourt townships sector and its lode-gold deposits agree with the key elements of the mantle degassing-granulitization model, as envisaged for Archean lode-gold mineralization of the Superior Province (Colvine et al., 1988; Fyon et al., 1989). The following points underline this consistency:

- 1) Gold mineralization related to undeformed quartz-tourmaline-carbonate-pyrite veins is associated regionally with the Larder Lake-Cadillac Tectonic Zone, a major crustal-scale fault, and is hosted essentially by shear zones subsidiary to the regional fault;

- 2) Important quantities of carbonate are associated with all scales of shearing and quartz veining, and CO₂ is recognized as an important hydrothermal fluid component as expected in a CO₂-degassing mantle model;
- 3) Enrichments in K, Rb, U, B, CO₂ and Au are noted in alteration zones adjacent to quartz veins. Notably, quartz veins and alteration zones in the study area are also characterized by the relative abundance of tourmaline, a boron-rich mineral;
- 4) Lode-gold deposits in the study area are spatially associated with felsic to intermediate intrusions, and a high number of gold deposits are hosted by intrusions; and
- 5) Gold mineralization in the study area is apparently ca 80-100 Ma younger than syn- to post-tectonic magmatism and regional metamorphism, and may be correlated with lower crustal magmatism and metamorphism, as recorded in the Kapuskasing Structural Zone.

4.8 SUMMARY

Although gold mineralization may be found in synvolcanic and syn- to late-tectonic environments in Archean terranes, gold mineralization in the study area consists essentially of the syn- to late-tectonic type (the Akasaba deposit could be an exceptional synvolcanic deposit).

After evaluation of the genetic models for mesothermal lode-gold mineralization, i.e., meteoric water, orthomagmatic, metamorphic dehydration, mantle degassing-granulitization models, and variations thereof, it is suggested that the mantle degassing-granulitization genetic gold model is the most comprehensive explanation for most Archean gold mineralization. It is also recommended to integrate the favourable aspects of amphibolite-facies fluids and meteoric fluids for the formation of some gold deposits with this model. This suggestion would agree with the proponents of multiple fluids and solute sources (cf., Colvine et al., 1988; Fyon et al., 1989).

Although geochronology is clearly helping us to better understand Archean terrane construction and events surrounding gold emplacement, it is also raising many questions and instigating further debate as a result of seemingly conflicting results or optional interpretations of data. Several studies attempting to date gold mineralization in the study area are evidence of the continuing debate surrounding

the interpretation of the geochronological data. In the present state of incomplete dating, final judgement on which gold-emplacment model(s) is (are) best must be reserved until those dates and their geodynamic interpretation are more complete.

Meanwhile, the Bourlamaque-Louvicourt townships sector and its lode-gold deposits have several characteristics (underplating; crustal-scale plumbing; carbonatization and CO₂-bearing hydrothermal fluids; enrichments in K, Rb, U, B and Au; spatial association between intrusions and gold deposits; apparent synchronicity between gold mineralization and lower crustal magmatism and metamorphism) consistent with the principal elements of the mantle degassing-granulitization genetic gold model. Also, the mesothermal lode-gold deposits of the North American Cordillera appear to be good Phanerozoic analogues of Archean mesothermal gold mineralization, and the characteristics of these young deposits clearly aid in interpreting the emplacement of gold in the Archean terrane of the study area.

CHAPTER 5

DISCUSSION AND SUMMARY

5.1 INTRODUCTION

This chapter summarizes the Archean greenstone belt geology that resulted in the two principal types of economic mineralization encountered in the Val d'Or-east mining district: synvolcanic base-metal massive sulphide deposits, and syn- to late-tectonic mesothermal lode-gold deposits. The geochemical characteristics of the principal lithotectonic domains hosting Archean volcanogenic massive sulphide (VMS) and lode-gold mineralization in the Val d'Or-east district are given in Chapter 2, and the justifications for the metallogenic origins of these two types of mineralization are presented in Chapters 3 and 4. The intent of the present chapter is to present an overall tectonochronological evolution of the southern Abitibi such that it can readily be seen that VMS and lode-gold deposits form a coherent, almost predictable part of this crustal-scale evolution.

This overview is, of course, not intended to be the final explanation of the metallogeny of the Bourlamaque-Louvicourt townships study area, for undoubtedly there will be many modifications and improvements to come, especially considering the rapid rate of revision of Abitibi geology witnessed in very recent years. Nor is it exclusive in the preferred genetic models chosen — again, better data may require significant

changes to be made to our interpretations. The scenario which follows is, however, considered to be the best interpretation of the base-metal and gold metallogeny of the Bourlamaque-Louvicourt townships study area in the light of currently available data and concepts.

5.2 SUMMARY OF GEOCHEMICAL DATA AND VMS AND LODGE-GOLD MODELS APPLIED TO THE VAL D'OR-EAST DISTRICT

The geochemical data for the principal lithotectonic domains of the Val d'Or district and the best genetic models for Archean VMS and lode-gold mineralization are reviewed briefly here as a precursor to the crustal-scale metallogenic interpretation of the Val d'Or-east (Bourlamaque and Louvicourt townships) geology.

5.2.1 Geochemical Data for the Val d'Or District

The Val d'Or domain (Desrochers et al., 1993), one of the major lithotectonic units of the Bourlamaque-Louvicourt townships study area, consists of flow and intrusive rocks that have experienced widespread and intense VMS hydrothermal alteration resulting in the peraluminous nature of these rocks. Despite this alteration, magmatic trends based on major-element behaviour are still evident, and trace-element and REE data (negative Nb and Ti and positive Zr anomalies, LREE-enriched) are suggestive of a calc-alkalic affinity for the Val d'Or domain rocks. This affinity is of special metallogenic importance because calc-alkalic rocks are commonly the hosts of VMS

deposits.

The other major lithotectonic domains (the Northern, Vassan, Central and Southern domains; Desrochers et al., 1993), located mostly in the Val d'Or-west district but also in part in the study area proper, have tholeiitic to komatiitic affinities based on major-element, trace-element and REE data. Although these data imply a genetic relationship between the komatiitic and tholeiitic rocks through magmatic processes, contrasting REE profiles (i.e., flat REE versus LREE-depleted/HREE-enriched profiles) suggest that the mafic flow rocks of both the Central and Southern domains come from two distinct mantle sources: a depleted tholeiitic mantle source, and a depleted tholeiitic mantle source which is also LREE-depleted. The provenances of these distinctive lithotectonic domains remains unknown, but they may represent segments of oceanic crust created south of the Abitibi protocontinent.

5.2.2 The Hydrothermal Convection-Cell Model for VMS Mineralization

The most favourable model for modern and ancient VMS mineralization is the hydrothermal convection-cell model. Irrespective of the VMS deposit classification (Mattabi-subtype versus Noranda-subtype) and thus aside from the precise model applied to a given deposit, the convection-cell model generally requires a relatively shallow (2-3 km below seafloor) subvolcanic intrusion to heat and convect seawater in the concomitant fault and fracture system of an oceanic rift environment. Heated, hydrothermally evolved and mineralized seawater would vent through the rocks overlying

the heat source resulting in distinctive hydrothermal-vent alteration patterns and mineral assemblages as well as VMS-type mineralization at the seafloor.

In the Val d'Or-east district, the Val d'Or domain, characterized by abundant autoclastic and volcanoclastic rocks of calc-alkalic affinities, overlies unconformably the neighbouring domains and hosts the known VMS deposits of the district. The comagmatic Bourlamaque pluton is the probable heat engine responsible for heating and thermally convecting an evolved base metal-mineralized seawater. The origin of the Val d'Or domain and the Bourlamaque pluton is thought to be due to an oceanic ridge subducted beneath oceanic plateau fragments (the Northern, Vassan, Central and Southern domains) accreted to the Abitibi protocontinent (Desrochers et al., 1993). An intracontinental back-arc environment, where rifting within a continental margin occurs as a result of the subduction of oceanic crust, is also a possible setting to explain the origin of the Val d'Or domain and the Bourlamaque pluton. This scenario is hypothesized for the formation of Kuroko massive sulphide deposits in the Green Tuff Belt (Cathles et al., 1983) and may explain the formation of the VMS deposits in Bourlamaque and Louvicourt townships. In any case, both of these tensional environments, capable of producing abundant calc-alkalic rocks and cogenetic intrusions, are consistent with the basic requirements of the hydrothermal convection-cell model for VMS mineralization.

5.2.3 The Mantle Degassing-Granulitization Model for Archean Lode-Gold Mineralization

Of the four current mesothermal lode-gold models (meteoric water, orthomagmatic, metamorphic dehydration, and mantle degassing-granulitization), the mantle degassing-granulitization concept appears at this time to be the most comprehensive explanation for most Archean lode-gold mineralization in the Bourlamaque-Louvicourt townships area. As proposed by Colvine et al. (1988) and others, Archean mesothermal lode-gold mineralization is seen as an integral part of the cratonization of the Superior Province, and this style of gold mineralization may be seen then as an almost inevitable product of crustal-mantle processes in Archean terrane.

In brief, the mantle degassing-granulitization model suggests that mantle diapirism supplies magma, heat and volatiles to the lower crust, resulting in the formation of a dehydrated granulitic residue. Small intrusions and a fluid containing CO_2 , H_2O , incompatible elements (Li, Rb, B, Cs, U, Th, K) and gold are channelled into deep regional deformation structures. Gold, CO_2 and companion elements may be extracted and transported to mesothermal, structural depositional sites either by exsolved magmatic fluids from ascending silicate magmas or by hydrothermal CO_2 -rich aqueous fluids rising directly from the dehydrating source. Because geochemical and isotopic data do not yet point unequivocally to any one source and because some studies suggest fluids other than those from a mantle-deep crustal magmatic source, metamorphic or meteoric water fluids may have played a part, along with abundant CO_2 -rich fluids from the mantle, in the

leaching, transport and deposition of gold and its companion elements in the Bourlamaque-Louvicourt townships situation.

5.3 CRUSTAL-SCALE METALLOGENIC INTERPRETATION OF THE VAL D'OR-EAST GEOLOGY

As proposed by Dimroth et al. (1983a,b), Ludden and Hubert (1986) and Jackson and Fyon (1991), the Abitibi crust appears to have evolved by accretion from north to south over a period extending from approximately 2,750-2,700 Ma (Corfu, 1993). Focusing in on the Val d'Or-Malartic district, we now find that even within a relatively limited portion of the southern Abitibi, a large lozenge-shaped block such as the Malartic Composite Block (MCB; Desrochers et al., 1993) consists of several discrete accreted terranes, arriving together or individually as exotic segments from some (southern?) oceanic region.

As these segments collided with the main Abitibi protocontinent to the north, they were welded onto it with distinctive overprinted D_1 deformations indicating possibly different oblique events. This accretion was necessarily complete by approximately 2,705 Ma, the age of volcanism for the superimposed Val d'Or domain (see below). It is not known yet whether all or some of the domains constituting the MCB extend east of Val d'Or, but, if not, it can be reasonably assumed that similar accreted terranes exist

there. From current mapping it appears that the Southern domain extends south of the Val d'Or domain, although this volcanic package of tholeiitic rocks could also constitute one or more additional domains east of Val d'Or.

In any case, the possibility of the Val d'Or calc-alkalic domain resting with a possible unconformity on the accreted and D_1 -deformed domains introduces an intriguing situation. Crustal extension is called for by the calc-alkalic lithologic composition of the Val d'Or domain and the formation of VMS mineralization in this calc-alkalic environment. Furthermore, it calls for an extensional regime within what is now a marginal continental block represented by the four newly-accreted D_1 -deformed domains.

Being within a continental margin, two tectonic situations are possible: 1) an intra-continental back-arc, and a subducted oceanic ridge. In order to get the oceanic-ridge extensional environment and its calc-alkalic affinities beneath the continental margin, Desrochers et al. (1993) propose subduction of an oceanic ridge with its accompanying rising plume, resulting in VMS-hosting volcanism of calc-alkalic affinity and subvolcanic plutonism piercing the newly accreted continental margin. Alternatively, extension can occur within the continental margin, behind an arc overlying a normally subducting oceanic plate (Fouquet et al., 1991, 1993).

The tectonic scenario for the MCB, involving accretionary tectonics and superimposed volcanism, is a plausible explanation for this terrane's evolution based on

analogies with similar tectonic developments on the west coast of North America. Recent reinterpretations of west-coast geology suggest that the North American continental margin along the Pacific Ocean is composed of allochthonous terranes accreted to the main continental mass, with major strike-slip or thrust faults commonly interpreted as accretionary sutures. These terranes include volcanic packages superimposed on the accreted terranes, a scenario similar to that suggested for the Val d'Or domain. For example, the Wrangell volcanic belt in Alaska records a transition from a subduction margin to a transform margin between the northeastern Pacific and North American plates. This transition resulted in the emplacement of subaerial volcanics overlying a leaky transform fault (Skulski et al., 1991). The Crescent basalts in the northern Coast Range volcanic province in Washington State and British Columbia also resulted from rifting, due to the subduction of a propagating rift in a fore-arc setting (Babcock et al., 1992).

Relating the above to the field area, the Bourlamaque pluton, which was intruded below the Val d'Or strata, probably acted as the heat engine to circulate modified seawater that generated the VMS deposits of the study area. All of this intrusive and extrusive activity is dated at approximately 2,705 Ma. Given the size of the Bourlamaque pluton, if it were all coeval and contemporaneous with Val d'Or domain volcanism, it would clearly have been sufficiently large to have created the VMS mineralization of several Rouyn-Noranda VMS camps.

Subsequent to the Val d'Or VMS environment, the Southern Abitibi underwent from approximately 2,700 to at least 2,688 Ma a north-south deformational event as part of the Kenoran orogeny, producing regional sub-greenschist- to greenschist-facies metamorphism and generally east/west-oriented D_2 deformation. This event could well be tied to the closure of the oceanic crust between the Abitibi and Pontiac subprovinces. Subduction to the north of intervening oceanic crust would have produced the large syntectonic plutonic suite (e.g., the Lacorne batholith). At the completion of this collision of the Pontiac protocontinent and adjacent oceanic crust with the Abitibi protocontinental crust, a major suture zone, the Larder Lake-Cadillac Tectonic Zone (LLCTZ), marked the line of closure. Deep seismic profiling suggests that this "break" along the southern margin of the Abitibi Subprovince dips steeply to the north and may become listric at depths of greater than 15 km. A number of major second-order subsidiary faults, and networks of more local third-order faults and fractures, formed an interconnected plumbing system on the north side of the LLCTZ.

With the D_2 north-south compression, Sigma-type brittle-ductile mesothermal level lode-gold deposits formed above the deep-reaching first-order LLCTZ. Auriferous fluids produced at great depth by mantle degassing-granulitization and possibly amphibolite-greenstone-type metamorphism could be tapped and rise through a fault-valve type hydrothermal system. According to Robert (1990, 1994), the vein system at any one time would extend over the width of the deformation zone (up to 15 km north of the main suture zone) and perhaps as much as 40 km along strike. The nature of the vein

fillings and wallrock alteration for the lode-gold deposits in the Val d'Or-east district are remarkably similar throughout the district, but there may be some indicators characteristic of locally different source rocks at depth (e.g., tourmaline vein-fillings due to boron derived from underthrust Pontiac sediments). Lode-gold mineralization appears to be the last geologic event, crosscutting all volcanic and intrusive lithologies except for Proterozoic dikes.

From the above, we see a reasonably well-constrained (temporal, tectonic, lithologic and geochemical) development and evolution of the southern Abitibi greenstone belt geology, within which two very major types of Archean mineralization occur as normal products of this crustal history. If in the future, there are significant changes, for example, to genetic models for ores or to our concepts of crustal development, such that new or highly-modified models and interpretations come forth, the probability is that these models and their reinterpretations will converge even better on a comprehensive interpretation of the Abitibi and its principal metallogeny.

CHAPTER 6

CONCLUSION AND RECOMMENDATIONS

The Val d'Or mining camp has long been known for its rich gold mineralization and more recently for its base-metal potential. Over the past fifty years, lithotectonic models have evolved for the Val d'Or region and for other regions as well, modifying our ideas on greenstone belt development. Concurrent with these advances, small- and large-scale modelling of VMS and mesothermal lode-gold mineralization in the Abitibi has progressed on both fronts, largely due to renewed research at all scales on both ancient and modern examples.

Based on the best-known geological interpretations for the Val d'Or region in general and more specifically for Bourlamaque and Louvicourt townships, VMS mineralization in the study area was clearly a synvolcanic event. This base-metal sulphide mineralization probably formed as a result of base metals leached from oceanic crust by hydrothermally convected fluids of evolved seawater origin in an intra-continental back-arc basin environment, or alternatively, in an environment with a subducting oceanic ridge.

In contrast, structural, mineralogical and geochronological data indicate that, for the most part, lode-gold mineralization in the study area had a syn- to late-tectonic timing. Based on all available information regarding the structural framework of the

area, the relationship between quartz-gold veining and tectonics, metamorphism and plutonism, and geochemical and geochronological data for this hydrothermal event, mesothermal lode-gold mineralization in the study area is best explained by the mantle degassing-granulitization model. Established from a wide range of geological information, this model suggests that CO₂-rich auriferous fluids resulted from the granulitization of the lower crust caused by the advection of mantle CO₂. These processes, as well as the emplacement of Archean gold mineralization, are thought to be linked to the cratonization of Archean terranes.

During the course of this research project, several questions were raised about various geologic aspects of the Val d'Or district, and it is clear that this information could aid in clarifying the paleovolcanic evolution of the area and understanding VMS and lode-gold mineralization. The following list, which is by no means complete, consists of several recommendations for continued research on different topics that could advance our understanding of the Val d'Or district, its metallogeny, and its economic mineral potential.

Structure

A structural analysis of the terrane east of Val d'Or as far as the Grenville Front should be done to define the boundaries and structural style of the Val d'Or and

Southern domains and to determine whether the Southern domain truly continues into Bourlamaque and Louvicourt townships or whether the dominantly tholeiitic volcanic succession in this area consists of one or more additional domains.

- Despite their relatively small extent and outcrop exposure, the Garden Island, Villebon, Trivio, Piché and Cadillac groups should be re-examined and re-evaluated, probably in light of the recent lithotectonic model of Desrochers et al. (1993).

Geochemistry

- In sectors of the Val d'Or domain where the stratigraphy and structure have been confidently established, a geochemical study should be conducted to attempt to explain the apparent intercalation of calc-alkalic and tholeiitic rocks, and to confirm (or not) the presence of isolated packages of Southern domain rocks within the Val d'Or domain.

VMS Mineralization

- A multi-faceted program consisting of several studies should be planned for the Louvicourt VMS deposit. An in-depth examination of this deposit would broaden our understanding of VMS mineralization in this camp and could possibly refine the Mattabi-type classification of VMS deposits. These studies should describe the morphology and alteration of the deposit, determine the lithological and structural control of mineralization and the relationship of this mineralization to the

neighbouring Louvem deposit. Also, a variety of isotope (O, H, Sr) studies should be done to determine numerous characteristics of the VMS mineralization, such as the temperature of sulphide deposition, the temperature and origin of mineralizing fluids, and the water/rock ratio in the source region.

Geochronology

- With regard to the relative timing (syn-, late-, post-tectonic) given to quartz-carbonate-tourmaline-pyrite vein mineralization, examples of "young", undeformed, gold-bearing quartz veins crosscut by intrusions should be located (if possible) so that the intrusions can be dated by U-Pb zircon geochronology in order to obtain lower age limits of this type of gold mineralization. From these same sites, hydrothermal minerals should be dated to see whether they give ages older than the magmatic zircon date. If younger dates are obtained, then dates already obtained from hydrothermal minerals may have to be re-evaluated as cooling or reset ages.
- Metamorphism in the Val d'Or region is not well constrained, and through further mineralogical and geochronological studies, the duration of this event should be better defined, addressing the question of two or more metamorphic events and examining their temporal relationship to gold mineralization and tectonism.
- Dating could be done on the main body of the Bourlamaque intrusion (as opposed to the Wong et al. (1991) date which comes from the western apophysis of the

intrusion) in order to determine whether the main part of the intrusion has an age more similar to that of the Val d'Or domain rocks than the age from the apophysis. If this age is consistent with the volcanic age, it could show the span of time taken to form the whole Bourlamaque intrusion and would help to define what volume of the pluton could have been involved in the hydrothermal fluid circulation related to VMS formation.

REFERENCES

- ALSAC, C. (1977) Pétrographie et géochimie de formations volcaniques minéralisées de l'Abitibi et de l'Estrie. Ministère des Ressources Naturelles du Québec, Final Report, DPV-519, 93 p, 3 maps.
- ALSAC, C., LAMARCHE, M. and LATULIPPE, M. (1970) Étude des caractères magmatiques des formations volcaniques des régions de Val d'Or et Weedon-Thetford (Canada). Bureau de Recherche Géologique et Minérale (France), Report 70, RME 031, 60 p.
- ALSAC, C. and LATULIPPE, M. (1979) Quelques aspects pétrographiques et géochimiques du volcanisme archéen du Malartic en Abitibi (Province du Québec, Canada). Canadian Journal of Earth Sciences, v.16, p.1041-1059.
- ALSAC, C., LATULIPPE, M. and LAMARCHE, R. (1971) Caractérisation pétrologique et géochimique des formations paléovolcaniques minéralisées d'après l'exemple des régions de Val-d'Or et Weedon-Thetford (Canada). Ministère des Ressources Naturelles du Québec, DP-0096, 42 p.
- ANGLIN, C.D. (1990) Preliminary Sm-Nd isotopic analyses of scheelites from Val d'Or gold deposits, Quebec, *in* Current Research, Part C, Geological Survey of Canada Paper 90-1C, p.255-259.
- ANHAEUSSER, C.R. (1976) The nature and distribution of Archaean gold mineralization in southern Africa. Minerals Science Engineering, v.8, p.46-84.
- ASSAD, J.R. (1958) The geology of the East Sullivan Deposit, Val d'Or, Quebec. Ph.D thesis, McGill University, Montreal, 238 p.
- BABCOCK, R.S., BURMESTER, R.F., ENGBRETSON, D.C. and WARNOCK, A. (1992) A rifted margin origin for the Crescent Basalts and related rocks in the northern coast range volcanic province, Washington and British Columbia. Journal of Geophysical Research, v.97, no.B5, p.6799-6821.
- BABINEAU, J. (1982) Évolution géochimique et pétrologique des séries volcaniques de la région de Cadillac-Malartic, Abitibi. Unpublished Master's thesis, Université de Montréal, Montreal, 112 p.
- BABINEAU, J. (1985) Géologie de la région de la Motte, Abitibi. Ministère de l'Énergie et des Ressources du Québec, ET 84-03, 17 p, 2 maps.

- BARLEY, M.E. (1992) A review of Archean volcanic-hosted massive sulfide and sulfate mineralization in western Australia. *Economic Geology*, v.87, p.855-872.
- BARNES, H.L. (1979) Solubilities of ore minerals, *in* Barnes, H.L., ed., *Geochemistry of Hydrothermal Ore Deposits*, Second Edition. John Wiley and Sons, Toronto, p.404-460.
- BELKABIR, A. (1990) Géologie du gisement filonien d'or Dumont et géochimie de ses épontes altérées, Val d'Or, Québec. M.Sc.A. thesis, École Polytechnique, Montreal, 150 p.
- BELL, K., ANGLIN, C.D. and FRANKLIN, J.M. (1989) Sm-Nd and Rb-Sr isotope systematics of scheelite: Possible implications for the age and genesis of vein-hosted gold deposits. *Geology*, v.17, p.500-504.
- BELL, L.V. and BELL, A.M. (1931) Région des sources de la rivière Bell, comté Abitibi. Rapport Annuel du Ministère des Mines du Québec, Part B, p.60-144.
- BELLEMARE, Y. and GERMAIN, M. (1987) Catalogue des gîtes minéraux du Québec. Ministère de l'Énergie et des Ressources du Québec, DV 87-23, 279 p.
- BENN, K., MILES, W. and GILLET, J. (1992b) Structural framework of the western Pontiac subprovince: an integrated geological and geophysical approach. Lithoprobe Abitibi-Grenville Project, Workshop IV, 1992, December 15-16, 1992, École Polytechnique, Program.
- BENN, K., SAWYER, E.W. and BOUCHEZ, J.-L. (1992a) Orogen parallel and transverse shearing in the Opatica belt, Quebec: implications for the structure of the Abitibi Subprovince. *Canadian Journal of Earth Sciences*, v.29, p.2429-2444.
- BICKLE, M.J., BETTENAY, L.F., BARLEY, M.E., CHAPMAN, H.J., GROVES, D.I., CAMPBELL, I.H. and DE LAETER, J.R. (1983) A 3500 Ma plutonic and volcanic calc-alkaline province in the Archean East Pilbara block. *Contributions to Mineralogy and Petrology*, v.84, p.25-35.
- BINNS, R.A. and SCOTT, S.D. (1993) Actively-forming polymetallic sulfide deposits associated with felsic volcanic rocks in the eastern Manus back-arc basin, Papua New Guinea. *Economic Geology*, v.88, p.2226-2236.
- BINNS, R.A., SCOTT, S.D., BOGDANOV, YU.A., LISITSIN, A.P., GORDEEV, V.V., GURVICH, E.G., FINLAYSON, E.J., BOYD, T., DOTTER, L.E., WHELLER, G.E. and MURAVYEV, K.G. (1993) Hydrothermal oxide and gold-

rich sulfate deposits of Franklin Seamount, western Woodlark Basin, Papua New Guinea. *Economic Geology*, v.88, p.2122-2153.

BOHLEN, S.R. (1987) Pressure-temperature-time paths and a tectonic model for the evolution of granulites. *Journal of Geology*, v.95, p.617-632.

BOUCHARD, M.-F. (1979) Région de Cadillac-Malartic. Ministère de l'Énergie et des Ressources du Québec, DPV-683, 10 p.

BOUCHARD, M.-F. (1980) Région de Cadillac-Malartic. Ministère de l'Énergie et des Ressources du Québec, DPV-791, 10 p, 1 map.

BOURNE, J. and DANIS, D. (1987) A proposed model for the formation of reversely zoned plutons based on a study of the Lacorne Complex, Superior Province, Quebec. *Canadian Journal of Earth Sciences*, v.24, p.2506-2520.

BROWN, A.C., CHOUTEAU, M., HUBERT, C., LUDDEN, J.N., MARESCHAL, M., CORRIVEAUX, L. and JENKINS, C.L. (1990) Predictive "downstream" models for the generation, circulation and focussing of auriferous fluids at deep levels in the Abitibi crust, *in*, Robert, F., Sheahan, P.A. and Green, S.B., eds., *Greenstone Gold and Crustal Evolution*, NUNA Conference Volume, Geological Association of Canada Mineral Deposits Division, p.136-137.

BUBAR, D.S., GILL, J.W., MANNARD, G.N. and STOCKFORD, H.R. (1989) La nouvelle découverte de Ressources Aur à Val-d'Or: Un important dépôt de sulfure massif dans un camp minier sous-estimé pour son potentiel en métaux de base. Ministère de l'Énergie et des Ressources, DV-89-07, p.36-37.

BUCHAN, K.L., MORTENSEN, J.K. and CARD, K.D. (1993) Northeast-trending Early Proterozoic dykes of southern Superior Province: multiple episodes of emplacement recognized from integrated paleomagnetism and U-Pb geochronology. *Canadian Journal of Earth Sciences*, v.30, p.1286-1296.

BURROWS, D.R. and SPOONER, E.T.C. (1987) Generation of a magmatic H₂O-CO₂ fluid enriched in Mo, Au and W within an Archean sodic granodiorite stock, Mink Lake, northwestern Ontario. *Economic Geology*, v.82, p.1931-1957.

BURROWS, D.R. and SPOONER, E.T.C. (1989) Relationships between Archean gold quartz vein-shear zone mineralization and igneous intrusions in the Val d'Or and Timmins areas, Abitibi Subprovince, Canada, *in* Keays, R.R., Ramsy, W.R.H. and Groves, D.I., eds., *The Geology of Gold Deposits: The Perspective in 1988*, *Economic Geology Monograph 6*. Economic Geology Publishing Company, El Paso, p.424-444.

- BURROWS, D.R., WOOD, P.C. and SPOONER, E.T.C. (1986) Carbon isotope evidence for a magmatic origin for Archean gold-quartz vein ore deposits. *Nature*, v.321, p.851-854.
- CAMERON, E. (1988) Archean gold: Relation to granulite formation and redox zoning in the crust. *Geology*, v.16, p.109-112.
- CAMERON, E.M. and CARRIGAN, W.J. (1987) Oxygen fugacity of Archean felsic magmas: relationship to gold mineralization, *in* Current Research, Part A, Geological Survey of Canada, Paper 87-1A, p.281-198, p.281-298.
- CAMERON, E.M. and HATTORI, K. (1987) Archean gold mineralization and oxidized hydrothermal fluids. *Economic Geology*, v.82, p.1177-1191.
- CAMPBELL, I.H., FRANKLIN, J.M., GORTON, M.P., HART, T.R. and SCOTT, S.D. (1981) The role of subvolcanic sills in the generation of massive sulfide deposits. *Economic Geology*, v.76, p.2248-2253.
- CAMPIGLIO, C. (1977) Batholite de Bourlamaque. Ministère des Richesses Naturelles du Québec, E.S. 26, 211 p.
- CAMPIGLIO, C. and DARLING, R. (1976) The geochemistry of the Archean Boulamaque batholith, Abitibi, Quebec. *Canadian Journal of Earth Sciences*, v.13, p.972-986.
- CAR, D. and AYRES, L.D. (1991) A thick dacitic debris flow sequence, Lake of the Woods greenstone terrane, central Canada: resedimented products of Archean vulcanian, plinian and dome-building eruptions. *Precambrian Research*, v.50, p.239-260.
- CARD, K.D. (1990) A review of the Superior Province of the Canadian Shield, a product of Archean accretion. *Precambrian Research*, v.48, p.99-156.
- CARD, K.D. and CIESIELSKI, A. (1986) DNAG#1. Subdivisions of the Superior Province of the Canadian Shield. *Geoscience Canada*, v.13, no.1, p.5-13.
- CAS, R.A.F. (1992) Submarine volcanism: Eruption styles, products, and relevance to understanding the host-rock successions to volcanic-hosted massive sulfide deposits. *Economic Geology*, v.87, p.511-541.
- CATHLES, L.M. (1981) Fluid flow and genesis of hydrothermal ore deposits, *in*, Skinner, B.J., ed., *Economic Geology 75th Anniversary Volume*. Economic Geology Publishing Company, El Paso, p.424-457.

- CATHLES, L.M. (1983) An analysis of the hydrothermal system responsible for massive sulfide deposition in the Hokuroku Basin of Japan *in* Ohmoto, H. and Skinner, B.J., eds., Kuroko and Related Volcanogenic Massive Sulphide Deposits, Economic Geology Monograph 5. Economic Geology Publishing Company, El Paso, p.439-487.
- CATHLES, L.M. (1986) The geologic solubility of gold from 200-350°C, and its implications for gold-base metal ratios in vein and stratiform deposits. Canadian Institute of Mining and Metallurgy, Special Volume 38, p.187-211.
- CATHLES, L.M. (1991) The importance of the 350°C isotherm in ore-forming hydrothermal systems. Geological Society of America, Abstracts with Programs, p.A21.
- CATHLES, L.M. (1983) Kuroko-type massive sulfide deposits of Japan: Products of an Aborted Island-Arc Rift, *in* Ohmoto, H. and Skinner, B.J., eds., Kuroko and Related Volcanogenic Massive Sulphide Deposits, Economic Geology Monograph 5. Economic Geology Publishing Company, El Paso, p.96-114.
- CHARTRAND, F. (1991) Geological setting of volcanogenic massive sulfide deposits in the Central Pyroclastic Belt, Val d'Or, *in* Chartrand, F., ed., Geology and Gold, Rare Element, and Base Metal Mineralization of the Val d'Or Area, Quebec, Society of Economic Geologists, Guidebook Series, v.9, p.75-89.
- CHARTRAND, F. and CATTALANI, S. (1990) Massive sulfide deposits in northwestern Quebec, *in* Rive, M., Verpaelst, P., Gagnon, Y., Lulin, J.-M., Riverin, G. and Simard, A., eds., The Northwestern Quebec Polymetallic Belt: A Summary of 60 Years of Mining Exploration, Canadian Institute of Mining and Metallurgy, Special Volume 43, p.77-91.
- CHARTRAND, F. and MOORHEAD, J. (1992) Synthèse géologique de Val d'Or. Ministère de l'Énergie et des Ressources du Québec, Rapport d'activité, DV 92-02, p.66-67.
- CHAYES, F. (1970) On the occurrence of corundum in the norms of the common volcanic rocks. Carnegie Institute of Washington Yearbook 68, p.179-182.
- CHOWN, E.H., DAIGNEAULT, R. and MUELLER, W. (1992) Tectonic evolution of the Northern Volcanic Zone, Abitibi belt, Quebec. Canadian Journal of Earth Sciences, v.29, p.2211-2225.

- CLAOUÉ-LONG, J.C., KING, R.W. and KERRICH, R. (1990) Archaean hydrothermal zircon in the Abitibi greenstone belt: Constraints on the timing of gold mineralisation. *Earth and Planetary Science Letters*, v.98, p.109-128.
- CLAOUÉ-LONG, J.C., KING, R.W. and KERRICH, R. (1992) Reply to comment by F. Corfu and D.W. Davis on "Archaean hydrothermal zircon in the Abitibi greenstone belt: constraints on the timing of gold mineralisation". *Earth and Planetary Science Letters*, v.109, p.601-609.
- CLIFFORD, B.A. (1987) Volcanic-sedimentary facies associations hosting the volcanogenic massive sulphide mineralisation at Gold Grove, Western Australia. *Pacific Rim Congress 87 Proceedings Volume, The Australasian Institute of Mining and Metallurgy*, p.871-875.
- COLVINE, A.C., FYON, J.A., HEATHER, K.B., MARMONT, S., SMITH, P.M. and TROOP, D.G. (1988) Archean lode gold deposits in Ontario. *Ontario Geological Survey, Miscellaneous Paper 139*, 136p.
- COMLINE, S.R. (1979) A study of the Piché Group and vein systems at Darius mine, Cadillac, Québec. M.Sc. thesis, University of Western Ontario, London, 141p.
- CONDIE, K.C. (1976) Trace-element geochemistry of Archean greenstone belts. *Earth Science Reviews*, v.12, p.393-417.
- CONEY, P.J. (1989) Structural aspects of suspect terranes and accretionary tectonics in western North America. *Journal of Structural Geology*, v.11, p.107-125.
- CONNOLLY, J.A.D. and THOMPSON, A.B. (1989) Fluid and enthalpy production during regional metamorphism. *Contributions to Mineralogy and Petrology*, v.102, p. 347-366.
- CORFU, F. (1987) Inverse age stratification in the Archaean crust of the Superior Province: Evidence for infra- and subcrustal accretion from high resolution U-Pb zircon and monazite ages. *Precambrian Research*, v.36, p.259-275.
- CORFU, F. (1993) The evolution of the southern Abitibi greenstone belt in light of precise U-Pb geochronology. *Economic Geology*, v.88, p.1323-1340.
- CORFU, F. and DAVIS, D.W. (1991) Comment on "Archean hydrothermal zircon in the Abitibi greenstone belt constraints on the timing of gold mineralization" by J.C. Clauoué-Long, R.W. King and R. Kerrich. *Earth and Planetary Science Letters*, v.104, p. 545-552.

- CORFU, F., JACKSON, S.L. and SUTCLIFFE, R.H. (1991) U-Pb ages and tectonic significance of late Archean alkalic magmatism and nonmarine sedimentation: Timiskaming Group, southern Abitibi belt, Ontario. *Canadian Journal of Earth Sciences*, v.28, p.489-503.
- CORFU, F., KROGH, T.E., KWOK, Y.Y. and JENSEN, L.S. (1989) U-Pb zircon geochronology in the southwestern Abitibi greenstone belt, Superior Province. *Canadian Journal of Earth Sciences*, v.26, p.1747-1763.
- CORFU, F. and STOTT, G.M. (1993) U-Pb geochronology of the central Uchi Subprovince, Superior Province. *Canadian Journal of Earth Sciences*, v.30, p.1179-1196.
- COUTURE, J.-F. (1991) Carte géologique des gîtes métallifères des districts de Rouyn-Noranda et de Val-d'Or. Ministère de l'Énergie et des Ressources, Map No. 2109 of report DV 90-11.
- CRAWFORD, A.J., BECCALUVA, L. and SERRI, G. (1981) Tectono-magmatic evolution of the west Philippine-Mariana region and the origin of boninites. *Earth and Planetary Science Letters*, v.54, p.346-356.
- DAHL, N., MCNAUGHTON, N.J. and GROVES, D.I. (1987) A lead-isotope study of sulphides associated with gold mineralization in selected deposits from the Archean Eastern Goldfield of Western Australia, *in* Ho, S.E. and Groves, D.I., eds., *Recent Advances in Understanding Precambrian Gold Deposits*, Geology Department and University Extension, University of Western Australia, Publication No. 11, 189-202.
- DAIGNEAULT, R., PERRAULT, G. and BÉDARD, P. (1983) Géologie et géochimie de la mine Lamaque, Val d'Or, Québec. *Canadian Institute of Mining and Metallurgy*, v.76, p.111-127.
- DAVIS, D.W. (1991) Age constraints on deposition and provenance of Archean sediments in the southern Abitibi and Pontiac subprovinces from U-Pb analyses of detrital zircons. *Geological Association of Canada—Mineralogical Association of Canada, Programs with Abstracts*, v.16, p.A29.
- DEBICHE, M.G., COX, A. and ENGBRETSON, D. (1987) The motion of allochthonous terranes across the North Pacific Basin. *Geological Society of America Special Paper* 207, 49 p.

- DEINES, P. and GOLD, D.P. (1973) The isotopic composition of carbonatite and kimberlite carbonates and their bearing on the isotopic composition of deep-seated carbon. *Geochimica et Cosmochimica Acta*, v.37, p.1709-1733.
- DESCARREAUX, J. (1972) *Géochimie des roches volcaniques de l'Abitibi*. Ph.D. thesis, Laval University, Ste-Foy, 283 p.
- DESCARREAUX, J. (1973) A petrochemical study of the Abitibi volcanic belt and its bearing on the occurrences of massive sulphide ores. *Canadian Institute of Mining and Metallurgy Bulletin* for February, p.61-69.
- DESROCHERS, J.-P. (1994) Ph.D. thesis, Université de Montréal, Montreal (in preparation).
- DESROCHERS, J.-P. and HUBERT, C. (1991) *Géologie de la région du Lac de Montigny*. Ministère de l'Énergie et des Ressources du Québec, Rapport d'activité, DV 91-25, p.63.
- DESROCHERS, J.-P., HUBERT, C., LUDDEN, J.N. and PILOTE, P. (1993) Accretion of Archean oceanic plateau fragments in the Abitibi greenstone belt, Canada. *Geology*, v.21, p.451-454.
- DEVANEY, J.R. and WILLIAMS, H.R. (1989) Evolution of an Archean subprovince boundary: a sedimentological and structural study of part of the Wabigoon-Quetico boundary in northern Ontario. *Canadian Journal of Earth Sciences*, v.26, p.1013-1026.
- DIMROTH, E., COUSINEAU, P., LEDUC, M. AND SANSCHAGRIN, Y. (1978) Structure and organization of Archean subaqueous basalt flows, Rouyn-Noranda area, Quebec, Canada. *Canadian Journal of Earth Sciences*, v.15, p.902-918.
- DIMROTH, E., IMREH, L., ROCHELEAU, M. and GOULET, N. (1982) Evolution of the south-central part of the Archean Abitibi Belt, Quebec. Part I: Stratigraphy and paleogeographic model. *Canadian Journal of Earth Sciences*, v.19, p.1729-1758.
- DIMROTH, E., IMREH, L., ROCHELEAU, M. and GOULET, N. (1983a) Evolution of the south-central segment of the Archean Abitibi Belt, Quebec. Part II: Tectonic evolution and geomechanical model. *Canadian Journal of Earth Sciences*, v.20, p.1355-1373.
- DIMROTH, E., IMREH, L., ROCHELEAU, M. and GOULET, N. (1983b) Evolution of the south-central segment of the Archean Abitibi Belt, Quebec. Part III:

Plutonic and metamorphic evolution and geotectonic model. *Canadian Journal of Earth Sciences*, v.20, p.1374-1388.

DRUMMOND, S.E. and OHMOTO, H. (1985) Chemical evolution and mineral deposition in boiling hydrothermal systems. *Economic Geology*, v.80, p.126-147.

DUDÁS, F.Ö. (1983) The effect of volatile content on the vesiculation of submarine basalts, *in* Ohmoto, H. and Skinner, B.J., eds., *Kuroko and Related Volcanogenic Massive Sulphide Deposits*, Economic Geology Monograph 5. Economic Geology Publishing Company, El Paso, p.134-141.

DUSSAULT, C. (1992) 1991 Rapports des géologues résidents sur l'activité minière régionale. Ministère de l'Énergie et des Ressources du Québec, DV 92-01, p. 38.

EISENLOHR, B.N., GROVES, D. and PARTINGTON, G.A. (1989) Crustal-scale shear zones and their significance to Archaean gold mineralization in Western Australia. *Mineralium Deposita*, v.24, p.1-8.

ELDER, J.W. (1977) Model of hydrothermal ore genesis, *in* *Volcanic Processes in Ore Genesis*, Institute of Mining and Metallurgy and Geological Society of London, Special Publication No. 7, p.4-13.

ENGBRETSON, D.C., COX, A. and GORDON, R.G. (1985) Relative motions between oceanic and continental plates in the Pacific Basin. Geological Society of America, Special Paper 206, 59p.

ETHERIDGE, M.A., WALL, V.J., COX, S.F. and VERNON, R.H. (1984) High fluid pressures during regional metamorphism and deformation - implications for mass transport and deformation mechanisms. *Journal of Geophysical Research*, v.89, p.4344-4358.

ETHERIDGE, M.A., WALL, V.J. and VERNON, R.H. (1983) The role of the fluid phase during regional metamorphism and deformation. *Journal of Metamorphic Geology*, v.1, p.205-226.

FENG, R. and KERRICH, R. (1990) Geobarometry, differential block movements, and crustal structure of the southwestern Abitibi greenstone belt, Canada. *Geology*, v.18, p.870-873.

- FENG, R. and KERRICH, R. (1991) Single zircon age constraints on the tectonic juxtaposition of the Archean Abitibi greenstone belt and Pontiac subprovince, Quebec, Canada. *Geochimica et Cosmochimica Acta*, v.55, p.3437-3441.
- FENG, R. and KERRICH, R. (1992) Geochemical evolution of granitoids from the Archean Abitibi Southern volcanic zone and the Pontiac subprovince, Superior Province, Canada: Implications for tectonic history and source regions. *Chemical Geology*, v.98, p.23-70.
- FENG, R., KERRICH, R., MCBRIDE, S. and FARRAR, E. (1992) $^{40}\text{Ar}/^{39}\text{Ar}$ age constraints on the thermal history of the Archean Abitibi greenstone belt and the Pontiac Subprovince: Implications for terrane collision, differential uplift, and overprinting of gold deposits. *Canadian Journal of Earth Sciences*, v.29, p.1389-1441.
- FINLOW-BATES, T. and STUMPFL, E.F. (1981) The behaviour of so-called immobile elements in hydrothermally altered rocks associated with volcanogenic submarine-exhalative ore deposits. *Mineralium Deposita*, v.16, p.319-328.
- FISHER, N.J. and FOSTER, R.P. (1991) Deformation, fluid-flow and gold precipitation in iron-formation, Zimbabwe, *in* Ladeira, E.A., ed., *Proceedings of Brazil Gold '91*, p.367-373.
- FISHER, R.V. (1984) Submarine volcanoclastic rocks, *in* Kokelaar, B.P. and Howells, M.F., eds., *Marginal Basin Geology - Volcanic and Associated Sedimentary and Tectonic Processes in Modern and Ancient Marginal Basins*. The Geological Society, p.5-27.
- FOUQUET, Y., VON STACKELBERG, U., CHARLOU, J.L., DONVAL, J.P., ERZINGER, J., FOUCHER, J.P., HERZIG, P., MÜHE, R., SOAKAI, S., M., WIEDICKE, M. and WHITECHURCH, H. (1991) Hydrothermal activity and metallogenesis in the Lau back-arc basin. *Nature*, v.349, p.778-781.
- FOUQUET, Y., VON STACKELBERG, U., CHARLOU, J.L., ERZINGER, J., HERZIG, P.M., MÜHE, R. and WIEDICKE, M. (1993) Metallogenesis in back-arc environments: The Lau basin example. *Economic Geology*, v.88, p.2154-2181.
- FRANKLIN, J.M. (1986) Volcanic-associated massive sulphide deposits - an update, *in* Andrea, C.J., Crowe, R.W.A., Finlay, S., Pennell, W.M. and Pyne, J.G., eds., *Geology and Genesis of Mineral Deposits in Ireland*. Dublin, Irish Association of Economic Geology, Special Publication 4, p.49-69.

- FRANKLIN, J.M. (1990) Volcanic-associated massive sulphide deposits, *in* Gold and Base Metal Mineralization in the Abitibi Subprovince, Canada, with Emphasis on the Quebec Segment. Short Course Notes, Compiled by S.E. Ho, F. Robert and D.I. Groves, University of Western Australia, Publication No. 24, p.211-241.
- FRANKLIN, J.M., GIBB, W. and POULSEN, K.H. (1977) Archean metallogeny and stratigraphy of the south Sturgeon Lake area. Institute on Lake Superior Geology, 23rd Annual Meeting, Thunder Bay, Ontario, Guidebook, 73 p.
- FRANKLIN, J.M., KASARDA, J. and POULSEN, K.H. (1975) Petrology and chemistry of the alteration zone of the Mattabi massive sulfide deposit. *Economic Geology*, v.70, p.63-79.
- FRANKLIN, J.M., LYDON, J.W. and SANGSTER, D.F. (1981) Volcanic-associated massive sulfide deposits, *in* Skinner, B.J., ed., *Economic Geology 75th Anniversary Volume*. Economic Geology Publishing Company, El Paso, p.485-627.
- FRANKLIN, J.M., ROSCOE, S.M., LOVERIDGE, W.D. and SANGSTER, D.F. (1983) Lead isotope studies in Superior and Southern provinces. *Geological Survey of Canada, Bulletin*, v.351, 60 p.
- FRANKLIN, J.M. and THORPE, R.I. (1982) Comparative metallogeny of the Superior, Slave and Churchill provinces, *in* Hutchinson, R.W., Spence, C.D. and Franklin, J.M., eds., *Precambrian Sulphide Deposits*, Geological Association of Canada, Special Paper 25, p.3-90.
- FRASER, R.J. (1993) The Lac Troilus gold-copper deposit, northwestern Quebec: A possible Archean porphyry system. *Economic Geology*, v.88, p.1685-1699.
- FRIPP, R.E.P. (1976a) Gold metallogeny in the Archaean of Rhodesia, *in* Windley, B.F., ed., *The Early History of the Earth*. John Wiley and Sons, Toronto, p.455-466.
- FRIPP, R.E.P. (1976b) Stratabound gold deposits in Archean banded iron-formation, Rhodesia. *Economic Geology*, v.71, p.58-75.
- FROST, B.R. and FROST, C.D. (1987) CO₂, melts and granulite metamorphism. *Nature*, v.327, p.503-506.
- FRYER, B.J., KERRICH, R., HUTCHINSON, R.W., PEIRCE, M.G. and ROGERS, D.S. (1979) Archaean precious-metal hydrothermal systems, Dome mine, Abitibi greenstone belt. I. *Canadian Journal of Earth Sciences*, v.16, p.421-439.

- FYON, J.A., CROCKET, J.H. and SCHWARCZ, H.P. (1983) The Carshaw and Malga iron formation-hosted gold deposits of the Timmins area, *in* Colvine, A.C., ed., *Gold Geology of Gold in Ontario*, Ontario Geological Survey, Miscellaneous Paper 110, p.98-110.
- FYON, J.A., TROOP, D.G., MARMONT, S. and MACDONALD, A.J. (1989) Introduction of old into Archean crust, Superior Province, Ontario - coupling between mantle-initiated magmatism and lower crustal thermal maturation, *in* Keays, R.R., Ramsy, W.R.H. and Groves, D.I., eds., *The Geology of Gold Deposits: The Perspective in 1988*, Economic Geology Monograph 6. Economic Geology Publishing Company, El Paso, p.479-490.
- GAÁL, G. and ISOHANNI, M. (1979) Characteristics of igneous intrusions and various wall rocks in some Precambrian porphyry copper-molybdenum deposits in Pohjinaama, Finlan. *Economic Geology*, v.74, p.1198-1210.
- GALLEY, A.G. and FRANKLIN, J.M. (1991) Semi-conformable hydrothermal alteration zones as a guide to VMS exploration. Geological Association of Canada—Mineralogical Association of Canada, Program with Abstracts, v.16, p.A41.
- GAUCHER, E. and ASSOCIATES (1982) Carte de compilation géoscientifique, 1 : 10,000 map. Ministère de l'Énergie et des Ressources du Québec, 32 C/4-0304.
- GAUDREAU, R., LACOSTE, P. and ROCHELEAU, M. (1986) Géologie et gîtologie du secteur de Louvicourt-Vauquelin, Abitibi. Ministère de l'Énergie et des Ressources, MB 86-67, 151 p., 1 map.
- GEIS, W.T., COOK F.A., GREEN, A.G., MILKEREIT, B., PERCIVAL, J.A. and WEST, G.F. (1990) Thin thrust sheet formation of the Kapuskasing structural zone revealed by Lithoprobe seismic reflection data. *Geology*, v.18, p.513-516.
- GÉLINAS, L., BROOKS, PERRAULT, G., CARIGNAN, J., TRUDEL, P. and GRASSO, F. (1977) Chemo-stratigraphic divisions within the Abitibi volcanic belt, Rouyn-Noranda district, Quebec, *in* W.R.A. Baragar, L.C. Coleman and J.H. Hall, eds., *Volcanic Regimes in Canada*, Geological Association of Canada, Special Paper 16, p.265-295.
- GÉLINAS, L., MELLINGER, M. and TRUDEL, P. (1982) Archean mafic metavolcanic from the Rouyn-Noranda district, Abitibi Greenstone Belt, Quebec. 1. Mobility of the major elements. *Canadian Journal of Earth Sciences*, v.19, p.2258-2275.

- GÉLINAS, L., TRUDEL, P. and HUBERT, C. (1984) Chemostratigraphic division of the Blake River Group, Rouyn-Noranda area, Abitibi, Quebec. *Canadian Journal of Earth Sciences*, v.21, p.220-231.
- GEOLOGICAL SURVEY OF CANADA (1981) Experimental colour compilation (high resolution aeromagnetic vertical gradient), Val d'Or, Abitibi county, Quebec. Map C40,074 G, scale 1:50,000.
- GIBSON, H.L., LICHTBLAU, A.P., COMBA, C.D.A. and WATKINSON, D.H. (1986) Subaqueous rhyolite flows of the central mine sequence, Noranda, Quebec. Geological Association of Canada - Mineralogical Association of Canada, Program with Abstracts, v.11, p.72.
- GIBSON, H.L., WATKINSON, D.H. and COMBA, C.D.A. (1983) Silicification: hydrothermal alteration in an Archean geothermal system within the Amulet Rhyolite Formation, Noranda, Quebec. *Economic Geology*, v.78, p.954-971.
- GILL, J.B. (1982) *Orogenic Andesites and Plate Tectonics*, 390 p.
- GIRAULT, M. (1986) *Pétrographie et géochimie de volcanites archéennes polymétamorphiques - reconstitution de l'histoire pétrologique (zone minière Manitou-Louvem, Val d'Or, Québec)*. Ph.D. thesis, Université scientifique, technique et médicale de Grenoble, Grenoble, France, 168 p.
- GLADNEY, E.S. and ROELANDTS, I. (1990) 1988 compilation of elemental concentration data for CCRMP reference rocks samples SY-2, SY-3 and MRG-1. *Geostandards Newsletter*, v.14, no.3, p.373-458.
- GOLDFARB, R.J., LEACH, D.L., PICKTHORN, W.J. and PATERSON (1988) Origin of lode-gold deposits of the Juneau gold belt, southeastern Alaska. *Geology*, v.16, p.440-443.
- GOLDIE, R., KOTILA, B. and SEWARD, D. (1979) The Don Rouyn mine: An Archean porphyry copper deposit near Noranda, Quebec. *Economic Geology*, v. 74, p.1680-1684.
- GOLDING, S.D., GROVES, D.I., MCNAUGHTON, N.J., BARLEY, M.E. and ROCK, N.M.S. (1987) Carbon isotopic composition of carbonates from contrasting alteration styles in supracrustal rocks of the Norseman-Wiluna belt, Yilgarn block, Western Australia: their significance to the source of Archaean auriferous fluids, in Ho, S.E. and Groves, D.I., eds., *Recent Advances in Understanding Precambrian Gold Deposits*, Geology Department and University Extension, The University of Western Australia, Publication No. 11, p.215-238.

- GOLDING, S.D. and WILSON, A.F. (1987) Oxygen and hydrogen isotope relationships in Archaean gold deposits of the Eastern Goldfields Province, Western Australia: constraints on the source of Archaean gold-bearing fluids, *in* Ho, S.E. and Groves, D.I., eds., *Recent Advances in Understanding Precambrian Gold Deposits*, University of Western Australia, Publication No. 11, p.203-213.
- GOODWIN, A.M. (1973) Archean iron-formations and tectonic basins of the Canadian Shield. *Economic Geology*, v.68, p.915-933.
- GORMAN, B.E. (1986) The Bousquet-Cadillac district, *in* Hubert, C and Robert, F., eds., *Structure and Gold, Rouyn to Val d'Or, Québec, Field Trip 14: Guidebook*, Geological Association of Canada — Mineralogical Association of Canada, p.43-70.
- GRANT, M. (1986) Étude du métamorphisme et de la distribution verticale des teneurs en Au, As et Sb à la mine Sigma, Val d'Or, Québec. M.Sc.A thesis, École Polytechnique, Montreal, 121 p.
- GREEN, A.G., MILKEREIT, B., MAYRAND, L.J., LUDDEN, J.N., HUBERT, C., JACKSON, S.L., SUTCLIFFE, R.H., WEST, G.F., VERPAELST, P. and SIMARD, A. (1990) Deep structure of an Archaean greenstone terrane. *Nature*, v.344, p.327-330.
- GRIFFIS, A.T. (1979) An Archean "porphyry-type" disseminated copper deposit, Timmins, Ontario — A discussion. *Economic Geology*, v.74, p.695-696.
- GROVES, D.A. (1984) Stratigraphy, lithology, and hydrothermal alteration of volcanic rocks beneath the Mattabi massive sulfide deposit, Sturgeon Lake, Ontario. M.Sc. thesis, University of Minnesota-Duluth, 115 p.
- GROVES, D.I., BARLEY, M.E., BARNICOAT, A.C., CASSIDY, K.F., FARE, R.J., HAGEMANN, S.G., HO, S.E., HRONSKY, J.M.A., MIKUCKI, E.J., MUELLER, A.G., MCNAUGHTON, N.J., PERRING, C.S., RIDLEY, J.R. and VEARNCOMBE, J.R. (1992) Sub-greenschist- to granulite-hosted Archaean lode-gold deposits of the Yilgarn craton: a depositional continuum from deep-sourced hydrothermal fluids in crustal-scale plumbing systems, *in* Glover, J.E. and Ho, S.E., eds., *The Archaean: Terrains, Processes and Metallogeny*. Geology Department and University Extension, The University of Western Australia, Publication No. 22, p.325-337.
- GROVES, D.I., BARLEY, M.E. and HO, S.E. (1989) Nature, genesis, and tectonic setting of mesothermal gold mineralization in the Yilgarn block, Western Australia, *in* Keays, R.R., Ramsay, W.R.H. and Groves, D.I., eds., *The*

Geology of Gold Deposits: The Perspective in 1988, Economic Geology Monograph 6, Economic Geology Publishing Company, El Paso, p.71-85.

GROVES, D.I., HO, S.E., MCNAUGHTON, N.J., MUELLE, A.G., PERRING, C.S., ROCK, N.M.S., and SKWARNECKI, M.S. (1988) Genetic models for Archaean lode-gold deposits in Western Australia, *in* Ho, S.E. and Groves, D.I., eds., *Advances in Understanding Precambrian Gold Deposits, Volume II*, Geology Department and University Extension, The University of Western Australia, Publication No. 12, p.1-22.

GROVES, D.A., MORTON, R.L. and FRANKLIN, J.M. (1984) Stratigraphy of the footwall volcanic rocks at the Mattabi massive sulfide deposit, Sturgeon Lake, Ontario. Geological Association of Canada - Mineralogical Association of Canada, Program with Abstracts, v.9, p.69.

GROVES, D.I. and PHILLIPS, N. (1987) The genesis and tectonic control on Archean gold deposits of the western Australian shield -a metamorphic replacement model. *Ore Geology Reviews*, v.2, p.287-322.

GROVES, D.I., PHILLIPS, G.N., FALCONER, L.J., HOUSTOUN, HO, S.E., BROWNING, P., DAHL, N. and MCNAUGHTON, N.J. (1987) Evidence of an epigenetic origin for BIF-hosted gold deposits in greenstone belts of the Yilgarn block, Western Australia, *in* Ho, S.E. and Groves, D.I., eds., *Recent Advances in Understanding Precambrian Gold Deposits*. University of Western Australia, Publication 11, p.167-179.

GROVES, D.I., PHILLIPS, G.N., HO, S.E., HENDERSON, C.A., CLARK, M.E. and WOAD, G.M. (1984) Controls on distribution of Archaean hydrothermal gold deposits in Western Australia, *in* R.P. Foster, ed., *Gold '82: The Geology, Geochemistry and Genesis of Gold Deposits*. Balkema, Rotterdam, p.689-712.

GUHA, J. (1984) Hydrothermal systems and correlations of mineral deposits in the Chibougamau mining district — An overview, *in* Guha, J. and Chown, E.H., eds., *Chibougamau — Stratigraphy and Mineralization*, Canadian Institute of Mining and Metallurgy, Special Volume 34, p.517-534.

GUHA, J., DUBÉ, B., PILOTE, P., CHOWN, E.H., ARCHAMBAULT, G., AND BOUCHARD, G. (1988) Gold mineralization patterns in relation to the lithologic and tectonic evolution of the Chibougamau mining district, Quebec, Canada. *Mineralium Deposita*, v.23, p.293-298.

- GUHA, J., LU, H-Z., DUBÉ, B., ROBERT, F. and GAGNON, M. (1991) Fluid characteristics of vein and altered wall rock in Archean mesothermal gold deposits. *Economic Geology*, v.86, p.667-684.
- GUNNING, H.C. (1937) Cadillac area, Quebec. Geological Survey of Canada, Memoir 206, 80 p.
- GUNNING, H.C. and AMBROSE, J.W. (1940) Malartic area, Quebec. Geological Survey of Canada, Memoir 222, 162 p.
- HAAS, J.L. (1971) The effect of salinity on the maximum thermal gradient of a hydrothermal system at hydrostatic pressure. *Economic Geology*, v.66, p.940-946.
- HALBACH, P., NAKAMURA, KO-ICHI., WAHSNER, M., LANGE, J., SAKAI, H., KÄSELITZ, HANSEN, R.-D., YAMANO, M., POST, J., PRAUSE, B., SEIFERT, R., MICHAELIS, W., TEICHMANN, F., KINOSHITA, M., MÄRTEN, A., ISHIBASHI, J., CZERWINSKI, S. and BLUM, N. (1989) Probable modern analogue of Kuroko-type massive sulphide deposits in the Okinawa Trough back-arc basin. *Nature*, v.338, p.496-499.
- HALBACH, P., PRACEJUS, B. and MÄRTEN, A. (1993) Geology and mineralogy of massive sulfide ores from the central Okinawa trough, Japan. *Economic Geology*, v.88, p.2210-2225.
- HAMILTON, W.B. (1988) Plate tectonics and island arcs. *Geological Society of America Bulletin*, v.100, p.1503-1527.
- HANES, J.A., ARCHIBALD, D.A., HODGSON, C.J. and ROBERT, F. (1989) Preliminary $^{40}\text{Ar}/^{39}\text{Ar}$ geochronology and timing of Archean gold mineralization at the Sigma Mine, Val d'Or, Quebec, *in* Current Research, Part C, Geological Survey of Canada, Paper 89-1C, p.135-142.
- HANES, J.A., ARCHIBALD, D.A., HODGSON, C.J. and ROBERT, F. (1992) Dating of Archean auriferous quartz vein deposits in the Abitibi greenstone belt, Canada: $^{40}\text{Ar}/^{39}\text{Ar}$ evidence for a 70- to 100-m.y.-time gap between plutonism-metamorphism and mineralization. *Economic Geology*, v.87, p.1849-1861.
- HANNINGTON, M., BLEEKER, W. and KJARSGAARD, I.M. (1994) Sulphide mineralogy and geochemistry of the Kidd Creek deposit, Ontario. Geological Survey of Canada, Minerals Colloquium, January 17-19, 1994, Ottawa, p.19 (oral presentation).

- HANNINGTON, M.D., PETER, J.M., SCOTT, S.D. (1986) Gold in sea-floor polymetallic sulfide deposits. *Economic Geology*, v.81, p.1867-1883.
- HANNINGTON, M.D. and SCOTT, S.D. (1989) Gold mineralization in volcanogenic massive sulfides: Implications of data from active hydrothermal vents on the modern sea floor, *in* Keays, R.R., Ramsay, W.R.H. and Groves, D.I., eds., *The Geology of Gold Deposits: The Perspective in 1988*, Economic Geology Monograph 6. Economic Geology Publishing Company, El Paso, p.491-507.
- HANSON, G.N. (1980) Rare earth elements in petrogenetic studies of igneous systems. *Annual Review of Earth and Planetary Sciences*, v. 8, p.371-406.
- HATTORI, K. (1987) Magnetic felsic intrusions associated with Canadian Archean gold deposits. *Geology*, v.15, p.1107-1111.
- HATTORI, K. and MUEHLENBACHS, K. (1980) Marine hydrothermal alteration at a Kuroko ore deposit, Kosaka, Japan. *Contributions to Mineralogy and Petrology*, v.74, p.285-292.
- HÉBERT, R., ROCHELEAU, M., GIGUÈRE, C., PERRIER, B. and GAUDREAU, R. (1991) Pétrologie et gîtologie d'un filon-couche différencié et minéralisé archéen: le gisement aurifère Sigma-2, canton de Louvicourt, Québec. *Canadian Journal of Earth Sciences*, v.28, p.1731-1743.
- Henley, R.W. (1984) Chemical structure of geothermal systems, *in* Henley, R.W., Truesdell, A.H. and Barton, P.B., Jr., eds., *Fluid-Mineral Equilibria in Hydrothermal Systems*, Reviews in Economic Geology. Society of Economic Geologists, v.1, p.9-27.
- HENLEY, R.W. (1985) The geothermal framework for epithermal deposits, *in* Berger, B.R. and Bethke, P.M., eds., *Geology and Geochemistry of Epithermal Systems*, Reviews in Economic Geology. Society of Economic Geologists, v.2, p.1-24.
- HENLEY, R.W. and ELLIS, A.J. (1983) Geothermal systems ancient and modern: a geochemical review. *Earth Science Reviews*, v.19, p.1-50.
- HENLEY, R.W. and THORNLEY, P. (1979) Some geothermal aspects of polymetallic massive sulfide formation. *Economic Geology*, v.74, p.1600-1612.
- HO, S.E. (1987) Fluid inclusions: their potential as an exploration tool for Archean gold deposits, *in* Ho, S.E. and Groves, D.I., eds., *Recent Advances in Understanding Precambrian Gold Deposits*. Geology Department and University Extension, University of Western Australia, Publication No.11, p.239-263.

- HODGSON, C.J. (1990) An overview of the geological characteristics of gold deposits in the Abitibi subprovince, in Short Course Notes, Gold and Base-Metal Mineralization in the Abitibi Subprovince, Canada, with Emphasis on the Quebec Segment. Geology Department and University Extension, The University of Western Australia, Publication No.24, p.63-100.
- HODGSON, C.J., CHAPMAN, R.S.G. and MACGEEHAN, P.J. (1982) Application of exploration criteria for gold deposits in the Superior Province of the Canadian Shield to gold exploration in the Cordillera, *in* Precious Metals in the Northern Cordillera. Association of Exploration Geochemists, Vancouver, British Columbia, p.173-206.
- HODGSON, C.J., HAMILTON, J.V. and PIROSHCO, D.W. (1990) Structural setting of gold deposits and the tectonic evolution of the Timmins-Kirkland Lake area, southwestern Abitibi greenstone belt, in Short Course Notes - Gold and Base-Metal Mineralization in the Abitibi Subprovince, Canada, with Emphasis on the Quebec Segment. The University of Western Australia, Publication No.24, p.101-120.
- HODGSON, C.J. and MACGEEHAN, P.J. (1982) A review of the geological characteristics of "gold-only" deposits in the Superior Province of the Canadian Shield, R.W. Hodder and W. Petruk, eds., *in* Geology of Canadian Gold Deposits, Canadian Institute of Mining and Metallurgy, Special Volume 24, p.211-229.
- HOLUBEC, J. (1972) Lithostratigraphy, structure and deep crustal relations of Archean rocks of the Canadian Shield, Rouyn—Noranda, Quebec. *Krystalinikum*, v.9, p.63-88.
- HONZA, E. (1991) The Tertiary arc chain in the western Pacific. *Tectonophysics*, v.187, p.285-303.
- HUBERT, C. (1990) Geologic framework, evolution and structural setting of gold and base metal deposits of the Abitibi greenstone belt, Canada, *in* Gold and base metal mineralization in the Abitibi subprovince Canada, with emphasis on the Quebec segment. Short course notes, compiled by S.E. Ho, F. Robert and D.I. Groves. University of Western Australia, Publication #24, p.53-62.
- HUBERT, C., TRUDEL, P. and GÉLINAS, L. (1984) Archean wrench-fault tectonics and structural evolution of the Blake River Group, Abitibi, Quebec. *Canadian Journal of Earth Sciences*, v.21, p.1024-1032.

- HUSTON, D.L. and LARGE, R.R. (1989) A chemical model for the concentration of gold in volcanogenic massive sulphide deposits. *Ore Geology Reviews*, v.4, p.171-200.
- HUTCHINSON, R.W., RIDLER, R.H. and SUFFEL, G.G. (1971) Metallogenic relationships in the Abitibi belt, Canada: A model for Archean metallogeny. *Canadian Institute of Mining and Metallurgy, Transactions*, v.74, p.106-115.
- IMREH, L. (1976) Nouvelle lithostratigraphie à l'ouest de Val-d'Or et son incidence géologique. *Quebec Department of Natural Resources, DPV-349*, 73 p.
- IMREH, L. (1984) Sillon de La Motte-Vassan et son avant-pays méridional: Synthèse volcanologique, lithostratigraphique et géologique. *Ministère de l'Énergie et des Ressources du Québec, MM 82-04*, 72 p, 2 maps.
- IMREH, L. (1990) Notes accompagnant les cartes préliminaires au 1:15 840 de l'Abitibi-Est méridional — Projet de géologie prévisionnelle — Coupure 32 C/04. *Ministère de l'Énergie et des Ressources du Québec, MB 90-36*, 17 p, 4 cartes.
- IRVINE, T.N. and BARAGAR, W.R.A. (1971) A guide to the chemical classification of the common volcanic rocks. *Canadian Journal of Earth Sciences*, v.8, p.523-548.
- ISHIHARA, S. (1975) Acid magmatism and mineralization — oxidation status of granitic magma and its relations to mineralization. *Marine Science Monograph*, v.7, p.756-759.
- JACKSON, S.L. and FYON, J.A. (1991) The western Abitibi Subprovince in Ontario, *in* Thurston, P.C., Williams, H.R., Sutcliffe, R.H. and Stott, G.M., eds., *Ontario Geological Survey, Special Volume 4, Part 1*, p.405-482.
- JACKSON, S.L., SUTCLIFFE, R.H., LUDDEN, J.N., HUBERT, C., GREEN, A.G., MILKEREIT, B., MAYRAND, L., WEST, G.F. and VERPAELST, P. (1990) Southern Abitibi greenstone belt: Archean crustal structure from seismic-reflection profiles. *Geology*, v.18, p.1086-1090.
- JAKEŠ, P. and WHITE, A.J.R. (1972) Major and trace element abundances in volcanic rocks of orogenic areas. *Geological Society of America Bulletin*, v.83, p.29-40.
- JAUPART, C. and PROVOST, A. (1985) Heat focussing, granite genesis and inverted metamorphic gradients in continental collision zones. *Earth and Planetary Science Letters*, v.73, p.385-397.

- JÉBRAK, M., LEQUENTREC, M.F., MARESCHAL, J.-C. and BLAIS, D. (1991) A gravity survey across the Bourlamaque massif, southeastern Abitibi greenstone belt, Québec, Canada: the relationship between the geometry of tonalite plutons and associated gold mineralization. *Precambrian Research*, v.50, p.261-268.
- JEMIELITA, R.A., DAVIS, D.W. and KROGH, T.E. (1990) U-Pb evidence for Abitibi gold mineralization post-dating greenstone magmatism and metamorphism. *Nature*, v.346, p.831-834.
- JEMIELITA, R.A., DAVIS, D.W., KROGH, T.E. and SPOONER, E.T.C. (1989) Chronological constraints on the origin of Archean lode gold deposits in the southern Superior Province from U/Pb isotopic analyses of hydrothermal rutile and titanite. Geological Society of America, Annual Meeting, Abstracts with Programs, v.21, p.A351.
- JENSEN, L.S. (1976) A new cation plot for classifying subalkalic volcanic rocks. Ontario Division of Mines, Miscellaneous Paper 66, 22 p.
- JOLLY, W.T. (1978) Metamorphic history of the Archean Abitibi Belt, *in* Metamorphism in the Canadian Shield, Geological Survey of Canada, Paper 78-10, p.63-78.
- KAPPEL, E.S. and FRANKLIN, J.M. (1989) Relationships between geologic development of ridge crests and sulfide deposits in the northeast Pacific Ocean. *Economic Geology*, v.84, p.485-505.
- KARIG, D.E. (1970) Ridges and basins of the Tonga-Kermadec Island arc system. *Journal of Geophysical Research*, v.75, p.239-254.
- KARIG, D.E. (1971) Origin and development of marginal basins in the western Pacific. *Journal of Geophysical Research*, v.76, p.2542-2561.
- KARIG, D.E. (1972) Remnant arcs. Geological Society of America, Bulletin, v.83, p.1057-1068.
- KARIG, D.E. (1974) Evolution of arc systems in the western Pacific. *Annual Review of Earth and Planetary Sciences*, v.2, p.51-75.
- KEAYS, R.R. (1984) Archean gold deposits and their source rocks: the upper mantle connection, *in* Foster, R.P., ed., Gold '82: The Geology, Geochemistry and Genesis of Gold Deposits, Geological Society of Zimbabwe, Special Publication No. 1, Rotterdam, p.17-51.

- KERR, D.J. and MASON, R. (1990) A re-appraisal of the geology and ore deposits of the Horne mine complex at Rouyn-Noranda, Quebec, *in* Rive, M. et al., eds., The Northwestern Quebec Polymetallic Belt: A Summary of 60 years of Mining Exploration, Canadian Institute of Mining and Metallurgy, Special Volume 43, p.153-165.
- KERRICH, R. (1983) Geochemistry of gold deposits in the Abitibi greenstone belt. Canadian Institute of Mining and Metallurgy, Special Volume 27, 71 p.
- KERRICH, R. (1986) Fluid infiltration into fault zones: chemical, isotopic and mechanical effects. *Journal of Pure and Applied Geophysics*, v.124, p.225-268.
- KERRICH, R. (1989a) Geochemical evidence on the sources of fluids and solutes for shear zone hosted mesothermal Au deposits, *in* Bursnall, J.T., ed., Mineralization and Shear Zones, Geological Association of Canada, Short Course Notes, Volume 6, p.129-218.
- KERRICH, R. (1989b) Geodynamic setting and hydraulic regimes: shear zone hosted mesothermal gold deposits, *in* Bursnall, J.T., ed., Mineralization and shear zones, Geological Association of Canada, Short Course Notes Volume 6, p.89-128.
- KERRICH, R. and ALLISON, I. (1978) Vein geometry and hydrostatics during Yellowknife mineralization. *Canadian Journal of Earth Sciences*, v.15, p.1653-1660.
- KERRICH, R. and FRYER, B.J. (1979) Archean precious-metal hydrothermal systems, Dome Mine, Abitibi Greenstone Belt: Part II. REE and oxygen isotope relations. *Canadian Journal of Earth Sciences*, v.16, p.440-458.
- KERRICH, R., FRYER, B.J., KING, R.W., WILLMORE, L.M. and VAN HEES, E. (1987) Crustal outgassing and LILE enrichment in major lithosphere structures, Archean Abitibi greenstone belt: Evidence on the source reservoir from strontium and carbon isotope tracers. *Contributions to Mineralogy and Petrology*, v.97, p.156-168.
- KERRICH, R. and KING, R. (1993) Hydrothermal zircon and baddeleyite in Val-d'Or Archean mesothermal gold deposits: characteristics, compositions, and fluid-inclusion properties, with implications for timing of primary gold mineralization. *Canadian Journal of Earth Sciences*, v.30, p.2334-2351.
- KERRICH, R. and WYMAN, D. (1990) Geodynamic setting of mesothermal gold deposits: An association with accretionary tectonic regimes. *Geology*, v.18, p.882-885.

- KERSWILL, J.A. (1986) Gold deposits hosted by iron formation in the Contwoyto Lake area, Northwest Territories, *in* Chater, A.M., ed., Gold '86 Poster Volume, p.82-85.
- KHEANG, L. and PERRAULT, G. (1987) Cl-rich and S-rich fluids related to the Archean gold deposits in the Val d'Or region, NW Quebec. Geological Association of Canada-Mineralogical Association of Canada, Program with Abstracts, v.12, p.61.
- KIRKHAM, R.V. (1972) Geology of copper and molybdenum deposits. Geological Survey of Canada, Paper 72-1, part A, p.82-87.
- KNUCKEY, M.J., COMBA, C.D.A. and RIVERIN, G. (1982) Structure, metal zoning, and alteration at the Millenbach Cu-Zn deposit, Noranda, Quebec. Geological Association of Canada, Special Paper 25, p.255-296.
- Knuckey, M.J. and Watkin, J.J. (1982) The geology of the Corbet massive sulfide deposit, Noranda, Quebec, Canada. Geological Association of Canada, Special Paper 25, p.297-318.
- KROGH, T.E. (1990) Direct evidence for tectonic underplating in an Archean granulite-greenstone terrane. American Geophysical Union, Transactions, v.71, no.17, p.617 (abstract).
- KROGH, T.E., HEAMAN, L.M. and MACHADO, N. (1988) Detailed U-Pb chronology of successive stages of zircon growth at medium and deep levels using parts of single zircon and titanite grains, p.243 in Project Lithoprobe, Kapuskasing Structural Zone Transect, Workshop, Toronto, University of Toronto, 252 p.
- KUSHIRO, J. and YODER JR., H.S. (1972) Origin of calc-alkalic peraluminous andesite and dacites. Carnegie Institution of Washington Year Book 71, p.411-413.
- KYSER, T.K. and KERRICH, R. (1990) Geochemistry of fluids in tectonically active crustal regions, *in* Nesbitt, B.E., ed., Short Course on Fluids in Tectonically Active Regimes of the Continental Crust, Mineralogical Association of Canada, p.133-230.
- KWONG, Y.T.J. and CROCKET, J.H. (1978) Background and anomalous gold in rocks of an Archean greenstone assemblage, Kakagi Lake area, northwestern Ontario. Economic Geology, v.73, p.50-63.

- LACROIX, R. (1986) Géologie et géochimie de la propriété New Pascalis, Val d'Or, Québec. M.Sc.A. thesis, Ecole Polytechnique, Montreal, 128 p.
- LADEIRA, E. (1991) Genesis of gold in Quadrilatero Ferrifero: a remarkable case of permanency, recycling and inheritance — A tribute to Djalma Guimaraes, Pierre Routhier and Hans Ramberg, *in* Ladeira, E., ed., Proceedings of Brazil Gold '91. Balkema, Rotterdam, p.11-30.
- LAFLÈCHE, M.R., DUPUY, C. and BOUGAULT, H. (1992) Geochemistry and petrogenesis of Archean mafic volcanic rocks of the southern Abitibi Belt, Quebec. *Precambrian Research*, v.57, p.207-241.
- LAJOIE, J. and LUDDEN, J. (1984) Petrology of the Archean Pontiac and Kewagama sediments and implications for the stratigraphy of the southern Abitibi belt. *Canadian Journal of Earth Sciences*, v.21, p.1305-1314.
- LAMB, W.M., VALLEY, J.W. and BROWN, P.E. (1987) Post-metamorphic CO₂-rich fluid inclusions in granulites. *Contributions to Mineralogy and Petrology*, v.96, p.485-495.
- LANDRY, J. (1991) Volcanologie physique et sédimentologie du groupe volcanique de Piché et relations stratigraphiques avec les groupes sédimentaires encaissants de Pontiac et de Cadillac. M.Sc. thesis, Université du Québec à Chicoutimi, Chicoutimi, 86 p.
- LANGFORD, F.F. and MORIN, J.A. (1976) The development of the Superior Province of northwestern Ontario by merging island arcs. *American Journal of Science*, v.276, p.1023-1034.
- LARGE, R.R. (1977) Chemical evolution and zonation of massive sulfide deposits in volcanic terrains. *Economic Geology*, v.72, p.549-572.
- LARGE, R.R. (1992) Australian volcanic-hosted massive sulfide deposits: Features, styles, and genetic models. *Economic Geology*, v.87, p.471-510.
- LARGE, R.R., HUSTON, D.L., MCGOLDRICK, P.J., RUXTON, P.A. and MCAUTHUR, G. (1989) Gold distribution and genesis in Australian volcanogenic massive sulfide deposits and their significance for gold transport models, *in* Keays, R.R., Ramsay, W.R.H. and Groves, D.I., eds., *The Geology of Gold Deposits: The Perspective in 1988*, Economic Geology Monograph 6. Economic Geology Publishing Company, El Paso, p.520-536.

- LAROCHE, C. (1979) Archean granitoid intrusions into the Pontiac Group, Lac Remigny area, northwestern Quebec. M.Sc. thesis, Carleton University, Ottawa, 176 p.
- LATULIPPE, M. (1966) The relationship of mineralization to Precambrian stratigraphy in the Matagami Lake and Val d'Or districts of Quebec. Geological Association of Canada, Special Paper Number 3, p.21-41.
- LATULIPPE, M. (1976) Excursion géologique: la région de Val-d'Or-Malartic. Quebec Department of Natural Resources/Canadian Institute of Mining and Metallurgy, DP 367, 124 p.
- LESHER, C.M., GOODWIN, A.M., CAMPBELL, I.H. and GORTON, M.P. (1986) Trace-element geochemistry of ore-associated and barren, felsic metavolcanic rocks in the Superior Province, Canada. Canadian Journal of Earth Sciences, v.23, p.222-237.
- LOWELL, J.D. (1974) Regional characteristics of porphyry copper deposits of the southwest. Economic Geology, v.69, p.601-617.
- LUDDEN, J.N., DAIGNEAULT, R., ROBERT, F. and TAYLOR, R.P. (1984) Trace element mobility in alteration zones associated with Archean Au lode deposits. Economic Geology, v.79, p.1131-1141.
- LUDDEN, J., GÉLINAS, L. and TRUDEL, P. (1982) Archean metavolcanics from the Rouyn-Noranda district, Abitibi greenstone belt, Quebec. 2. Mobility of trace elements and petrogenetic constraints. Canadian Journal of Earth Sciences, v.19, p.2276-2287.
- LULIN, J.-M. (1990) Une analyse du développement minier du nord-ouest québécois, *in* Rive, M., Verpaelst, P., Gagnon, Y., Lulin, J.-M., Riverin, G. and Simard, A., eds., The Northwestern Quebec Polymetallic Belt: A Summary of 60 Years of Mining Exploration, Canadian Institute of Mining and Metallurgy, Special Volume 43, p.17-34.
- LYDON, J.W. (1988) Volcanogenic massive sulphide deposits. Part 2: Genetic models. Geoscience Canada, v.15, p.43-65.
- LYDON, J.W. and GALLEY, A. (1986) Chemical and mineralogical zonation of the Mathiati alteration pipe, Cyprus, and its genetic significance, *in* Gallagher, M.J., Ixer, R.A., Neary, C.R. and Prichard, H.M., eds., Metallogeny of Basic and Ultrabasic Rocks, Institution of Mining and Metallurgy, London, p.49-68.

- MACDONALD, A.J. (1983) The iron formation-gold association: Evidence from the Geraldton area, *in* Colvine, A.C., ed., *Geology of Gold in Ontario*, Ontario Geological Survey, Miscellaneous Paper 110, p.75-83.
- MACDONALD, A.J. and FYON, J.A. (1986) Sulphidation — The key to gold mineralization in banded iron formation (extended abstract), *in* Chater, A.M., ed., *Gold '86 Poster Volume*, p.96-97.
- MACGEEHAN, P.J. (1978) The geochemistry of altered volcanic rocks at Matagami, Quebec: a geothermal model for massive sulfide genesis. *Canadian Journal of Earth Sciences*, v.15, p.551-570.
- MACGEEHAN, P.J. and MACLEAN, W.H. (1980) Tholeiitic basalt-rhyolite magmatism and massive sulphide deposits at Matagami, Quebec. *Nature*, v.283, p.153-157.
- MACHADO, N., RIVE, M., GARIÉPY, C. and SIMARD, A. (1991) U-Pb geochronology of granitoids from the Pontiac subprovince: Preliminary results. Geological Association of Canada — Mineralogical Association of Canada, Program with Abstracts. v. 16, p.A78.
- MANNARD, G.N. and BUBAR, D.S. (1991) The role of litho-geochemistry in the discovery of the Louvicourt copper-zinc-silver-gold massive sulphide deposit. Geological Association of Canada — Mineralogical Association of Canada, Program with Abstracts, v.16, p.A79.
- MARQUIS, P., BROWN, A.C., HUBERT, C. and RIGG, D.M. (1990a) Progressive alteration associated with auriferous massive sulfide bodies at the Dumagami mine, Abitibi greenstone belt, Quebec. *Economic Geology*, v.85, p.746-764.
- MARQUIS, P., HUBERT, C., BROWN, A.C. and RIGG, D.M. (1990b) An evaluation of genetic models for gold deposits of the Bousquet district, Quebec, based on their mineralogic, geochemical, and structural characteristics, *in* Rive, M., Verpaelst, P., Gagnon, Y., Lulin, J.-M., Riverin, G. and Simard, A., eds., *The Northwestern Quebec Polymetallic Belt: A Summary of 60 Years of Mining Exploration*, Canadian Institute of Mining and Metallurgy, Special Volume 43, p. 383-399.
- MARQUIS, R. and GOULET, N. (1987) Essai de corrélation stratigraphique et structurale à l'est de Val-d'Or: Implication pour la prospection aurifère du secteur. *Canadian Journal of Earth Sciences*, v.24, p.2412-2421.

- MARTIN, H. (1986) Effect of steeper Archean geothermal gradient on the geochemistry of subduction-zone magmas. *Geology*, v.14, p.753-756.
- MASLIWEC, A., YORK, D., KUYBIDA, P, AND HALL, C.M. (1986) The dating of Ontario's gold deposits. Ontario Geological Survey Miscellaneous Paper 127, p.223-228.
- MCBIRNEY, A.R. (1963) Factors governing the nature of submarine volcanism. *Bulletin of Volcanology*, v.26, p.455-469.
- MCMILLAN, W.J. and PANTELEYEV, A. (1980) Ore deposit model - 1. Porphyry copper deposits. *Geoscience Canada*, v.7, no.2, p.52-63.
- MCNAUGHTON, N.J., CASSIDY, K.F., DAHL, N., DE LAETER, J.R., GOLDINGIN, S.D., GROVES, D.I., HO, S.E., MUELLER, A.G., PERRING, C.S., SANG, J.H. and TURNER, J.V. (1992) The source of ore components in lode-gold deposits of the Yilgarn block, Western Australia *in* Glover, J.E. and Ho, S.E., eds., *The Archaean: Terrains, Processes and Metallogeny*. Geology Department and University Extension, The University of Western Australia, Publication No. 22, p.351-363.
- MEINERT, L.D. (1992) Skarns and skarn deposits. *Geoscience Canada*, v.19, p.145-162.
- MONGER, J.W.H. (1993) Canadian Cordilleran tectonics: from geosynclines to crustal collage. *Canadian Journal of Earth Sciences*, v.30, p.209-231.
- MOORE, J.G. (1965) Petrology of deep-sea basalt near Hawaii. *American Journal of Science*, v.263, p.40-52.
- MOORE, J.G. (1979) Vesicularity and CO₂ in mid-ocean ridge basalt. *Nature*, v.282, p.250-253.
- MOORE, J.G. and SCHILLING, J.-G. (1973) Vesicles, water and sulfur in Reykjanes Ridge basalts. *Contributions to Mineralogy and Petrology*, v.41, p.105-118.
- MOORHEAD, J. and CHARTRAND, F. (1993) Synthèse géologie de Val d'Or. Rapport d'activité, Ministère de l'Énergie et des Ressources du Québec, DV93-02, p.66.
- MORASSE, S., WASTENEYS, H.A., CORMIER, M., HELMSTAEDT, H. and MASON, R. (1993) La mine d'or Kiena: minéralisation magmatique hydrothermale kénoréenne précoce dans la ceinture minérale de Val-d'Or, sud-est

de l'Abitibi. Séminaire d'information 1993, Ministère de l'Énergie et des Ressources du Québec, DV 93-03, p.67-71.

- MORRIS, D.J., LEEMAN, W.P. and TERA, F. (1990) The subducted component in island arc lavas: constraints from Be isotopes and B-Be systematics. *Nature*, v.344, p.31-36.
- MORRISON, J. and VALLEY, J.W. (1988) Post-granulite facies fluid infiltration in the Adirondack Mountains. *Geology*, v.16, p.513-516.
- MORTON, R.L. and FRANKLIN, J.M. (1987) Two-fold classification of Archean volcanic-associated massive sulfide deposits. *Economic Geology*, v.82, p.1057-1063.
- MORTON, R.L., WALKER, J.S., HUDAK, G.J. and FRANKLIN, J.M. (1991) The early development of an Archean submarine caldera complex with emphasis on the Mattabi ash-flow tuff and its relationship to the Mattabi massive sulfide deposit. *Economic Geology*, v.86, p.1002-1011.
- MOTTL, M.J. (1983) Metabasalts, axial hot springs, and the structure of hydrothermal systems at mid-ocean ridges. *Geological Society of America, Bulletin*, v.94, p.161-180.
- MUELLER, A.G. (1988) Archaean gold-silver deposits with prominent calc-silicate alteration in the Southern Cross greenstone belt, Western Australia: Analogues of Phanerozoic skarn deposits, *in* Ho, S.E. and Groves, D.I., eds., *Advances in Understanding Precambrian Gold Deposits, Volume II*. The University of Western Australia, Publication No.12, p.141-163.
- NESBITT, B.E. (1988) Gold deposit continuum: A genetic model for lode Au mineralization in the continental crust. *Geology*, v.16, p.1044-1048.
- NESBITT, B.E. and MUEHLENBACHS, K. (1988) Genetic implication of the association of mesothermal gold deposits with major strike-slip fault systems, *in* Kisvarsanyi, G and Grant, S.K., eds., *North American Conference on Tectonic Control of Ore Deposits and the Vertical and Horizontal Extent of Ore Systems*. University of Missouri-Rolla, p.57-66.
- NESBITT, B.E. and MUEHLENBACHS (1989a) Geology, geochemistry, and genesis of mesothermal lode gold deposits of the Canadian Cordillera: evidence for ore formation from evolved meteoric water, *in* Keays, R.R., Ramsay, W.R.H. and Groves, D.I., eds., *The Geology of Gold Deposits: The Perspective in 1988*,

Economic Geology Monograph 6. Economic Geology Publishing Company, El Paso, p.553-563.

NESBITT, B.E. and MUEHLENBACHS, K. (1989b) Origins and movement of fluids during deformation and metamorphism in the Canadian Cordillera. *Science*, v.245, p.733-736.

NESBITT, B.E., MUEHLENBACHS, K. and MUROWCHICK, J.B. (1987) Reply on "Dual origins of lode gold deposits in the Canadian Cordillera". *Geology*, v.15, p.471-473.

NESBITT, B.E., MUEHLENBACHS, K. and MUROWCHICK, J.B. (1989) Genetic implications of stable isotope characteristics of mesothermal Au deposits and related Sb and Hg deposits in the Canadian Cordillera, *Economic Geology*, v.84, p.1489-1506.

NESBITT, B.E., MUROWCHICK, J.B. and MUEHLENBACHS, K. (1986) Dual origins of lode gold deposits in the Canadian Cordillera. *Geology*, v.14, p.506-509.

NEWTON, R.C., SMITH, J.V. and WINDLEY, B.F. (1980) Carbonic metamorphism, granulites and crustal growth. *Nature*, v.288, p.45-50.

NORMAN, G.W.H. (1941) Vassan-Dubuisson map-area, Abitibi County, Quebec. Geological Survey of Canada, Paper 41-6, 9 p.

NORMAN, G.W.H. (1942) The Cadillac synclinal belt of northwestern Quebec. *Transactions of the Royal Society of Canada*, v.36, p.89-98.

NORMAN, G.W.H. (1943a) Bourlamaque Township, Abitibi County, Quebec. Geological Survey of Canada, Paper 43-2, 14 p.

NORMAN, G.W.H. (1943b) Notes sur la structure de la région de Cadillac-Bourlamaque, comté d'Abitibi, Québec. Geological Survey of Canada, Memoir 43-6.

NORMAN, G.W.H. (1945) Carte préliminaire de Louvicourt, comté d'Abitibi, Québec. Geological Survey of Canada, Memoir 45-10.

NORMAN, G.W.H. (1947) Dubuisson-Bourlamaque-Louvicourt, Abitibi County, Quebec. Geological Survey of Canada, Paper 47-20.

- OBERTHÜR, T., SAAGER, R. and TOMSCHI, H.-P. (1990) Geological, mineralogical and geochemical aspects of Archean banded iron-formation-hosted gold deposits: some examples from southern Africa. *Mineralium Deposita*, v.25, p. S125-S135.
- OHMOTO, H. and RYE, R.O. (1974) Hydrogen and oxygen isotopic compositions of fluid inclusions in the Kuroko deposits, Japan. *Economic Geology*, v.69, p.947-953.
- OHMOTO, H. and RYE, R.O. (1979) Isotopes of sulfur and carbon, *in* H.L. Barnes, ed., *Geochemistry of Hydrothermal Ore Deposits*, Second Edition. John Wiley and Sons, Toronto, p.509-567.
- OLDOW, J.S., BALLY, A.W., AVE LALLEMANT, H.G. and LEEMAN, W.P. (1989) Phanerozoic evolution of the North American Cordillera; United States and Canada, *in* Bally, A.W. and Palmer, A.R., eds., *The Geology of North America - An Overview*, Volume A, Geological Society of America Special Publication, p.139-232.
- O'NIONS, R.K. and OXBURGH, E.R. (1988) Helium volatiles fluxes and the development of continental crust. *Earth and Planetary Science Letters*, v.90, p.331-347.
- PARENT, G. (1985) Géochimie du groupe volcanique de Malartic, d'âge archéen, région de l'Abitibi. M.Sc. thesis, Université de Montréal, Montreal, 104 p.
- PEARCE, J.A. and CANN, J.R. (1973) Tectonic setting of basic volcanic rocks determined using trace element analyses. *Earth and Planetary Science Letters*, v.19, p.290-300.
- PEARCE, J.A. and NORRY, M.J. (1979) Petrogenetic implications of Ti, Zr, Y, and Nb variation in volcanic rocks. *Contributions to Mineralogy and Petrology*, v.69, p.33-47.
- PÉLOQUIN, A.S., POTVIN, R., PARADIS, S., LAFLÈCHE, M.R., VERPAELST, P. and GIBSON, H.L. (1990) The Blake River Group, Rouyn-Noranda area, Quebec: a stratigraphic synthesis, *in* Rive, M., Verpaelst, P., Gagnon, Y., Lulin, J.-M., Riverin, G. and Simard, A., eds., *The Northwestern Quebec Polymetallic Belt: A Summary of 60 Years of Mining Exploration*. Canadian Institute of Mining and Metallurgy Special Volume 43, p.108-117.
- PERCIVAL, J.A. (1989) A regional perspective of the Quetico metasedimentary belt, Superior Province, Canada. *Canadian Journal of Earth Sciences*, v.26, p.677-693.

- PERCIVAL, J.A. and KROGH, T.E. (1983) U-Pb zircon geochronology of the Kapuskasing structural zone and vicinity in the Chapleau-Foley area, Ontario. *Canadian Journal of Earth Sciences*, v.20, p.830-843.
- PERFIT, M.R. and FORNARI, D.J. (1983) Geochemical studies of abyssal lavas recovered by DSRV "Alvin" from eastern Galapagos Rift, Inca Transform, and Ecuador Rift: 2. Phase chemistry and crystallization history. *Journal of Geophysical Research*, v.88, p.10530-10550.
- PERFIT, M.R., FORNARI, D.J., MALAHOFF, A. and EMBLEY, R.W. (1983) Geochemical studies of abyssal lavas recovered by DSRV "Alvin" from eastern Galapagos Rift, Inca Transform, and Ecuador Rift: 3. Trace element abundances and petrogenesis. *Journal of Geophysical Research*, v.88, p.10551-10572.
- PERRING, C.S., BARLEY, M.E., CASSIDY, K.F., GROVES, D.I., MCNAUGHTON, N.J., ROCK, N.M.S., BETTENAY, L.F., GOLDING, S.D. and HALLBERG, J.A. (1989) The association of linear orogenic belts, mantle-crustal magmatism, and Archean gold mineralization in the eastern Yilgarn block of Western Australia, *in* Keays, R.R., Ramsay, W.R.H. and Groves, D.I., eds., *The Geology of Gold Deposits: The Perspective in 1988*, Economic Geology Monograph 6. Economic Geology Publishing Company, El Paso, p.571-584.
- PERRING, C.S., GROVES, D.I. and HO, S.E. (1987) Constraints on the source of auriferous fluids for Archean gold deposits. University of Western Australia Geology Department, University Extension Publication No. 11, p.287-306.
- PETERSON, J.W. and NEWTON, R.C. (1989) CO₂-enhanced melting of biotite-bearing rocks at deep-crustal pressure-temperature conditions. *Nature*, v.340, p.378-380.
- PETERSON, J.W. and NEWTON, R.C. (1990) Experimental CO₂-melting of granite and its bearing on the Archean gold association, *in* Robert, F., Sheahan, P.A. and Green, S.B., eds., *Greenstone Gold and Crustal Evolution*, NUNA Conference Volume, Val d'Or, Quebec. Geological Association of Canada-Mineral Deposits Division, p.192.
- PHILLIPS, G.N. and GROVES, D.I. (1983) The nature of Archean gold-bearing fluids as deduced from gold deposits of Western Australia. *Journal of the Geological Society of Australia*, v.30, p.215-39.
- PHILLIPS, G.N., GROVES, D.I. and MARTYN, J.E. (1984) An epigenetic origin for Archean banded iron formation hosted gold deposits. *Economic Geology*, v.79, p.162-171.

- PICKTHORN, W.J., GOLDFARB, R.J. and LEACH, D.L. (1987) Comment on "Dual origins of lode gold deposits in the Canadian Cordillera". *Geology*, v.15, p.471-473.
- PILOTE, P., COUTURE, J.-F., DESROCHERS, J.-P., MACHADO, N. and PELZ, P. (1993) Minéralisations aurifères multiphasées dans la région de Val d'Or: l'exemple de la mine Norlartic. Séminaire d'information, Ministère de l'Énergie et des Ressources du Québec, DV 93-03, p.61-66.
- PISUTHA-ARNOND, V. and OHMOTO, H. (1983) Thermal history, chemical and isotopic compositions of the ore-forming fluids responsible for the Kuroko massive sulfide deposits in the Hokuroku District of Japan, *in* Ohmoto, H. and Skinner, B.J., eds., *Kuroko and Related Volcanogenic Massive Sulphide Deposits*, Economic Geology Monograph 5. Economic Geology Publishing Company, El Paso, p.523-558.
- POPOV, V. (1976) La mine Manitou-Barvue, *in* Excursion géologique, La région de Val-d'Or — Malartic. Quebec Department of Natural Resources/Canadian Institute of Mining and Metallurgy, DP 367, p.84-91.
- POULSEN, K.H., CARD, K.D. and FRANKLIN, J.M. (1992) Archean tectonic and metallogenic evolution of the Superior Province of the Canadian Shield. *Precambrian Research*, v.58, p.25-54.
- POULSEN, K.H. and ROBERT, F. (1989) Shear zones and gold: Practical examples from the southern Canadian Shield, *in* Bursnall, J.T., ed., *Mineralization and Shear Zones*. Geological Association of Canada, Short Course Notes, v.6, p.239-266.
- POWELL, R., WILL, T.M. and PHILLIPS, G.N. (1991) Metamorphism in Archaean greenstone belts: calculated fluid compositions and implications for gold mineralization. *Journal of Metamorphic Geology*, v.9, p.141-150.
- POWELL, W.G., CARMICHAEL, D.M. and HODGSON, C.J. (1992) Low-grade metamorphism in the Rouyn-Duparquet area, southern Abitibi greenstone belt, Quebec. Geological Association of Canada — Mineralogical Association of Canada, Abstracts Volume 17, p.A91.
- POWELL, W.G., CARMICHAEL, D.M. and HODGSON, C.J. (1993) Relative timing of metamorphism and tectonism during the evolution of the southern Abitibi greenstone belt, *in* Séminaire d'information 1993, Ministère de l'Énergie et des Ressources du Québec, DV 93-03, p.49-50.

- RAMSAY, J.G. (1980) The crack-seal mechanism of rock deformation. *Nature*, v.284, p.83-99.
- RAY, G.E., DAWSON, G.L. and SIMPSON, R. (1988) Geology, geochemistry and metallogenic zoning in the Hedley gold-skarn camp. British Columbia Ministry of Energy, Mines and Petroleum Resources, Geological Fieldwork, 1987, Paper 1988-1, p.59-80.
- RAYMOND, D. (1983) Dispersion et altération lithogéochimiques à la mine Louvem et ses environs, Val d'Or, Québec. M.Sc. thesis, Laval University, Ste.-Foy, 209 p.
- RIDLER, R.H. (1970) Relationship of mineralization to volcanic stratigraphy in the Kirkland-Larder Lakes area, Ontario. Geological Association of Canada Annual Meeting, Proceedings, v.21, p.33-42.
- RIVERIN, G. and HODGSON, C.J. (1980) Wall-rock alteration at the Millenbach Cu-Zn mine, Noranda, Quebec. *Economic Geology*, v.75, p.424-444.
- ROBERT, F. (1980) Pétrographie et pétrochimie des roches encaissantes du gîte de Zn-Cu-Ag de Manitou-Barvue, Val d'Or, Québec. M.Sc.A. thesis, Ecole Polytechnique, Montreal, 208 p.
- ROBERT, F. (1989) Internal structure of the Cadillac tectonic zone southeast of Val d'Or, Abitibi greenstone belt, Quebec. *Canadian Journal of Earth Sciences*, v.26, p.2661-2675.
- ROBERT, F. (1990a) Structural setting and control of gold-quartz veins of the Val d'Or area, southeastern Abitibi subprovince, *in* Gold and Base Metal Mineralization in the Abitibi Subprovince Canada, with Emphasis on the Quebec Segment. Short Course Notes, Compiled by S.E. Ho, F. Robert and D.I. Groves. University of Western Australia, Publication No. 24, p.167-209.
- ROBERT, F. (1990b) An overview of gold deposits in the eastern Abitibi subprovince, *in* Rive, M. et al., eds., The Northwestern Quebec Polymetallic Belt: A Summary of 60 years of Mining Exploration. The Canadian Institute of Mining and Metallurgy, Special Volume 43, p.93-105.
- ROBERT, F. (1991a) Gold metallogeny of greenstone belts: Considerations from the eastern Abitibi Subprovince, Canada, *in* Ladeira, E.A., ed., Brazil Gold '91, Rotterdam, p.31-47.

- ROBERT, F. (1991b) Gold metallogeny of greenstone belts: Considerations from the eastern Abitibi Subprovince, Canada. Brazil Gold '91, Belo Horizonte, Gravaso e Imagem (publisher), Video Tape No.17.
- ROBERT, F. (1994) Vein fields in gold districts: The example of Val d'Or, southeastern Abitibi, *in* Current Research, Geological Survey of Canada, Paper (in press).
- ROBERT, F. and BOULLIER, A.-M. (1994) Mesothermal gold-quartz veins and earthquakes, *in* Proceedings Volume of USGS Red Book Conference, The Mechanical Involvement of Fluids in Faulting, convened by S. Hickman, R. Sibson and R. Bruhn, June 6-10, 1993, Tenaya Lodge, Fish Camp, California (in press).
- ROBERT, F., BROMMECKER, R. and BUBAR, D.S. (1990) The Orenada zone 4 deposit: Deformed vein-type gold mineralization within the Cadillac tectonic zone, SE of Val d'Or, *in* Rive, M. et al., eds. The Northwestern Quebec Polymetallic Belt: A Summary of 60 Years of Mining Exploration. Canadian Institute of Mining and Metallurgy Special, Volume 43, p.255-268.
- ROBERT, F. and BROWN, A.C. (1984) Progressive alteration associated with gold-quartz-tourmaline veins at the Sigma mine, Abitibi greenstone belt, Quebec. *Economic Geology*, v.79, p.393-399.
- ROBERT, F. and BROWN, A.C. (1986a) Archean gold-bearing quartz veins at the Sigma mine, Abitibi greenstone belt, Quebec: Part I. Geologic relations and formation of the vein system. *Economic Geology*, v.81, p.578-592.
- ROBERT, F. and BROWN, A.C. (1986b) Archean gold-bearing quartz veins at the Sigma mine, Abitibi greenstone belt, Quebec: Part II. Vein paragenesis and hydrothermal alteration. *Economic Geology*, v.81, p.593-616.
- ROBERT, F., BROWN, A.C. and AUDET, A.J. (1983) Structural control of gold mineralization at the Sigma mine, Val d'Or, Quebec. *Canadian Institute of Mining and Metallurgy, Bulletin*, v.76, no.850, p.72-80.
- ROBERT, F. and KELLY, W.C. (1987) Ore-forming fluids in Archean gold-bearing quartz veins at the Sigma mine, Abitibi greenstone belt, Quebec, Canada. *Economic Geology*, v.82, p.1464-1482.
- ROCHELEAU, M., GAUDREAU, R., LACOSTE, P., HÉBERT, S. ST-JULIEN, P., PERRIER, B. and RACINE, M. (1987) Synthèse stratigraphique, paléogéographique et gîtologique du secteur de Vauquelin, de Pershing et de Haig

- Rapport intérimaire. Ministère de l'Énergie et des Ressources du Québec, MB 87-52, 153 p.

- ROCHELEAU, M., HÉBERT, R., ST-JULIEN, P., RACINE, M., GAUDREAU, R. and LACOSTE, P. (1990) La ceinture de l'Abitibi à l'est de Val-d'Or: un secteur économiquement méconnu, affecté par la tectonique et le métamorphisme grenvillien, *in* Rive, M., Verpaelst, P., Gagnon, Y., Lulin, J.-M., Riverin, G. and Simard, A., eds., *The Northwestern Quebec Polymetallic Belt: A Summary of 60 Years of Mining Exploration*, Canadian Institute of Mining and Metallurgy, Special Volume 43, p.269-283.
- ROCK, N.M.S. and GROVES, D.I. (1988a) Do lamprophyres carry gold as well as diamonds? *Nature*, v.332, p.253-255.
- ROCK, N.M.S. and GROVES, D.I. (1988b) Can lamprophyres resolve the genetic controversy over mesothermal gold deposits? *Geology*, v.16, p.538-541.
- ROCK, N.M.S., GROVES, D.I., PERRING, C.S. and GOLDING, S.D. (1989) Gold, lamprophyres, and porphyries: What does their association mean?, *in* Keays, R.R., Ramsay, W.R.H. and Groves, D.I., eds., *The Geology of Gold Deposits: The Perspective in 1988*, Economic Geology Monograph 6. Economic Geology Publishing Company, El Paso, p.609-635.
- ROEDDER, E. (1984) Fluid inclusions. *Reviews in Mineralogy*, v.12, p.343, 357-359.
- ROGERS, J.J.W. and GREENSBERG, J.K. (1990) Late-orogenic, post-orogenic, and anorogenic granites: distinction by major-element and trace-element chemistry and possible origins. *The Journal of Geology*, v.98, p.291-309.
- ROMBERGER, S.B. (1986a) Ore Deposits #9. Disseminated gold deposits. *Geoscience Canada*, v.13, p.23-31.
- ROMBERGER, S.B. (1986b) The solution chemistry of gold applied to the origin of hydrothermal deposits, *in* L.A. Clark, ed., *Gold in the Western Shield*, Canadian Institute of Mining and Metallurgy, Special Volume 38, p.168-186.
- ROMBERGER, S.B. (1992) A model for bonanza gold deposits. *Geoscience Canada*, v.19, No.2, p.63-72.
- RONA, P.A. (1984) Hydrothermal mineralization at seafloor spreading centers. *Earth-Science Reviews*, v.20, p.1-104.

- RONA, P.A. (1988) Hydrothermal mineralization at oceanic ridges. *Canadian Mineralogist*, v.26, p.431-465.
- RONA, P.A. and SCOTT, S.D. (1993) A special issue on sea-floor hydrothermal mineralization: Preface. *Economic Geology*, v.88, p.1935-1976.
- ROSCOE, S.M. (1973) The Huronian Supergroup, a Paleoproterozoic succession showing evidence of atmospheric evolution. *The Geological Association of Canada, Special Paper 12*, p.31-47.
- ROY, C. (1983) Géologie de la mine d'or Kiena. M.Sc.A. thesis, École Polytechnique, Montreal, 201 p.
- RYE, D.M. and RYE, R.O. (1974) Homestake gold mine, South Dakota: I Stable isotope studies. *Economic Geology*, v.69, p.293-317.
- SAAGER, R. and MEYER, M. (1984) Gold distribution in Archaean granitoids and supracrustal rocks from southern Africa: A comparison, *in* Foster, R.P., ed., *Gold '82: The Geology, Geochemistry and Genesis of Gold Deposits*, Geological Society of Zimbabwe, Special Publication No. 1, Rotterdam, p.53-70.
- SAAGER, R., OBERTHÜR, T. and TOMSCHI, H.-P. (1987) Geochemistry and mineralogy of banded iron-formation-hosted gold mineralization in the Gwanda greenstone belt, Zimbabwe. *Economic Geology*, v.82, p.2017-2032.
- SAKAI, H. (1991) Expedition east Manus Basin hydrothermal field, Kakuro-Maru cruise KH90-3, leg 2. A brief summary report for SOPAC. South Pacific Applied Geoscience Commission, SOPAC Cruise Report 138, 3 p.
- SANGSTER, D.F. (1972) Precambrian volcanogenic massive sulphide deposits in Canada: A review. *Geological Survey of Canada, Paper 72-22*, 44p.
- SANSFAÇON, R. (1986) The Malartic district, *in* Hubert, C. and Robert, F., eds., *Structure and gold, Rouyn to Val d'Or, Québec*, Geological Association of Canada — Mineralogical Association of Canada, Field Trip 14: Guidebook, p.27-42.
- SATO, K. (1975) Unilateral isotopic variation of Miocene ore leads from Japan. *Economic Geology*, v.70, p.800-805.
- SAUVÉ, P. (1985) Géologie de la mine d'or Akasaba, région de Val-d'Or. Ministère de l'Énergie et des Ressources du Québec, MB 85-40, 40 p.

- SAUVÉ, P., IMREH, L. and TRUDEL, P. (1993) Description des gîtes d'or de la région de Val-d'Or. Ministère de l'Énergie et des Ressources du Québec, MM 91-03, 178 p.
- SAUVÉ, P., PERRAULT, G. and TRUDEL, P. (1986) Compilation et données nouvelles sur les gîtes d'or du camp minier de Val-d'Or. Ministère de l'Énergies et des Ressources du Québec, MB 86-24, 117p.
- SAWKINS, F.J. (1982) The formation of Kuroko-type deposits viewed within the broader context of ore genesis theory. *Mining Geology*, v.32, p.25-33.
- SAWKINS, F.J. (1986) Some thoughts on the genesis of kuroko-type deposits. *Geology in the real world—the Kingsley Dunham volume*. London, Institute of Mining Metallurgy, p.387-394.
- SCHANDL, E.S. and WICKS, F.J. (1993) Carbonate and associated alteration of ultramafic and rhyolitic rocks at the Hemingway property, Kidd Creek volcanic complex, Timmins, Ontario. *Economic Geology*, v.88, p.1615-1635.
- SEWARD, T.M. (1973) Thio complexes of gold and the transport of gold in hydrothermal ore solutions. *Geochimica et Cosmochimica Acta*, v.37, p.379-399.
- SEWARD, T.M. (1984) The formation of lead(II) chloride complexes to 300°C: A spectrophotometric study. *Geochimica et Cosmochimica Acta*, v.48, p.121-134.
- SEYFRIED, W.E., JR. (1987) Experimental and theoretical constraints on hydrothermal alteration processes at mid-ocean ridges. *Annual Review of Earth and Planetary Sciences*, v.15, p.317-335.
- SEYFRIED, W.E., JR. and JANECKY, D.R. (1985) Heavy metal and sulfur transport during subcritical and supercritical hydrothermal alteration of basalt: Influence of fluid pressure and basalt composition and crystallinity. *Geochimica et Cosmochimica Acta*, v.49, p.2545-2560.
- SHARPE, J.I. (1968) Canton de Louvicourt, Comté d'Abitibi-Est. Quebec Department of Natural Resources, Geological Report 135, 59 p, 4 maps.
- SHENBERGER, D.M. and BARNES, H.L. (1989) Solubility of gold in aqueous sulfide solutions from 150 to 350°C. *Geochimica et Cosmochimica Acta*, v.53, p.269-278.

- SIBSON, R.H. (1990) Faulting and fluid flow, *in* Nesbitt, B.E., ed., Short Course on Fluids in Tectonically Active Regimes of the Continental Crust, Mineralogical Association of Canada, p.93-132.
- SIBSON, R.H., ROBERT, F. and POULSEN, H. (1988) High angle faults, fluid pressure cycling and mesothermal gold-quartz deposits. *Geology*, v.16, p.551-555.
- SIMS, P.K., CARD, K.D., MOREY, G.B. and PETERMAN, Z.E. (1980) The Great Lakes tectonic zone—A major crustal structure in central North America. *Geological Society of America, Bulletin*, v.91, p.690-698.
- SKULSKI, T., FRANCIS, D. and LUDDEN, J. (1991) Arc-transform magmatism in the Wrangell volcanic belt. *Geology*, v.19, p.11-14.
- SOLOMON, M. (1990) Subduction, arc reversal, and the origin of porphyry copper-gold deposits in island arcs. *Geology*, v.18, p.630-633.
- SMITH, P.E., SCHANDL, E.S. and YORK, D. (1993) Timing of K-metasomatic alteration of the Kidd Creek massive sulphide deposit, Ontario, using $^{40}\text{Ar}/^{39}\text{Ar}$ laser dating of single crystals of fuchsite. *Geological Association of Canada - Mineralogical Association of Canada, Program with Abstracts*, v. 16, p.A116.
- SMITH, P.E., SCHANDL, E.S. and YORK, D. (1993) Timing of metasomatic alteration of the Archean Kidd Creek massive sulfide deposit, Ontario, using $^{40}\text{Ar}-^{39}\text{Ar}$ laser dating of single crystals of fuchsite. *Economic Geology*, v.88, p.1636-1643.
- SPITZ, G. and DARLING, R. (1973) Pétrographie des roches encaissantes du gisement cuprifère de Louvem. *Canadian Journal of Earth Sciences*, v.10, p.760-776.
- SPITZ, G. and DARLING, R. (1975) The petrochemistry of altered volcanic rocks surrounding the Louvem copper deposit, Val d'Or, Quebec. *Canadian Journal of Earth Sciences*, v.12, p.1820-1849.
- SPITZ, G. and DARLING, R. (1978) Major and minor element lithogeochemical anomalies surrounding the Louvem copper deposit, Val d'Or, Quebec. *Canadian Journal of Earth Sciences*, v. 15, p.1116-1169.
- SPOONER, E.T.C. and BRAY, C.J. (1977) Hydrothermal fluids of seawater salinity in ophiolitic sulphide ore deposits in Cyprus. *Nature*, v.266, p.808-812.

- STANTON, R.L. (1991) Understanding volcanic massive sulfides—past, present, and future, *in* Hutchinson, R.W. and Grauch, R.I., eds., *Historical Perspectives of Genetic Concepts and Case Histories of Famous Discoveries*, Economic Geology Monograph 8. Economic Geology Publishing Company, El Paso, p.82-95.
- STAUDIGEL, H. and SCHMINCKE, H.-U. (1984) The Pliocene seamount series La Palma/Canary Islands. *Journal of Geophysical Research*, v.89, p.11195-11215.
- STOCKWELL, C.H. (1982) Proposals for time classification and correlation of Precambrian rocks and events in Canada and adjacent areas of the Canadian Shield, Part 1: A time classification of Precambrian rocks and events. *Geological Survey of Canada*, Paper 80-19, 135 p.
- STOREY, M., MAHONEY, J.J., KROENKE, L.W. and SAUNDERS, A.D. (1991) Are oceanic plateaus sites of komatiite formation? *Geology*, v.19, p.376-379.
- STOTT, G.M. and CORFU, F. (1991) Uchi Subprovince, *in* Thurston, P.C., Williams, H.R., Sutcliffe, R.H. and Stott, G.M., eds., *Geology of Ontario*, Ontario Geological Survey, Special Volume 4, Part I, p.144-236.
- STYRT, M.M., BRACKMANN, A.J., HOLLAND, H.D., CLARK, P.C., PISUTHARNOND, V., ELDRIDGE, C.S. and OHMOTO, H. (1981) The mineralogy and isotopic composition of sulfur in hydrothermal sulfide/sulfate deposits on the East Pacific Rise, 21°N latitude. *Earth and Planetary Science Letters*, v.53, p.382-390.
- SUN, S.-S. and MCDONOUGH, W.F. (1989) Chemical and isotopic systematics of oceanic basalts: implications for mantle composition and processes, *in* A.D. Saunders and M.J. Norry, eds., *Magmatism in the Ocean Basins*. Geological Society, Special Publication No.42, p.313-345.
- SUN, S.-S., NESBITT, R.W. and SHARASKIN, A.Y. (1979) Geochemical characteristics of mid-ocean ridge basalts. *Earth and Planetary Science Letters*, v.44, p.119-138.
- SWAGER, C.D., WITT, W.K., GRIFFIN, T.G., AHMAT, A.L., HUNTER, W.M., MCGOLDRICK, P.J. and SYCHE, S. (1992) Late Archaean granite-greenstones of the Kalgoorlie terrane, Yilgarn Craton, Western Australia, *in* Glover, J.E. and Ho, S.E., eds., *The Archean: Terrains, Processes and Metallogeny*, Proceedings Volume for the Third International Archaean Symposium held in Perth, Western Australia, The University of Western Australia, Publication No. 22, p.107-122.

- SYMONS, P.M., ANDERSON, G., BEARD, T.J., HAMILTON, L.M., REYNOLDS, G.D., ROBINSON, J.M. and STALEY, R.W. (1988) The Boddington gold deposit, *in* Bicentennial Gold 88, Extended Abstracts, Oral Programme, Geological Society of Australia, v. 22, p.56-61.
- TANER, M.F. (1986) Metallogenic signification of alkaline intrusions: East Sullivan monzonitic stock, Val d'Or, Quebec. Canadian Institute of Mining and Metallurgy, v.79, no.887, p.62.
- TANER, M.F. and TRUDEL, P. (1989) Bourlamaque batholith and its gold potential, Val d'Or, Quebec. Canadian Institute of Mining and Metallurgy, Bulletin 82, p.33-42.
- TARNEY, J., WEAVER, S.D., SAUNDERS, A.D., PANKHURST, R.J. and BARKER, P.F. (1982) Volcanic evolution of the northern Antarctica peninsula and the Scotia arc, *in* Thorpe, R.S., ed., Andesites: Orogenic Andesites and Related Rocks. John Wiley Sons, New York, p.371-400.
- TAYLOR, B.E., ROBERT, F., BALL, M. and LEITCH, C.H.B. (1991) Mesozoic "Mother Lode type" gold deposits in North America: Primary vs secondary (meteoric) fluids. Geological Association of Canada/Mineralogical Association of Canada, Program with Abstracts, v. 16, p.A122.
- TESSIER, A.C. (1986) La géochimie du Stock de Siscoe et ses relations avec la géologie environnante, Val d'Or, Québec. B.Sc.A. thesis, Génie minéral, École Polytechnique, Montreal, 132 p.
- TESSIER, A. (1990) Structural evolution and host rock dilation during emplacement of gold-quartz vein at the Perron deposit, Val d'Or Quebec. M.Sc. thesis, Queen's University, Kingston, 242 p.
- TESSIER, A.C., TRUDEL, P. and IMREH, L. (1990) Petrology and alteration of the Siscoe stock at the Siscoe gold mine, Val d'Or, Quebec, *in* Rive, M., Verpaelst, P., Gagnon, Y., Lulin, J.-M., Riverin, G. and Simard, A., eds., The Northwestern Quebec Polymetallic Belt: A Summary of 60 Years of Mining Exploration. Canadian Institute of Mining and Metallurgy, Special Volume 43, p.285-298.
- THE NORTHERN MINER (1994) Aur downgrades reserves at Louvicourt significantly. Article in the April 25, 1994 Edition, p.1-2.
- THOMPSON, R.N., MORRISON, M.A., HENDRY, G.L., AND PARRY, S.J. (1984) An assessment of the relative roles of crust and mantle in magma genesis: An

elemental approach. Royal Society of London, Philosophical Transactions, v.A310, p.549-590.

TITLEY, S.R. and BEANE, R.E. (1981) Porphyry copper deposits, Part I. Geologic settings, petrology, and tectogenesis, *in* Skinner, B.J., ed., Economic Geology 75th Anniversary Volume. Economic Geology Publishing Company, El Paso, p.214-235.

TOURET, J. and DIETVORST, P. (1983) Fluid inclusions in high-grade anatectic metamorphites. Journal of Geological Society of London, v.140, p.635-649.

TOURIGNY, G. (1984) Géologie structurale et métamorphisme des roches précambriennes du Groupe de Kewagama dans la région de Cadillac-Malartic, Abitibi, Québec. M.Sc. thesis, Université de Montréal, Montreal, 85 p.

TOURIGNY, G., BROWN, A.C., HUBERT, C. and CRÉPEAU, R. (1989a) Synvolcanic and syntectonic gold mineralization at the Bousquet mine, Abitibi greenstone belt, Quebec. Economic Geology, v.84, p.1875-1890.

TOURIGNY, G., HUBERT, C., BROWN, A.C. and CRÉPEAU, R. (1989b) Structural control of gold mineralization at the Bousquet mine, Abitibi, Quebec. Canadian Journal of Earth Sciences, v.26, p.157-175.

TOURIGNY, G., DOUCET, D. and BOURGET, A. (1993) Geology of the Bousquet 2 mine: an example of a deformed, gold-bearing polymetallic sulfide deposit. Economic Geology, v.88, p.1578-1597.

UJIKE, O. (1975) Petrogenetic significance of normative corundum in calc-alkaline volcanic rock series. Journal of the Japanese Association of Mineralogists, Petrologists and Economic Geologists, v.70, p.85-92.

URABE, T. and SATO, T. (1978) Kuroko deposits of the Kosaka mine, northeast Honshu, Japan - products of submarine hot springs on Miocene sea floor. Economic Geology, v.73, p.161-179.

URABE, T. and MARUMO, K. (1991) A new model for Kuroko-type deposits of Japan. Episodes, v.14, p.246-251.

VALLEY, J.M. (1988) Granulites; melts and fluids in the deep crust. Journal of the Geological Society of India, v.31, p.161 (abstract).

VALLIANT, R.I. and HUTCHINSON, R.W. (1982) Stratigraphic distribution and genesis of gold deposits, Bousquet region, northwestern Quebec, *in* Hodder,

R.W. and Petruk, W., eds., *Geology of Canadian Gold Deposits*, Canadian Institute of Mining and Metallurgy, Special Volume 24, p.27-40.

VALLIANT, R.I., MONGEAU, C. and DOUCET, R. (1982) The Bousquet pyritic gold deposits, Bousquet region, *in* Hodder, R.W. and Petruk, W., eds., *Geology of Canadian Gold Deposits*, Canadian Institute of Mining and Metallurgy, Special Volume 24, p.41-49.

VERVOORT, J.D., WHITE, W.M., THORPE, R.I. and FRANKLIN, J.M. (1993) Postmagmatic thermal activity in the Abitibi greenstone belt, Noranda and Matagami districts: evidence from whole-rock Pb isotope data. *Economic Geology*, v.88, p.1598-1614.

VINOGRADOV, A.P. (1962) Average contents of the chemical elements in the principal types of igneous rocks of the Earth's crust. *Geokhimiya*, v.7, p.641-664.

VOGEL, D.E. (1972) *Geology of Villebon township, Abitibi-East county, and the north part of Frevill township, Pontiac county*. Ministère des Ressources Naturelles du Québec, DP-80, 90 p.

VRY, J., BROWN, P.E., VALLEY, J.W. and MORRISON, J. (1988) Constraints on granulite genesis from carbon isotope compositions of cordierite and graphite. *Nature*, v.332, p.66-68.

VU, L. (1990) *Geology of the Ferderber gold deposit and gold potential of the Bourlamaque batholith, Belmoral Mines Ltd., Val d'Or, Quebec*, *in* Rive, M., Verpaelst, P., Gagnon, Y., Lulin, J.-M., Riverin, G. and Simard, A., eds., *The Northwestern Quebec Polymetallic Belt: A Summary of 60 Years of Mining Exploration*. Canadian Institute of Mining and Metallurgy Special Volume 43, p.237-244.

WALSHE, J.F., KESLER, S.E., DUFF, D. and CLOKE, P.L. (1988) Fluid inclusion geochemistry of high-grade vein-hosted gold ore at the Pamour mine, Porcupine camp, Ontario. *Economic Geology*, v.83, p.1347-1368.

WEIR, R.H. JR. and KERRICK, D.M. (1984) Mineralogic and stable isotope relationships in gold-quartz veins in the southern Mother Lode, California. *Geological Society of America, Abstracts with Programs*, v.16, p.688.

WELLS, P.R.A. (1980) Thermal models for the magmatic accretion and subsequent metamorphism of continental crust. *Earth and Planetary Science Letters*, v.46, p.253-265.

- WHITFORD, D.J. and ASHLEY, P.M. (1992) The Scuddles volcanic-hosted massive sulfide deposit, western Australia: Geochemistry of the host rocks and evaluation of lithochemistry for exploration. *Economic Geology*, v.87, p.873-888.
- WINCHESTER, J.A. and FLOYD, P.A. (1976) Geochemical magma type discrimination: application to altered and metamorphosed basic igneous rocks. *Earth and Planetary Science Letters*, v.28, p.459-469.
- WINCHESTER, J.A. and FLOYD, P.A. (1977) Geochemical discrimination of different magma series and their differentiation products using immobile elements. *Chemical Geology*, v.20, p.325-343.
- WONG, L., DAVIS, D.W., KROGH, T.E. and ROBERT, F. (1991) U-Pb zircon and rutile chronology of Archean greenstone formation and gold mineralization in the Val d'Or region, Quebec. *Earth and Planetary Science Letters*, v.104, p.325-336.
- WONG, L., DAVIS, D.W., HANES, J.A., ARCHIBALD, D.A., HODGSON, C.J. and ROBERT, F. (1989) An integrated U/Pb and Ar/Ar geochronological study of the Archean Sigma gold deposit, Val d'Or, Quebec. *Geological Association of Canada/Mineralogical Association of Canada, Program with Abstracts*, v.14, p.A45.
- WYMAN, D. and KERRICH, R. (1988) Alkaline magmatism, major structures, and gold deposits: Implications for greenstone belt gold metallogeny. *Economic Geology*, v.83, p.454-461.
- WYMAN, D. and KERRICH, R. (1989) Archean shoshonitic lamprophyres associated with Superior Province gold deposits: Distribution, tectonic setting, noble metal abundances, and significance for gold mineralization, *in* Keays, R.R., Ramsay, W.R.H. and Groves, D.I., eds., *The Geology of Gold Deposits: The Perspective in 1988*, *Economic Geology Monograph 6*. Economic Geology Publishing Company, El Paso, p.661-667.
- WYMAN, D. and KERRICH, R. (1990) The genetic association of mesothermal gold deposits with accretionary plate tectonic regimes, *in* Robert, F., Sheahan, P.A. and Green, S.B., eds., *Greenstone Gold and Crustal Evolution*, NUNA Conference Volume, Val d'Or, Quebec. Geological Association of Canada-Mineral Deposits Division, p.226-227.
- YAMADA, E. (1984) Subaqueous pyroclastic flows: their development and their deposits, *in* Kokelaar, B.P. and Howells, M.F., eds., *Marginal Basin Geology -*

Volcanic and Associated Sedimentary and Tectonic Processes in Modern and Ancient Marginal Basins, The Geological Society, p.29-35.

YAMADA, R., SUYAMA, T. and OGUSHI, O. (1987) Gold-bearing siliceous ore of the Nurukawa kuroko deposit, Akita prefecture, Japan. *Mining Geology*, v.37, p.109-118.

ZWENG, P.L. and MORTENSEN, J.K. (1989) U/Pb age constraints on Archean magmatism and gold mineralization at the Camflo mine, Malartic, Quebec. Geological Society of America Annual Meeting, Abstracts with Programs, p.A351.

ZWENG, P.L., MORTENSEN, J.K. and DALRYMPLE, G.B. (1993) Thermochronology of the Camflo gold deposit, Malartic, Quebec: Implications for magmatic underplating and the formation of gold-bearing quartz veins. *Economic Geology*, v.88, p.1700-1721.

Appendix 1.

Sampling and Laboratory Analytical Techniques

Rocks with the freshest possible appearance were sampled, avoiding obvious alteration and surface alteration rinds. All samples came from outcrops, except samples 3851-91, 3867-91, 5685-92, 3846-91, and 3847-91 which were drill core samples and 5686-92 which was a grab sample taken from the muck pile of the dacitic caprock in which is sunk the shaft of the Louvicourt massive sulphide deposit. Samples gathered in 1991 may include < 1 millimetre-wide fracture-plane surfaces. Samples of 1991 were sent directly to the laboratory of the Centre de Recherches minérales in Sainte-Foy, Quebec for analytical preparation and analysis. Conversely, the samples taken in 1992 were \leq 1 centimetre-size chips, prepared in the field, avoiding all apparent alteration and fracture plane surfaces. These samples were crushed to < 200 mesh grain size, using a ceramic jaw crusher and an agate shatter box in the rock preparation laboratory of the Mineral Engineering Department at the École Polytechnique. All precautions were taken to minimize contamination during all stages of crushing. The prepared rock powders were then sent for analysis to the Centre de Recherches minérales in Sainte-Foy, Quebec. Sample numbers correspond to **designation** numbers used to identify samples sent to the laboratory. The last two numbers indicate the year of sampling.

Major element oxides were determined by X-ray fluorescence. A sample weighing two grammes was prepared as a borate capsule. The following table summarizes the detection limits and estimates of analytical precision.

Oxides	Detection Limit (%)	Range of Concentration (%)	Relative 2 Sigma Deviation (%)
SiO ₂	0.04	40.0 75.0	1 1
Al ₂ O ₃	0.04	2.00 20.0	5 2
Fe ₂ O ₃ (total)	0.02	2.0 10.0	5 2.5
MgO	0.05	0.5 15.0	5 2
CaO	0.02	1.00 10.0	10 2
Na ₂ O	0.1	2.0	5
K ₂ O	0.01	1.00 5.00	10 2
TiO ₂	0.01	0.50 2.00	2 1
MnO	0.01	0.10	10
P ₂ O ₅	0.01	0.20	5

Trace elements such as barium, cobalt, copper, lithium, nickel, scandium, vanadium and zinc were analyzed by plasma emission spectrometry using a 2 g sample taken into solution by perchloric and fluorhydric acids. The following table gives the detection limits and estimates of analytical precision of these analyses.

Element	Detection Limit (ppm)	Range of Concentration (ppm)	Relative 2 Sigma Deviation (ppm)
Barium	1	143 832	34 88
Cobalt	3	40 3	6 2
Copper	1	81 15	16 4
Lithium	1	21 15	6 2
Nickel	1	168 4	18 4
Scandium	1	N.A.	N.A.
Vanadium	2	200 8	34 6
Zinc	2	189 78	80 16

N.A. = not available

Other trace elements such as niobium, rubidium, strontium, tantalum, yttrium and zirconium were determined by X-ray fluorescence using a 4 g sample prepared as a pressed pellet. The following table gives the detection limits and estimates of analytical precision for these elements.

Element	Detection Limit (ppm)	Concentration (ppm)	Relative 2 Sigma Deviation (%)
Niobium	3	25	15
Rubidium	3	150	10
Strontium	3	250	10
Tantalum	5	25	15
Yttrium	3	50	15
Zirconium	3	200	10

Rare earth elements (lanthanum, cerium, neodymium, samarium, terbium, thulium and ytterbium) and some trace elements such as cesium, hafnium, scandium, tantalum, thorium and uranium were analyzed by neutron activation using a 0.5 g sample. The following table gives the detection limits and estimates of analytical precision by neutron activation for these elements.

Element	Detection Limit (ppm)	Concentration (ppm)	2 Sigma Deviation (ppm)
Cerium	2	37	2
Cesium	0.2	<0.2	---
Europium	0.1	2.0	0.1
Lanthanum	0.5	15.5	0.3
Lutecium	0.05	0.29	0.01
Neodymium	2	23	1
Samarium	0.05	6.34	0.18
Scandium	0.02	29.8	0.4
Tantalum	0.1	1.2	0.1
Terbium	0.1	0.9	0.05
Thorium	0.05	1.13	0.05
Uranium	0.5	0.6	0.4
Ytterbium	0.2	1.9	0.1

Total carbon in CO₂ was determined by a LECO CR-12 conduction oven using a 2 g sample, whereas total sulphur was determined by LECO SC-432 and LECO CS-132 conduction ovens using a 1 g sample.

For detailed explanations of the techniques used by the Centre de Recherches minérales in Sainte-Foy, Quebec, the reader is referred to the Centre's Volume 5 and Report 89-PR-05 (X-ray Fluorescence), Tome 1, p. 173 (Plasma Emission Spectrometry), Report 86-SP-011-A (Neutron Activation) and Volume 4 (LECO ovens).

Tables A2.1 to A2.6 of Appendix 2 compile analyses of extrusive and intrusive rocks gathered by the author from the Vassan, Central, Southern and Val d'Or domains. Various duplicate analyses for 1992 samples are included, as well as an accepted standard, the Mont Royal Gabbro (Gladney and Roelandts, 1990). No duplicate analyses were done on 1991 samples. However, one outcrop of pillowed flow material was sampled both in 1991 and 1992. The results in the following table show that 1) the clean and careful sampling and crushing techniques of 1992 may have helped avoid carbonate alteration but they did not help in detecting and avoiding hydrated samples, and 2) the trace element and especially the major element results of 1991 are comparable to those of 1992. This last point indicates, along with the other duplicate analyses included in Appendix 2, that the Centre de Recherches minérales obtains reproducible results from one year to the next and that "extremely clean and careful" sampling and crushing techniques are not necessarily needed, unless elements chosen for analysis are known to

Table A1.1 Analyses for the Same Outcrop Sampled in 1991 and 1992.

Element	3862-91	5666-92
SiO ₂ (%)	51.3	51.5
Al ₂ O ₃ (%)	19.4	20.8
Fe ₂ O ₃ (T) (%)	8.37	8.39
MgO (%)	4.56	4.97
CaO (%)	7.20	4.37
Na ₂ O (%)	4.37	5.64
K ₂ O (%)	0.01	0.01
TiO ₂ (%)	0.81	0.88
MnO (%)	0.14	0.14
P ₂ O ₅ (%)	0.10	0.09
L.O.I. (%)	4.25	3.62
CO ₂ (%)	1.21	0.15
S (%)	0.02	<0.01
Ba (ppm)	10	13
Co (ppm)	20	26
Cu (ppm)	52	54
Li (ppm)	32	33
Ni (ppm)	37	53
V (ppm)	171	197
Zn (ppm)	59	88
Nb (ppm)	5	5
Rb (ppm)	<3	<3
Sr (ppm)	210	170
Y (ppm)	27	27
Zr (ppm)	98	110
Zr/Y	3.6	4.1

be susceptible to contamination during crushing (e.g. Fe, Ni, and Cr contamination from a tungsten carbide shatter box).

Analyses in Appendix 4 were selected with permission from Desrochers (1994). These samples are from the Vassan, Central and Southern domains west of Val d'Or. Sample numbers correspond to **designation** numbers used to identify samples sent to the laboratory, and the last two numbers indicate the year of sampling and the letter indicates the domain (V: Vassan; C: Central; S: Southern). Samples were prepared and analyzed at the Centre de Recherches minérales in Sainte-Foy, Quebec. Scandium values in Appendix 4 were determined by plasma emission spectrometry whereas scandium results in Appendix 2 were produced by neutron activation analysis.

Appendix 5 contains selected analyses from Gaudreau et al. (1986) and Girault (1986). Analyses from Gaudreau et al. (1986) are identified by sample numbers starting with the designation **GAU** and the accompanying numbers corresponds to the analysis numbers used in that publication. Alteration rinds and quartz-carbonate veinlets of these samples were eliminated using a diamond saw at l'Université Laval. Samples were crushed at Chimatec Limited using a steel crusher for all samples except for those selected for analyses of low-concentration elements. For low-concentration elements, a part of the sample was crushed in a ceramic crusher in order to reduce contamination in Cr and Fe. The analyses were done at Chimatec Limited. Analyses from Girault (1986) are identified by sample numbers starting with the designation **GIR** and the

accompanying numbers correspond to the analysis numbers used in that thesis. Samples were prepared and analyzed at the Université scientifique, technique et médicale de Grenoble. No details are given regarding preparation and analytical techniques.

Appendix 2.

**Sampling Location Map, Major, Trace and Rare-Earth Element
Analyses, and the CIPW Norm for Flow and Intrusive Rock Samples
from the Vassan, Central, Southern and Val d'Or Domains.**

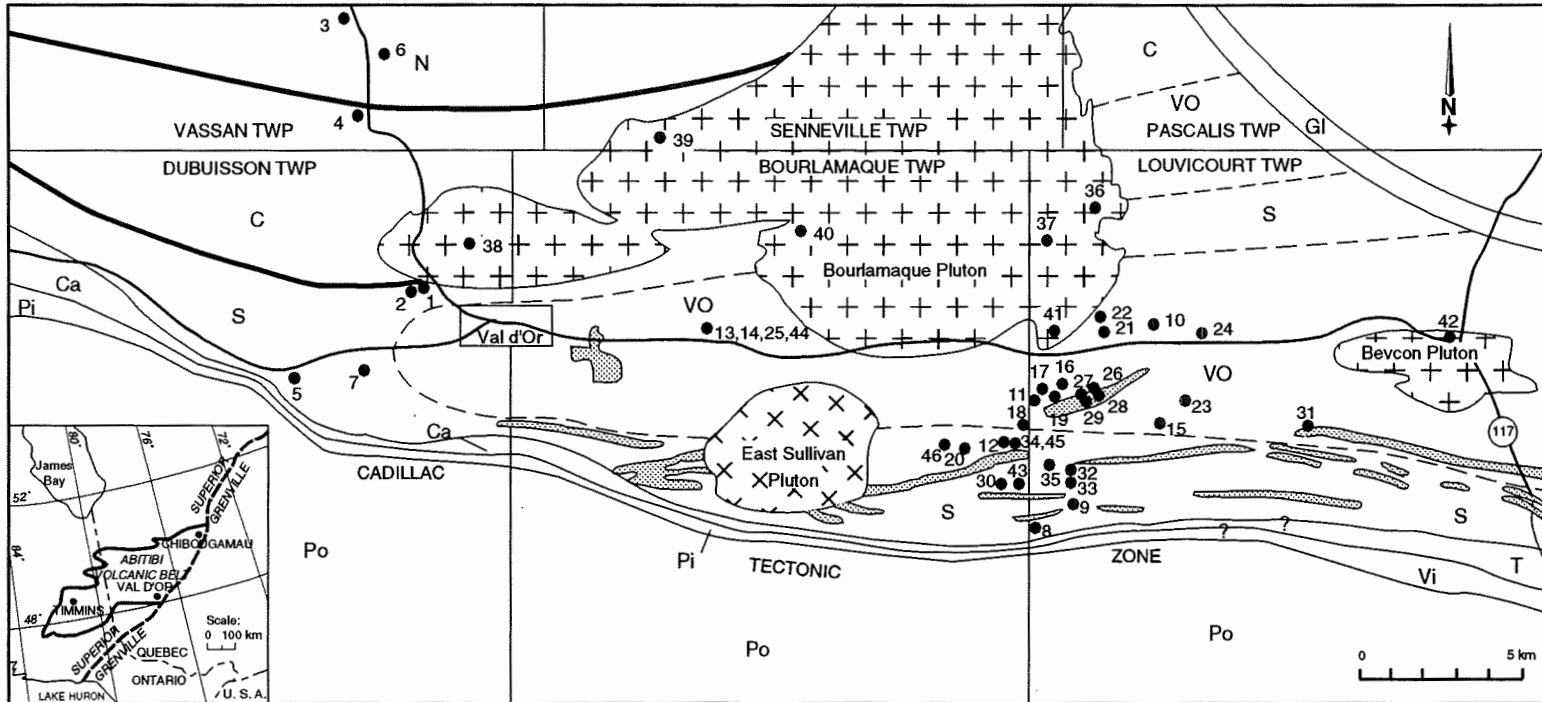


Figure A2.1 Location map of flow and intrusive samples taken by the author. These numbers are noted with the analyses and in Appendix 3 with the microscopic and macroscopic descriptions.

Table A2.1 . Major element (wt. %) analyses of extrusive rocks from the Southern, Central and Vassan domains, presented in recalculated volatile-free weight percent and the CIPW norm of recalculated analyses.

Sample No.	3833-91	3834-91	3835-91	3837-91	3838-91
UTM ZONE	18	18	18	18	18
UTM-EAST	290100	29000	287550	287800	285950
UTM-NORTH	5332450	5332400	5340550	5338000	5330450
Map No.	1	2	3	4	5
Name	Basalt flow	Mg Basalt flow	Basalt flow	Pillow. Basalt	Basalt flow
Affinity	Thol.	Thol.	Thol.	Thol.	Thol.
SiO ₂	54.71	48.15	52.57	55.31	53.00
TiO ₂	0.87	0.37	0.53	0.63	0.48
Al ₂ O ₃	14.14	19.91	16.59	14.16	15.67
Fe ₂ O ₃	14.14	8.48	11.44	13.34	12.48
MnO	0.22	0.14	0.20	0.22	0.21
MgO	5.31	11.48	8.11	5.44	7.23
CaO	7.38	8.39	7.86	8.29	8.89
Na ₂ O	3.11	2.80	2.48	2.52	1.73
K ₂ O	0.05	0.26	0.16	0.04	0.27
P ₂ O ₅	0.07	0.01	0.05	0.05	0.05
CO ₂ (%)	0.07	0.07	0.08	0.08	0.13
LOI (%)	1.91	4.21	3.11	2.37	2.93
S (%)	0.05	0.02	0.03	0.07	0.02
CIPW norm (weight %)					
Q	8.60	0.00	4.09	11.15	8.14
Or	0.31	1.57	0.98	0.25	1.60
Ab	26.66	23.88	21.21	21.59	14.80
An	24.72	41.23	33.94	27.48	34.53
Di	9.47	0.13	3.75	11.01	7.26
Hy	24.17	8.38	31.44	23.20	28.79
Ol	0.00	21.51	0.00	0.00	0.00
Mt	4.15	2.48	3.35	3.91	3.65
Il	1.67	0.71	1.01	1.20	0.93
Ap	0.17	0.03	0.12	0.12	0.12
Cc	0.16	0.16	0.18	0.18	0.30
Sp	0.02	0.05	0.03	0.01	0.02

Table A2.1 . Major element (wt. %) analyses of extrusive rocks from the Southern, Central and Vassan domains, presented in recalculated volatile-free weight percent and the CIPW norm of recalculated analyses (end).

Sample No.	3864-91	3865-91	5667-92	5668-92
UTM ZONE	18	18	18	18
UTM-EAST	288350	288100	308200	308900
UTM-NORTH	5339600	5330750	5324200	5324650
Map No.	6	7	8	9
Name	Komatiite	Mg Basalt flow	Basalt flow	Basalt flow
Affinity	Komat.	Thol.	Thol.	Thol.
SiO ₂	46.13	48.97	51.20	49.07
TiO ₂	0.35	0.39	0.87	1.14
Al ₂ O ₃	6.05	20.72	15.50	15.91
Fe ₂ O ₃	12.05	9.09	8.37	13.06
MnO	0.15	0.14	0.15	0.20
MgO	28.76	8.42	5.93	5.13
CaO	5.98	10.52	14.99	12.96
Na ₂ O	0.48	1.44	2.87	2.08
K ₂ O	0.03	0.27	0.08	0.41
P ₂ O ₅	0.02	0.02	0.03	0.04
CO ₂ (%)	0.63	0.04	0.70	0.12
LOI (%)	7.83	3.22	2.01	1.97
S (%)	0.02	0.04	0.03	0.06
CIPW norm (weight %)				
Q	0.00	0.53	0.10	0.77
Or	0.19	1.60	0.49	2.44
Ab	4.08	12.30	24.41	17.79
An	14.39	49.63	29.40	33.23
Di	9.08	2.06	33.24	25.47
Hy	30.77	30.38	7.32	14.06
Ol	36.65	0.00	0.00	0.00
Mt	3.53	2.66	2.44	3.83
Il	0.67	0.75	1.66	2.19
Ap	0.05	0.05	0.07	0.10
Cc	1.43	0.09	1.59	0.27
Sp	0.01	0.02	0.00	0.00

Table A2.2. Trace and rare earth element analyses in ppm of extrusive rocks from the Southern, Central and Vassan domains.

Sample No.	3833-91	3834-91	3835-91	3837-91	3838-01
UTM ZONE	18	18	18	18	18
UTM-EAST	290100	29000	287550	287800	285950
UTM-NORTH	5332450	5332400	5340550	5338000	5330450
Map No.	1	2	3	4	5
Name	Basalt flow	Mg basalt flow	Basalt flow	Pillow. flow	Basalt flow
Affinity	Thol.	Thol.	Thol.	Thol.	Thol.
Ni	84	206	125	65	82
Co	42	45	43	36	36
Sc	74	34	52	63	64
V	316	124	160	255	191
Cu	217	42	44	121	139
Zn	78	40	54	72	55
Li	10	28	19	7	9
K	420	2080	1320	330	2160
Rb	< 3	7	4	< 3	8
Cs	< 0.2	< 0.2	0.4	< 0.2	< 0.2
Ba	21	43	46	15	44
Sr	57	130	53	69	74
Ta	< 0.1	1.0	0.2	< 0.1	< 0.1
Nb	5	3	4	3	< 3
Hf	1.6	0.4	1.0	1.2	1.1
Zr	76	27	60	57	47
Ti	5100	2100	3060	3660	2820
Y	42	6	26	32	19
Th	0.21	< 0.05	0.16	0.07	0.15
U	1.1	0.5	< 0.5	< 0.5	< 0.5
La	3.3	0.9	2.6	2.9	1.8
Ce	9	< 2	6	7	4
Nd	5	2	3	4	5
Sm	2.3	0.5	1.6	1.8	1.1
Eu	0.8	0.2	0.5	0.7	0.5
Tb	0.7	< 0.1	0.4	0.5	0.3
Tm	1.0	0.3	0.6	0.7	0.6
Yb	5.8	1.3	3.4	4.4	3.2
Lu	0.92	0.22	0.58	0.71	0.59
Zr/Y	1.8	4.5	2.3	1.8	2.5
(La/Sm)N**	0.9	1.2	1.0	1.0	1.1
(La/Yb)N**	0.4	0.5	0.5	0.5	0.4
(Sm/Yb)N**	0.4	0.4	0.5	0.5	0.4

** Normalizing values of the C1 chondrite from Sun and McDonough (1989).

Table A2.2. Trace and rare earth element analyses in ppm of extrusive rocks from the Southern, Central and Vassan domains (end).

Sample No.	3864-91	3865-91	5667-92	5668-92
UTM ZONE	18	18	18	18
UTM-EAST	288350	288100	308200	308900
UTM-NORTH	5339600	5330750	5324200	5324650
Map No.	6	7	8	9
Name	Komatiite	Mg Basalt flow	Basalt flow	Basalt flow
Affinity	Komat.	Thol.	Thol.	Thol.
Ni	1500	96	100	178
Co	89	37	32	64
Sc	20	39	38	46
V	95	115	231	338
Cu	27	43	72	200
Zn	56	42	30	69
Li	5	11	< 1	2
K	250	2160	660	3320
Rb	3	10	< 3	14
Cs	0.8	0.3	< 0.2	0.4
Ba	12	43	11	39
Sr	12	100	98	110
Ta	< 0.1	0.2	0.1	< 0.1
Nb	3	3	3	4
Hf	0.5	0.6	1.1	1.1
Zr	30	36	60	57
Ti	1920	2280	5100	6700
Y	5	11	15	17
Th	< 0.05	0.09	0.17	0.07
U	< 0.5	< 0.5	< 0.5	< 0.5
La	0.7	1.4	1.6	2.1
Ce	4	3	5	6
Nd	3	5	3	5
Sm	0.7	0.8	1.6	1.8
Eu	0.2	0.3	0.5	0.7
Tb	0.2	0.2	0.4	0.4
Tm	0.3	< 0.2	0.3	0.3
Yb	0.5	1.6	1.7	1.9
Lu	0.09	0.28	0.26	0.29
Zr/Y	6.0	3.3	4.0	3.4
(La/Sm)N**	0.7	1.2	0.6	0.8
(La/Yb)N**	1.0	0.6	0.7	0.8
(Sm/Yb)N**	1.5	0.5	1.0	1.1

** Normalizing values of the C1 chondrite from Sun and McDonough (1989).

Table A2.3 . Major element (wt. %) analyses of extrusive rocks from the Val d'Or Domain, presented in recalculated volatile-free weight percent and the CIPW norm of recalculated analyses.

Sample No.	3840-91	3841-91	3851-91	3856-91	3859-91
UTM ZONE	18	18	18	18	18
UTM-EAST	310950	308200	307500	297300	297300
UTM-NORTH	5330650	5328200	5326200	5330900	5330900
Map No.	10	11	12	13	14
Name	Rhyol. flow	Rhyol. flow	Pillowed flo	Pillowed flo	Mafic flow
Affinity	Calc.	Calc.	Calc.	Calc.	Calc.
SiO ₂	74.73	76.04	58.53	64.75	58.29
TiO ₂	0.38	0.54	1.02	1.29	0.69
Al ₂ O ₃	14.05	12.98	17.66	14.66	19.29
Fe ₂ O ₃	2.18	0.66	7.13	8.40	6.33
MnO	0.02	0.02	0.10	0.06	0.12
MgO	1.42	0.19	5.47	3.30	5.28
CaO	0.59	2.97	6.92	1.17	6.61
Na ₂ O	5.71	5.65	2.78	5.40	0.95
K ₂ O	0.62	0.86	0.18	0.66	2.25
P ₂ O ₅	0.31	0.11	0.21	0.30	0.18
CO ₂ (%)	0.07	2.37	0.49	1.29	0.13
LOI (%)	1.32	2.71	3.70	2.99	3.88
S (%)	0.09	0.02	< 0.01	< 0.01	< 0.01
CIPW norm (weight %)					
Q	36.68	39.86	17.58	23.42	20.07
C	3.80	2.77	1.93	5.09	3.98
Z	0.01	0.01	0.01	0.01	0.01
Or	3.68	5.06	1.06	3.93	13.38
Ab	48.38	47.79	23.66	46.01	8.12
An	0.51	0.00	30.09	0.00	31.02
Di	0.00	0.00	0.00	0.00	0.00
Hy	3.85	0.11	20.50	14.51	19.67
Ol	0.00	0.00	0.00	0.00	0.00
Mt	1.58	0.00	2.08	2.45	1.84
Hm	0.00	0.00	0.00	0.00	0.00
Il	0.72	0.68	1.96	2.47	1.33
Ru	0.00	0.00	0.00	0.00	0.00
Ap	0.73	0.27	0.50	0.72	0.42
Cc	0.16	5.05	1.12	1.40	0.30
Ma	0.00	0.29	0.00	1.30	0.00
Sp	0.02	0.01	0.07	0.03	0.05

Table A2.3 . Major element (wt. %) analyses of extrusive rocks from the Val d'Or Domain, presented in recalculated volatile-free weight percent and the CIPW norm of recalculated analyses (continued).

Sample No.	3867-91	5654-92	5681-92*	5657-92
UTM ZONE	18	18	18	18
UTM-EAST	288100	309900	309900	308600
UTM-NORTH	5330600	5328525	5328525	5328050
Map No.	15	16	16	17
Name	Mafic flow	Rhyol. flow	Rhyol. flow	Silic. fels. flow
Affinity	Calc.	Calc.	Calc.	Calc.
SiO ₂	55.77	74.14	73.93	73.10
TiO ₂	1.29	0.77	0.78	1.03
Al ₂ O ₃	15.99	13.67	13.61	13.43
Fe ₂ O ₃	10.14	1.40	1.29	3.57
MnO	0.14	0.05	0.05	0.05
MgO	5.70	0.25	0.26	0.67
CaO	9.69	3.17	3.18	1.97
Na ₂ O	0.89	5.34	5.62	4.98
K ₂ O	0.09	1.06	1.10	0.99
P ₂ O ₅	0.30	0.16	0.18	0.22
CO ₂ (%)	0.67	2.48	2.46	1.51
LOI (%)	4.15	3.06	3.07	2.50
S (%)	0.14	0.02	0.03	< 0.01
	CIPW norm (weight %)			
Q	19.81	38.87	36.79	39.62
C	0.00	3.74	3.17	4.16
Z	0.01	0.02	0.06	0.01
Or	0.56	6.25	6.53	5.89
Ab	7.62	45.24	47.58	42.23
An	39.67	0.00	0.00	0.00
Di	2.13	0.00	0.00	0.00
Hy	23.24	0.28	0.34	1.25
Ol	0.00	0.00	0.00	0.00
Mt	2.96	0.00	0.00	2.38
Hm	0.00	0.70	0.64	0.14
Il	2.47	1.45	1.34	1.95
Ru	0.00	0.00	0.08	0.00
Ap	0.72	0.37	0.42	0.51
Cc	1.52	5.32	5.32	3.03
Ma	0.00	0.28	0.25	0.35
Sp	0.02	0.00	0.01	0.02

* 5681-92 is the duplicate analysis of 5654-92.

Table A2.3. Major element (wt. %) analyses of extrusive rocks from the Val d'Or domain, presented in recalculated volatile-free weight percent and the CIPW norm of recalculated analyses (end).

Sample No.	5655-92	5658-92	5671-92	5677-92	5683-92	5684-92	5686-92
UTM ZONE	18	18	18	18	18	18	18
UTM-EAST	308050	308650	306650	310450	310300	312800	313000
UTM-NORTH	5327300	5328150	5327200	5330700	5330600	5327850	5330000
Map No.	18	19	20	21	22	23	24
Name	Intermed. flow	Intermed. flow	Intermed. flow	Rhyol. flow	Rhyol. flow	Intermed. flow	Intermed. flow
Affinity	Calc.	Calc.	Calc.	Calc.	Calc.	Calc.	Calc.
SiO ₂	64.13	61.20	65.44	74.35	70.88	62.08	67.91
TiO ₂	0.95	1.29	1.37	0.40	0.79	1.02	0.74
Al ₂ O ₃	14.10	16.93	16.88	13.07	13.95	16.89	15.17
Fe ₂ O ₃	5.84	6.15	6.19	3.53	5.20	6.02	4.46
MnO	0.06	0.11	0.09	0.06	0.12	0.10	0.06
MgO	5.62	4.00	1.04	2.02	1.95	3.74	1.54
CaO	4.27	5.49	2.38	1.24	1.35	3.13	2.19
Na ₂ O	4.69	4.37	5.26	5.27	5.51	6.60	2.09
K ₂ O	0.01	0.24	1.07	< 0.01	0.08	0.22	5.48
P ₂ O ₅	0.33	0.22	0.29	0.06	0.16	0.21	0.36
CO ₂ (%)	2.86	1.75	1.52	0.49	0.09	1.54	2.83
LOI (%)	5.67	4.24	3.15	1.87	1.69	3.63	4.06
S (%)	< 0.01	< 0.01	< 0.01	< 0.01	0.01	< 0.01	< 0.01
CIPW norm (weight %)							
Q	25.62	20.17	26.82	39.17	32.99	12.87	32.67
C	5.99	4.05	6.95	3.43	2.94	4.16	5.80
Z	0.01	0.01	0.02	0.02	0.02	0.01	0.02
Or	0.06	1.44	6.34	0.00	0.49	1.32	32.54
Ab	39.83	37.19	44.73	44.66	46.73	56.10	17.77
An	1.09	14.89	0.40	2.65	5.10	4.48	0.00
Hy	19.43	15.23	7.70	5.97	5.94	14.84	4.57
Ol	0.00	0.00	0.00	0.00	0.00	0.00	0.00
Mt	1.70	1.79	1.80	2.57	3.78	1.75	1.30
Il	1.82	2.47	2.61	0.76	1.50	1.95	1.42
Ap	0.78	0.53	0.69	0.15	0.39	0.50	0.85
Cc	6.51	3.98	3.47	1.11	0.20	3.51	3.13
Ma	0.00	0.00	0.00	0.00	0.00	0.00	2.81
Sp	0.09	0.06	0.05	0.03	0.04	0.09	0.06

Table A2.4 . Trace and rare earth element analyses in ppm of extrusive rocks from the Val d'Or Domain.

Sample No.	3840-91	3841-91	3851-91	3856-91	3859-91
UTM ZONE	18	18	18	18	18
UTM-EAST	310950	308200	307500	297300	297300
UTM-NORTH	5330650	5328200	5326200	5330900	5330900
Map No.	10	11	12	13	14
Name	Rhyol. flow	Rhyol. flow	Pillowed flow	Pillowed flow	Mafic flow
Affinity	Calc.	Calc.	Calc.	Calc.	Calc.
Ni	8	38	74	71	56
Co	16	15	22	20	15
Sc	14	12	n.d.	33	n.d.
V	8	17	177	159	130
Cu	110	13	66	57	9
Zn	21	174	57	61	62
Li	11	4	37	18	28
K	5060	6890	1410	5310	18000
Rb	13	25	6	9	77
Cs	< 0.2	1.2	n.d.	1.3	n.d.
Ba	144	235	177	75	403
Sr	80	140	340	200	180
Ta	0.7	0.5	n.d.	3.6	n.d.
Nb	10	10	6	6	6
Hf	7.0	6.2	n.d.	5.9	n.d.
Zr	270	270	130	130	120
Ti	2220	3120	5880	7490	4020
Y	45	25	23	21	20
Th	4.1	2.6	n.d.	2.9	n.d.
U	0.9	1.0	n.d.	1.2	n.d.
La	29	16	n.d.	25	n.d.
Ce	75	39	n.d.	57	n.d.
Nd	48	23	n.d.	34	n.d.
Sm	11.0	5.7	n.d.	8.9	n.d.
Eu	1.6	1.2	n.d.	1.8	n.d.
Tb	1.4	0.8	n.d.	1.0	n.d.
Tm	0.6	0.2	n.d.	0.8	n.d.
Yb	5.2	2.7	n.d.	3.8	n.d.
Lu	0.82	0.36	n.d.	0.59	n.d.
Zr/Y	6.0	10.8	5.7	6.2	6.0
(La/Sm)N**	1.7	1.8	n.d.	1.8	n.d.
(La/Yb)N**	4.0	4.3	n.d.	4.7	n.d.
(Sm/Yb)N**	2.4	2.3	n.d.	2.6	n.d.

** Normalizing values of the C1 chondrite from Sun and McDonough (1989).
n.d. signifies not determined.

Table A2.4 . Trace and rare earth element analyses in ppm of
extrusive rocks from the Val d'Or Domain (continued).

Sample No.	3867-91	5654-92	5681-92*	5657-92
UTM ZONE	18	18	18	18
UTM-EAST	288100	309900	309900	308600
UTM-NORTH	5330600	5328525	5328525	5328050
Map No.	15	16	16	17
Name	Mafic flow	Rhyol. flow	Rhyol. flow	Silic. fels. flow
Affinity	Calc.	Calc.	Calc.	Calc.
Ni	115	18	18	12
Co	40	12	12	9
Sc	n.d.	n.d.	n.d.	22
V	135	40	38	125
Cu	51	85	81	118
Zn	47	38	43	59
Li	13	< 1	2	10
K	750	8880	9160	8050
Rb	3	24	23	34
Cs	n.d.	n.d.	n.d.	1.7
Ba	53	316	294	299
Sr	300	110	110	120
Ta	n.d.	n.d.	n.d.	0.8
Nb	7	11	10	10
Hf	n.d.	n.d.	n.d.	9.2
Zr	150	290	290	280
Ti	7430	4620	4700	6000
Y	27	35	34	35
Th	n.d.	n.d.	n.d.	3.1
U	n.d.	n.d.	n.d.	< 0.5
La	n.d.	n.d.	n.d.	18
Ce	n.d.	n.d.	n.d.	44
Nd	n.d.	n.d.	n.d.	24
Sm	n.d.	n.d.	n.d.	6.5
Eu	n.d.	n.d.	n.d.	1.9
Tb	n.d.	n.d.	n.d.	1.0
Tm	n.d.	n.d.	n.d.	0.5
Yb	n.d.	n.d.	n.d.	3.5
Lu	n.d.	n.d.	n.d.	0.50
Zr/Y	5.6	8.3	8.5	8.0
(La/Sm)N**	n.d.	n.d.	n.d.	1.8
(La/Yb)N**	n.d.	n.d.	n.d.	3.7
(Sm/Yb)N**	n.d.	n.d.	n.d.	2.1

* 5681-92 is the duplicate analysis of 5654-92.

** Normalizing values of the C1 chondrite from Sun and McDonough (1989).

n.d. signifies not determined.

Table A2.4 . Trace and rare earth element analyses in ppm of extrusive rocks from the Val d'Or Domain (end).

Sample No.	5655-92	5658-92	5671-92	5677-92	5683-92	5684-92	5686-92
UTM ZONE	18	18	18	18	18	18	18
UTM-EAST	308050	308650	306650	310450	310300	312800	313000
UTM-NORTH	5327300	5328150	5327200	5330700	5330600	5327850	5330000
Map No.	18	19	20	21	22	23	24
Name	Intermed. flow	Intermed. flow	Intermed. flow	Rhyol. flow	Rhyol. flow	Intermed. flow	Intermed. flow
Affinity	Calc.	Calc.	Calc.	Calc.	Calc.	Calc.	Calc.
Ni	183	95	23	8	3	47	0
Co	23	28	13	8	6	15	6
Sc	22	39	22	13	17	24	18
V	91	191	236	16	29	172	51
Cu	111	84	129	20	115	46	30
Zn	68	95	109	44	97	96	49
Li	47	31	26	18	20	50	35
K	80	1910	8550	0	660	1740	43500
Rb	< 3	8	39	< 3	3	7	79
Cs	< 0.2	0.8	1.8	< 0.2	< 0.2	0.4	1.7
Ba	150	169	380	5	33	135	849
Sr	410	290	180	110	110	160	99
Ta	1.0	0.5	0.6	0.5	0.5	0.3	0.6
Nb	10	9	11	10	12	8	11
Hf	6.9	5.6	6.8	7.3	7.1	4.2	5.9
Zr	230	190	300	310	330	210	280
Ti	5400	7370	7910	2340	4620	5820	4260
Y	21	23	37	38	40	27	38
Th	2.9	1.7	2.9	2.9	3.1	2.3	3.4
U	1.0	0.9	1.0	1.0	1.3	< 0.5	1.0
La	21	14	20	21	20	17	24
Ce	52	35	45	50	46	39	59
Nd	33	21	31	30	27	24	37
Sm	7.6	5.5	7.3	7.0	7.6	6.4	9.8
Eu	2.2	1.7	1.3	1.3	1.2	1.3	1.4
Tb	0.9	0.8	1.0	1.0	1.0	0.8	1.0
Tm	0.4	0.5	0.4	0.6	0.5	0.4	0.5
Yb	2.0	2.5	3.4	3.8	4.4	2.7	3.3
Lu	0.36	0.37	0.53	0.64	0.61	0.42	0.59
Zr/Y	11	8.3	8.1	8.2	8.3	7.8	7.4
(La/Sm)N**	1.8	1.6	1.8	1.9	1.7	1.7	1.6
(La/Yb)N**	7.5	4.0	4.2	4.0	3.3	4.5	5.2
(Sm/Yb)N**	4.2	2.4	2.4	2.0	1.9	2.6	3.3

** Normalizing values of the C1 chondrite from Sun and McDonough (1989).

Table A2.5. Major element analyses of intrusive rocks from the Val d'Or and Southern domains, presented in recalculated volatile-free weight percent and the CIPW norm of recalculated analyses.

Sample No.	3860-91	3869-91	3870-91	5652-92	5653-92	3847-91	5651-92
UTM ZONE	18	18	18	18	18	18	18
UTM-EAST	297350	310500	310300	310600	310625	307800	316800
UTM-NORTH	5330900	5328200	5328200	5328200	5328250	5325350	5326600
Map No.	25	26	27	28	29	30	31
Name	Gabbroic Intrusion	Dunrairie Sill	Dunrairie Sill	Dunrairie Sill	Dunrairie Sill	Dioritic Intrusion	Sigma-2 Gabbro
Affinity	Calc.	Calc.	Calc.	Calc.	Calc.	Thol.	Thol.
SiO ₂	55.83	67.25	67.08	67.08	65.90	50.89	47.78
TiO ₂	0.67	0.77	0.76	0.77	0.78	0.52	4.09
Al ₂ O ₃	14.52	15.73	14.58	15.57	15.40	13.29	12.94
Fe ₂ O ₃	7.93	6.39	8.89	6.97	8.17	10.49	18.54
MnO	0.13	0.06	0.07	0.07	0.09	0.19	0.23
MgO	7.39	4.24	5.76	4.65	4.32	14.02	4.23
CaO	7.27	0.89	0.45	0.85	1.29	7.87	8.22
Na ₂ O	3.58	2.89	0.30	2.11	2.20	2.60	3.44
K ₂ O	2.34	1.43	1.74	1.56	1.50	0.11	0.43
P ₂ O ₅	0.33	0.36	0.36	0.37	0.36	0.02	0.09
CO ₂ (%)	0.85	0.39	0.06	0.61	1.16	0.17	1.44
LOI (%)	2.50	3.51	4.11	3.95	4.34	3.71	2.43
S (%)	< 0.01	< 0.01	< 0.01	< 0.01	< 0.01	0.02	0.15

	CIPW norm (Weight %)						
Q	1.33	35.99	46.21	39.31	37.98	0.00	2.13
C	0.00	9.45	12.25	10.44	10.21	0.00	0.00
Z	0.03	0.05	0.05	0.05	0.06	0.01	0.02
Or	13.96	8.49	10.37	9.26	8.92	0.68	2.57
Ab	30.47	24.55	2.57	17.96	18.74	22.15	29.58
An	16.74	0.00	0.00	0.00	0.00	24.44	18.83
Di	10.11	0.00	0.00	0.00	0.00	11.03	10.85
Hy	22.06	16.80	23.55	17.93	18.10	26.18	20.63
Ol	0.00	0.00	0.00	0.00	0.00	11.16	0.00
Mt	2.32	1.86	2.60	2.03	2.39	3.07	5.46
Il	1.29	1.46	1.45	1.48	1.48	0.99	7.88
Ap	0.79	0.88	0.92	0.89	0.86	0.05	0.22
Cc	1.95	0.79	0.00	0.71	1.52	0.39	3.28
Ma	0.00	0.09	0.12	0.58	0.96	0.00	0.00
Sp	0.05	0.10	0.12	0.09	0.07	0.07	0.06

Table A2.5. Major element analyses of intrusive rocks from the Val d'Or and Southern domains, presented in recalculated volatile-free weight percent and the CIPW norm of recalculated analyses (continued).

Sample No.	5663-92	5669-92	5673-92	5674-92	5678-92*	MRG-1*
UTM ZONE	18	18	18	18	—	—
UTM-EAST	308850	308900	307600	308650	—	—
UTM-NORTH	5325850	5325475	5326200	5326025	—	—
Map No.	32	33	34	35	—	—
Name	Dioritic Intrusion	Dioritic Intrusion	Paramaque Sill	Dioritic Intrusion	Mont Royal Standard	Mont Royal Standard
Affinity	Thol.	Thol.	Thol.	Thol.		
SiO ₂	52.33	48.96	51.20	49.85	39.10	39.12+/-0.54
TiO ₂	1.27	2.19	0.93	1.29	3.75	3.77+/-0.15
Al ₂ O ₃	13.80	14.42	14.86	14.44	8.46	8.47+/-0.28
Fe ₂ O ₃	14.83	19.61	11.93	14.64	17.70	17.94+/-0.39
MnO	0.21	0.23	0.16	0.25	0.17	0.17+/-0.01
MgO	6.43	4.38	7.05	7.30	13.50	13.55+/-0.32
CaO	9.06	6.80	9.36	8.79	14.60	14.70+/-0.34
Na ₂ O	1.87	2.73	2.46	2.81	0.59	0.74+/-0.08
K ₂ O	0.10	0.17	2.01	0.58	0.18	0.18+/-0.03
P ₂ O ₅	0.09	0.52	0.03	0.05	0.05	0.08+/-0.03
CO ₂ (%)	0.40	0.22	5.06	0.51	1.30	1.07+/-0.08
LOI (%)	2.88	3.00	8.19	2.86	1.39	1.56+/-0.43
S (%)	< 0.01	< 0.01	0.15	0.13	0.06	610+/-100ppm

	CIPW norm (Weight %)					
Q	9.17	5.08	6.60	0.00	n.d.	n.d.
C	0.00	0.00	3.27	0.00	n.d.	n.d.
Z	0.02	0.03	0.01	0.01	n.d.	n.d.
Or	0.62	1.00	12.01	3.49	n.d.	n.d.
Ab	16.05	23.45	21.03	24.10	n.d.	n.d.
An	29.26	27.01	14.81	25.30	n.d.	n.d.
Di	10.88	2.12	0.00	12.60	n.d.	n.d.
Hy	26.48	29.81	30.44	24.98	n.d.	n.d.
Ol	0.00	0.00	0.00	1.99	n.d.	n.d.
Mt	4.35	5.78	3.49	4.30	n.d.	n.d.
Il	2.44	4.22	1.79	2.47	n.d.	n.d.
Ap	0.22	1.25	0.08	0.12	n.d.	n.d.
Cc	0.91	0.50	11.53	1.16	n.d.	n.d.
Ma	0.00	0.00	0.00	0.00	n.d.	n.d.
Sp	0.06	0.05	0.10	0.06	n.d.	n.d.

* Major element oxide analysis for 5678-92 and MRG-1 (Gladney and Roelandts, 1990) are given in volatile-bearing weight percent form.

n.d. signifies not determined.

Table A2.5 . Major element analyses of intrusive rocks from the Val d'Or and Southern domains, presented in recalculated volatile-free weight percent and the CIPW norm of recalculated analyses (continued).

Sample No.	3878-91	3880-91	5659-92	5660-92	5661-92	5680-92*	5662-92
UTM ZONE	18	18	18	18	18	18	18
UTM-EAST	310350	308700	291000	297525	300500	300500	309100
UTM-NORTH	5333900	5332800	5333575	5336950	5333625	5333625	5330150
Map No.	36	37	38	39	40	40	41
Name	Bourl. Int.	Bourl. Int.	Bourl. Int.	Bourl. Int.	Bourl. Int.	Bourl. Int.	Bourl. Int.
	Diorite	Diorite	Diorite	Diorite	Diorite	Diorite	Diorite
Affinity	Chal.	Chal.	Chal.	Chal.	Chal.	Chal.	Chal.
SiO ₂	69.24	62.78	60.76	59.83	58.65	58.90	61.42
TiO ₂	0.43	0.69	0.75	0.65	0.91	0.90	0.87
Al ₂ O ₃	15.79	16.62	17.98	17.79	17.86	17.61	15.97
Fe ₂ O ₃	4.35	6.68	6.82	7.24	7.03	7.23	6.49
MnO	0.04	0.09	0.10	0.11	0.07	0.07	0.09
MgO	1.77	2.49	2.90	3.33	3.79	3.71	4.73
CaO	2.77	6.02	5.84	6.69	5.85	5.82	5.42
Na ₂ O	4.48	3.61	3.99	3.56	5.56	5.48	4.59
K ₂ O	1.04	0.86	0.59	0.67	0.12	0.12	0.28
P ₂ O ₅	0.08	0.15	0.26	0.13	0.16	0.16	0.15
CO ₂ (%)	0.91	0.99	1.92	0.51	2.19	2.17	3.50
LOI (%)	2.66	3.15	3.93	2.75	4.60	4.54	6.10
S (%)	< 0.01	< 0.01	< 0.01	< 0.01	< 0.01	< 0.01	< 0.01
	CIPW norm (weight %)						
Q	31.35	21.88	21.28	15.60	10.95	11.69	22.14
C	4.53	1.41	5.16	0.48	3.34	3.23	6.69
Z	0.04	0.21	0.03	0.02	0.03	0.03	0.04
Or	6.20	5.10	3.51	3.98	0.69	0.69	1.65
Ab	38.02	30.74	33.93	30.27	47.30	46.65	39.02
An	7.60	22.91	15.47	29.45	14.45	14.41	4.00
Di	0.00	0.00	0.00	0.00	0.00	0.00	0.00
Hy	8.85	13.03	14.15	15.91	16.32	16.36	18.11
Mt	1.27	1.95	1.99	2.11	2.05	2.11	1.89
Il	0.83	1.32	1.44	1.24	1.74	1.72	1.67
Ap	0.20	0.37	0.62	0.32	0.38	0.38	0.36
Cc	2.08	2.26	4.38	1.16	4.99	4.95	7.97
Sp	0.04	0.03	0.07	0.05	0.05	0.05	0.05

* 5680-92 is the duplicate analysis of 5661-92.

Table A2.5. Major element analyses of intrusive rocks from the Val d'Or and Southern domains, presented in recalculated volatile-free weight percent and the CIPW norm of recalculated analyses (end).

Sample No.	5685-92	3846-91	3857-91	5672-92	5682-92	5687-92*
UTM ZONE	18	18	18	18	18	18
UTM-EAST	320400	307900	297300	307550	306800	306800
UTM-NORTH	5329400	5325350	5330900	5326300	5327500	5327500
Map No.	42	43	44	45	46	46
Name	Bevcon Int. Diorite	Feld.(Qz-Hbd) Porphyry	Feldspar Porphyry	Feld.(Qz) Porphyry	Feld.(Qz) Porphyry	Feld.(Qz) Porphyry
Affinity	Chal.	Chal.	Chal.	Chal.	Chal.	Chal.
SiO ₂	68.51	61.20	59.19	64.26	63.63	63.71
TiO ₂	0.49	0.46	0.86	0.43	0.35	0.36
Al ₂ O ₃	15.81	15.89	17.44	16.85	16.68	16.65
Fe ₂ O ₃	4.64	5.94	7.76	3.61	3.73	3.71
MnO	0.04	0.07	0.11	0.06	0.07	0.07
MgO	1.90	4.92	3.49	3.13	3.28	3.35
CaO	2.82	5.74	6.13	6.08	5.82	5.82
Na ₂ O	4.60	4.40	4.27	5.22	5.18	5.05
K ₂ O	1.14	1.18	0.40	0.24	1.11	1.13
P ₂ O ₅	0.06	0.20	0.35	0.12	0.14	0.14
CO ₂ (%)	1.61	0.11	0.07	2.49	4.14	4.24
LOI (%)	3.41	1.80	2.69	4.37	6.37	6.42
S (%)	< 0.01	0.09	0.32	< 0.01	< 0.01	< 0.01

CIPW norm (weight %)

Q	30.98	10.77	12.25	20.69	21.66	22.57
C	5.71	0.00	0.00	2.91	6.17	6.54
Z	0.04	0.03	0.04	0.02	0.02	0.02
Or	6.76	7.00	2.38	1.42	6.61	6.72
Ab	39.05	37.37	36.33	44.29	43.92	42.84
An	3.57	20.23	27.42	13.90	2.14	1.54
Di	0.00	5.50	0.52	0.00	0.00	0.00
Hy	9.41	15.96	16.30	11.43	12.10	12.24
Mt	1.35	1.73	2.26	1.05	1.09	1.08
Il	0.93	0.89	1.65	0.81	0.67	0.69
Ap	0.15	0.47	0.83	0.30	0.33	0.33
Cc	3.68	0.25	0.16	5.68	9.48	9.72
Sp	0.07	0.10	0.04	0.10	0.10	0.14

* 5687-92 is the duplicate analysis of 5682-92.

Table A2.6. Trace and rare earth element analyses in ppm for intrusive rocks from the Val d'Or and Southern domains.

Sample No.	3860-91	3869-91	3870-91	5652-92	5653-92	3847-91	5651-92
UTM ZONE	18	18	18	18	18	18	18
UTM-EAST	297350	310500	310300	310600	310625	307800	316800
UTM-NORTH	5330900	5328200	5328200	5328200	5328250	5325350	5326600
Map No.	25	26	27	28	29	30	31
Name	Gabbroic Intrusion	Dunraine Sill	Dunraine Sill	Dunraine Sill	Dunraine Sill	Dioritic Intrusion	Sigma-2 Gabbro
Affinity	Calc.	Calc.	Calc.	Calc.	Calc.	Thol.	Thol.
Ni	112	53	53	55	51	204	13
Co	30	14	22	17	17	44	51
Sc	21	18	n.d.	n.d.	n.d.	34	66
V	114	79	76	88	82	151	235
Cu	36	4	4	8	7	20	124
Zn	67	48	59	50	49	58	73
Li	19	35	44	33	24	24	22
K	17900	11500	13900	12300	11900	910	3490
Rb	71	23	28	25	29	5	11
Cs	3.0	1.0	n.d.	n.d.	n.d.	0.8	1.1
Ba	636	398	629	455	314	28	196
Sr	850	37	19	34	55	69	100
Ta	2.8	3.4	n.d.	n.d.	n.d.	0.1	< 0.1
Nb	4	10	9	10	10	3	5
Hf	3.2	5.6	n.d.	n.d.	n.d.	0.7	2.6
Zr	150	250	230	260	260	38	74
Ti	3780	4440	4380	4440	4440	3000	24000
Y	17	30	27	31	32	9	43
Th	4.80	3.40	n.d.	n.d.	n.d.	< 0.05	0.19
U	0.8	0.9	n.d.	n.d.	n.d.	1.0	0.5
La	32	25	n.d.	n.d.	n.d.	1	3
Ce	66	61	n.d.	n.d.	n.d.	4	11
Nd	31	38	n.d.	n.d.	n.d.	3	11
Sm	6.5	9.4	n.d.	n.d.	n.d.	0.9	4.9
Eu	1.6	1.8	n.d.	n.d.	n.d.	0.3	2.0
Tb	0.6	1.0	n.d.	n.d.	n.d.	0.2	1.3
Tm	0.5	0.5	n.d.	n.d.	n.d.	0.3	0.7
Yb	1.5	3.3	n.d.	n.d.	n.d.	1.3	4.3
Lu	0.30	0.49	n.d.	n.d.	n.d.	0.20	0.60
Zr/Y	8.8	8.3	8.5	8.4	8.1	4.2	1.7
(La/Sm)N**	3.2	1.7	n.d.	n.d.	n.d.	1.0	0.4
(La/Yb)N**	15	5.4	n.d.	n.d.	n.d.	0.8	0.5
(Sm/Yb)N**	4.8	3.2	n.d.	n.d.	n.d.	0.8	1.3

n.d. signifies not determined.

** Normalizing values of the C1 chondrite from Sun and McDonough (1989).

Table A2.6. Trace and rare earth element analyses in ppm for intrusive rocks from the Val d'Or and Southern domains (continued).

Sample No.	5663-92	5669-92	5673-92	5674-92	5678-92	MRG-1*
UTM ZONE	18	18	18	18	—	—
UTM-EAST	308850	308900	307600	308650	—	—
UTM-NORTH	5325850	5325475	5326200	5326025	—	—
Map No.	32	33	34	35	—	—
Name	Dioritic Intrusion	Dioritic Intrusion	Paramaque Sill	Dioritic Intrusion	Mont Royal Standard	Mont Royal Standard
Affinity	Thol.	Thol.	Thol.	Thol.		
Ni	89	22	84	127	225	193.2+/-18
Co	43	32	34	41	85	87+/-7
Sc	44	n.d.	n.d.	n.d.	51#	55+/-5
V	315	129	249	317	462	526+/-33
Cu	94	73	83	134	188	134+/-14
Zn	118	170	34	71	210	191+/-15
Li	20	16	33	21	7	4.2+/-1.0
K	830	1330	15400	4650	1490	0.151 +/-0.022 (%)
Rb	3	< 3	75	22	8	8.5+/-2.4
Cs	0.5	n.d.	n.d.	n.d.	n.d.	0.57+/-0.16
Ba	37	41	278	105	46	61+/-23
Sr	94	130	150	110	300	266+/-13
Ta	0.1	n.d.	n.d.	n.d.	n.d.	0.80+/-0.5
Nb	5	8	4	4	19	20+/-4
Hf	2.1	0.0	0.0	0.0	n.d.	3.76+/-0.22
Zr	100	160	53	68	130	108+/-16
Ti	7370	12600	5160	7430	22500	2.26+/-0.09 (%)
Y	32	73	16	22	13	14+/-5
Th	0.26	n.d.	n.d.	n.d.	n.d.	0.93+/-0.18
U	0.8	n.d.	n.d.	n.d.	n.d.	0.24+/-0.04
La	4	n.d.	n.d.	n.d.	n.d.	—
Ce	11	n.d.	n.d.	n.d.	n.d.	—
Nd	7	n.d.	n.d.	n.d.	n.d.	—
Sm	3.4	n.d.	n.d.	n.d.	n.d.	—
Eu	1.0	n.d.	n.d.	n.d.	n.d.	—
Tb	0.7	n.d.	n.d.	n.d.	n.d.	—
Tm	0.5	n.d.	n.d.	n.d.	n.d.	—
Yb	3.1	n.d.	n.d.	n.d.	n.d.	—
Lu	0.52	n.d.	n.d.	n.d.	n.d.	—
Zr/Y	3.1	2.2	3.3	3.1	10	—
(La/Sm)N**	0.8	n.d.	n.d.	n.d.	n.d.	—
(La/Yb)N**	0.9	n.d.	n.d.	n.d.	n.d.	—
(Sm/Yb)N**	1.2	n.d.	n.d.	n.d.	n.d.	—

n.d. signifies not determined.

* Values of Mont Royal Standard from Gladney and Roelandts (1990).

** Normalizing values of the C1 chondrite from Sun and McDonough (1989).

Determined by plasma emission spectrometry.

Table A2.6. Trace and rare earth element analyses in ppm of intrusive rocks from the Val d'Or and Southern domains (continued).

Sample No.	3878-91	3880-91	5659-92	5660-92	5661-92	5680-92*	5662-92
UTM ZONE	18	18	18	18	18	18	18
UTM-EAST	310350	308700	291000	297525	300500	300500	309100
UTM-NORTH	5333900	5332800	5333575	5336950	5333625	5333625	5330150
Map No.	36	37	38	39	40	40	41
Name	Bourl. Int.	Bourl. Int.	Bourl. Int.	Bourl. Int.	Bourl. Int.	Bourl. Int.	Bourl. Int.
Affinity	Diorite	Diorite	Diorite	Diorite	Diorite	Diorite	Diorite
	Calc.	Calc.	Calc.	Calc.	Calc.	Calc.	Calc.
Ni	9	19	23	39	42	46	58
Co	8	13	16	21	18	20	16
Sc	13	n.d.	16	18	n.d.	n.d.	23
V	56	99	98	119	130	150	142
Cu	7	17	118	50	11	10	8
Zn	27	37	80	83	32	29	31
Li	14	11	25	19	16	18	19
K	8380	6890	4730	5400	920	910	2080
Rb	37	25	12	19	< 3	3	7
Cs	0.4	n.d.	0.5	< 0.2	n.d.	n.d.	0.2
Ba	274	246	164	186	120	144	68
Sr	160	260	390	280	260	260	180
Ta	5.7	n.d.	0.5	0.3	n.d.	n.d.	0.4
Nb	8	7	9	7	7	7	8
Hf	5.1	n.d.	3.8	2.5	n.d.	n.d.	4.4
Zr	170	1000	150	110	150	150	190
Ti	2520	4020	4320	3780	5160	5160	4860
Y	27	34	19	22	28	27	23
Th	6.00	n.d.	0.83	2.60	n.d.	n.d.	1.90
U	2.7	n.d.	0.6	0.7	n.d.	n.d.	< 0.5
La	23	n.d.	14	14	n.d.	n.d.	14
Ce	50	n.d.	29	30	n.d.	n.d.	32
Nd	21	n.d.	16	14	n.d.	n.d.	20
Sm	5.2	n.d.	4.3	3.7	n.d.	n.d.	5.0
Eu	1.0	n.d.	1.2	1.2	n.d.	n.d.	1.1
Tb	0.8	n.d.	0.5	0.6	n.d.	n.d.	0.7
Tm	0.5	n.d.	0.3	0.4	n.d.	n.d.	0.4
Yb	3.7	n.d.	1.9	2.4	n.d.	n.d.	2.6
Lu	0.57	n.d.	0.22	0.39	n.d.	n.d.	0.35
Zr/Y	6.3	29	7.9	5.0	5.4	5.6	8.3
(La/Sm)N**	2.9	n.d.	2.1	2.4	n.d.	n.d.	1.8
(La/Yb)N**	4.5	n.d.	5.3	4.2	n.d.	n.d.	3.9
(Sm/Yb)N**	1.6	n.d.	2.5	1.7	n.d.	n.d.	2.1

* 5680-92 is the duplicate analysis of 5661-92.

n.d. signifies not determined.

** Normalizing values of the C1 chondrite from Sun and McDonough (1989).

Table A2.6. Trace and rare earth element analyses in ppm of intrusive rocks from the Val d'Or and Southern domains (end).

Sample No.	5685-92	3846-91	3857-91	5672-92	5682-92	5687-92*
UTM ZONE	18	18	18	18	18	18
UTM-EAST	320400	307900	297300	307550	306800	306800
UTM-NORTH	5329400	5325350	5330900	5326300	5327500	5327500
Map No.	42	43	44	45	46	46
Name	Bevcon Int.	Feld.(Qz-Hbd)	Feldspar	Feld.(Qz)	Feld.(Qz)	Feld.(Qz)
Affinity	Diorite	Porphyry	Porphyry	Porphyry	Porphyry	Porphyry
	Calc.	Calc.	Calc.	Calc.	Calc.	Calc.
Ni	6	123	21	58	58	66
Co	8	21	11	15	11	13
Sc	19	12	15	n.d.	n.d.	n.d.
V	64	74	99	69	62	64
Cu	62	102	42	6	5	2
Zn	37	48	53	15	47	50
Li	25	36	15	34	36	50
K	9130	9460	3240	1910	8630	8800
Rb	36	30	14	7	40	41
Cs	0.6	1.3	0.6	n.d.	n.d.	n.d.
Ba	257	325	141	138	529	712
Sr	150	800	300	440	460	450
Ta	0.4	0.3	0.7	n.d.	n.d.	n.d.
Nb	7	4	12	4	4	5
Hf	4.6	2.7	3.6	n.d.	n.d.	n.d.
Zr	200	120	170	110	100	100
Ti	2820	2700	5040	2460	1980	2040
Y	31	8	17	4	7	7
Th	1.90	3.30	2.20	n.d.	n.d.	n.d.
U	< 0.5	1.0	< 0.5	n.d.	n.d.	n.d.
La	12	22	19	n.d.	n.d.	n.d.
Ce	27	50	37	n.d.	n.d.	n.d.
Nd	16	27	19	n.d.	n.d.	n.d.
Sm	5.2	4.8	4.3	n.d.	n.d.	n.d.
Eu	1.0	1.3	1.2	n.d.	n.d.	n.d.
Tb	0.7	0.4	0.6	n.d.	n.d.	n.d.
Tm	0.4	0.2	0.4	n.d.	n.d.	n.d.
Yb	3.1	0.8	1.5	n.d.	n.d.	n.d.
Lu	0.50	0.14	0.28	n.d.	n.d.	n.d.
Zr/Y	6.5	14	10	26	14	14
(La/Sm)N**	1.5	3.0	2.9	n.d.	n.d.	n.d.
(La/Yb)N**	2.8	20	9.1	n.d.	n.d.	n.d.
(Sm/Yb)N**	1.9	6.7	3.2	n.d.	n.d.	n.d.

* 5687-92 is the duplicate analysis of 5682-92.

n.d. signifies not determined.

** Normalizing values of the C1 chondrite from Sun and McDonough (1989).

Appendix 3.

**Macroscopic and Microscopic Descriptions of Flow and
Intrusive Rock Samples from the Vassan, Central, Southern and Val d'Or Domains.**

Appendix 3a. Macroscopic and microscopic descriptions of extrusive rock samples from the Southern, Central and Vassan domains.

Sample No.	3833-91	3834-91	3835-91
Map No.*	1	2	3
Field Description	Massive, aphanitic, mafic flow, beige-green a/s, green-black f/s, no HCl reaction, no vesicularity, epidote alteration.	Massive, aphanitic mafic flow, whitish a/s; grey f/s, no HCl reaction.	Massive, aphanitic mafic flow, buff a/s, green-black f/s, no HCl reaction, epidote alteration observed.
Microscopic Description	Composed of abundant actinolite/tremolite and plagioclase and epidote, minor chlorite.	Composed essentially of tremolite/ actinolite and talc with abundant epidote, plagioclase broken up and altered to epidote.	Highly epidotized mafic rock where primary mafic minerals are altered to actinolite - tremolite, chlorite and minor amounts of talc.

Sample No.	3837-91	3838-91	3864-91
Map No.*	4	5	6
Field Description	Pillowed mafic flow, light green a/s, green fresh surface with chlorite porphyroblasts, no HCl reaction, selvages 1-2 cm wide.	Massive mafic flow, aphanitic, creamy a/s, green-black f/s, no HCl reaction.	Massive mafic flow, aphanitic, buff-green a/s, dark green f/s, epidote alteration, calcite veinlets present but avoided.
Microscopic Description	Extremely fine-grained, homogeneous texture of abundant epidote, chlorite and small amounts of quartz and talc, traces of opaques, plagioclase grains are not identifiable.	Felted mass of actinolite/tremolite, chlorite and epidote, plagioclase altered to epidote or to albite.	Felted mass composed primarily of actinolite/tremolite and lesser amounts of chlorite, minor carb. alteration, minor plagioclase.

a/s: altered surface; f/s: fresh surface; rxn: reaction; qz: quartz; plag: plagioclase; ser: sericite; carb: carbonate; opa: opaques; *: Map number on Figure A2.1 in Appendix 2.

Appendix 3a. Macroscopic and microscopic descriptions of extrusive rock samples from the Southern, Central and Vassan domains (end).

Sample No.	3865-91	5667-92	5668-92
Map No.*	7	8	9
Field Description	Massive mafic flow, aphanitic with minor amounts of plagioclase phenocrysts, buff/cream a/s, dark green f/s,	Massive, mafic flow, aphanitic, cream a/s, green-grey f/s, abundant epidote, traces of magnetite.	Massive mafic flow, aphanitic, buff a/s, light grey f/s, no HCl reaction, traces of sulphides.
Microscopic Description	Felted-pilotaxitic texture of plagioclase and actinolite/tremolite, abundant epidote alteration.	Composed essentially of epidote with lesser quantities of actinolite/tremolite, little plagioclase left, traces of carbonate and opaques.	Ophitic texture made of flaky masses of actinolite-tremolite, chlorite, plagioclase and epidote, traces of opaques and quartz.

a/s: altered surface; f/s: fresh surface; rxn: reaction; qz: quartz; plag: plagioclase; ser: sericite; carb: carbonate; opaq: opaques; *: Map number on Figure A2.1 in Appendix 2.

Appendix 3b. Macroscopic and microscopic descriptions of extrusive rock samples from the Val d'Or domain.

Sample No.	3840-91	3841-91	3851-91
Map No.*	10	11	12
Field Description	Felsic flow, aphanitic, with porphyroblasts of chlorite, white a/s, light grey f/s, no HCl rxn, traces of pyrite.	Sheared felsic flow, aphanitic, creamy a/s, light grey f/s, HCl rxn along schistosity planes, traces of pyrite.	Drill core sample of pillowed flow, aphanitic, medium green f/s, little chlorite and carbonate alteration, 1 cm average width of pillow selvage.
Microscopic Description	Felsic flow with glomeroporphyritic plagioclase, small amounts of sericite and chlorite.	Evidence of silicification, fine plag. phenocrysts altered to carb., set in very fine matrix of plag-qz-carb-ser-opaq.	Evidence of silicification, plag. grains are highly epidotized, clear albite grains present, small amount of carb., traces of chlorite and leucoxene.

Sample No.	3856-91	3859-91	3867-91
Map No.*	13	14	15
Field Description	Pillowed basalt, evidence of silicification, light green a/s, medium green f/s, 1 cm thick selvages.	Massive mafic flow, fine grained to aphanitic, cream a/s, medium green f/s, no HCl rxn, no apparent pyrite.	Drill core of mafic flow, light grey/green f/s, < 10 % qz-(cc) amygdules, varying quantities of plag. phenocrysts, slightly chloritic.
Microscopic Description	Small quantity of highly epidotized plagioclase phenocrysts set in a microlitic textured matrix composed of lath-like albite and chlorite grains and fine and coarse-grained epidote.	Evidence of silicification and albitization, abundant sericite and epidote, small amount of chlorite, traces of carbonate.	Glomeroporphyritic texture of epidotized plagio. grains, set in matrix composed of highly epidotized plagioclase, chlorite and minor carbonate.

a/s: altered surface; f/s: fresh surface; rxn: reaction; qz: quartz; plag: plagioclase; ser: sericite; carb: carbonate; opaq: opaques; *: Map number on Figure A2.1 in Appendix 2.

Appendix 3b. Macroscopic and microscopic descriptions of extrusive rock samples from the Val d'Or domain (continued).

Sample No.	5654-92	5655-92	5657-92
Map No.*	16	18	17
Field Description	Felsic flow, aphanitic, creamy a/s, medium grey f/s, HCl rxn, sericite alteration.	Plagioclase-phyric, quartz (minor carbonate) amygdaloidal, mafic flow, buff a/s, greenish f/s, light chloritization	Intermediate, plagiophyric, quartz-carb. amygdaloidal flow, grey-cream a/s, greenish grey f/s, no HCl rxn on sampled pieces, ubiquitous presence of fine chlorite porphyroblasts.
Microscopic Description	Embayment textures common of plagioclase phenocrysts, abundant sericite, small amounts of chlorite and carbonate; evidence of albitization.	Plagioclase phenocrysts have light to medium carbonate alteration, matrix is chloritized and carbonated, traces of epidote, the quantity of quartz in the matrix suggests an intermediate composition.	Matrix sericitized, plagioclase phenocrysts lightly to strongly sericitized with minor carbonate alteration.
Sample No.	5658-92	5671-92	5677-92
Map No.*	19	20	21
Field Description	Mafic flow, similar to 5657-92, presence of large pillow/lobe selvages, very hard sample, probably due to silicification.	Intermediate, feldspar-phyric, quartz-calcite amygdaloidal flow, cream-white a/s, medium grey f/s, sampled where phenocrysts and amygdules were least abundant.	Felsic flow, aphanitic with traces of fine-grained quartz eyes (?), cream a/s, light grey f/s, minor chlorite and calcite alteration.
Microscopic Description	Highly epidotized, pilotaxitic matrix with minor amounts of chlorite and carbonate, plagioclase phenocrysts altered to sericite, carbonate and/or epidote.	Carbonate-altered plagioclase phenocrysts, set in a plagioclase-rich matrix with carbonate alteration and minor chlorite and epidote alteration.	Minor amount of plagioclase phenocrysts, set in quartz-rich matrix with abundant chlorite and minor epidote and carbonate, minor concentrations of polygonal-like quartz.

Appendix 3b. Macroscopic and microscopic descriptions of extrusive rock samples from the Val d'Or domain (end).

Sample No.	5683-92	5684-92	5686-92
Map No.*	22	23	24
Field Description	Felsic flow, aphanitic, white-cream a/s, dark green f/s, local calcite alteration, chlorite porphyroblasts, traces of pyrite.	Feldspar-phyric mafic flow with calcite amygdules, buff a/s, light grey f/s, no apparent chloritization or other alteration.	Caprock unit of Louvicourt VMS mine, sample taken from the muck pile, intermediate flow, aphanitic, light grey f/s, massive with no amygdules, local calcite veinlets.
Microscopic Description	Plagioclase phenocrysts highly altered to epidote and chlorite with traces of sericite, matrix composed of epidote, chlorite, plagioclase polygonal quartz concentrations (amygdules?).	Glomeroporphyritic plagio. phenocrysts with carbonate alteration, matrix consists of microlitic plagioclase with relatively abundant chlorite and lesser quantities of epidote.	Composed essentially of plagioclase with appreciable amounts of biotite and sericite, small amount of carbonate, traces of epidote.

a/s: altered surface; f/s: fresh surface; rxn: reaction; qz: quartz; plag: plagioclase; ser: sericite; carb: carbonate; opa: opaques; *: Map number on Figure A2.1 in Appendix 2.

Appendix 3c. Macroscopic and microscopic descriptions of intrusive rock samples from the Val d'Or and Southern domains.

Sample No.	3860-91	3869-91	3870-91
Map No.*	25	26	27
Field Description	Gabbroic textured intrusion, green-buff a/s, grey-black f/s, rare clots or phenocrysts of mafic minerals, weak HCl rxn.	Fine grained dioritic mafic intrusion, green-buff a/s, medium green f/s, weak schistosity.	Same as 3869-91.
Microscopic Description	Actinolite-biotite rich, subophitic texture, fine-grained epidote alteration of plagioclase, minor amount of quartz present interstitial to plagioclase, trace amounts of apatite.	Feldspar phenocrysts set in a micrographitic matrix of quartz - feldspar - chlorite, granophyric textures are present around some phenocrysts, feldspar is highly sericitized, minor amounts of carbonate - chlorite - quartz clots, trace amounts of leucoxene.	Highly sericitized. unequigranular feldspar surrounded by abundant chlorite \pm fibrous sericite aggregates; minor quartz and fine-grained leucoxene present.
Sample No.	5652-92	5653-92	3847-91
Map No.*	28	29	30
Field Description	Same as 3869-91, minor Fe carbonate.	Same as 3869-91, minor Fe carbonate.	Drill core sample of dioritic intrusion, massive, medium green, with mafic, subhedral phenocrysts.
Microscopic Description	No thin section available.	No thin section available.	Actinolite-tremolite rich intrusion with abundant, fine-grained epidote affecting the majority of the grains, minor amounts of plagioclase, ilmenite and leucoxene present, trace amounts of carbonate.

a/s: altered surface; f/s: fresh surface; rxn: reaction; qz: quartz; plag: plagioclase; ser: sericite; carb: carbonate; opaq: opaques; *: Map number on Figure A2.1 in Appendix 2.

Appendix 3c. Macroscopic and microscopic descriptions of intrusive rock samples from the Val d'Or and Southern domains (continued).

Sample No.	5651-92	5663-92	5669-92
Map No.*	31	32	33
Field Description	Gabbroic intrusion, fine-grained, weak HCl reaction, traces of sulphides.	Massive, diaclosed dioritic intrusion, fine-grained, no HCl reaction.	Dioritic intrusion, medium grained, lath-like mafic minerals visible, weak HCl reaction.
Microscopic Description	Composed essentially of actinolite-tremolite grains and plagioclase altered to epidote and carbonate, minor amounts of biotite and quartz present.	Composed essentially of actinolite with abundant epidote, plagioclase and quartz are fine grained and interstitial to actinolite.	Composed essentially of plagioclase grains altered to epidote, carbonate and chlorite and of a mixture of actinolite-chlorite-epidote, minor quartz present.

Sample No.	5673-92	5674-92
Map No.*	34	35
Field Description	Fine-grained dioritic sill, massive, green-buff a/s, grey-green f/s, HCl reaction, traces of pyrite.	Fine-grained dioritic sill, massive, slightly diaclosed, chloritic, weak HCl reaction, traces of pyrite.
Microscopic Description	Composed essentially of highly carbonatized and epidotized plagioclase and biotite transforming to chlorite.	Composed essentially of actinolite \pm chlorite and highly epidotized plagioclase, minor biotite clots surrounded by actinolite.

a/s: altered surface; f/s: fresh surface; rxn: reaction; qz: quartz; plag: plagioclase; ser: sericite; carb: carbonate; opa: opaques; *: Map number on Figure A2.1 in Appendix 2.

Appendix 3c. Macroscopic and microscopic descriptions of intrusive rock samples from the Val d'Or and Southern domains (continued).

Sample No.	3878-91	3880-91	5659-92
Map No.*	36	37	38
Field Description	Medium-grained granitic rock, composed of white and bluish qz, cream-green epidotized feldspar, and chloritized mafic minerals, HCl rxn.	Medium-grained granitic rock, weak schistosity, same description as 3878-91.	Medium- to coarse-grained granitic rock, composed of quartz, carbonatized feldspar, and chloritized mafic minerals, weak schistosity.
Microscopic Description	Composed essentially of quartz and sericitized and carbonatized feldspar, epidote alteration is weak, chlorite with zircons.	Composed of large, single grains of qz and highly epidotized and sericitized feldspar grains, fine-grained qz + chlorite ± carbonate occur interstitial to large grains, minor amounts of ilmenite and leucoxene are present, trace amounts of apatite.	Plagioclase altered to small amounts of epidote, sericite and carbonate, albitization and silicification present.
Sample No.	5660-92	5661-92	5662-92
Map No.*	39	40	41
Field Description	Fine-medium-grained granitic rock, white and minor blue quartz interstitial to feldspar, chloritized mafics, weak HCl reaction.	Massive medium-grained granitic rock, quartz not visible, composed of plagioclase, epidote and chlorite, weak HCl reaction.	Same as 3878-91.
Microscopic Description	Composed essentially of feldspar and quartz with lesser amounts of chlorite, weak epidote and weak but ubiquitous sericite alteration of feldspar, trace amounts of carbonate and hornblende.	Compared to 5660-92 and 5669-92, minor quartz present, feldspar rich, no sericite, more carbonate, epidote and chlorite as abundant.	Feldspar grains affected by carbonate, epidote and minor sericite alteration, myrmekitic texture present, mafic minerals completely transformed to chlorite.

a/s: altered surface; f/s: fresh surface; rxn: reaction; qz: quartz; plag: plagioclase; ser: sericite; carb: carbonate; opaq: opaques; *: Map number on Figure A2.1 in Appendix 2.

Appendix 3c. Macroscopic and microscopic descriptions of intrusive rock samples from the Val d'Or and Southern domains (end).

Sample No.	5685-92	3846-91	3857-91
Map No.*	42	43	44
Field Description	Drill core sample, medium- to coarse-grained, composed of large feldspar grains with interstitial clots of epidote and chlorite and bluish quartz, HCl rxn.	Drill core sample, feldspar and amphibole-phyric dyke, subhedral, creamy-white phenocrysts locally epidotized, matrix is fine-grained to aphanitic, little to no HCl reaction.	Feldspar-phyric dyke, variable size and shape of phenocrysts, creamy with light epidotization, traces of pyrite, no HCl reaction.
Microscopic Description	Composed essentially of interlocking grains of quartz and feldspar altered to sericite, carbonate and chlorite with interstitial clots of chlorite, carbonate and epidote.	Fine- to coarse-grained feldspar phenocrysts altered to epidote, carb. and biotite; fine-grained hornblende altered to actinolite ± chlorite, matrix composed of fine-grained plag., hornblende, qz, carb, traces of opaq. and apatite.	Highly epidotized plagioclase phenocrysts and trace amounts of quartz phenocrysts are set in a fine-grained matrix of albite, epidote, zircon-bearing chlorite, relics of brown biotite and minor amounts of quartz.
Sample No.	5672-92	5682-92	
Map No.*	45	46	
Field Description	Massive feldspar-phyric dike, chalk white phenocrysts, subhedral to euhedral, green chlorite-epidote clots interstitial to phenocrysts.	Feldspar-phyric dike, equant to rounded, cream-pink phenocrysts, carbonatized, chlorite clots interstitial to phenocrysts, weak schistosity.	
Microscopic Description	Feldspar phenocrysts are carbonatized and sericitized, minor quantity of quartz phenocrysts, matrix composed of carbonate, epidote, chlorite and feldspar.	Feldspar phenocrysts are highly sericitized with less carbonate alteration, minor quartz phenocrysts, chlorite clots interstitial to phenocrysts, matrix contains abundant sericite and less carbonate.	

a/s: altered surface; f/s: fresh surface; rxn: reaction; qz: quartz; plag: plagioclase; ser: sericite; carb: carbonate; opaq: opaques; *: Map number on Figure A2.1 in Appendix 2.

Appendix 4.

**Selected Major and Trace Element Analyses from Desrochers (1994)
and the CIPW Norm of Mafic to Ultramafic Flow Rocks
from the Vassan, Central and Southern Domains.**

Table A4. Major (wt %) and trace (ppm) element analyses from Desrochers (1994) of mafic to ultramafic extrusive rocks from the Vassan, Central and Southern domains, major element analyses presented in recalculated volatile-free weight percent and the CIPW norm of recalculated analyses.

Sample No.	90-33614-S	90-33640-S	90-33670-S	90-33653-S	90-33668-S	91-03630-S	91-03637-S
UTM ZONE	18	18	18	18	18	18	18
UTM EAST	285886	288881	289350	284879	280381	288425	288750
UTM NORTH	5330264	5330047	5330296	5331186	5334884	5332100	5331850
Mg Number	53.92	65.39	59.73	69.91	39.91	42.16	42.32
SiO ₂	53.10	54.86	52.38	50.72	52.38	53.42	53.86
TiO ₂	0.48	0.73	0.82	0.50	0.84	0.79	0.79
Al ₂ O ₃	15.85	17.53	18.89	16.21	14.53	14.43	14.86
Fe ₂ O ₃	12.45	8.31	9.32	9.13	15.35	15.04	14.65
MnO	0.22	0.15	0.16	0.17	0.28	0.25	0.24
MgO	7.36	7.92	6.98	10.71	5.15	5.54	5.43
CaO	8.24	8.39	9.06	10.03	6.76	8.68	8.14
Na ₂ O	1.99	1.32	2.31	2.06	4.55	1.67	1.90
K ₂ O	0.28	0.72	0.03	0.42	0.09	0.11	0.06
P ₂ O ₅	0.03	0.08	0.06	0.06	0.08	0.07	0.06
LOI (%)	2.91	3.13	0.29	3.36	1.44	2.45	2.68
Ni	93	89	66	290	94	84	99
Co	47	30	32	58	50	43	47
Sc	55	38	29	45	67	68	72
V	235	188	225	226	369	299	340
Cu	59	64	55	10	118	99	232
Zn	87	79	69	50	110	104	111
Li	10	13	8	7	10	22	9
K	2240	5730	250	3320	750	910	500
Rb	7	20	3	14	< 3	4	< 3
Ba	60	151	39	62	20	24	14
Sr	55	170	120	160	62	37	38
Nb	< 3	4	4	< 3	4	4	4
Zr	41	71	76	44	74	57	55
Ti	2820	4200	4920	2940	4980	4620	4320
Y	23	19	21	15	46	39	40
Zr/Y	1.8	3.7	3.6	2.9	1.6	1.5	1.4
CIPW norm (weight %)							
Q	7.14	11.25	5.52	0.00	0.00	11.57	11.76
Z	0.01	0.01	0.02	0.01	0.02	0.01	0.01
Or	1.66	4.27	0.18	2.48	0.55	0.68	0.37
Ab	16.97	11.22	19.68	17.54	39.00	14.29	16.26
An	33.83	40.06	41.40	34.02	19.16	31.90	32.21
Di	6.00	1.14	2.87	12.68	11.95	9.35	6.89
Hy	29.75	28.08	25.93	25.95	19.93	26.08	26.55
Ol	0.00	0.00	0.00	3.61	3.13	0.00	0.00
Mt	3.65	2.42	2.72	2.67	4.51	4.42	4.30
Il	0.93	1.39	1.57	0.95	1.59	1.51	1.53
Ap	0.07	0.20	0.14	0.15	0.20	0.17	0.15
Sp	0.03	0.04	0.02	0.02	0.03	0.06	0.03

Table A4. Major (wt %) and trace (ppm) element analyses from Desrochers (1994) of mafic to ultramafic extrusive rocks from the Vassan, Central and Southern domains, major element analyses presented in recalculated volatile-free weight percent and the CIPW norm of recalculated analyses (continued).

Sample No.	91-03641-S	91-03643-S	91-03644-S	91-03647-N	91-03653-S	91-03654-N	91-03655-N
UTM ZONE	18	18	18	18	18	18	18
UTM EAST	288650	289400	291100	287500	291050	287300	287560
UTM NORTH	5331700	5332425	5331850	5340600	5331900	5342850	5342800
Mg Number	38.48	40.72	55.12	55.69	54.30	71.33	71.39
SiO ₂	54.49	52.83	52.75	52.19	53.82	49.33	48.87
TiO ₂	0.80	0.79	0.49	0.49	0.50	0.72	0.73
Al ₂ O ₃	14.03	13.99	16.10	15.93	15.39	10.29	10.05
Fe ₂ O ₃	14.13	14.50	12.88	11.54	12.91	12.59	12.79
MnO	0.22	0.22	0.19	0.20	0.18	0.19	0.20
MgO	4.46	5.03	7.99	7.32	7.75	15.82	16.12
CaO	8.53	10.34	8.29	8.19	8.53	8.83	9.40
Na ₂ O	3.17	2.12	1.27	3.99	0.86	2.13	1.73
K ₂ O	0.09	0.11	0.03	0.11	0.03	0.04	0.07
P ₂ O ₅	0.07	0.05	0.03	0.03	0.03	0.05	0.05
LOI (%)	0.88	0.54	3.20	1.69	3.35	3.09	3.03
Ni	63	98	94	120	93	484	504
Co	44	45	47	42	49	78	75
Sc	74	77	66	60	66	32	32
V	300	340	239	219	244	197	198
Cu	39	57	86	57	15	52	172
Zn	70	82	84	64	78	83	84
Li	6	3	18	14	20	20	25
K	750	1000	330	1080	250	420	660
Rb	3	3	< 3	3	3	< 3	3
Ba	40	35	23	65	14	29	15
Sr	36	79	69	69	70	53	42
Nb	4	4	3	< 3	3	4	3
Zr	64	58	36	36	38	60	57
Ti	4440	4560	2580	22700	2880	4020	4020
Y	46	41	24	25	24	23	22
Zr/Y	1.4	1.4	1.5	1.4	1.6	2.6	2.6
CIPW norm (weight %)							
Q	7.90	8.28	9.77	0.00	13.36	0.00	0.00
Z	0.01	0.01	0.01	0.01	0.01	0.01	0.01
Or	0.55	0.67	0.19	0.67	0.19	0.25	0.44
Ab	27.14	18.14	10.83	34.10	7.33	18.24	14.75
An	24.04	28.68	38.51	25.43	38.42	18.54	19.62
Di	15.32	19.14	2.34	12.62	3.43	20.37	21.80
Hy	19.20	19.22	33.57	15.97	32.44	20.56	22.25
Ol	0.00	0.00	0.00	6.82	0.00	16.89	15.89
Mt	4.14	4.25	3.77	3.38	3.78	3.69	3.75
Il	1.54	1.52	0.94	0.94	0.95	1.38	1.40
Ap	0.17	0.12	0.07	0.07	0.07	0.12	0.12
Sp	0.02	0.01	0.05	0.04	0.06	0.06	0.07

Table A4. Major (wt %) and trace (ppm) element analyses from Desrochers (1994) of mafic to ultramafic extrusive rocks from the Vassan, Central and Southern domains, major element analyses presented in recalculated volatile-free weight percent and the CIPW norm of recalculated analyses (continued).

Sample No.	91-03682-S	91-03684-S	91-03685S	91-03688-N	91-03689-N	91-03691-S	91-03697-N
UTM ZONE	18	18	18	18	18	18	18
UTM EAST	290800	287950	292800	289100	280450	286000	291200
UTM NORTH	5331900	5331950	5332050	5340400	5344575	5331050	5339600
Mg Number	54.89	43.31	43.87	79.32	72.86	40.24	80.30
SiO ₂	50.18	55.11	53.98	47.43	48.70	56.99	45.89
TiO ₂	0.84	0.94	0.82	0.36	0.68	0.92	0.40
Al ₂ O ₃	13.77	13.59	13.88	8.49	9.64	12.99	6.96
Fe ₂ O ₃	14.07	13.91	15.44	11.52	12.65	13.30	12.52
MnO	0.22	0.23	0.25	0.18	0.19	0.19	0.21
MgO	8.65	5.37	6.09	22.31	17.14	4.52	25.76
CaO	8.51	8.54	7.23	8.71	9.05	9.43	7.69
Na ₂ O	3.48	2.03	2.21	0.94	1.84	1.47	0.51
K ₂ O	0.23	0.21	0.04	0.05	0.05	0.08	0.05
P ₂ O ₅	0.05	0.07	0.06	< 0.01	0.06	0.08	0.02
LOI (%)	1.82	3.19	2.66	3.22	3.41	1.91	3.88
Ni	85	52	90	1100	542	91	1200
Co	63	35	49	90	74	29	104
Sc	29	75	69	26	29	64	25
V	259	377	352	146	187	357	138
Cu	61	149	139	33	25	68	42
Zn	83	115	122	70	97	88	66
Li	22	9	9	15	33	8	5
K	2080	1660	330	500	420	660	420
Rb	7	8	3	3	< 3	< 3	5
Ba	56	36	20	20	31	19	23
Sr	38	58	36	28	63	34	20
Nb	3	5	4	3	3	4	< 3
Zr	59	75	69	33	66	83	34
Ti	5040	5460	4740	2100	3900	5400	2280
Y	16	37	38	8	17	47	8
Zr/Y	3.7	2.0	1.8	4.1	3.9	1.8	4.3
CIPW norm (weight %)							
Q	0.00	12.83	10.59	0.00	0.00	18.89	0.00
Z	0.01	0.02	0.01	0.01	0.01	0.02	0.01
Or	1.41	1.24	0.25	0.31	0.31	0.49	0.31
Ab	29.76	17.40	18.91	8.07	15.72	12.60	4.37
An	21.47	27.65	28.19	18.92	18.00	28.90	16.69
Di	17.11	12.26	6.43	19.73	21.62	14.92	17.32
Hy	12.02	22.56	29.37	19.57	19.48	18.34	19.65
Ol	12.35	0.00	0.00	30.78	19.71	0.00	38.79
Mt	4.13	4.08	4.53	3.38	3.70	3.90	3.67
Il	1.61	1.81	1.57	0.70	1.30	1.77	0.76
Ap	0.12	0.17	0.15	0.00	0.15	0.20	0.05
Sp	0.06	0.03	0.03	0.04	0.09	0.02	0.01

Table A4. Major (wt %) and trace (ppm) element analyses from Desrochers (1994) of mafic to ultramafic extrusive rocks from the Vasean, Central and Southern domains, major element analyses presented in recalculated volatile-free weight percent and the CIPW norm of recalculated analyses (continued).

Sample No.	91-03698-N	91-03707-N	91-03708-S	91-03710-NC	91-03718-S	91-03724-C	91-03629N
UTM ZONE	18	18	18	18	18	18	18
UTM EAST	289925	287425	288425	287375	293900	284000	287800
UTM NORTH	5339275	5340650	5331500	5337200	5330375	5332550	5340800
Mg Number	64.78	53.58	52.88	59.40	65.29	49.57	85.47
SiO ₂	50.45	51.77	52.79	50.91	49.71	51.63	44.68
TiO ₂	0.47	0.48	0.79	0.49	0.46	0.64	0.26
Al ₂ O ₃	16.82	15.49	17.98	15.61	7.88	15.36	5.23
Fe ₂ O ₃	10.80	12.43	11.16	11.83	14.22	13.91	11.20
MnO	0.19	0.20	0.14	0.16	0.46	0.23	0.16
MgO	10.03	7.25	6.32	8.74	13.50	6.91	33.26
CaO	10.10	8.37	5.54	9.74	12.89	9.48	4.85
Na ₂ O	0.98	3.85	4.94	2.45	0.64	1.76	0.32
K ₂ O	0.13	0.12	0.28	0.03	0.21	0.03	0.02
P ₂ O ₅	0.04	0.03	0.06	0.03	0.02	0.05	0.01
LOI (%)	3.72	1.76	2.45	2.86	1.39	3.28	8.47
Ni	161	119	33	114	1000	103	1700
Co	46	46	36	45	106	44	106
Sc	46	61	62	48	29	65	19
V	176	218	237	197	179	245	90
Cu	14	74	68	65	75	56	34
Zn	66	65	57	62	91	91	59
Li	29	15	22	23	6	11	< 1
K	1080	1000	2320	250	1740	250	170
Rb	5	< 3	11	< 3	4	< 3	3
Ba	45	60	39	20	16	14	5
Sr	85	70	67	89	32	60	10
Nb	4	3	4	3	3	4	3
Zr	46	48	72	47	37	60	18
Ti	2700	2820	4800	2880	2700	3720	1380
Y	15	22	25	20	10	30	7
Zr/Y	3.1	2.2	2.9	2.4	3.7	2.0	2.6
CIPW norm (weight %)							
Q	4.14	0.00	0.00	0.25	0.00	6.56	0.00
Z	0.01	0.01	0.02	0.01	0.01	0.01	0.00
Or	0.81	0.73	1.67	0.18	1.29	0.19	0.13
Ab	8.33	32.92	42.16	20.91	5.52	15.08	2.72
An	41.42	24.84	26.26	31.77	18.16	34.27	12.88
Di	7.20	13.89	0.89	13.73	37.71	10.71	8.97
Hy	33.92	15.93	14.83	28.64	30.17	27.77	20.16
Ol	0.00	7.05	9.23	0.00	3.37	0.00	51.57
Mt	3.16	3.64	3.26	3.46	4.18	4.08	3.28
Il	0.89	0.92	1.50	0.94	0.89	1.23	0.51
Ap	0.10	0.07	0.15	0.07	0.05	0.12	0.03
Sp	0.08	0.04	0.06	0.06	0.02	0.03	0.00

Table A4. Major (wt %) and trace (ppm) element analyses from Desrochers (1994) of mafic to ultramafic extrusive rocks from the Vasean, Central and Southern domains, major element analyses presented in recalculated volatile-free weight percent and the CIPW norm of recalculated analyses (continued).

Sample No.	91-03657-S	91-03658-N	91-03659-S	91-03669-S	91-03674-S	91-03678-S	91-03679NC
UTM ZONE	18	18	18	18	18	18	18
UTM EAST	288600	290900	290350	289150	288050	287850	288925
UTM NORTH	5331850	5339650	5332225	5332000	5331800	5331775	5337575
Mg Number	46.14	77.13	38.85	65.44	38.45	42.89	45.41
SiO ₂	53.07	47.80	53.66	54.32	53.54	53.01	55.73
TiO ₂	0.79	0.43	0.86	0.70	0.90	0.78	0.57
Al ₂ O ₃	14.10	7.53	13.64	15.45	14.70	14.57	15.17
Fe ₂ O ₃	15.24	12.57	16.19	8.12	14.70	14.88	12.90
MnO	0.24	0.22	0.24	0.17	0.26	0.24	0.17
MgO	6.59	21.40	5.19	7.76	4.63	5.64	5.42
CaO	8.11	9.30	7.07	10.95	8.44	8.40	9.09
Na ₂ O	1.75	0.72	3.02	2.31	2.65	2.30	0.88
K ₂ O	0.07	0.01	0.06	0.15	0.11	0.11	0.02
P ₂ O ₅	0.05	0.02	0.07	0.06	0.07	0.06	0.05
LOI (%)	2.81	3.52	1.74	1.54	1.90	2.62	2.98
Ni	115	1000	69	135	59	93	77
Co	49	96	47	51	40	44	45
Sc	76	27	75	34	76	75	68
V	323	152	354	217	368	342	292
Cu	100	12	30	84	98	115	29
Zn	110	79	99	81	121	112	85
Li	17	1	8	9	8	9	11
K	580	166	580	1330	830	910	170
Rb	4	3	< 3	5	4	< 3	< 3
Ba	23	4	19	117	33	29	9
Sr	74	17	22	150	28	35	87
Nb	4	3	< 3	4	4	3	4
Zr	55	31	58	60	63	55	47
Ti	4320	2460	4740	3780	4920	4200	3540
Y	37	11	36	17	45	40	29
Zr/Y	1.5	2.8	1.6	3.5	1.4	1.4	1.6
CIPW norm (weight %)							
Q	10.04	0.00	7.53	6.39	8.61	8.17	18.37
Z	0.01	0.01	0.01	0.01	0.01	0.01	0.01
Or	0.44	0.06	0.37	0.91	0.68	0.68	0.12
Ab	15.00	6.13	25.92	19.69	22.70	19.73	7.50
An	30.73	17.48	23.77	31.52	28.19	29.42	37.77
Di	8.01	23.21	9.44	18.43	11.48	10.30	6.22
Hy	29.66	25.34	26.40	19.24	22.13	25.70	25.02
Ol	0.00	24.57	0.00	0.00	0.00	0.00	0.00
Mt	4.47	3.69	4.76	2.37	4.31	4.37	3.78
Il	1.51	0.82	1.65	1.33	1.74	1.49	1.09
Ap	0.12	0.05	0.17	0.15	0.17	0.15	0.12
Sp	0.05	0.00	0.02	0.02	0.02	0.03	0.03

Table A4. Major (wt %) and trace (ppm) element analyses from Desrochers (1994) of mafic to ultramafic extrusive rocks from the Vasean, Central and Southern domains major element analyses presented in recalculated volatile-free weight percent and the CIPW norm of recalculated analyses (end).

Sample No.	91-03633N	91-03658N	91-03681S	91-03690N	90-33666C
UTM ZONE	18	18	18	18	18
UTM EAST	287950	290900	290650	289150	281358
UTM NORTH	5340800	5339650	5331875	5340300	5334325
Mg Number	80.70	77.13	84.31	82.47	83.08
SiO ₂	47.32	47.65	46.09	45.70	52.17
TiO ₂	0.41	0.42	0.34	0.35	0.33
Al ₂ O ₃	6.76	7.82	5.03	6.57	5.14
Fe ₂ O ₃	11.56	12.53	11.74	11.58	10.20
MnO	0.18	0.22	0.15	0.17	0.13
MgO	24.41	21.34	31.85	27.53	25.29
CaO	9.08	9.27	4.76	7.38	6.74
Na ₂ O	0.24	0.71	< 0.10	0.57	< 0.10
K ₂ O	0.01	0.01	< 0.01	0.13	< 0.01
P ₂ O ₅	0.03	0.02	0.03	0.02	0.01
LOI (%)	6.66	3.52	8.55	5.31	5.42
Ni	1300	1000	1800	1300	1500
Co	97	96	110	101	92
Sc	22	27	19	22	19
V	125	152	110	130	125
Cu	40	12	32	30	10
Zn	62	79	86	72	66
Li	15	< 1	1	7	< 1
K	80	170	80	1000	80
Rb	3	3	3	5	4
Ba	6	4	11	13	2
Sr	30	17	11	18	4
Nb	3	3	4	3	3
Zr	24	31	30	32	27
Ti	2160	2460	1860	1200	1860
Y	12	11	5	7	7
Zr/Y	2.0	2.8	6.0	4.6	3.9
CIPW norm (weight %)					
Q	0.00	0.00	0.00	0.00	0.00
Z	0.01	0.01	0.01	0.01	0.01
Or	0.07	0.06	0.00	0.76	0.00
Ab	2.01	6.11	0.00	4.90	0.00
An	17.51	18.29	13.86	15.11	14.15
Di	22.06	22.38	7.74	17.21	15.44
Hy	29.17	26.49	35.51	17.08	64.09
Ol	25.13	22.28	38.98	41.00	2.88
Mt	3.39	3.67	3.44	3.39	2.98
Il	0.78	0.81	0.65	0.67	0.63
Ap	0.08	0.05	0.08	0.05	0.03
Sp	0.00	0.00	0.00	0.00	0.00

Appendix 5.

**Sampling Location Maps, Selected Major and Trace Element Analyses
from Girault (1986) and Gaudreau et al. (1986), and the CIPW Norm
for these Flow Rocks from the Val d'Or Domain.**

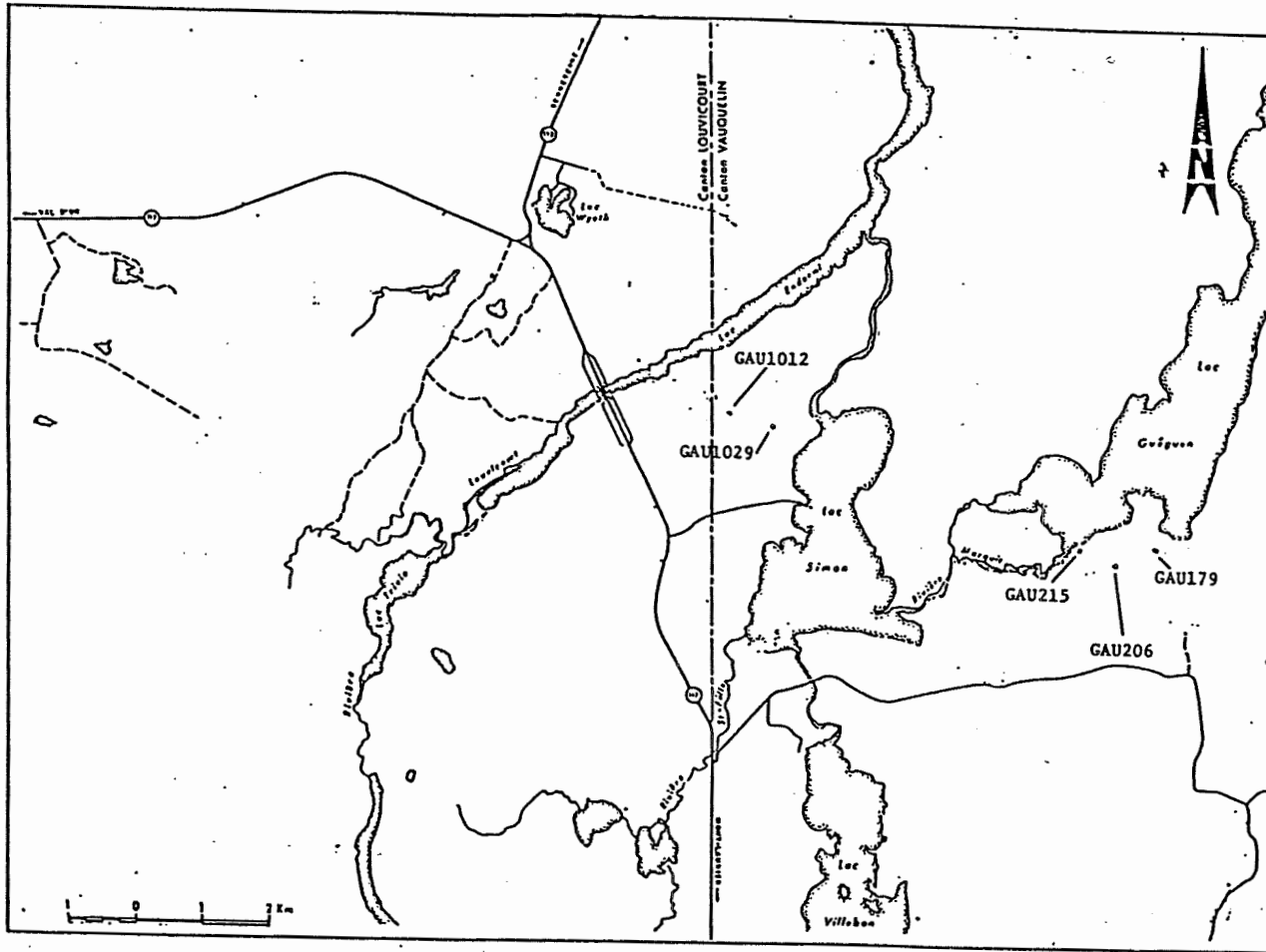


Figure A5.2 Location map of selected analyses from Gaudreau et al. (1986).

Table A5. Selected major element (wt %) and trace element (ppm) analyses of flow rocks, major element analyses presented in recalculated volatile-free weight percent, from Girault (1986) and Gaudreau et al. (1986), and the CIPW norm of recalculated analyses. Sample locations given in Figures A5.1 and A5.2 (end).

Sample No.	GIR47	GIR9	GIR63	GAU179	GAU206	GAU215	GAU1012	GAU1029
Map No.	47	9	63	179	206	215	1012	1029
UTM ZONE	—	—	—	18	18	18	18	18
UTM EAST	—	—	—	330710	330100	329550	324225	324900
UTM NORTH	—	—	—	5324350	5324340	5324550	5326775	5326650
Name	Rhyolite	Dacite	Dacite	And. Basalt	Basalt	Basalt	Andesite	Rhyodacite
Affinity	Calc.	Calc.	Calc.	Thol.	Thol.	Thol.	Calc.	Calc.
SiO ₂	74.33	65.67	76.57	53.47	56.44	56.02	60.02	70.54
TiO ₂	0.35	1.23	0.22	1.08	1.00	0.88	0.93	0.96
Al ₂ O ₃	12.88	14.10	9.94	15.97	16.96	18.64	17.07	13.72
Fe ₂ O ₃	3.72	6.39	3.74	12.22	9.19	7.46	7.00	5.16
MnO	0.03	0.09	0.12	0.18	0.15	0.16	0.09	0.15
MgO	1.53	1.84	1.50	5.64	5.15	5.65	5.12	1.05
CaO	2.04	4.35	3.83	9.05	7.44	5.31	4.43	5.69
Na ₂ O	4.99	5.28	3.46	2.05	2.83	5.19	3.80	2.17
K ₂ O	0.06	0.82	0.54	0.18	0.48	0.39	1.31	0.30
P ₂ O ₅	0.06	0.24	0.09	0.15	0.25	0.30	0.22	0.25
CO ₂ (%)	n.d.	n.d.	n.d.	0.32	0.12	0.47	0.12	0.14
LOI (%)	n.d.	n.d.	n.d.	2.00	2.35	3.80	3.40	0.95
S (%)	n.d.	n.d.	n.d.	0.01	0.01	0.16	0.01	0.01
K	500	6800	4480	1490	3980	3240	10800	2490
Rb	2	21	12	0.5	8	6	28	2
Sr	140	163	67	144	257	210	261	185
Nb	10.0	8.0	12.0	n.d.	n.d.	n.d.	n.d.	n.d.
Zr	317	195	190	48	107	98	181	230
Ti	2100	7370	1320	6480	6000	5300	5580	5760
Y	47	36	29	21	27	27	30	44
Zr/Y	6.7	5.4	6.6	2.3	4.0	3.6	6.0	5.2

n.d. signifies not determined.

	CIPW norm (weight %)							
Q	38.17	19.74	45.43	10.41	11.44	3.27	13.73	43.82
C	1.03	0.00	0.00	0.00	0.00	1.84	2.16	0.40
Z	0.06	0.04	0.04	0.01	0.02	0.02	0.04	0.05
Or	0.36	4.88	3.20	1.07	2.86	2.32	7.79	1.78
Ab	42.30	44.74	29.33	17.52	24.98	44.18	32.34	18.41
An	9.80	12.51	10.02	34.19	31.95	21.56	19.90	25.78
Di	0.00	6.38	6.79	6.72	2.32	0.00	0.00	0.00
Wo	0.00	0.00	0.00	0.00	0.00	0.00	0.00	0.00
Hy	4.83	6.98	1.89	23.68	21.11	21.67	19.59	3.45
Mt	2.70	1.86	2.72	3.58	2.68	2.18	2.04	3.75
Hm	0.00	0.00	0.00	0.00	0.00	0.00	0.00	0.00
Il	0.67	2.35	0.42	2.07	1.91	1.68	1.78	1.83
Sn	0.00	0.00	0.00	0.00	0.00	0.00	0.00	0.00
Ap	0.14	0.57	0.21	0.36	0.60	0.71	0.52	0.59
Cc	0.00	0.00	0.00	0.73	0.27	1.07	0.27	0.32

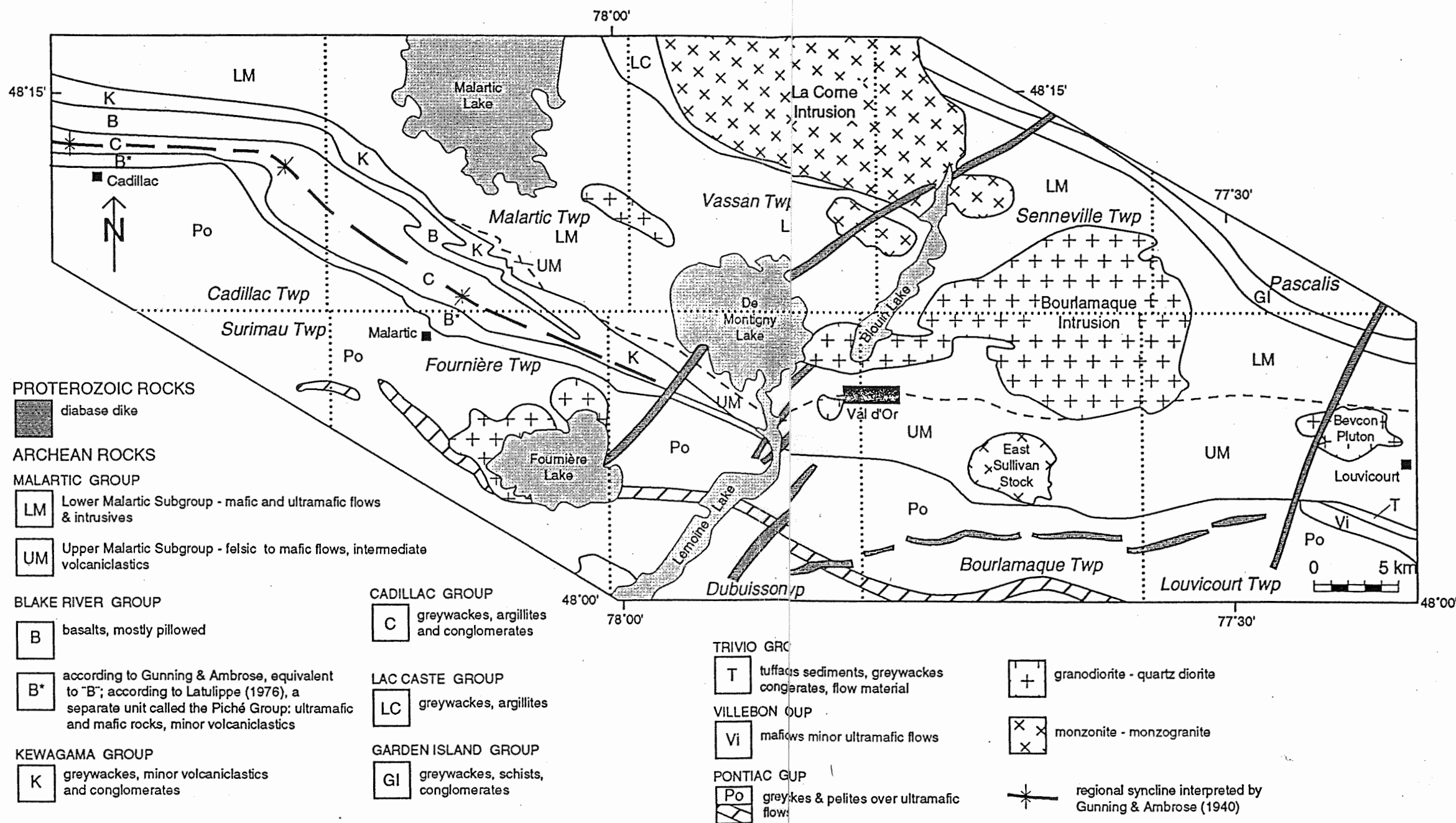


Figure 3. General geologic map of the Val d'Or region illustrating the regional syncline interpreted by Gunning and Ambrose (1940) and the division (broken line) of the Malartic Group into upper and lower subgroups (Latulippe 1976). The dotted lines represent township boundaries. The Bourlamaque and Louvicourt townships comprise the study area.

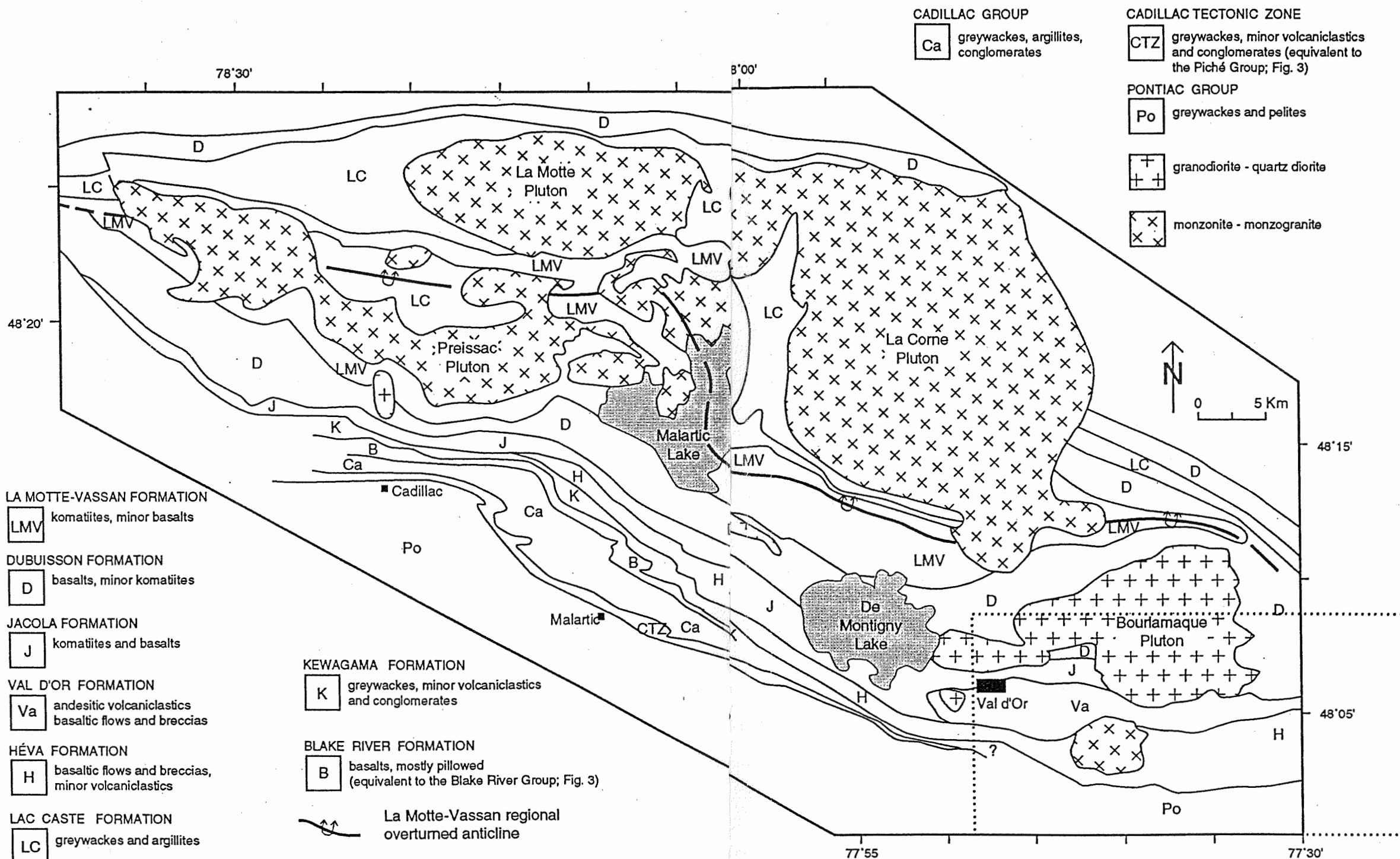


Figure 4. Geologic map of the Val d'Or region interpreted by Imreh (1984). The La Motte-Vassan overturned anticline is the dominant, regional structure and the Malartic Group as defined by Gunning and Ambrose (1940) and Latulipe (1966, 1976) is divided into the La Motte-Vassan, Dubuisson, Jacola, Val d'Or and Héva formations. The dotted line outlines the study area.

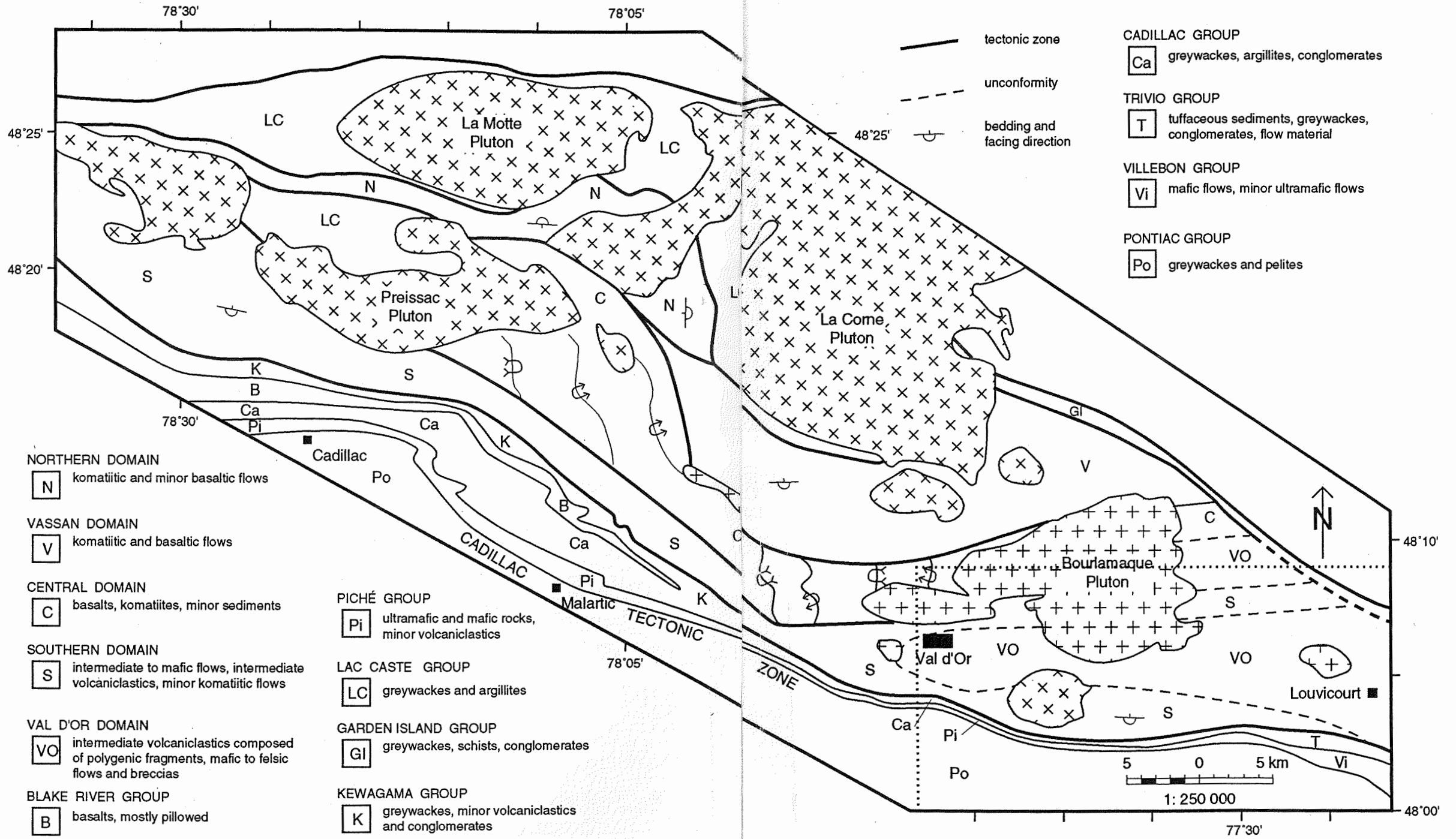


Figure 5. Tectonostratigraphic map of the Val d'Or region highlighting the five lithotectonic domains of the Malartic Composite Block (modified after Desrochers et al., 1993). The dotted line outlines the study area.

ÉCOLE POLYTECHNIQUE DE MONTRÉAL



3 9334 00223534 7